DEVELOPMENT OF ENERGY EFFICIENT SOLAR POWERED AQUA-AMMONIA ABSORPTION REFRIGERATION AND AIR-CONDITIONING SYSTEM

BY

MUHAMMAD UMAR SIDDIQUI

A Dissertation Presented to the

DEANSHIP OF GRADUATE STUDIES

KING FAHD UNIVERSITY OF PETROLEUM & MINERALS

DHAHRAN, SAUDI ARABIA

In Partial Fulfillment of the

Requirements for the Degree of

DOCTOR OF PHILOSOPHY

In

MECHANICAL ENGINEERING

MAY 2014

KING FAHD UNIVERSITY OF PETROLEUM & MINERALS

DHAHRAN- 31261, SAUDI ARABIA

DEANSHIP OF GRADUATE STUDIES

This thesis, written by **Muhammad Umar Siddiqui** under the direction his thesis advisor and approved by his thesis committee, has been presented and accepted by the Dean of Graduate Studies, in partial fulfillment of the requirements for the degree of **DOCTOR OF PHILOSOPHY IN MECHANICAL ENGINEERING.**

Dr. Syed A. M. Said
(Advisor)

Dr. Zuhair M. Gasem
Department Chairman

Dr. Maged A.I. El-Shaarawi
(Co-Advisor)

Dr. Salam A. Zummo
Dean of Graduate Studies

Dr. Habib I. Abualhamayel
(Member)

25/5/14
Date

Dr. Haitham Bahaidarah
(Member)

Dr. Amro M. Al-Qutub
(Member)

DEDICATED TO MY BELOVED PARENTS, MY WIFE, MY SISTERS

AND ONLY BROTHER

ACKNOWLEDGMENTS

All praise and thanks are due to Almighty Allah, Most Gracious and Most Merciful, for his immense beneficence and blessings. He bestowed upon me health, knowledge and patience to complete this work. May peace and blessings be upon prophet Muhammad (PBUH), his family and his companions. Thereafter, acknowledgement is due to KFUPM for the support extended towards my research by granting me the opportunity to pursue post-graduate studies through its remarkable facilities at the Mechanical Engineering Department and Centre of Research Excellence – Renewable Energy (CoRE-RE). I would also like to acknowledge the support of KACST under an NSTIP project # 08-ENE56-04 in conducting this research.

I acknowledge, with deep gratitude and appreciation, the inspiration, encouragement, valuable time and continuous guidance given to me by Dr. Syed. A. M. Said, my dissertation advisor. I am highly grateful to my dissertation co-advisor Dr. Maged A.I. El-Shaarawi for his valuable guidance, suggestions and motivation. Their strong support and co-operation towards this research was a boon to me. I am also grateful to my Committee members, Dr. Habib Abulhamayel, Dr. Haitham Bahaidarah & Dr. Amro Al-Qutub for their constructive guidance and support.

My heartfelt thanks are due to my parents for their prayers, guidance, and moral support throughout my academic life. My parents' advice, to strive for excellence has made all this work possible. I am also grateful to my wife who stood beside me through the last stages of completing my research. Special thanks are due to my senior colleagues at the University for their Help and prayers. I also acknowledge KFUPM for providing excellent research opportunities and a healthy academic environment.

TABLE OF CONTENTS

LIST OF TABLES

LIST OF FIGURES

LIST OF ABBREVIATIONS

ABS	:	Absorber
APC	:	Absorber Pre-cooler
COND	:	Condenser
COP	:	Coefficient of Performance
c_P	:	Specific heat capacity at constant pressure, $kJ.kg^{-1}. K^{-1}$
CR	:	Circulation Ratio
del	:	Absolute exergy loss across any component
DEPH	:	Dephlegmator
$\dot{E}$	:	Exergy loss ratio
ECOP	:	Exergetic Coefficient of Performance
EVAP	:	Evaporator
EV1	:	Liquid Expansion Valve
EV2	:	Refrigerant expansion valve
G	:	Solar Intensity, $W.m^{-2}$
GEN	:	Generator
GHX	:	Heat Recovery Coils inside the Generator Assembly

h	:	Enthalpy, $kJ.kg^{-1}$
HRHX	:	Heat Rejection Heat Exchanger
$\dot{m}$	:	Mass flow rate, $kg.s^{-1}$
$Mass_{initial}$	:	Initial Mass of strong solution in the chiller, kg
$Mass_{reservoir}$	:	Mass of refrigerant stored in the reservoir, kg
P	:	Pressure, kPa
POL	:	Principal operating line
$Pole_{dephl}$	:	Enthalpy at pole of dephlagmator, $kJ.kg^{-1}$
$Pole_{gen}$	:	Enthalpy at pole of generator, $kJ.kg^{-1}$
PUMP	:	Solvent/Solution Pump
Q	:	Thermal energy input, rejected or recovered, kW
RPC	:	Refrigerant Pre-cooler
SHE	:	Solution Heat Exchanger
T	:	Temperature, ºC
T_{abs}	:	Absorber temperature, ºC
T_{amb}	:	Ambient temperature, ºC
T_{cond}	:	Condenser temperature, ºC

T_{evap}	:	Evaporator temperature, ºC
T_{gen}	:	Weak solution temperature at exit of generator, ºC
x_{ss}	:	Concentration of strong solution
x_{ws}	:	Concentration of weak solution

Greek Symbols

η	:	Efficiency
ρ	:	Density, $kg.m^{-3}$
ε	:	Effectiveness

ABSTRACT

Full Name : Muhammad Umar Siddiqui

Thesis Title : Development of Energy Efficient Solar Powered Aqua-Ammonia Absorption Refrigeration and Air-Conditioning System

Major Field : Mechanical Engineering

Date of Degree : May 2014

The residential sector in the Kingdom of Saudi-Arabia consumes more than 50% of the electrical energy production. More than 80% of this goes to power the air-conditioning systems. The air-conditioning sector is considered a service sector and reducing this high percentage of electrical energy consumption by the use of solar energy will avail such high quality of energy for production sector or exportation. Hence, utilization of solar energy to power air-conditioning systems is a matter of key interest for the Kingdom of Saudi-Arabia. Absorption systems are one of the most effective ways to be powered by solar energy. The main advantage of aqua-ammonia absorption system is that it can be operated to provide refrigeration (below 0ºC temperatures) as well as air-conditioning (above 0ºC temperatures). Hence, the focus of the present dissertation topic is to develop an energy efficient solar powered aqua-ammonia absorption refrigeration and air-conditioning system that can operate effectively in the hot climatic conditions of Saudi-Arabia. The development includes an in-depth review of the design and operation of conventional solar-assisted absorption refrigeration systems. This in-depth review is followed by proposing an energy efficient design that have a better performance compared to the conventional design. The detailed results of first law and second laws of thermodynamic analysis of the proposed design is presented.

ARABIC ABSTRACT

ملخص الرسالة

الاسم الكامل: محمد عمر صديقي

عنوان الرسالة: تصميم وتحليل لنظام تبريد وتكييف هواء يعمل بالطاقة الشمسية ويُستخدم ماء الأمونيا كوسيط تبريد

التخصص: الهندسة الميكانيكية

تاريخ الدرجة العلمية: مايو 2014

القطاع السكني في المملكة العربية السعودية تستهلك أكثر من 50 ٪ من إنتاج الطاقة الكهربائية. أكثر من 80 ٪ من هذا يذهب الى قطاع تكييف الهواء. يعتبر قطاع تكييف الهواء قطاع خدمي وليس قطاع انتاجي، من الممكن تقليل هذه النسبة العالية من استهلاك الطاقة الكهربائية عن طريق استخدام الطاقة الشمسية. إن استخدام الطاقة الشمسية لتشغيل أنظمة تكييف الهواء في القطاع السكني والتجاري هو موضوع اهتمام رئيسي للمملكة العربية السعودية. إن أنظمة تكييف الهواء التي تعمل بالامتصاص تُعتبر واحدة من أكثر الطرق فعالية لتشغيل أنظمة تكييف الهواء باستخدام الطاقة الشمسية. وقد تم تركيب العديد من أنظمة تكييف الهواء التي تعمل باليثيم بروماید داخل المملكة. ولكن حسب علم الباحثين، لا توجد بالمملكة أنظمة تعمل بخاصية نظام امتصاص الماء من الأمونيا. نظام امتصاص ماء الأمونيا يتمتع بميزة إضافية على الأنظمة التي تعمل باليثيم بروماید لأنها يمكن أن توفر تبريد بدرجات حرارة أقل من الصفر (التبريد) إلى جانب تكييف الهواء. تعرض هذه الدراسة تصميم وتحليل لنظام تبريد وتكييف هواء يعمل بالطاقة الشمسية ويُستخدم ماء الأمونيا كوسيط تبريد. الملامح الرئيسية للتصميم المقترح هو أنه مزود بخزان تبريد وجهاز تخليص الماء من الأمونيا (dephlegmator). أن كلا من هذه الميزتين تساعد على زيادة كفاءة النظام. وقد تم تصنيع مكونات التصميم المقترح وتجميعها وتركيبها واختبارها.

نتائج الدراسة النظرية والمعملية أثبتت أن التصميم الجديد ذا كفاءة عالية مقارنة بالتصميم الذي لا يحتوي على خزان تبريد و جهاز تخليص الماء من الأمونيا (dephlegmator).

CHAPTER 1

INTRODUCTION

The technological advancement and economic growth of any country rest on the availability of utilizable form of energy in that country. The quantity of available energy also reflects its quality of life. So far, fossil fuel is considered and utilized as the prominent source of generating utilizable form of energy [1]. However concerns are growing on daily basis over the negative effects on the environment that are caused by burning of fossil fuels that includes global warming and green-house gas effect on the ozone. Thus serious efforts are being made to explore alternatives that could reduce the fossil fuels burning. So far renewable energy represents the best alternative to reduce the burning of fossil fuels.

Renewable energy refers to the form of energy that either do not get depleted or has the natural ability to renew itself. Renewable energy sources include biomass, geothermal, hydropower, wave, wind, solar and tidal energy sources. Among all of these naturally available and environmentally friendly sources, solar energy stands top on the list of renewable energy sources. The main reason behind the enormous potential of solar energy is its cleanliness and natural availability. It has also been calculated that the total solar radiation transmitted to the earth is about 1.74×10^{17} W [2] while the overall energy consumption of the world is about 1.84×10^{13} W [3]. Thus solar energy presents an enormous potential renewable energy source.

It is not possible to completely replace the conventional source of energy by renewable energy. However, a major portion of the consumption sector energy requirements can be met with the utilization of renewable energy. Hence, this will contribute to the reduction of fossil fuel consumption. So the recent focus is on utilizing renewable energy sources to meet the energy requirements for the consumption sector. Within the consumption sector in the gulf region, air-conditioning and refrigeration presents one of the highly energy consuming field. This can be acknowledged by the fact that as per the statistic of 2010 [4], about 52% of the electrical energy produced in the KSA is consumed by the residential sector whereas more than 70% of this residential energy consumption goes to the comfort conditioning as shown in figure 1-1. Thus, more than 36% of electrical energy produced in the KSA is consumed by the air-conditioning sector.

Furthermore the energy requirements for air-conditioning sector is also increasing each year [5]. Hence, utilization of renewable energy sources is being given a serious consideration to meet the power requirements of the air-conditioning sector. In this regard, solar energy is considered as the most appropriate option among other renewable energy sources since its peak coincides with the peak demand of air-conditioning [6]. Solar electrical and thermal powered refrigeration systems can be used to produce cooling [7]. The first is a photo-voltaic based solar energy system, in which solar energy is initially converted into electrical energy and then utilized for producing the refrigeration much like conventional methods. The second one utilizes solar thermal energy to power the generator of an absorption refrigeration system.

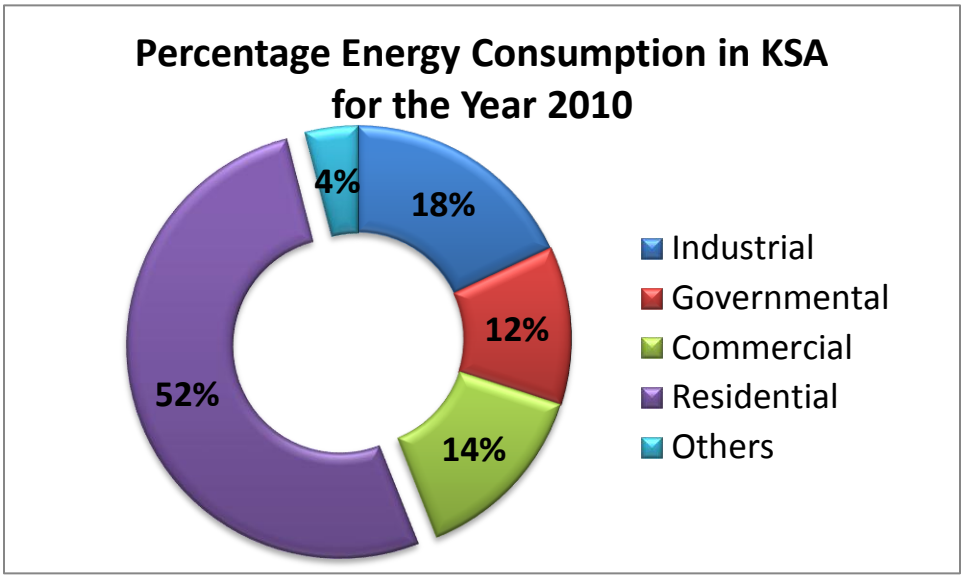

Figure 1-1 Pie-Chart for the Energy Consumption in KSA

Kim & Ferreira [8] made a comparison between the two systems both from the point of view of energy efficiency and economic feasibility. They reported that the collector efficiency of photovoltaic systems is approximately 15% where the COP of the compressor based refrigeration systems is typically 4.0. Thus, the solar cooling efficiency for the Solar electric refrigeration system is determined as

$$\text{Solar Cooling Efficiency} = 0.15 \text{ of Collector Efficiency} \times 4.0\ COP_{comp,systems}$$

$$= 0.60 \text{ approx. for vapor compression systems}$$

However, the collector efficiency of solar thermal systems is approximately 90% where the COP of the absorption based refrigeration systems is typically 0.7. Thus, the solar cooling efficiency for the Solar thermal refrigeration system is determined as

$$\text{Solar Cooling Efficiency} = 0.90 \text{ of Collector Efficiency} \times 0.7\ COP_{absorp,systems}$$

$$= 0.63 \text{ approx. for vapor absorption systems}$$

The comparison by Kim & Ferreira [8] also indicated that solar electric systems are expensive than solar thermal systems. Otanicar et al. [9] showed that a very small portion (less than 35%) of the incident solar radiation is converted into electrical energy using photovoltaic cells while solar thermal systems can utilize more than 95% of the incident solar radiation. Due to these advantages of solar thermal systems over solar photovoltaic systems, recently more research has been carried out in the field of solar thermal cooling systems [10]. Absorption systems represent an efficient way to produce cooling. Therefore, this dissertation is focused over the development of an energy efficient solar powered absorption refrigeration and air-conditioning system.

CHAPTER 2

LITERATURE REVIEW

This chapter presents an intensive review on the recent developments in the field of solar powered absorption systems. The main focus of the literature review is the recent, simulation and experimental, work done in the field of solar powered absorption systems with respect to the different pairs of working fluid used in such systems.

The absorption refrigeration system operates on the principles of absorption cycle rather than the compression cycle. This absorption cycle eliminates the need of a compressor by replacing it with an absorber and a generator [11]. In case of a compression cycle, the refrigerant pressurization is required which is performed by the compressor in the vapor phase. However, in case of an absorption cycle, the refrigerant pressurization is not performed in the vapor phase. Rather the refrigerant is first absorbed in an absorbing material and is then pressurized in the absorbed liquid phase. The pressurized absorption mixture is then reheated in the generator to regenerate the pressurized refrigerant vapor. The advantage of the absorption system over the compression system is that very little or no electrical power is required to pressurize the refrigerant compared to conventional compression system which requires considerably large amount of electrical power [12]. However such absorption systems require heat input to regenerate the refrigerant vapor. Such heat is provided by solar thermal collectors in case of solar powered absorption refrigeration systems [13].

One of the earliest solar absorption chillers was developed by Trombe and Foex [14]. They reported preliminary experimental results with a pilot plant using aqua-ammonia. Followed their work, Chinnappa [15] made a systematic experimental study of an absorption refrigeration cycle employing two binary systems (NH_3-H^20 and NH_3-$LiNO_3$) with maximum solution temperatures up to about 405 K. In addition to those a simple refrigerator operated with flat plate collectors was built at Colombo, Ceylon by Chinnappa [16] as well. They reported that an evaporator temperature of 10^0F can be reached on a clear day for every three to four square feet of collector area using flat plate collectors. Solar powered absorption refrigeration systems are generally classified as continuous operation systems and intermittent operation systems.

2.1 Continuous Operation Systems

The continuous operation systems belongs to a specific classification of absorption refrigeration system in which both the generation and absorption processes take place simultaneously. Such systems operate in a cyclic behavior with a cycle time of less than a day (24 hours). The pressurization process in such systems is carried out by the solution pump. Solution pump's electrical power requirement is much less compared to the electrical power requirements of compressors in the vapor compression systems.

The basic components of a continuous operation absorption refrigeration system are the generator, absorber, condenser, evaporator, throttling valves and a solution pump. The generator is powered by solar collectors in case of a solar powered absorption system. The effect of different types of solar collectors in the performance of solar powered absorption systems have recently been analyzed by Kundu et al. [17]. Their results indicated that concave parabolic shape collectors present the best design for the

absorption system. The condensation process within the absorption systems have been studied in detail by Fernandez-Seara et al. [18]. They investigated the condensation of refrigerant-absorbent solution on a horizontal smooth tube both experimentally and theoretically. They reported that refrigerant vapor mass transfer significantly effects heat and mass transfer coefficients and consequently overall condensation heat transfer coefficients within the condenser of the absorption system. Similarly, the absorption process alone, have also been recently studied for spray absorbers by Venegas et al. [19]. Their results indicated that about 60% of the mass transfer takes place during the deceleration period of the drops within the spray absorbers.

Along with basic components, certain heat recovery components are also added to the continuous operation absorption system to increase its coefficient of performance. These heat recovery components are solution heat exchanger and a refrigerant pre-cooler. Without using the refrigerant pre-cooler drops the performance of the absorption system by 3-5% whereas not using the solution heat exchanger will cause a drop in the performance by 35-50% [20]. Also additional refrigerant rectification equipment such as a rectifier and a dephlegmator is added in the design to rectify the refrigerant vapor in case of having a volatile absorbent. Rectification equipment are added to restrict the volatile absorbent (such as water) within the generator and absorber thus preventing it from entering into the evaporator. The rectification equipment is normally constructed in the form of a column and divided into two sub-sections i.e. rectifying strip and stripping strip [21]. Improper rectification with the volatile absorbent such as water will cause water accumulation in the evaporator that significantly deteriorates the performance of the absorption system [22]. The construction of the rectifier plays a very important role in

refrigerant purification process. In this regard, Sieres & Fernandez-Seara [23] experimentally determined that there are appreciable differences between experimental results and the available correlations that describe the volumetric mass transfer coefficient within the rectification column. Sieres et al. [24] also used large specific area corrugated sheet structured packing within the rectification column and experimentally determined its correlation for volumetric vapor phase mass transfer coefficient. They also used 10 mm metal Pall rings as the packing material for the rectifier column [25] and reported the correlation for volumetric vapor phase mass transfer coefficient based on the experimental results. Fernandez-Seara et al. [26] used helical coil rectifier in an absorption refrigeration system and analyzed the influence of heat and mass transfer coefficients on the rectifier performance.

Along with the component to component analysis, several simulation and experimental studies have also been conducted on the continuous operation based solar powered absorption refrigeration systems. Some of the recent studies have been reviewed and presented in the next section of this chapter.

2.1.1 Simulation Studies

The simulation work conducted over the continuous operation based solar powered absorption refrigeration systems can further be classified based on the refrigerant-absorbent working pair used. The most common working pairs are the aqua-ammonia and LiBr-water, however certain other working pairs have also been used in simulating the performance of solar powered absorption refrigeration systems. The aqua-ammonia represents the most commonly used refrigerant-absorbent working pair in the continuous operation based solar powered absorption refrigeration system. Several

simulation studies have been conducted in this regard using the simulation software such as MATLAB, EES, TRANSYS, ASPEN, etc . One of the recent simulation study over this topic was performed by Raghuvanshi & Maheshwari [27] over the MATLAB software. They showed that a coefficient of performance of 0.227 can be reached by operating the absorption system at generator temperature as low as 50ºC. Said et al. [28] conducted the simulation study over Engineering Equation Solver (EES) software and concluded that an aqua-ammonia absorption system equipped with a refrigerant storage provides better coefficient of performance when operated continuously on a day and night basis. The comparison was made between refrigerant storage, heat storage and cold storage system for continuous operation of the aqua-ammonia absorption chiller.

Darwish et al. [29] conducted the simulation studies over the aqua-ammonia absorption system using ASPEN simulation software. They provided the experimental validation of their work and reported that their results have a maximum deviation of 1.8% from the experimental results. Their results indicated an increase of 15-20% in the coefficient of performance of the aqua-ammonia absorption system by the use of separator at the top of the rectifying column within the absorption system. Another simulation study was conducted by Beccali et al. [30] to estimate the life cycle of an aqua-ammonia absorption refrigeration system using TRANSYS software. Their simulation results indicated that a cooling system of 12 kW, when installed at Palmero & Zurich, is estimated to have a life cycle of approximately 25 years. Artificial Neural Networks (ANN) can also be effectively used to simulate the performance of absorption refrigeration systems [31]. Sencan [32,33] used ANN to estimate the performance of aqua-ammonia absorption refrigeration systems. They developed a new formulation

independent of ANN software that can be used with any programming language to estimate the performance of absorption systems. They compared their results from ANN with the linear regression and M5' Rules models using WEKA software [34] and showed that the best results were obtained from ANN.

The thermodynamic design for the absorption system leads to the heat exchanger design for its components. In this regard, Bangotra & Mahajan [35] performed the UA analysis of the different components of aqua-ammonia absorption system. A similar form of detailed UA analysis for the heat exchanger design of different components of absorption system have also been presented by Lavanya & Murthy [36]. First law thermodynamic analysis of an aqua-ammonia absorption system has been recently carried out by Abdulateef et al. [37]. They showed the influence of the effectiveness of solution heat exchanger over the performance of the system. Their simulation results indicated 50% increase in the coefficient of performance of the system when increasing the effectiveness of solution heat exchanger from 0 to 1.

Along with first law thermodynamic analysis, a couple of second law thermodynamic analysis and exergy analysis have also been simulated recently for continuous operation aqua-ammonia absorption refrigeration systems. In this regard, Chua et al. [38] performed the second law thermodynamic analysis to estimate the losses within the different components of the system. Their results indicated that 30% of the thermal energy input is dissipated within the rectifier and regenerative heat exchanger. While the liquid and vapor phases in the absorber contributes to about 6% and 3% thermal energy dissipation respectively. Lostec et al. [39] performed the second law optimization of the absorption refrigeration system. Their results indicated the presence

of three optimum values of COP 0.56, 0.62 & 0.69 for the absorption system that minimizes UA value, irreversibility and exergetic efficiency respectively. Their results also showed that all of these three optimum COP values are lower than the maximum COP value. Also their results indicated that 33% and 34% of the exergy destruction takes place inside the absorber and desorber of the absorption system respectively. Similarly, a simulation study of the aqua-ammonia absorption system based on the first and second law of thermodynamic have been carried out by Caciula et al. [40]. They utilized compound parabolic collectors and developed a mathematical model of aqua-ammonia mixture based on mass and energy conservation equations. Their results indicated a maximum COP 0.66 & 0.73 at a generator temperature of 90°C & 74°C when operated at an evaporator temperature of -3°C & 6°C respectively.

Along with the steady state analysis, several unsteady analysis have also been recently simulated for continuous operation based aqua-ammonia absorption refrigeration systems. In this regard, Cai et al. [41] performed the lumped-parameter dynamic simulation of aqua-ammonia based continuous operation absorption system. Their results indicated an oscillation in time before reaching steady state in transient response to the step parameter change (one percent pressure rise by the pump) of the absorption system. Kim & Park [42] also conducted the lumped-parameter dynamic simulation for a commercially available 10.5 kW absorption chiller and showed that that there exists an optimum volume of the generator and optimum mass & concentration of strong solution for achieving maximum cooling capacity in an absorption system. They recommended a stepwise turn-up and turn-down of the system's input parameter to decrease the time constant of the system. They also showed that the time constant of the system decreases

with the increase of refrigerant concentration of the strong aqua-ammonia solution. However Kim et al. [43] showed that high concentration of refrigerant in the system deteriorate the performance by increasing the system pressures. Ozgoren et al. [44] predicted the hourly performance of a 3.5 kW cooling capacity aqua-ammonia absorption system using evacuated tube collectors for Adana province, Turkey. Their simulation results indicated a cooling coefficient of performance of 0.243-0.454 while heating coefficient of performance was predicted to be in the range of 1.243-1.454.

Recently, the approach of direct air cooling of the solar powered aqua-ammonia chiller have been simulated by Lin et al. [45] for two stage absorption system. They tested several arrangements for the series connection of condenser (CON), low pressure absorber (LABS) and medium pressure absorber (MABS). Their results indicated that the best thermal performance is achieved for the CON-LABS-MABS air cooling sequence in a series connection. The simulation results for the best arrangement indicated a thermal COP of 0.34 and electrical COP of 26 under typical summer conditions. The analysis for producing lowest possible evaporation temperature using aqua-ammonia absorption system have been conducted by Rogdakis & Antonopoulos [46]. They suggested two stage aqua-ammonia absorption system in which the high pressure condenser and medium pressure absorber rejects heat to the ambient while low pressure absorber rejects heat to the medium pressure evaporator. Their simulation results indicated the production of evaporation temperatures of about -70°C.

The costing analysis and optimization is another important topic in the analysis of aqua-ammonia absorption systems. In this regard, the sensitivity analysis over the total annual cost have been conducted by Bayramoglu & Bulgan [47] for aqua-ammonia

absorption system. They designed the major components of their system as shell and tube heat exchangers. Their analysis resulted in an optimized total annual cost for their system which is 4.6% lower than the conventional systems. The thermoeconomic optimization of such a system has been conducted by Misra et al. [48]. They developed a code for optimization of aqua-ammonia absorption system in which the thermodynamic properties of aqua-ammonia mixture were taken from the work of Ziegler & Trepp [49]. The iterative scheme used for the optimization resulted in an increase of about 44.2% & 44.6% in the COP and exergetic efficiency of the system respectively.

Apart from aqua-ammonia, the LiBr-water represents another commonly used refrigerant-absorbent working pair in the continuous operation based solar powered absorption refrigeration system [50]. Several simulation studies have been conducted in this regard using the simulation software such as FORTRAN, MATLAB, EES, ASPEN, TRANSYS, etc . One of the recent simulation study over this topic was performed by Gomri [51] using the mathematical code developed in FORTRAN simulation software. He compared performance of single effect and double effect absorption systems. His results indicated that the double effect systems have COP approximately double to that of single effect systems. His case study indicated a COP of 1.22-1.42 for the double effect systems where the single effect system could only reach a COP of 0.73-0.79 when operating under the same conditions. He also determined the optimum generator temperature for varying condenser and evaporator temperatures while keeping the exergy to its minimum. Onan et al. [52] utilized MATLab software to simulate the hourly performance of a 106 kW system in an environment where the ambient temperature varies from 40.3 °C to 13.2 °C. Their results indicated that the total exergy loss in the

collector ranges from 10-70% which is maximum compared to the other components of the solar powered LiBr-water system.

Somers et al. [53] compared the results of ASPEN simulation software to the EES software for the performance of solar powered LiBr-water system. They successfully modeled the single effect and double effect LiBr-water system using ASPEN and their results indicated an error of less than 3% & 5% respectively when compared to EES results. Cascales et al. [54] used artificial neural networks (ANN) to model a solar powered LiBr-water system. They trained and validated the ANN code using two years of experimental data. Their results indicated that ANN predicted approximately accurate absorber outlet and condenser outlet temperatures however the COP prediction was not accurate probably due to high anomalous experimental results.

Balghouthi et al. [55,56] used TRANSYS & EES to simulate the performance of solar powered LiBr-water system installed with a 800 litres hot water storage tank in Tunisia. Flat plate solar collectors were used with the collector area of 30 m^2 and tilted at an angle of 35°. The simulation results indicated a COP of 0.74 for their system. Ortiz et al. [57] also used TRANSYS to develop a numerical model to simulate the performance of solar powered LiBr-water system. Their simulation results indicated that such a system can reduce the total external cooling energy requirement by 33% to 43%. Eicker et al. [58] went through the dynamic simulation models for 15 kW single effect solar powered LiBr-water system. Their simulation results indicated a maximum primary energy ratio of 88% for solar fraction which is almost triple than the conventional electrical compression system. Recently Hong et al. [59] proposed an Evaporator-Absorber-Exchange (EAX) absorption cycle than can utilize the heat of condensation of the vapors generated from

the high temperature generator. Their simulation results indicated that the COP of such system is 40% higher than the conventional single effect cycle but lower than the conventional double effect cycle when operating between the generator temperature of 127.5 to 150 °C.

Kayankli & Kilic [60] performed a parametric study over the COP of the LiBr-water system for varying operating parameters. The results indicated that solution heat exchanger increases the COP by 44% compared to refrigerant heat exchanger which increases the COP by only 2.8%. Gomri [61] performed both the 1st law and 2nd law thermodynamic analysis of LiBr-water system for single effect, double effect and triple effect systems. His simulation results indicated that the maximum second law efficiency for single effect, double effect & triple effect systems are in the range of 0.125-0.232, 0.143-0.251 & 0.177-0.252 respectively. Kaushik & Arora [62] performed the 1st and 2nd law thermodynamic analysis of single effect and double effect LiBr-water system which is connected in series. Their 1st law analysis results indicate that the COP of series flow double effect system is 60 to 70% greater than the single effect system where the optimum COP is reached at 91°C for single effect and 150°C for double effect system. Similarly their 2nd law analysis results indicate that the optimum exergetic efficiency is reached at 80°C for single effect and 130°C for double effect system. Kilic & Kaynakli [63] also performed the 1st and 2nd law thermodynamic analysis of LiBr-water absorption chiller. Their results indicated that irrespective of the working conditions, the generator presents the highest exergy loss component i.e. 45.6% of the overall exergy loss in the chiller while the pump and refrigerant heat exchanger represents the lowest exergy loss component in the chiller.

Aside from purely aqua-ammonia or purely LiBr-water systems, Kouremenos et al. [64] developed a hybrid system in which both the aforementioned systems cooperate to produce a highly-efficient cooling with a theoretical COP upto 2.3. In their system, heat output from the aqua-ammonia system is used to power the LiBr-water system. Micallef & Micallef [65] also developed a mathematical model to solve the vapor absorption problems relating to aqua-ammonia or LiBr-water systems. Eicker & Pietruschka [66] performed the cost analysis of solar powered LiBr-water absorption system. Their cost analysis indicated that for long operation hours in Southern European locations, cooling costs are around 200 euros per MWh and about 280 euros per MWh for buildings with lower internal gains and shorter cooling periods. Florides et al. [67] simulated the performance of LiBr-water system equipped with $15m^2$ compound parabolic collector and a 600 litre hot water storage tank and performed the cost optimization for Cyprus. Their optimization results indicated a life cycle savings of C£1376 without subsidized fuel cost.

Farshi et al. [68] performed the exergoeconomic analysis of double effect absorption cooling system. Their analysis results indicated that lower cost are obtained at high evaporator and generator temperatures, low condenser temperature and low solution heat exchanger effectiveness. Koroneos et al. [69] performed the cost analysis of a 70 kW solar powered LiBr-water absorption chiller. Their analysis results indicated that the cost of such a system is 138,000 euros which is 107,640 euros higher than the cost of conventional system leading to a payback time of approximately 24 years.

Apart from aqua-ammonia & LiBr-water, some other refrigerant-absorbent working pairs have also been recently tested theoretically in the continuous operation

based solar powered absorption refrigeration system. In this regards, Abdulateef et al. [70] performed a comparative study between the performances of aqua-ammonia, lithium nitrate-ammonia and sodium thiocyanate-ammonia mixtures for absorption systems. Their results indicated that lithium nitrate-ammonia and sodium thiocyanate-ammonia mixtures gives better performance compared to aqua-ammonia mixture at temperatures below the freezing point of water; however above the freezing point of water aqua-ammonia has comparatively better performance than the other two. They also stated that lithium nitrate-ammonia and sodium thiocyanate-ammonia mixtures are simpler in operation because of no requirement of rectifier in their operation. Their results also indicated that sodium thiocyanate-ammonia mixture cannot operate below -10°C because of possibility of crystallization.

Saghiruddin & Siddiqui [71] simulated a two stage absorption system that operates on dual mixtures. They utilized LiBr-water for the first stage but analyzed the overall performance of the system by varying the mixture for the second stage. The mixtures used for the second stage were aqua-ammonia, lithium nitrate-ammonia and sodium thiocyanate-ammonia. Their results indicated that lithium nitrate-ammonia and sodium thiocyanate The mixtures used for the second stage were aqua-ammonia, lithium nitrate-ammonia and sodium thiocyanate-ammonia. Lithium nitrate-ammonia and sodium thiocyanate-ammonia required 20% and 45% high generator temperatures respectively compared to the aqua-ammonia system. Thus, based on the overall economic analysis of the absorption system, the authors concluded that the aqua-ammonia absorption system powered by flat plate solar collectors is the most economically feasible option. Medrano et al. [72] simulated double lift absorption system by comparing the aqua-ammonia

working mixture with TFE-TEGDME and methanol-TEDGME working mixtures. Their simulation results indicated that the COP of TFE-TEGDME and methanol-TEDGME is 0.45 which is almost 15% higher than aqua-ammonia. However, they reported that methanol-TEDGME has twice the circulation ratio compared to TFE-TEGDME. The authors therefore concluded that TFE-TEGDME is the best working pair.

Pilatowsky et al. [73] analyzed the monomethyleamine-water working pair for flat plate solar collectors powered absorption cooling system. Their simulation results indicated that a COP of 0.72 can be reached while operating the system at a generator temperature of 60°C producing cooling effect at 10°C. Fong et al. [74] optimized solar thermal refrigeration system working on LiCl-water mixtures. The optimization results indicated reduction in the primary energy consumption of 12.2% for LiCl-water systems. Crepinsek et al. [75] analyzed the performance of possible alternative working pairs for aqua-ammonia absorption system. Their simulation results indicated that for single effect cycles R124-DMEU, R125-DMEU, NH_3-$LiNO_3$ and NH_3-NaSCN represents the most suitable alternatives for aqua-ammonia whereas for half effect cycle, R134a-DMAC and TFE-TEGDME represents as the most suitable alternative working pairs for aqua-ammonia.

2.1.2 Experimental Studies

The experimental work conducted over the continuous operation based solar powered absorption refrigeration systems can also further be classified based on the refrigerant-absorbent working pair used. The most common working pairs are the aqua-ammonia and LiBr-water, however certain other working pairs have also been used in

simulating the performance of solar powered absorption refrigeration systems. Some of the recent developments regarding these will be reviewed in this section.

Brendel et al. [76] developed an experimental setup for small scale solar powered 10 kW aqua-ammonia absorption system. They used plate heat exchangers in the system except for generator which is fabricated as helical coil heat exchanger inside a cylindrical shell. They reported a COP of 0.58 to 0.74 for the absorption system to be operating at a generator temperature ranging from 80 to 120°C. Lostec et al. [77] also performed an experimental study of a 10 kW aqua-ammonia absorption system which uses water-ethylene glycol solution inside the cooling circuit and all heat exchangers were used as plate heat exchangers. They reported a COP of 0.6 when operated at the evaporator temperature of 16°C. Their results indicated a significant decrease in COP when decreasing the evaporator temperature. They reported that such an incompliance to the design specifications is mainly due to the overfeeding of the evaporator. This phenomenon was also observed by Albers & Ziegler [78] and Asdrubali & Grignaffini [79] at the increase of generator temperature.

Cerezo et al. [80,81] went through the mathematical modeling and experimental study of a bubble absorber constructed as a plate heat exchanger for aqua-ammonia absorption system. Their results indicated an increase in solution heat transfer and mass absorption flux with increasing absorber pressure while the solution concentration and temperature decreases with increasing absorber pressure. De-Francisco et al. [82] tested a prototype of a 2 kW solar powered aqua-ammonia absorption chiller that utilizes concentrating collectors and uses a transfer tank instead of a pump. Their experimentation resulted in a COP of 0.05 when the collectors operated at temperature

greater than 150°C. They suggested the inefficient operation of the transfer tank being responsible for such a low COP of their system. Boudéhenn et al. [83] developed a 5 kW solar powered aqua-ammonia absorption chiller. They constructed the chiller components using the industrially available brazed plate heat exchangers using 0.735 kg of water and 2.4 kg of ammonia. Their experimentation resulted in a COP of 0.65 however it was reported that their solution heat exchanger, which was designed to operate at 0.83 efficiency, was showing poor efficiency of 0.16.

Sohel & Dawoud [84] modeled an aqua-ammonia absorption system that utilizes a gravity assisted solution pump for its operation. They designed the solution pump as a hermetic vessel connected through vapor and liquid tubes between generator and absorber. Their study results indicated that the flow rate is independent of the diameter of the pump vessel whereas it depends over the diameter of the liquid tubes connecting absorber and generator such that doubling the diameter increases the flow rate by 323-400%. Abdulateef et al. [85] also performed an experimental investigation in Malaysia over the 1.5 ton solar powered aqua-ammonia absorption chiller. Their experimentation resulted in a maximum COP of 0.6 of the absorption chiller where most of the components of the chiller were constructed as shell & tube heat exchangers and $10m^2$ evacuated tube solar collectors used in the operation. Arias-Varela et al. [86] designed a solar powered aqua-ammonia absorption chiller to preserve sea food i.e. 200 kg of fish and economically analyzed the feasibility of the system. Their analysis results indicated that the payback time of the investment done over the absorption system is approximately 23 years. Their experimentation resulted in a COP of 0.426 for their system when operated at an evaporator temperature of -10°C.

Along with aqua-ammonia systems, much of the experimental work have also been conducted over LiBr-water systems [87]. Agyemin et al. [88] performed the experimental analysis of a domestic-scale 4.5 kW solar powered LiBr-water absorption system equipped with a 1000 litres cold storage. Vacuum tube solar collectors were used with the collector area of 12 m^2 in the experiment. The experimental results indicated a COP of 0.58 while producing the chilled water at a temperature of 7.4°C in the cold storage. Balghouthi et al. [89] installed and tested the performance of 16 kW double effect LiBr-water absorption system in Tunisia. Their system utilizes parabolic trough collectors for the operation and was equipped with tanks for storage and drain-back storage. Their experimentation resulted in a COP ranging from 0.8 to 0.91 with the maximum output of 12 kW from the absorption chiller at 8°C in the evaporator. Their results also indicated an energy saving of 1154 liters of gasoline using the absorption chiller.

Darkwa et al. [90] performed the experimental analysis of a LiBr-water absorption system powered by evacuated tubular and flat plate solar collectors and integrated with four hot water storage tanks. Their experimental results indicated that a COP of 0.69 could be achieved when supplied by the heated water at 96.3°C by the solar collectors. Hu et al. [91] performed an experimental study of a 40 W micro absorption heat pump. The absorption system was constructed of micro-evaporator, micro-condenser, expansion channel. They reported an experimental COP ranging from 0.465 to 0.511 when operating at a generator temperature of 100°C while producing an evaporation at a temperature ranging from 11 to 19°C. Bermejo et al. [92] developed a 174 kW gas/solar powered double effect LiBr-water absorption chiller in Spain using 352

m^2 linear concentrating Fresnel collectors. Their experimentation results indicated the solar energy contributed 75% of the total heat input to the generator producing a COP of 1.1-1.25 when operated at the evaporator temperature of 8°C.

Similarly, another experimental setup was established in Reunion Island by Praene et al. [93] of 30 kW solar powered LiBr-water absorption refrigeration system. Their installed system consists of 90 m^2 double glazed flat plate solar collectors and equipped with hot and cold water storages of 1500 & 1000 litres respectively. The economic analysis of their experimental setup indicated that the solar collector field contributes to more than 57% of the overall capital cost of the absorption system. Sumathy et al. [94] developed a 100 kW double stage solar powered LiBr-water absorption chiller in south China. Their experimental test results indicated that their system could be operated at the generator temperature ranging from 60 to 75°C. The economic analysis over the experimental setup also revealed that the double stage systems are 50% cheaper than the single stage systems when operating roughly at the same COP.

Apart from aqua-ammonia and LiBr-water, certain other absorbent-refrigerant working pairs have also been utilized in the experimental investigation of solar powered absorption refrigeration systems. Zhu et al. [95] performed an experimental investigation over the solar powered absorption refrigeration system that uses sodium thiocyanate-ammonia ($NaSCN-NH_3$) as the working mixture. The experimental results indicated that such a system could be operated at comparatively lower generator and evaporator temperatures and at higher COP than the conventional systems. Thus, if the generator outlet temperature is below 58°C while the condenser and absorber temperature is 15°C

and evaporator temperature being -20°C, the system COP will be close to zero i.e. the system does not work at all. From 58 to 75°C, the COP increases rapidly; after the generator outlet temperature of 80°C, the COP will increase in a comparatively slower pace.

2.2 Intermittent Operation Systems

The intermittent operation systems belongs to a specific classification of absorption refrigeration system in which both the generation and absorption processes do not take place simultaneously rather they follow each other in an intermittent manner. Because of the intermittent nature, it is possible to utilize the aqua-ammonia vessel to behave as a generator during the daytime while behaving as an absorber during the night time. Such systems operate in a cyclic behavior with a cycle time of one complete day (24 hours). The pressurization process in the intermittent operation systems is carried out by isochoric heating of the aqua-ammonia solution in the generator. In this way, electrical energy is not required at all in the operation of intermittent absorption systems. Hence such systems significantly helps in reducing the fossil fuel consumption.

2.2.1 Simulation Studies

The simulation work conducted over the intermittent operation based solar powered absorption refrigeration systems can further be classified based on the refrigerant-absorbent working pair used. The most common working pair is the aqua-ammonia however certain other working pairs have also been used in simulating the performance of solar powered absorption refrigeration systems. The aqua-ammonia represents the most commonly used refrigerant-absorbent working pair in the intermittent operation based solar powered absorption refrigeration system. El-Shaarawi & Ramadan

[96] investigated the performance of solar powered intermittent aqua-ammonia absorption system under varying condenser temperature. They reported that decreasing the condenser temperature at any fixed initial solution concentration and temperature results in an increase in the COP of the system. Their simulation results also indicated that there exist an optimum generator temperature for achieving maximum COP at a specified condenser temperature [97]. In another research, the same group of authors also showed that the temperature of the condensate at the beginning of the aqua-ammonia absorption process has considerable influence on the performance of intermittent solar refrigerators [98].

A theoretical simulation have also been conducted by Said et al. [28] over intermittent solar absorption system designed to provide 120 kW-hr of cooling effect throughout the day and night operation. Their simulation results indicated that the intermittent absorption system can achieve a COP of 0.23 when operating at the generator temperature of 120°C while producing cooling effect at a temperature of -9°C. Recently El-Shaarawi et al. [99] went through the comparative analysis between constant pressure and constant temperature absorption processes in an intermittent solar absorption system. The results of their simulation indicated that the COP of constant pressure absorption is 20% higher than the COP of constant temperature absorption processes. Their simulation results also indicated that the optimum generator temperature for constant pressure absorption is approximately 12% higher than the constant temperature absorption process.

El-Shaarawi et al. [100] recently also developed simplified correlation for aqua-ammonia intermittent solar powered absorption refrigeration system. They developed a

set of polynomial form of correlations for directly estimating the performance of intermittent absorption systems as a function of generator, absorber, condenser and evaporator temperatures. They reported that their developed correlation estimate the design parameters of intermittent absorption refrigeration systems with an accuracy of greater than 97%. Recently Said et al. [101] also modified the design of conventional intermittent absorption system by introducing an economizer in the design. The economizer behaves as a waste energy storage and helps in the recovery of waste energy from the system. The simulation results of their modified design indicated an increase of 20% in the coefficient of performance of the intermittent absorption system using the economizer.

Fong et al. [74] optimized solar thermal adsorption refrigeration system working on Silica Gel-water mixtures. The optimization results indicated reduction in the primary energy consumption of 7.1% for Silica Gel-water systems. They recommended the sizing of ΔT = 6°C & ΔT = 4-4.5°C of the cooling water pump and chilled water pump respectively for such systems. Rivera & Rivera [102] simulated the performance of a solar powered intermittent absorption refrigeration chiller with lithium nitrate-ammonia as the working mixture for Mexico. They used compound parabolic concentrator with glass cover for powering their system with solar energy while behaving as the generator/absorber for the system. They reported that the lithium nitrate-ammonia system do not require rectifier because of non-volatile nature of the lithium nitrate absorbent. The results of their simulation indicated that 11.8 kg of ice could be produced at a COP ranging from 0.15 to 0.4 when operating at the generator temperature of 120°C.

2.2.2 Experimental Studies

The experimental work conducted over the intermittent operation based solar powered absorption refrigeration systems can also further be classified based on the refrigerant-absorbent working pair used. The most common working pair is again the aqua-ammonia however certain other working pairs have also been used in simulating the performance of solar powered absorption refrigeration systems. Some of the recent developments regarding these will be reviewed in this section.

El-Shaarawi and Ramadan [103] developed an experimental setup for testing intermittently operating solar powered aqua-ammonia refrigeration system in the Egyptian climate. Although the experimental setup was designed to produce cooling effect at around -13°C, however, the experimental results indicated a COP of 0.5 when producing cooling effect at an evaporator temperature of -2°C. They investigated the reason for low performance of the system claiming that it was found difficult to prevent water from being transferred into condenser. They suggested that the rectifier needs to be re-designed for efficient performance in refrigeration applications.

El-Ghalban [104] constructed a prototype for intermittently operating 20 W solar powered absorption refrigeration system working on lithium chloride-water mixture. The results of the experimentation indicated a COP of 0.19 which was 2% less than the theoretical design of the model. It was reported that the intermittent system completed its cycle in around 8 hours approximately. The system operated at a generator temperature of 70°C with a condensation temperature of 40°C producing the cooling load at an evaporator temperature of 10°C.

Hernandez et al. [105] used the experimental results for the intermittently operating solar powered absorption refrigeration system working with lithium nitrate-ammonia mixture to predict the performance using direct and inverse artificial neural network. The results for the sensitivity analysis of their system indicated that generation pressure is the most significant variable that affects the performance of such a system. They also showed that it's possible to use inverse artificial neural networks to predict the input parameters for achieving a specific desired COP of the system.

Rasul & Murphy [106] constructed a prototype for intermittently operating absorption refrigeration system powered by parabolic solar trough working on calcium chloride-ammonia mixture. They reported that during the first run, the system operated at a COP of 0.65 however for the second run the system operated at a very low COP of 0.26 with evaporator temperature around 17°C. They attributed the low COP of the system towards less affinity of ammonia for calcium chloride compared to water. They recommended re-designing of the absorber proper absorption of ammonia in calcium chloride. A summary of the recent work done over solar powered absorption refrigeration system is shown in Table 2-1.

Table 2-1 Summary of recent work done over Solar Powered Absorption Refrigeration Systems

Reference	Research type	Working Pair	Type of Operation	Cooling Load	Temperatures (°C)				Operating Pressure	COP	Features/Results
					Generator	Absorber	Condenser	Evaporator			
Raghuvanshi & Maheshwari [27] (2011)	Simulation (MATLAB)	Aqua-Ammonia	Continuous Operation	62.7 kW	50	20	50	2.5	20.33 bar	0.227	First Law Analysis was conducted An energy analysis of each component has been carried out and numerical results for the cycle are tabulated Emperical Correlations for evaluating the thermodynamic properties of aqua-ammonia have been used
Said et al. [28] (2012)	Simulation (EES)	Aqua-Ammonia	Continuous Operation & Intermittent Operation	5 kW for 24 hrs i.e. 120 kW-hr	120	45	45	-9		0.427 (Continuous Operation) 0.23 (Intermittent Operation)	Comparison of refrigerant storage system done with heat and cold storage systems First Law Analysis was conducted Analysis was conducted for 120 kW-hr cooling load for the 24 hour period
Darwish et al. [29] (2008)	Simulation (ASPEN)	Aqua-Ammonia	Continuous Operation	10 kW	166	40	40	-7	15.55 bar	0.45	Experimental Validation of the simulation was provided Maximum deviation of 1.8% from the experimental results Used seperator at the top of rectifying column Showed 15-20% increase in COP using a seperator
Sencan [32,33] (2006,2007)	Simulation (Artificial Neural Networks)	Aqua-Ammonia	Continuous Operation		60-90	20-40	20-40	2.5-7.5		0.67-0.81	Developed new formulation independent of dedicated ANN software Compared their results with the linear regression and M5' Rules models Obtained correlation coefficient of 0.9996 & 0.9873 for circulation ratio and COP respectively Showed that ANN gives the best results
Bangotra & Mahajan [35] (2012)	Simulation	Aqua-Ammonia	Continuous Operation	10.548 kW	120	52	54	2	10.7 bar	0.2079	Analyzed basic absorption refrigeration system Performed first law thermodynamic analysis Determined UA values for the different components of the system

Reference	Research type	Working Pair	Type of Operation	Cooling Load	Temperatures (°C)				Operating Pressure	COP	Features/Results
					Generator	Absorber	Condenser	Evaporator			
Lavanya & Murthy [36] (2013)	Simulation	Aqua-Ammonia	Continuous Operation	116.9 W	90	28	34	-18	14 bar	0.6	Analyzed advanced absorption refrigeration system Performed first law thermodynamic analysis for 200 litre Capacity solar water cooler Determined UA & LMTD values for the different components of the system
Chua et al. [38] (2002)	Simulation	Aqua-Ammonia	Continuous Operation	6.17 kW	145	45	51	3.5	20.7 bar	0.519	Performed first and second law thermodynamic analysis 30% of thermal energy dissipation within the rectifier and the regenrative heat exchanger 6% & 3% energy dissipation by liquid and vapor phases respectively in the absorber
Lostec et al. [39] (2010)	Simulation	Aqua-Ammonia	Continuous Operation	3 kW	72	17	17	-11	8 bar	0.69	Performed first and second law thermodynamic analysis Results indicated the presence of three optimum values of COP 0.56, 0.62 & 0.69 for the absorption system that minimizes UA value, irreversibility and exergetic efficiency respectively Results also showed that all of these three optimum COP values are lower than the maximum COP value Results indicated that 33% and 34% of the exergy destruction takes place inside the absorber and desorber of the absorption system respectively
Caciula et al. [40] (2013)	Simulation	Aqua-Ammonia	Continuous Operation	100 kW	70-150	30	30	-3 to 6		0.6-0.73	Performed first and second law thermodynamic analysis Utilized compund parabolic collectors Results indicated variation in exergetic efficiency from 0.12 to 0.22
Cai et al. [41] (2010)	Simulation (Dynamic)	Aqua-Ammonia	Continuous Operation	1109 kW	100	30	40	10	15.6 bar	0.642	performed the lumped-parameter dynamic simulation Transient response for step parameter change of one percent pressure rise is analyzed in the system Results indicated an oscillation in time before reaching steady state

Reference	Research type	Working Pair	Type of Operation	Cooling Load	Temperatures (°C)				Operating Pressure	COP	Features/Results
					Generator	Absorber	Condenser	Evaporator			
Kim & Park [42] (2007)	Simulation (Dynamic)	Aqua-Ammonia	Continuous Operation	10.5 kW	165	58.6	54.5	4.8	21.68 bar	0.557	Time constant of the system decreases with the increase of ammonia concentration of the strong solution An optimum volume of generator and optimum mass & concentration of strong solution exist for achieving maximum cooling capacity Stepwise turnup and turndown is recommended for decreasing the time constant of the system
Kim et al. [43] (2003)	Simulation (Dynamic)	Aqua-Ammonia	Continuous Operation	10 kW	120	30	30	12.5	17.5 bar		Dynamic Model developed to simulate the chiller's transient behavior The model predicted that the chiller would react quite sensitively to some design and operation parameters Heat loss to the environment was neglected in the analysis High concentration of refrigerant in the system was shown to deteriorate the performance by increasing the system pressures
Ozgoren et al. [44] (2012)	Simulation (Dynamic)	Aqua-Ammonia	Continuous Operation	3.5 kW	110	36-52	36-52	10		0.243-0.454 (for cooling) 1.243-1.454 (for heating)	Hourly performance was predicted for Adana Province, Turkey Analysis was conducted for July 29 Evacuated tubular collectors used for the analysis Maximum Solar collector efficiency was found to be 0.784 Calculated collector area was 35.95 sq.m
Lin et al. [45] (2011)	Simulation	Aqua-Ammonia	Continuous Operation	5 kW	80	46 (low pressure) 50 (medium	42	10	16.5 bar	0.34 (thermal) 26 (electrical)	Analysis was conducted for two stage system Direct air cooling of absorber and condenser Tested several air cooling sequence
Rogdakis & Antonopoulos [46] (1992)	Simulation	Aqua-Ammonia	Continuous Operation	300 - 1100 kJ/kg	130 to 180	15 to 35	10 to 30	-70 to -30	15 bar	0.2-0.65	Analysis was conducted for two stage system high pressure condenser and medium pressure absorber rejects heat to the ambient low pressure absorber rejects heat to the medium pressure evaporator

Reference	Research type	Working Pair	Type of Operation	Cooling Load	Temperatures (°C)				Operating Pressure	COP	Features/Results
					Generator	Absorber	Condenser	Evaporator			
Bayramoglu & Bulgan [47] (1995)	Simulation	Aqua-Ammonia	Continuous Operation	1000 kW	110 (Heat Source Temperature)	25 (Cooling Water Temp)	25 (Cooling Water Temp)	-5			Performed sensitivity analysis over the total annual cost Major components are designed as shell and tube heat exchangers Optimized total annual cost is 4.6% lower than the conventional systems.
Misra et al. [48] (2006)	Simulation	Aqua-Ammonia	Continuous Operation		155	33.75	37	7.5	15.64 bar	0.25	Thermoeconomic optimization has been carried out Both 1st and 2nd law analysis have been carried out Simulation resulted in an increase of about 44.2% & 44.6% in the COP and exergetic efficiency of the system respectively
Gomri [51,61] (2009,2010)	Simulation (Fortran)	LiBr-water	Continuous Operation	300 kW	60 to 190	33 to 39	33 to 39	04 to 10		0.73 to 0.79 (single effect) 1.22 to 1.42 (double effect) 1.62 to 1.90 (triple effect)	Performed both the 1st and 2nd law thermodynamic analysis Compared performance of single effect, double effect and triple effect absorption systems Determined the optimum generator temperature for varying condenser and evaporator temperatures while keeping the exergy to its minimum Maximum second law efficiency for single effect, double effect & triple effect systems are in the range of 0.125-0.232, 0.143-0.251 & 0.177-0.252 respectively.
Onan et al. [52] (2010)	Simulation (MatLAB)	LiBr-water	Continuous Operation	106 kW	80.039	39.6	38.28	6	0.06776 bar	0.7	Ambient temperature varies from 40.3 °C to 13.2 °C Total exergy loss in the collector ranges from 10-70% which is maximum compared to the other components of the solar powered LiBr-water system.

Reference	Research type	Working Pair	Type of Operation	Cooling Load	Temperatures (°C)				Operating Pressure	COP	Features/Results
					Generator	Absorber	Condenser	Evaporator			
Somers et al. [53] (2011)	Simulation (EES & ASPEN)	LiBr-water	Continuous Operation	10.772 kW	89.9	32.7	40.2	1.3	0.07445 bar	0.738 (ASPEN)	Compared the results of ASPEN simulation software to the EES software
											Modeled the single effect and double effect LiBr-water system
										0.72 (EES)	Single effect and double effect simultion results indicated an error of less than 3% & 5% respectively
Balghouthi et al. [55,56] (2005,2008)	Simulation (TRANSYS)	LiBr-water	Continuous Operation	11.31 kW	84.6	36.2	38	5.5	0.06601 bar	0.74	Installed with a 800 litres hot water storage tank in Tunisia
											Flat plate solar collectors were used with the collector area of 30 m2 and tilted at an angle of 35°.
Hong et al. [59] (2011)	Simulation	LiBr-water	Continuous Operation		95 (Single Effect	40	40	5		0.76 (Single Effect)	Proposed an Evaporator-Absorber-Exchange (EAX) absorption cycle
											Can utilize the heat of condensation of the vapors generated from the high temperature generator
					160 (Double Effect)					1.29 (Double Effect)	COP is 40% higher than the conventional single effect cycle
Kaynakli & Kilic [60] (2007)	Simulation	LiBr-water	Continuous Operation	2400 kJ/kg	81 to 104	40	40	5		0.2 to 0.7	Performed a parametric study over the COP of the LiBr-water system for varying operating parameters
											Results indicated that solution heat exchanger increases the COP by 44% compared to refrigerant heat exchanger which increases the COP by only 2.8%.
Kaushik & Arora [62] (2009)	Simulation (EES)	LiBr-water	Continuous Operation	2355.45 kW	87.8 (single effect)	37.8	37.8	7.2		0.6 to 0.75 (single effect)	Performed the 1st and 2nd law thermodynamic analysis of single effect and double effect LiBr-water system
					140.6 (series flow double effect)					1 to 1.28 (series flow double effect)	1st law analysis results indicate that the COP of series flow double effect system is 60 to 70% greater than the single effect system
											2nd law analysis results indicate that the optimum exergetic efficiency is reached at 80°C for single effect and 130°C for double effect system

Reference	Research type	Working Pair	Type of Operation	Cooling Load	Temperatures (°C)				Operating Pressure	COP	Features/Results
					Generator	Absorber	Condenser	Evaporator			
Kilic & Kaynakli [63] (2007)	Simulation	LiBr-water	Continuous Operation	10 kW	90	40	35	5		0.77	1st and 2nd law thermodynamic analysis of LiBr-water absorption chiller The generator presents the highest exergy loss component i.e. 45.6% of the overall exergy loss in the chiller The pump and refrigerant heat exchanger represents the lowest exergy loss component in the chiller
Kouremenos et al. [64] (1989)	Simulation	Aqua-Ammonia & LiBr-water	Continuous Operation	3597 to 4563 kJ/kg NH3	56 to 76 (LiBr-water) 156 to 211 (Aqua-ammonia)	30 to 35 (LiBr-water) 71 to 81 (Aqua-ammonia)	30 to 35 (LiBr-water) 71 to 108 (Aqua-ammonia)	6.3 to 7.5 (LiBr-water) 3.3 to 4.5 (Aqua-ammonia)	32 to 42 torr (LiBr-water) 33 to 41 bar (Aqua-ammonia)	0.88 to 0.91 (LiBr-water) 0.41 to 0.61 (Aqua-ammonia)	Developed a hybrid system in which both the Aqua-ammonia and LiBr-water systems cooperate to produce a highly-efficient cooling with a theoretical combined COP upto 2.3 Heat output from the aqua-ammonia system is used to power the LiBr-water system
Abdulateef et al. [70] (2008)	Simulation	Aqua-Ammonia	Continuous Operation		90	25	25	-5		0.606 (Aqua-ammonia)	lithium nitrate-ammonia and sodium thiocyanate-ammonia mixtures gives better performance compared to aqua-ammonia mixture at temperatures below the freezing point of water
		Lithium nitrate-ammonia								0.61 (Lithium nitrate-ammonia)	above the freezing point of water aqua-ammonia has comparatively better performance than the other two
		Sodium thiocyanate-ammonia								0.65 (Sodium thiocyanate-ammonia)	results also indicated that sodium thiocyanate-ammonia mixture cannot operate below -10°C because of possibility of crystallization.
Saghiruddin & Siddiqui [71] (2001)	Simulation	Aqua-Ammonia	Continuous Operation	3.5 kW	35 to 150	25 to 45 (first stage) 10 (second stage)	25 to 45 (first stage) 25 to 45 (second stage)	5 (first stage) 0 to -60 (second stage)			simulated a two stage absorption system that operates on dual mixtures utilized LiBr-water for the first stage
		Lithium nitrate-ammonia									The mixtures used for the second stage were aqua-ammonia, lithium nitrate-ammonia and sodium thiocyanate-ammonia
		Sodium thiocyanate-ammonia									aqua-ammonia absorption system powered by flat plate solar collectors is the most economically feasible option

Reference	Research type	Working Pair	Type of Operation	Cooling Load	Temperatures (°C)				Operating Pressure	COP	Features/Results
					Generator	Absorber	Condenser	Evaporator			
Medrano et al. [72] (2001)	Simulation	TFE-TEGDME	Continuous Operation		105	35 to 45	35 to 45	-5 to -10		0.45 (TFE-TEGDME)	simulated double lift absorption system
		Methanol-TEGDME								0.45 (Methanol-TEGDME)	COP of TFE-TEGDME and methanol-TEDGME is 0.45 which is almost 15% higher than aqua-ammonia
		Aqua-ammonia								0.3825 (Aqua-Ammonia)	methanol-TEDGME has twice the circulation ratio compared to TFE-TEGDME
											TFE-TEGDME is the best working pair
Pilatowsky et al. [73] (2001)	Simulation	Monomethyl eamine-water	Continuous Operation		60 to 80	25 to 35	25 to 35	-10 to 10		0.1 to 0.7	Used flat plate solar collectors powered absorption cooling system
											Performed the 1st law thermodynamic analysis
Brendel et al. [76] (2010)	Experimental	Aqua-Ammonia	Continuous Operation	10 kW	80 to 120	30 to 45	30 to 45	5 to 15	13 to 18 bar	0.58 to 0.74	Developed an experimental setup
											Used plate heat exchangers for all components except generator
											Generatorfabricated as helical coil heat exhanger in a cylindrical shell
Lostec et al. [77] (2012)	Experimental	Aqua-Ammonia	Continuous Operation	10 kW	68 to 75	24 to 29	24 to 29	16 to 19	13 bar	0.6	all heat exchangers were used as plate heat exchangers
											Their results indicated a significant decrease in COP when decreasing the evaporator temperature
											They reported overfeeding of the evaporator causing drop in COP of the system
De-Francisco et al. [82] (2002)	Experimental	Aqua-Ammonia	Continuous Operation	2 kW	150		35	10		0.05	Absorption chiller utilizes concentrating collectors and uses a transfer tank instead of a pump
											They suggested the inefficient operation of the transfer tank being responsible for such a low COP of their system
Boudéhenn et al. [83] (2012)	Experimental	Aqua-Ammonia	Continuous Operation	4.2 kW	80	27	27	18		0.65	chiller components were constructed using the industrially available brazed plate heat exchangers
											Their system uses 0.735 kg of water and 2.4 kg of ammonia
											They reported poor operation of solution heat exchanger in their system

Reference	Research type	Working Pair	Type of Operation	Cooling Load	Temperatures (°C)				Operating Pressure	COP	Features/Results
					Generator	Absorber	Condenser	Evaporator			
Abdulateef et al. [85] (2010)	Experimental	Aqua-Ammonia	Continuous Operation	1.5 ton	60 to 98	23 to 39	23 to 39	3 to 16		0.6	most of the components of the chiller were constructed as shell & tube heat exchangers 10m2 evacuated tube solar collectors used in the operation
Arias-Varela et al. [86] (2000)	Experimental	Aqua-Ammonia	Continuous Operation	2 kW	106	34	34	-10	13.4 atm	0.426	economically analyzed the feasibility of the system analysis results indicated that the payback time of approximately 23 years for the chiller
Agyenim et al. [88] (2010)	Experimental	LiBr-water	Continuous Operation	4.5 kW	75-92	24	24	7.4		0.58	The system was equipped with 1000 litres of cold storage water Vacuum tube solar collectors were used with the collector area of 12 m2
Balghouthi et al. [89] (2012)	Experimental	LiBr-water	Continuous Operation	12 kW	165	35	35	8		0.8 to 0.91	double effect LiBr-water absorption system was tested in Tunisia Their system utilizes parabolic trough collectors for the operation Equipped with tanks for storage and drain-back storage Their results also indicated an energy saving of 1154 litres of gasoline using the absorption chiller
Darkwa et al. [90] (2012)	Experimental	LiBr-water	Continuous Operation		91			12.2		0.69	Performed analysis of an absorption system powered by evacuated tubular and flat plate solar collectors Their system was also integrated with four hot water storage tanks
Hu & Chao [91] (2008)	Experimental	LiBr-water	Continuous Operation	40 W	100	30	39 to 50	11 to 19		0.465 to 0.511	Performed an experimental study of micro absorption heat pump The absorption system was constructed of micro-evaporator, micro-condenser, expansion channel
Bermejo et al. [92] (2010)	Experimental	LiBr-water	Continuous Operation	174 kW	145	36	36	8		1.1 to 1.25	Developed a gas/solar powered double effect LiBr-water absorption chiller in Spain Used 352 m2 linear concentrating Fresnel collectors

Reference	Research type	Working Pair	Type of Operation	Cooling Load	Temperatures (°C)				Operating Pressure	COP	Features/Results
					Generator	Absorber	Condenser	Evaporator			
Sumathy et al. [94] (2002)	Experimental	LiBr-water	Continuous Operation	100 kW	65 to 80	32	32	9		0.31 to 0.39	Developed a double stage solar powered absorption chiller in south China Double stage systems are 50% cheaper than the single stage systems when operating roughly at the same COP.
Zhu et al. [95] (2008)	Experimental	Sodium thiocyanate-ammonia	Continuous Operation	1 kW	80	15	15	-20		0.55	The experimental results indicated that such a system could be operated at comparatively lower generator and evaporator temperatures and at higher COP than the conventional systems
Rivera & Rivera [102] (2003)	Simulation	Lithium Nitrate-Ammonia	Intermittent Operation	11.8 kg of ice	120	40 to 44	40 to 44	Less than 0		0.15 to 0.4	They used compound parabolic concentrator with glass cover They reported that the lithium nitrate-ammonia system do not require rectifier because of non-volatile nature of the lithium nitrate absorbent
El-Shaarawi & Ramadan [103] (1986)	Experimental	Aqua-Ammonia	Intermittent Operation	700 to 760 kcal	85 to 95	30	30	-2 to 4	12.3 to 14.9 atm	0.495 to 0.513	Designed to produce cooling effect at around -13°C, however, experimentally reached an evaporator temperature of -2°C only it was found difficult to prevent water from being transferred into condenser They suggested that the rectifier needs to be re-designed for efficient performance
El-Ghalban [104] (2002)	Experimental	Lithium Chloride-water	Intermittent Operation	20 W	70	40	40	10		0.19	The results of the experimentation indicated a COP of 0.19 which was 2% less than the theoretical design of the model.
Rasul & Murphy [106] (2006)	Experimental	Calcium Chloride-Ammonia	Intermittent Operation	0.08 to 0.204 kW	130	20 to 30	20 to 30	1 to 20		0.26 to 0.65	Their absorption refrigeration system was powered by parabolic solar trough They attributed the low COP of the system towards less affinity of ammonia for calcium chloride compared to water They recommended re-designing of the absorber for proper absorption of ammonia in calcium chloride.

The thermodynamic properties of the absorbent-refrigerant working pair is the most important factor in analyzing and optimizing the performance of the absorption systems. Aqua-Ammonia is one of the most widely used absorbent-refrigerant working pair in absorption systems. In this regard, a generalized equation of state based on a four-parameter corresponding states principle have been utilized by Park & Sonntag [107] to determine the thermodynamic properties of aqua-ammonia mixtures. Their work was basically an extension to the work done by IGT (Institute of Gas Technology) [108] to cover the operating range of power cycles as well. Later Ibrahim & Klein [109] utilized Gibbs excess energy to estimate the VLE thermodynamic properties of aqua-ammonia mixtures. Another approach was utilized by Patek & Klomfar [110] in this regard. They developed the thermodynamic property correlations by fitting experimental data using simple functional forms. Tillner-Roth & Friend [111] utilized the approach of Helmholtz free energy for developing the correlations estimating the VLE thermodynamic properties of aqua-ammonia mixtures. Although equations developed utilizing Gibbs excess energy and Helmholtz free energy were implicit in nature, yet, they were utilized in a software of Engineering Equation Solver (EES) [112] to facilitate the users of directly estimating the thermodynamic properties. Recently, El-Shaarawi et al. [113] utilized EES to develop polynomial forms of explicitly defined thermodynamic property correlations that can be utilized by any simulation software. They also reported a comparison of their work with other reported literatures [107,109,110,111] and reported that their work is in an excellent agreement with those of Ibrahim & Klein [109]. The working temperature and pressure range of the VLE thermodynamic properties of aqua-ammonia working mixtures is listed in Table 2-2.

Table 2-2 Summary of working temperature and pressure ranges

Methodology Utilized	Year	Working Range		Reference
		Temperature [C]	Pressure [bar]	
Generalized Equation of State	*1990*	*upto 377*	*upto 200*	[107]
Gibbs Excess Energy	*1993*	*upto 327*	*upto 110*	[109]
Simple Functional Form	*1995*	*upto 180*	*upto 20*	[110]
Helmholtz Free Energy	*1998*		*upto 400*	[111]
Polynomial Form of Equations	*2013*		*upto 100*	[113]

Based on the intensive literature review, the following conclusions can be made:-

- ✓ Absorption refrigeration system is the most suitable option to be powered by solar energy.
- ✓ Aqua-Ammonia presents so far best proven absorbent-refrigerant working pair.
- ✓ Intermittent systems have very less coefficient of performance and very large size.
- ✓ Gibbs excess energy presents the best property correlation for aqua-ammonia.
- ✓ Several theoretical researches have been conducted on conventional absorption systems.
- ✓ Several experimental researches have also been conducted on conventional absorption systems.
- ✓ Solar collectors presents the most expensive component of absorption cooling system.

Hence, there is still a need to improve the efficiency of solar powered continuous operation based aqua-ammonia vapor absorption refrigeration & air-conditioning systems.

CHAPTER 3

OBJECTIVES AND METHODOLOGY

After going through the detailed literature review in Chapter 2, this chapter deals with the problem definition of this dissertation. The problem definition is followed by the objectives of this dissertation which is further followed by the description of methodology adopted to solve the problem.

3.1 Problem Definition

The aim of this dissertation is to modify the design of a conventional aqua-ammonia vapor absorption system to make it comparatively more energy efficient. Thus, for defining the problem, firstly it is important to understand a typical aqua-ammonia vapor absorption system. A typical aqua-ammonia vapor absorption system can be subdivided into basic components and non-basic components. Basic components are those components which are necessary for the operation of the refrigeration system i.e. without it the refrigeration system will not function at all. However, the non-basic components are those components which are not essential for the operation of the refrigeration system, although their presence may substantially improve the performance of the system. Figure 3-1 distinguishes between the basic components and non-basic components of a typical aqua-ammonia vapor absorption refrigeration system.

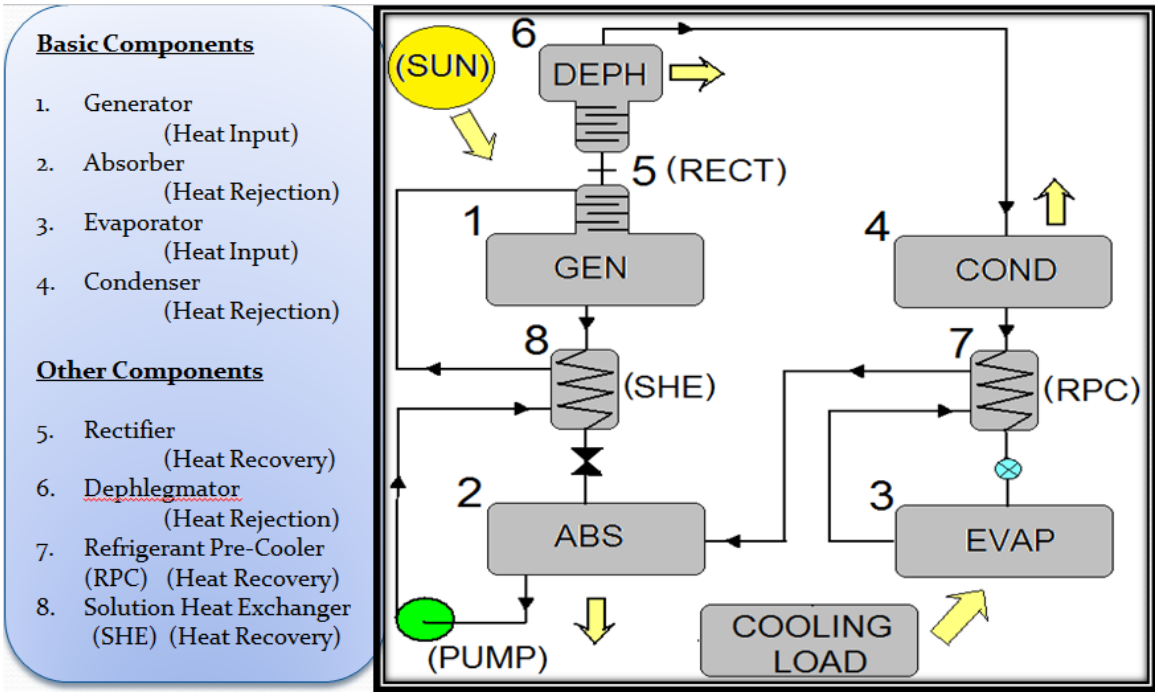

Figure 3-1 Typical Solar powered Aqua-Ammonia Absorption System

It can be seen from figure 3-1 that there are essentially four basic components of the aqua-ammonia absorption system i.e. generator, absorber, condenser and evaporator and there are four non-basic components of the absorption systems i.e. rectifier, dephlegmator, refrigerant pre-cooler and solution heat exchanger. A pump is also one of the basic components for continuous operation systems however for intermittent systems, a solution pump is not needed for the operation of the cooling system, therefore pump is not included in the list of basic components for aqua-ammonia absorption system.

These eight components of the aqua-ammonia absorption systems can also be classified in term of heat input, heat rejection and heat recovery components. It can also be seen from figure 3-1 that both generator and evaporator acts as the heat input components for the absorption chiller. Similarly there are a total of three heat rejection components in a typical aqua-ammonia absorption system i.e. absorber, condenser and dephlegmator. Also, there are a total of three heat recovery components in a typical aqua-ammonia absorption system. These are rectifier, solution heat exchanger and refrigerant pre-cooler.

The overall efficiency of an absorption system depends upon the amount of heat recovery from the heat recovery components. Hence the coefficient of performance of a cooling system is a direct function of overall heat recovery within the absorption system. Conventionally dephlegmator is used as a heat rejection component, however, recovering heat from the dephlegmator will increase the overall heat recovery from the system. Thus, the higher the heat recovery, the higher will be the coefficient of performance of the absorption system. This will result in the reduction of overall solar collector area requirement for a specific cooling load. The reduction in solar collector area will reduce

the capital cost of such systems as solar collectors present the most expensive component in such systems. Hence, one of the aim of this dissertation is to improve the performance of conventional absorption systems by utilizing heat rejection from the dephlegmator.

The coefficient of performance of absorption systems, also depends upon the high and low ammonia mass concentration. The high concentration of ammonia in the absorption system is further a function of absorber temperature which in itself is a function of ambient temperature. Since, the design of any specific cooling system is based upon the yearly local average high ambient temperature, this limits the total amount of refrigerant introduced in the absorption system. The limitation of the total amount of refrigerant in an absorption system limits the high ammonia mass concentration within such systems.

Due to the variation of ambient conditions throughout the year, more than 75% of the time, the absorption chiller operates at ambient temperatures lower than the design temperature. Therefore theoretically, the absorption system should operate at a much higher coefficient of performance than the design coefficient of performance for more than 75% of the year. However due to the limitation of total amount of refrigerant in the system, the coefficient of performance do not increase as expected at lower ambient temperatures. In other words, due to limited amount of refrigerant in the system, the absorption system does not operate at full cooling capacity. Hence the limited amount of refrigerant in the system makes the system inflexible to the change of ambient conditions. An inclusion of a refrigerant storage unit will remove this limitation of the conventional absorption systems. Hence, another aim of this dissertation is to improve the performance

of conventional absorption systems by introducing an ammonia storage in the design of the system.

3.2 Objectives

The overall objective of the present dissertation is to develop an energy efficient solar powered aqua-ammonia absorption refrigeration and air-conditioning system based on continuous operation. The specific objectives include:

1. Designing a solar absorption chiller that utilizes dephlegmator waste heat.
2. Equip the proposed design with the refrigerant storage unit
3. Perform the 1st and 2nd law analysis on the proposed new design
4. Analyze the proposed design based on Dhahran ambient conditions.

3.3 Methodology

To achieve the above mentioned objectives, initially an intensive literature review for refrigeration systems is carried out. This includes a thorough study of absorption refrigeration systems and the state-of-the-art of their utilization in both air-conditioning and refrigeration applications. This is followed by the designing an energy efficient solar powered absorption system that recovers waste heat from the dephlegmator as well as utilizes a refrigerant storage unit for higher performance of the cooling system. Mathematical model is then developed for the proposed design to carry out the first and second law of thermodynamic analysis in order to analyze the performance of the proposed design at Dhahran ambient conditions. A performance comparison between the proposed design and conventional design is also carried out.

CHAPTER 4

DESIGN OF THE PROPOSED ABSORPTION SYSTEM

After stating the objectives and methodology in Chapter 3, this chapter presents the design of the proposed solar powered aqua-ammonia vapor absorption refrigeration and air-conditioning system. The proposed design is a modified form of conventional aqua-ammonia absorption system aimed at improving its performance by heat recovering from the dephlegmator. The proposed system is also designed to operate at full cooling capacity with varying ambient conditions by introducing a refrigerant storage in the design of the system.

4.1 Description of the Proposed Design

The schematic design & enthalpy-concentration diagram of the proposed absorption refrigeration system is shown in figure 4-1 & 4-2 respectively. The detailed description of the proposed energy efficient solar powered absorption refrigeration and air-conditioning system is described in this section as follows.

4.1.1 Solar Collector Circuit

The absorption system consists of a generator which takes in the heat from solar collectors and generates ammonia vapors to be used for refrigeration purposes. Water from the solar collectors enters the generator heating coils at state point 27. The energy from the solar collectors is added into the generator causing the collector fluid to leave the generator at state point 28. As a result of heat addition from the solar collectors, the aqua-ammonia vapors are generated which is represented by state point 1.

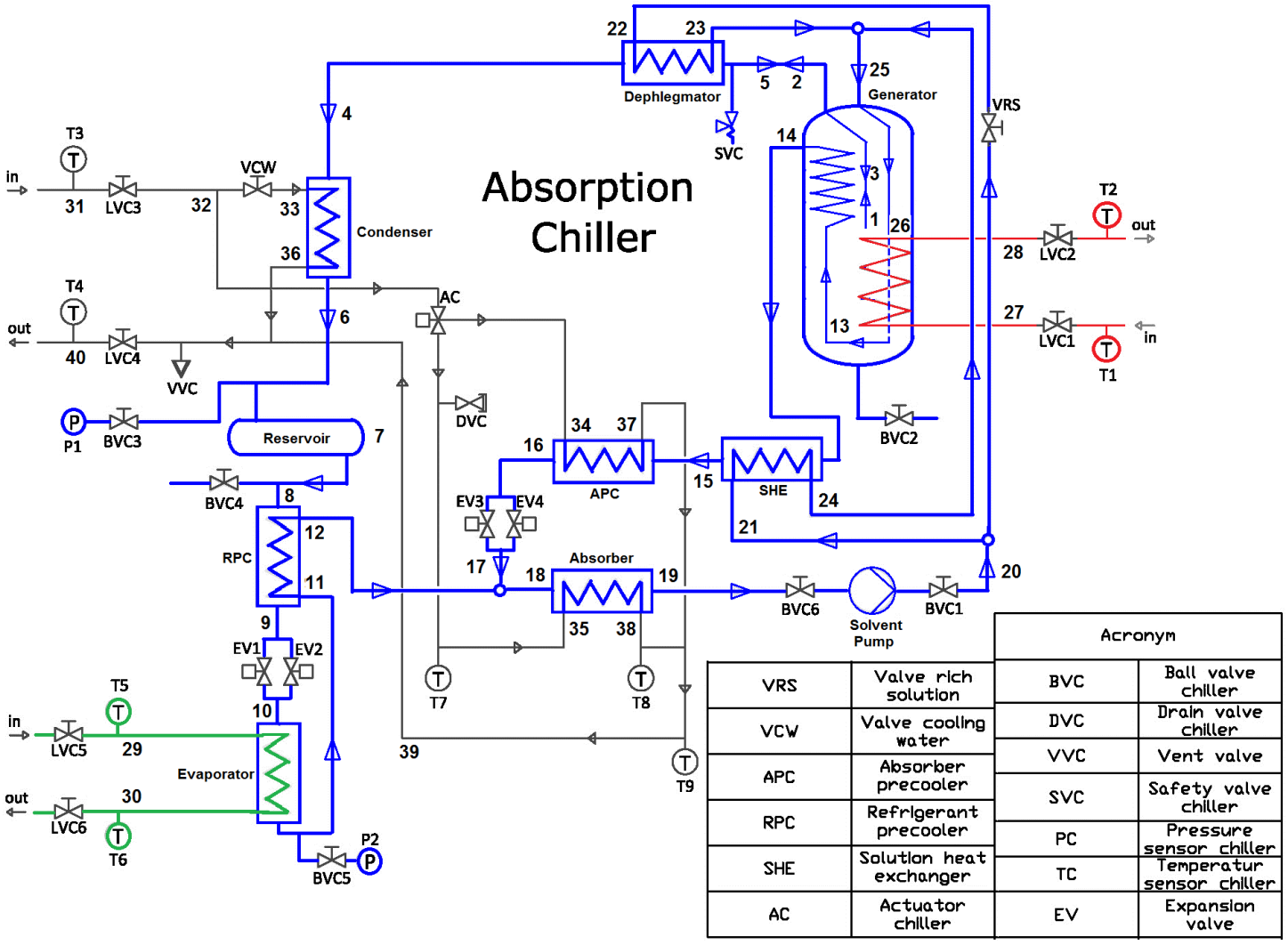

		Acronym	
VRS	Valve rich solution	BVC	Ball valve chiller
VCW	Valve cooling water	DVC	Drain valve chiller
APC	Absorber precooler	VVC	Vent valve
RPC	Refrigerant precooler	SVC	Safety valve chiller
SHE	Solution heat exchanger	PC	Pressure sensor chiller
AC	Actuator chiller	TC	Temperatur sensor chiller
		EV	Expansion valve

Figure 4-1 Schematic Design of the Proposed Absorption Refrigeration System

4.1.2 The Generation And Rectification

The generator consists of heater coils situated below heat recovery coils. The generated aqua-ammonia vapors moves in the upward direction around the generator heat recovery coils. The path way for the aqua-ammonia vapors around the generator heat recovery coils is filled with stainless steel net causing partial rectification of aqua-ammonia vapors within the generator. The strong aqua-ammonia solution enters the generator from the top location represented by state point 25. Initially this strong solution is preheated around the tubes of generator heat recovery coils. This preheated strong solution is represented by state point 26. The preheated strong solution then takes in the heat from the heater coils generating aqua-ammonia vapors and becoming weak solution represented by state point 13.

The weak heated solution is then transported to the heat recovery coils preheating the strong solution outside the heat recovery coils and exiting the generator represented by state point 14. The aqua-ammonia vapors generated represented by state point 1 is rectified around the generator heat recovery coils. The rectification process causes a drop in the temperature of aqua-ammonia vapors producing condensate inside the generator represented by state point 3 and comparatively rich aqua-ammonia vapors leaving the generator at state point 2. However at any location within the generator, the aqua-ammonia vapors are comparatively at higher temperature than the aqua-ammonia liquid inside the generator.

4.1.3 Dephlegmator (Hot Side)

The comparatively rich aqua-ammonia vapors represented by state point 2 then enter into the dephlegmator where it loses heat to the comparatively cold strong solution until the temperature aqua-ammonia vapors drop to the level where all (or most of) the water content is condensed inside the dephlegmator and only pure ammonia vapor leaves the dephlegmator represented by state point 4. The dephlegmator condensate represented by state point 5 is returned back to the generator.

4.1.4 The Condensation And Refrigerant Storage

The pure ammonia vapors then enters into the condenser where it condenses to pure saturated ammonia liquid represented by state point 6. The saturated pure ammonia liquid is then stored in the refrigerant storage vessel represented by state point 7.

4.1.5 Refrigerant Pre-cooler (Liquid Side) & Expansion

The pure saturated ammonia liquid is then withdrawn from the refrigerant storage vessel by the refrigerant pre-cooler, represented by state point 8, where the liquid ammonia is cooled before passing through the refrigerant expansion valves. The pre-cooled refrigerant ammonia is represented by state point 9. A set of two refrigerant expansion valves are provided which maintains the required pressure differential across them by alternate opening and closing. Due to refrigerant expansion valves, the throttling process takes place producing the vapor-liquid mixture of cold refrigerant represented by state point 10. The vapor content of this mixture depends upon the extent of pre-cooling that takes place inside the refrigerant pre-cooler. Greater the pre-cooling lower will be the vapor content at state point 10 and vice versa.

4.1.6 Water Glycol Circuit (Chilling Circuit) And Evaporation

The liquid content of the mixture at state point 10 then moves into the evaporator to produce the required refrigeration effect at the evaporator. Since evaporation is expected to take place at temperatures below the freezing point of water, so water glycol solution is used inside the evaporator to takes in the refrigeration effect. The water glycol solution enters the evaporator represented by state point 29, takes in the refrigeration effect at the evaporator and then leaves the evaporator at state point 30. The pre-cooled ammonia refrigerant evaporates while providing the refrigeration effect at the evaporator. Hence saturated ammonia refrigerant vapors leave the evaporator which is represented by state point 11.

4.1.7 Refrigerant Pre-Cooler (Vapor Side)

This saturated refrigerant vapor then moves to the refrigerant pre-cooler where it is superheated while pre-cooling the liquid ammonia refrigerant and leaves the refrigerant pre-cooler represented by state point 12.

4.1.8 Solution Heat Exchanger (Hot Side)

The weak aqua-ammonia solution as it leaves the generator, represented by state point 14 then moves to the solution heat exchanger. The solution heat exchanger is also a heat recovery component which undergoes heat transfer between the hot weak solution from the generator and cold strong solution from the absorber. So the weak solution from the generator after further sub-cooling by the solution heat exchanger is represented by state point 15.

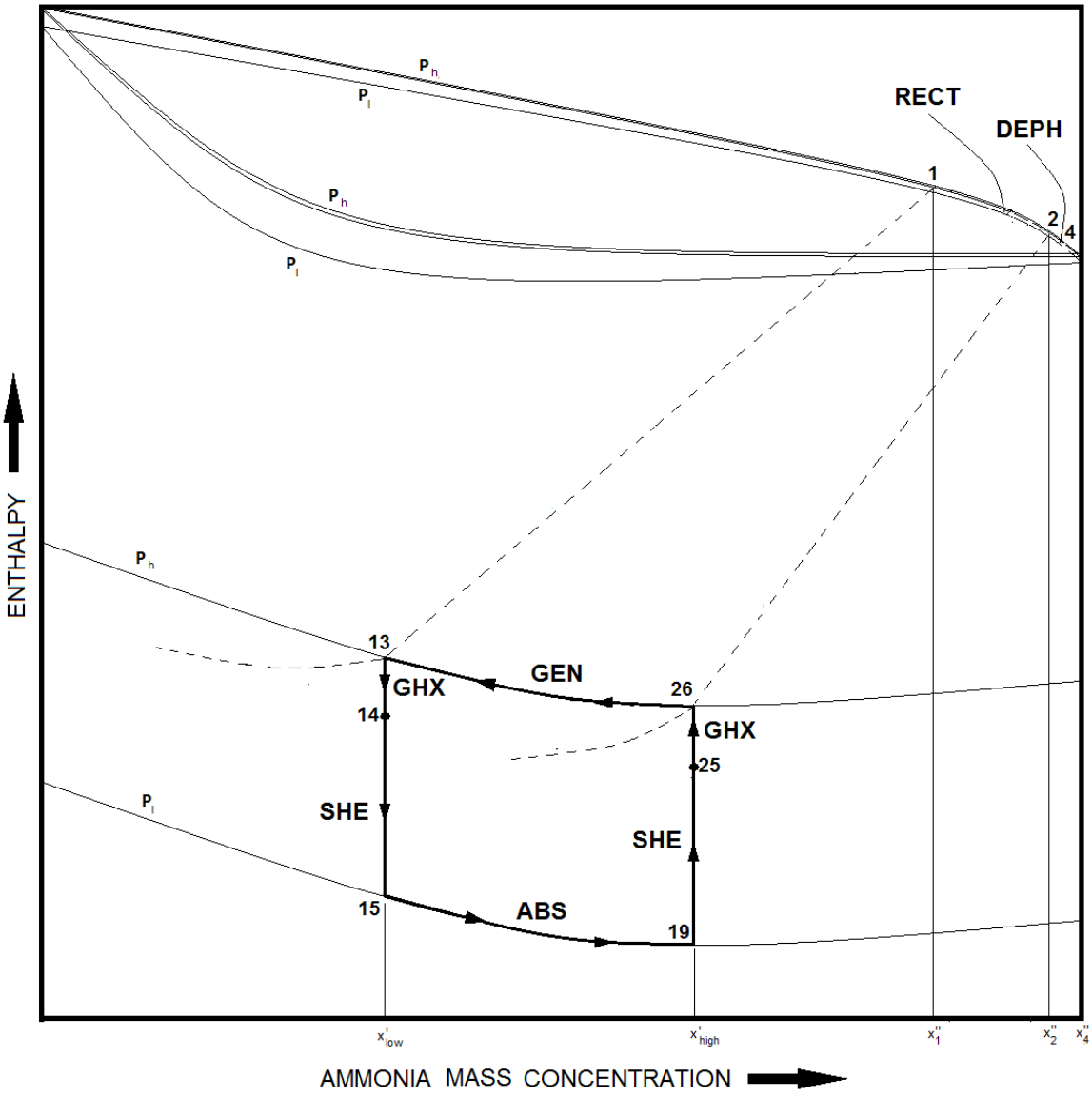

Figure 4-2 Enthalpy-Concentration Diagram of the proposed Absorption Refrigeration System

4.1.9 Absorber Pre-Cooler

After passing through the solution heat exchanger, still there is some potential left inside weak solution to reject heat before entering inside the absorber. Absorption inside the absorber takes place in two parts, i.e. spontaneous absorption and non-spontaneous absorption. Spontaneous absorption takes place when ammonia is mixed with the weak solution which is pre-cooled to the level that no heat rejection is required for the generated heat of absorption. However, non-spontaneous absorption takes place when ammonia is mixed with the weak solution such that heat is required to be rejected for further absorption process to takes place. Spontaneous absorption process is the most efficient process, however non-spontaneous absorption is comparatively very less efficient due to the existence of vapor and liquid in the mixture from which heat is required to be rejected.

So in order to increase the spontaneous form of absorption, an absorber pre-cooler is added in the system. The absorber pre-cooler is located upstream of the absorber and downstream of the solution heat exchanger. So the pre-cooled weak solution represented by state point 15, enters into the absorber pre-cooler where it is further pre-cooled leaving the absorber pre-cooler at state point 16.

4.1.10 The Absorption Process & Throttling

The pre-cooled weak solution then moves through the solution expansion valves to get throttled by pressure reduction. A set of two solution expansion valves are provided which maintains the required pressure differential across them by alternate opening and closing. The throttled weak pre-cooled aqua-ammonia solution represented by state point 17 is then mixed with superheated pure ammonia vapor represented by state point 12.

The mixture initially causes an spontaneous absorption followed by a non-spontaneous absorption requiring heat rejection from the absorber. As a result of absorption process, strong aqua-ammonia solution is formed at the exit of absorber represented by state point 19. This strong aqua-ammonia solution is then pressurized by the solution pump which is represented by state point 20.

4.1.11 Solution Heat Exchanger & Dephlegmator (Cold Side)

The pressurized strong aqua-ammonia solution is then split into two parts. One part moves to the solution heat exchanger which is represented by state point 21 whereas the other part moves to the dephlegmator which is represented by the state point 22. The portion of strong aqua-ammonia solution which moves to the solution heat exchanger is then preheated and represented by state point 24. Similarly, the portion of the strong aqua-ammonia solution which moves to the dephlegmator is also preheated and represented by state point 23. The splitting of strong aqua-ammonia solution is performed by a 3-way valve such that the temperature at state point 24 remains the same as the temperature at state point 15. The strong preheated aqua-ammonia solution at state point 23 is then mixed with the strong aqua-ammonia solution at state point 24 and is represented by state point 25. This strong aqua-ammonia solution at state point 25 is then fed into the generator for continuation of the generation process.

4.1.12 Cooling Water Circuit

The cooling water circuit starts with a cooling water supply represented by state point 31. This inlet cooling water is then split into two parts. One part goes into the condenser inlet and is represented by state point 33 while the other part is represented by state point 32. The cooling water takes in the heat of rejection from the condenser and

then leaves the condenser represented by state point 36. The other part of the inlet cooling water represented by state point 32 is further split into two parts. One part goes to the inlet of absorber pre-cooler and is represented by state point 34 whereas the other part goes into the inlet of absorber and is represented by state point 35.

The portion of cooling water going into the absorber pre-cooler takes in the heat of rejection and leaves the absorber pre-cooler at state point 37. Similarly, the portion of cooling water going into the absorber takes in the heat of rejection and leaves the absorber at state point 38. The cooling water outlet represented by state point 37 is then mixed with the cooling water outlet represented by state point 38. This mixture is represented by state point 39. Similarly, the cooling water outlet represented by state point 39 is then mixed with the cooling water outlet represented by state point 36. This mixture is represented by state point 40. Finally the cooling water moves out of the absorption refrigeration system at state point 40.

The cooling water inlet and cooling water outlet are connected to the heat rejection unit which rejects the heat of the cooling water into the atmosphere to be able to supply it back into the absorption system for cooling purposes.

4.2 Distinguishing Features of the Proposed Design

In comparison to the conventional aqua-ammonia absorption systems, following are the distinguishing features of the proposed design.

4.2.1 Heat Recovery from the Dephlegmator

One distinguishing feature of the proposed design compared to the conventional aqua-ammonia absorption systems is the heat recovery from the dephlegmator. In conventional designs, the dephlegmator used to reject heat to the ambient. However, in the proposed design, the dephlegmator rejects heat to the strong cold aqua-ammonia solution from the absorber thus recovering energy within the absorption system. For allowing heat recovery from the dephlegmator, the strong cold aqua-ammonia solution from the absorber is therefore split into two parts such that one part recovers heat from the solution heat exchanger whereas the other part recovers heat from the dephlegmator.

4.2.2 Two Solution Heat Exchangers

Another distinguishing feature of the proposed design compared to the conventional aqua-ammonia absorption systems is the use of two solution heat exchangers in the system. In the conventional absorption systems, the amount of heat recovery from the solution heat exchanger is limited by the generation starting temperature of the strong aqua-ammonia solution. As the generation starting temperature is reached, the aqua-ammonia vapors start to generate within the solution heat exchanger. Since the solution heat exchanger is not designed to handle two phase flows, this causes a significant drop in the effectiveness of the solution heat exchanger. Therefore in our proposed design, another solution heat exchanger is introduced within the cylindrical

shell of the generator assembly. This second solution heat exchanger, which is located inside the generator assembly, allows the heat recovery to take place while generating aqua-ammonia vapors.

The heat recovery arrangement in the proposed design is shown in figure 4-3. It can be seen from the figure 4-3 that the cold aqua-ammonia solution from the absorber, after splitting, first recovers heat from the dephlegmator and the solution heat exchanger and then enters into the generator assembly where it further recovers heat from the heat recovery coils within the generator. Thus the proposed heat recovery arrangement allows the maximum possible heat recovery from the absorption system compared to conventional systems.

4.2.3 Absorber Pre-Cooler

Another distinguishing feature of the proposed design compared to the conventional aqua-ammonia absorption systems is use of absorber pre-cooler. The use of absorber pre-cooler is optional and can be used if proper heat rejection is not taking place at the absorber. The absorber pre-cooler cools down the weak solution allowing more spontaneous absorption to take place thus reducing the load of heat rejection over the absorber.

4.2.4 Refrigerant Storage

Another distinguishing feature of the proposed design compared to the conventional aqua-ammonia absorption systems is use of refrigerant storage. The refrigerant storage will allow the proposed absorption system to operate at full cooling capacity when operating at ambient temperatures lower than the design temperature.

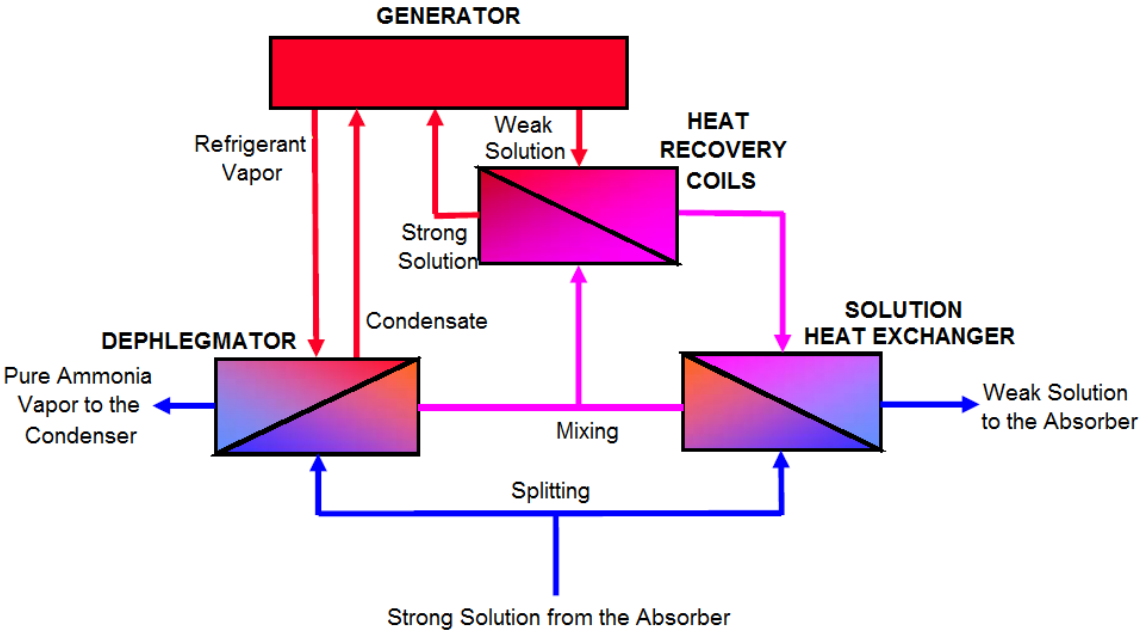

Figure 4-3 Heat Recovery Arrangement in the proposed design

CHAPTER 5

MATHEMATICAL MODELLING

After describing the design of the proposed absorption system in Chapter 4, this chapter provides the mathematical modeling for simulating the performance of the proposed energy efficient solar powered aqua-ammonia vapor absorption refrigeration and air-conditioning system. In this chapter, the specific focus has been given to the first and second laws of thermodynamic analysis conducted over the proposed absorption chiller.

5.1 First Law of Thermodynamic

First law of thermodynamic analysis states that the mass and energy of a closed system is conserved. This means that in any process, if there is mass not stored within the system, then the total mass inlet will be equal to the total mass outlet from the system. Similarly, in case of energy for any process, energy can change its form but the total energy within a system remains conserved. Thus the total amount of energy added into the system, either by means of heat or work, is equal to the sum of total amount of energy lost by the system, either by heat or work, and the change in internal energy of the system. Thus, mass and energy balance is applied to each and every component of the proposed absorption chiller, to determine all the parameters of the chiller.

Following are assumption used in the analysis of first law of thermodynamic for the proposed absorption chiller.

1) The pressure drop through the heat exchangers and their connecting pipes is negligible.
2) The ammonia mass concentration of the aqua-ammonia solution remains uniform inside the generator and the absorber.
3) The pressure difference between generator and condenser is negligible.
4) The pressure difference between absorber and evaporator is negligible.
5) The refrigerant expansion/flashing processes are adiabatic.
6) Proper rectification of generated aqua-ammonia vapors take place inside the rectifier.
7) The aqua-ammonia solution inside the generator and the absorber remains as saturated liquid throughout the operation.
8) The refrigerant condenses as saturated liquid inside the condenser.
9) The aqua-ammonia vapor remains as saturated vapor throughout the heat exchange inside the rectifier.
10) There are no leaks in the piping or the components of the system.
11) The temperature of cooling water inlet for heat rejection system is 1.25°C higher than the ambient.
12) The heat losses from the solar collectors to the absorption chiller is negligible.
13) It is assumed that the generator could reach up to 1°C less than the temperature of heated water from the solar collectors.

14) It is assumed that there is approximately 4°C rise in the temperature of cooling water as it takes in the heat of rejection from the absorber.

15) It is assumed that there is approximately 4°C rise in the temperature of cooling water as it takes in the heat of rejection from the condenser.

16) It is assumed that the condenser and absorber operates at a temperature approximately 1.7°C higher than the cooling water outlet temperature.

17) The volume flow rates of the cooling water in the heat rejection circuit, heated water in the solar collector circuit and water-glycol mixture in the chilling circuit is assumed to be constant.

18) Thermal inertia of all the components of the absorption chiller is negligible.

The component to component analysis of the proposed absorption chiller is given as follows:

5.1.1 Solar Collector Circuit

The solar collector circuit purchased by Millennium Energy Industries (MEI) are evacuated tubular solar collectors. The efficiency of these collectors depends upon the ambient temperature and solar radiation intensity. Based on the loss coefficients provided by the manufacturer equation (1) is used to calculate the collector efficiency within the developed experimental setup for the proposed absorption chiller.

$$\eta_{sc} = 0.6574 - 1.58 \cdot \left(\frac{T_i - T_a}{G} \right) - 0.0057 \cdot G \cdot \left(\frac{T_i - T_a}{G} \right)^2 \qquad (1)$$

The solar energy incident over the solar collectors which are available to the collectors are calculated using equation (2).

$$Q_{available} = G / 1000 \cdot A_{collector} \tag{2}$$

Using the efficiency of the solar collectors, the actual useable amount of solar energy that could be used to operate the generator of the proposed absorption system is calculated using equation (3).

$$Q_{useable} = \eta_{sc} \cdot Q_{available} \tag{3}$$

The energy balance equation for the heated water in the solar collector circuit can be given as equation (4)

$$Q_{useable} = \rho_{heat} \cdot \frac{\dot{V}_{heat}}{1000 \cdot 3600} \cdot Cp_{heat} \cdot \left(T_{27} - T_{28}\right) \tag{4}$$

5.1.2 Aqua-Ammonia Mass Balance

The aqua-ammonia mass balance within the proposed absorption chiller is determined by the following set of equations (5) to (9). Because of the addition of ammonia storage tank in the proposed absorption chiller, it is required to determine the mass flow rates of strong solution and the initial mass flow rate as they could be different based on the quantity of ammonia stored in the ammonia storage unit.

$$\frac{\dot{m}_{ss}}{\dot{m}_{initial}} = \frac{x_{ss,max} - 1}{x_{high} - 1} \tag{5}$$

$$\dot{m}_{ar} = \dot{m}_{initial} - \dot{m}_{ss} \tag{6}$$

$$\frac{\dot{m}_{ws}}{\dot{m}_{initial}} = \frac{x_{high} - 1}{x_{low} - 1} \tag{7}$$

$$\dot{m}_{au} = \dot{m}_{ss} - \dot{m}_{ws} \tag{8}$$

$$CR = \dot{m}_{ss} / \dot{m}_{au} \tag{9}$$

After determining the actual mass flow rate of the strong solution, the mass flow rate of the refrigerant and weak solution could be determined using equations (10) & (11).

$$\dot{m}_{ws} + \dot{m}_{ref} = \dot{m}_{ss} \tag{10}$$

$$CR = \dot{m}_{ss} / \dot{m}_{ref} \tag{11}$$

5.1.3 Generator

The energy balance over the generator is applied using the following set of equations (12) to (15). Equation (12) & (13) are used to determine the slope and constant for the principal operating line for the generator.

$$Slope = \frac{h_2 - h_{25}}{x_2 - x_{high}} \tag{12}$$

$$h_2 = Slope \cdot x_2 + constant \tag{13}$$

Once the slope and the constant are determined, the pole of the generator is determined using equation (14) while the energy balance can then be applied over the generator using equation (15).

$$Pole_{Generator} = Slope \cdot x_{low} + constant \tag{14}$$

$$Q_{GEN} = \dot{m}_{ws} \cdot \left(h_{14} - Pole_{Generator} \right) \tag{15}$$

5.1.4 Dephlegmator

The dephlegmator heat recovery can be determined using the equation (16) and (17) for the liquid and vapor sides of the heat exchanger.

$$Q_{DEPH} = \dot{m}_{23} \cdot h_{23} - \dot{m}_{22} \cdot h_{22} \tag{16}$$

$$Q_{DEPH} = \dot{m}_{2} \cdot h_{2} - \dot{m}_{4} \cdot h_{4} - \dot{m}_{5} \cdot h_{5} \tag{17}$$

The maximum possible heat rejection from the dephlegmator is calculated using the equation for the principal operating line of the absorption chiller as follows using equation (18) & (19)

$$Pole_{Dephlegmator} = Slope \cdot x_{pure,ammonia} + constant \tag{18}$$

$$Q_{DEPH,pole} = \dot{m}_{ref} \cdot \left(Pole_{Dephlegmator} - h_4 \right) \tag{19}$$

The ratio of heat recovery from dephlegmator compared to maximum heat recovery is given by equation (20)

$$RecoveryRatio_{Deph} = Q_{DEPH} \,/\, Q_{DEPH,pole} \tag{20}$$

The split ratio of mass flow rate for the optimum heat recovery from the dephlegmator is given by equation (21)

$$Split\ Ratio = \frac{\dot{m}_{22}}{\dot{m}_{20}} \tag{21}$$

5.1.5 Heat Recovery Coils inside Generator

The heat recovery from the heat recovery coils inside the generator which behaves as a second solution heat exchanger is given by equation (22).

$$Q_{GHX} = \dot{m}_{13} \cdot h_{13} - \dot{m}_{14} \cdot h_{14} \quad (22)$$

5.1.6 Solution Heat Exchanger

The heat recovery from the solution heat exchanger is given by equation (23)

$$Q_{SHE} = \dot{m}_{14} \cdot h_{14} - \dot{m}_{15} \cdot h_{15} \quad (23)$$

5.1.7 Absorber Pre-Cooler

The heat recovery from the absorber pre-cooler is given by equation (24)

$$Q_{APC} = \dot{m}_{15} \cdot h_{15} - \dot{m}_{16} \cdot h_{16} \quad (24)$$

5.1.8 Pump

The electrical input required from the solution pump is given by equation (25)

$$Q_{PUMP} = \dot{m}_{20} \cdot h_{20} - \dot{m}_{19} \cdot h_{19} \quad (25)$$

5.1.9 Absorber

The energy required to be rejected out of the absorber is calculated from the energy balance over the absorber as follow:

$$Q_{ABS} = \dot{m}_{17} \cdot h_{17} + \dot{m}_{12} \cdot h_{12} - \dot{m}_{19} \cdot h_{19} \quad (26)$$

5.1.10 Refrigerant Pre-Cooler

The heat recovery from the refrigerant pre-cooler is given by equation (27)

$$Q_{RPC} = \dot{m}_{12} \cdot h_{12} - \dot{m}_{11} \cdot h_{11} \tag{27}$$

5.1.11 Condenser

The energy required to be rejected out of the condenser is calculated from the energy balance over the absorber as follow:

$$Q_{COND} = \dot{m}_{4} \cdot h_{4} - \dot{m}_{6} \cdot h_{6} \tag{28}$$

5.1.12 Evaporator

The refrigeration effect produced by the evaporator is calculated using equation (29) for the proposed absorption chiller

$$Q_{EVAP} = \dot{m}_{11} \cdot h_{11} - \dot{m}_{10} \cdot h_{10} \tag{29}$$

5.1.13 Coefficient of Performance

The overall coefficient of performance of the proposed absorption system is calculated using equation (30).

$$COP = \frac{Q_{EVAP}}{Q_{GEN} + Q_{PUMP}} \tag{30}$$

5.1.14 Energy Balance

Knowing that the overall energy remains conserved in the system, the overall energy balance must be such that the energy input into the system is equal to the energy out of the system as given by equation (31) & (32).

$$Energy_{IN} = Q_{EVAP} + Q_{GEN} + Q_{PUMP} \quad (31)$$

$$Energy_{OUT} = Q_{COND} + Q_{APC} + Q_{ABS} \quad (32)$$

Finally the overall energy recovery by the proposed absorption chiller can be calculated using equation (33)

$$Energy_{Recovery} = Q_{DEPH} + Q_{SHE} + Q_{RPC} + Q_{GHX} \quad (33)$$

5.2 Second Law of Thermodynamic

Thermodynamic analysis using mass and energy balance equations present the quantitative aspect of any system. However, for comparison purposes, a more detailed qualitative analysis needs to be carried out. Exergy analysis based on second law of thermodynamics presents the quality of a system. The fact that exergy is not conserved and part of it is destroyed is of more significance than energy analysis in the design of thermal systems. Exergy analysis can be used to identify the components with high exergy losses. Once such components are identified, they can be modified to increase the overall efficiency of the system. As energy is conserved and does not reveal any information on energy losses of the system, it is inappropriate to design a thermal system based solely on energy analysis.

Exergy is defined as the minimum theoretical useful work required to form a quantity of matter from substances present in the environment and to bring the matter to a specified state. While discussing exergy, it is important to consider the difference between the surrounding and the environment. Surrounding is everything outside the system where as environment is a part of the surrounding, the intensive properties of which are uniform and do not change significantly as a result of any process.

Exergy destruction which is mainly due to friction and other resistances will not be considered in this exergy analysis. However irreversibilities due to finite temperature heat transfer processes produce exergy losses that will be considered in each component of the proposed absorption system. Exergy analysis for the proposed absorption system is performed keeping in view the same assumptions as used for the first law of thermodynamic analysis.

The exergetic efficiency, also known as second law efficiency, is a suitable parameter for determining the performance of a thermal system. Refrigeration systems must be compared using exergetic efficiencies rather than vales of coefficient of performance. This is because a system with high COP may have more exergy losses as compared to a system with low COP. Thus comparison on the basis of COP values does not give a true measure of a real performance of any system.

Along with the assumptions for first law of thermodynamic analysis, following assumption are also used in the second law of thermodynamic analysis.

1) Kinetic exergy of all the components of the absorption chiller is neglected.
2) Potential exergy of all the components of the absorption chiller is also neglected.
3) As no chemical reaction occurs in any component of absorption chiller, the value of chemical exergy remains the same at inlet and outlet of all the components. Thus chemical exergy can be neglected for absorption chiller as the difference between the exergy values at inlet and outlet for each component will eventually make it zero.
4) Reference temperature is assumed as the ambient temperature in the exergy/second law thermodynamic analysis of absorption chiller.
5) It is assumed that the heat extracted from the condenser is not used, therefore, it is omitted in the exergy loss calculation for the condenser.
6) Similarly, it is also assumed that the heat extracted from the absorber is also not used, therefore, it is also omitted in the exergy loss calculation for the absorber.

5.2.1 Specific Exergy

The specific exergy of all the state points in the proposed absorption chiller can be determined using equation (34)

$$E_i = x_i \left(h_i - T_a s_i \right) \text{ where i = 1 to 26} \quad (34)$$

5.2.2 Evaporator

The exergy loss across the evaporator and the percentage exergy loss for the evaporator is given by equation (35) & (36)

$$del_{evap} = \left(\dot{m}_{10} \cdot E_{10} - \dot{m}_{11} \cdot E_{11}\right) + Q_{EVAP} \cdot \left(1 - \left(\frac{T_{ambient} + 273}{T_{10} + 273}\right)\right) \tag{35}$$

$$\dot{E}_{loss,evap} = \frac{\left(del_{evap}\right)}{del_{total}} \tag{36}$$

5.2.3 Absorber

The exergy loss across the absorber and the percentage exergy loss for the absorber is given by equation (37) & (38)

$$del_{abs} = \dot{m}_{12} \cdot E_{12} + \dot{m}_{17} \cdot E_{17} - \dot{m}_{19} \cdot E_{19} \tag{37}$$

$$\dot{E}_{loss,abs} = del_{abs} \,/\, del_{total} \tag{38}$$

5.2.4 Condenser

The exergy loss across the condenser and the percentage exergy loss for the condenser is given by equation (39) & (40)

$$del_{cond} = \dot{m}_{4} \cdot E_{4} - \dot{m}_{6} \cdot E_{6} \tag{39}$$

$$\dot{E}_{loss,cond} = del_{cond} \,/\, del_{total} \tag{40}$$

5.2.5 Generator

The exergy loss across the generator and the percentage exergy loss for the generator is given by equation (41) & (42)

$$del_{gen} = \dot{m}_{26} \cdot E_{26} - \dot{m}_{13} \cdot E_{13} - \dot{m}_{1} \cdot E_{1} + Q_{GEN} \cdot \left(1 - \left(\frac{T_{ambient} + 273}{T_{13} + 273}\right)\right) \quad (41)$$

$$\dot{E}_{loss,gen} = del_{gen} / del_{total} \quad (42)$$

5.2.6 Heat Recovery Coils in the Generator

The exergy loss across the heat recovery coils in the generator and the percentage exergy loss for the heat recovery coils in the generator is given by equation (43) & (44)

$$del_{GHX} = \dot{m}_{1} \cdot E_{1} - \dot{m}_{2} \cdot E_{2} - \dot{m}_{3} \cdot E_{3} + \dot{m}_{25} \cdot E_{25} - \dot{m}_{26} \cdot E_{26} + \dot{m}_{13} \cdot E_{13} - \dot{m}_{14} \cdot E_{14} \quad (43)$$

$$\dot{E}_{loss,GHX} = del_{GHX} / del_{total} \quad (44)$$

5.2.7 Solution Heat Exchanger

The exergy loss across the solution heat exchanger and the percentage exergy loss for the solution heat exchanger is given by equation (45) & (46)

$$del_{SHE} = \dot{m}_{14} \cdot E_{14} + \dot{m}_{21} \cdot E_{21} - \dot{m}_{24} \cdot E_{24} - \dot{m}_{15} \cdot E_{15} \quad (45)$$

$$\dot{E}_{loss,SHE} = \frac{\left(del_{SHE}\right)}{del_{total}} \quad (46)$$

5.2.8 Refrigerant Pre-Cooler

The exergy loss across the refrigerant pre-cooler and the percentage exergy loss for the refrigerant pre-cooler is given by equation (47) & (48)

$$del_{RPC} = \dot{m}_8 \cdot E_8 + \dot{m}_{11} \cdot E_{11} - \dot{m}_9 \cdot E_9 - \dot{m}_{12} \cdot E_{12} \quad (47)$$

$$\dot{E}_{loss,RPC} = del_{RPC} / del_{total} \quad (48)$$

5.2.9 Dephlegmator

The exergy loss across the dephlegmator and the percentage exergy loss for the dephlegmator is given by equation (49) & (50)

$$del_{Deph} = \dot{m}_{22} \cdot E_{22} + \dot{m}_2 \cdot E_2 - \dot{m}_5 \cdot E_5 - \dot{m}_4 \cdot E_4 - \dot{m}_{23} \cdot E_{23} \quad (49)$$

$$\dot{E}_{loss,Deph} = del_{Deph} / del_{total} \quad (50)$$

5.2.10 Refrigerant Expansion Valve

The exergy loss across the refrigerant expansion valve and the percentage exergy loss for the refrigerant expansion valve is given by equation (51) & (52)

$$del_{EV,ref} = \dot{m}_9 \cdot E_9 - \dot{m}_{10} \cdot E_{10} \quad (51)$$

$$\dot{E}_{loss,EV,ref} = del_{EV,ref} / del_{total} \quad (52)$$

5.2.11 Solution Expansion Valve

The exergy loss across the solution expansion valve and the percentage exergy loss for the solution expansion valve is given by equation (53) & (54)

$$del_{EV,sol} = \dot{m}_{16} \cdot E_{16} - \dot{m}_{17} \cdot E_{17} \tag{53}$$

$$\dot{E}_{loss,EV,sol} = del_{EV,sol} / del_{total} \tag{54}$$

5.2.12 Pump

The exergy loss across the pump and the percentage exergy loss for the pump is given by equation (55) & (56)

$$del_{pump} = \dot{m}_{19} \cdot E_{19} - \dot{m}_{20} \cdot E_{20} + Q_{pump} \tag{55}$$

$$\dot{E}_{loss,pump} = del_{pump} / del_{total} \tag{56}$$

5.2.13 Exergetic Coefficient of Performance

The maximum coefficient of performance and the exergetic coefficient of performance for the proposed absorption chiller is given by equation (57) & (58)

$$COP_{max} = \left(\frac{T_{gen} - T_{ambient}}{T_{gen} + KC} \right) \cdot \left(\frac{T_{10} + KC}{T_{ambient} - T_{10}} \right) \tag{57}$$

$$ECOP = COP / COP_{max} \tag{58}$$

CHAPTER 6

RESULTS AND DISCUSSION

After describing the design of the proposed absorption system in Chapter 4 and the mathematical modeling in Chapter 5, this chapter provides the results and discussion for simulating the performance of the proposed energy efficient solar powered aqua-ammonia vapor absorption refrigeration and air-conditioning system. In this chapter, the specific focus has been given to the first and second laws of thermodynamic analysis conducted over the proposed absorption chiller. Along with that, the experimental validation of the simulated work, effect of dephlegmator heat recovery and the effect of refrigerant storage unit over the performance of the proposed absorption chiller have also been studied in this chapter.

6.1 Thermodynamic Analysis for the Design Condition

The proposed absorption chiller has been designed for an ambient temperature of 40°C. The thermodynamic analysis of the design condition for the proposed energy efficient solar powered aqua-ammonia vapor absorption refrigeration and air-conditioning system has been carried out using the mass and energy balance equations described in chapter 5. Also, for the second law analysis, the exergy balance has been carried out. A detailed list of state points for the proposed absorption chiller for operating at the design ambient condition has been provided in Table 6-1. Also, the detailed thermodynamic properties for each state point of the proposed absorption chiller when operating at design conditions has been provided in Table 6-2.

Table 6-1 List of state points for the proposed absorption chiller for the design condition

State Point	Medium	State	Location	Vapor/Liquid Ratio	Ammonia Mass Concentration
				q[i]	x[i]
[i]					
1	*Aqua-Ammonia*	*Saturated Vapor*	*Generation*	*1*	*0.8384*
2	*Aqua-Ammonia*	*Saturated Vapor*	*Generator Exit*	*1*	*0.934*
3	*Aqua-Ammonia*	*Saturated Liquid*	*Rectifier Condensate*	*0*	*0.3123*
4	*Aqua-Ammonia*	*Saturated Vapor*	*Dephlegmator Exit*	*1*	*0.9826*
5	*Aqua-Ammonia*	*Saturated Liquid*	*Dephlegmator Condensate*	*0*	*0.4259*
6	*Aqua-Ammonia*	*Saturated Liquid*	*Condenser Condensate*	*0*	*0.9826*
7	*Aqua-Ammonia*	*Saturated Liquid*	*Ammonia Reservoir*	*0*	*0.9826*
8	*Aqua-Ammonia*	*Saturated Liquid*	*RPC Liquid Inlet*	*0*	*0.9826*
9	*Aqua-Ammonia*	*Sub-Cooled Liquid*	*RPC Liquid Outlet*	*-*	*0.9826*
10	*Aqua-Ammonia*	*Vapor Liquid Mixture*	*Evaporator Inlet*	*0.1281*	*0.9826*
11	*Pure Ammonia*	*Saturated Vapor*	*Evaporator Outlet*	*1*	*0.9826*
12	*Pure Ammonia*	*Superheated Vapor*	*RPC Vapor Outlet*	*-*	*0.9826*
13	*Aqua-Ammonia*	*Saturated Liquid*	*Inside Generator*	*0*	*0.2645*
14	*Aqua-Ammonia*	*Sub-Cooled Liquid*	*Generator Outlet*	*-*	*0.2645*
15	*Aqua-Ammonia*	*Sub-Cooled Liquid*	*SHE Weak Solution Outlet*	*-*	*0.2645*
16	*Aqua-Ammonia*	*Sub-Cooled Liquid*	*APC Weak Solution Outlet*	*-*	*0.2645*
17	*Aqua-Ammonia*	*Vapor Liquid Mixture*	*Weak Solution Expansion*	*-*	*0.2645*
18	*Aqua-Ammonia*	*Vapor Liquid Mixture*	*Absorber Inlet*	*0.1737*	*0.3935*
19	*Aqua-Ammonia*	*Saturated Liquid*	*Absorber Outlet*	*0*	*0.3935*
20	*Aqua-Ammonia*	*Sub-Cooled Liquid*	*Solution Pump Outlet*	*-*	*0.3935*

State Point	Medium	State	Location	Vapor/Liquid Ratio	Ammonia Mass Concentration
				q[i]	x[i]
[i]					
21	*Aqua-Ammonia*	*Sub-Cooled Liquid*	*SHE Strong Solution Inlet*	*-*	*0.3935*
22	*Aqua-Ammonia*	*Sub-Cooled Liquid*	*Dephlegmator Inlet*	*-*	*0.3935*
23	*Aqua-Ammonia*	*Sub-Cooled Liquid*	*Dephlegmator Outlet*	*-*	*0.3935*
24	*Aqua-Ammonia*	*Sub-Cooled Liquid*	*SHE Strong Solution Outlet*	*-*	*0.3935*
25	*Aqua-Ammonia*	*Sub-Cooled Liquid*	*Rectifier Inlet*	*-*	*0.3935*
26	*Aqua-Ammonia*	*Vapor Liquid Mixture*	*Generator Inlet*	*0.04835*	*0.3935*
27	*Pure Water*	*Sub-Cooled Liquid*	*Inlet from Solar Collector*	*-*	*0*
28	*Pure Water*	*Sub-Cooled Liquid*	*Outlet to Solar Collector*	*-*	*0*
29	*Water-Glycol Mixture*	*Sub-Cooled Liquid*	*Inlet to the Evaporator*	*-*	
30	*Water-Glycol Mixture*	*Sub-Cooled Liquid*	*Outlet from the Evaporator*	*-*	
31	*Pure Water*	*Sub-Cooled Liquid*	*Coolant Main Inlet*	*-*	*0*
32	*Pure Water*	*Sub-Cooled Liquid*	*Coolant to the Actuator*	*-*	*0*
33	*Pure Water*	*Sub-Cooled Liquid*	*Coolant to the Condenser*	*-*	*0*
34	*Pure Water*	*Sub-Cooled Liquid*	*Coolant to the APC*	*-*	*0*
35	*Pure Water*	*Sub-Cooled Liquid*	*Coolant to the Absorber*	*-*	*0*
36	*Pure Water*	*Sub-Cooled Liquid*	*Coolant out of the Condenser*	*-*	*0*
37	*Pure Water*	*Sub-Cooled Liquid*	*Coolant out of the APC*	*-*	*0*
38	*Pure Water*	*Sub-Cooled Liquid*	*Coolant out of the Absorber*	*-*	*0*
39	*Pure Water*	*Sub-Cooled Liquid*	*Coolant Sub-header*	*-*	*0*
40	*Pure Water*	*Sub-Cooled Liquid*	*Coolant Main Outlet*	*-*	*0*

Table 6-2 Detailed thermodynamic properties for proposed absorption chiller at design condition

State Point	Temperature	Pressure	Mass Flow Rate	Specific Enthalpy	Specific Entropy	Specific Internal Energy	Density	Specific Exergy
	T[i]	P[i]	m_dot[i]	h[i]	s[i]	u[i]	rho[i]	E
[i]	[C]	[bar]	[kg/hr]	[kJ/kg]	[kJ/kg-C]	[kJ/kg]	[kg/m^3]	[kJ/kg]
1	*140.5*	*18.38*	*43.272*	*1735*	*5.234*	*1551*	*9.97*	*81.33*
2	*117.1*	*18.38*	*36.612*	*1572*	*4.877*	*1398*	*10.57*	*42.77*
3	*128.8*	*18.38*	*6.6564*	*374.7*	*1.611*	*372.4*	*784.93*	*-40.49*
4	*90.34*	*18.38*	*33.4044*	*1448*	*4.556*	*1288*	*11.53*	*21.46*
5	*103.7*	*18.38*	*3.19464*	*234.7*	*1.289*	*232.3*	*771.01*	*-71.91*
6	*46.95*	*18.38*	*33.4044*	*212.1*	*0.7709*	*208.9*	*574.38*	*-28.66*
7	*46.95*	*18.38*	*33.4044*	*212.1*	*0.7709*	*208.9*	*574.38*	
8	*46.95*	*18.38*	*33.4044*	*212.1*	*0.7709*	*208.9*	*574.38*	*-28.66*
9	*30.43*	*18.38*	*33.4044*	*130.6*	*0.5094*	*127.6*	*602.05*	*-28.32*
10	*-5*	*3.529*	*33.4044*	*130.6*	*0.552*	*114.4*	*21.72*	*-41.42*
11	*-5*	*3.529*	*33.4044*	*1263*	*4.701*	*1140*	*2.87*	*-209*
12	*28.77*	*3.529*	*33.4044*	*1344*	*4.987*	*1202*	*2.49*	*-217*
13	*140.5*	*18.38*	*157.068*	*445.8*	*1.758*	*443.4*	*789.27*	*-27.6*
14	*121.8*	*18.38*	*157.068*	*358.5*	*1.542*	*356.2*	*815.66*	*-32.81*
15	*69.39*	*18.38*	*157.068*	*126.1*	*0.9106*	*124*	*874.89*	*-42.03*
16	*69.39*	*18.38*	*157.068*	*126.1*	*0.9106*	*124*	*874.89*	*-42.03*
17	*69.65*	*3.529*	*157.068*	*126.1*	*0.9155*	*125.7*	*874.13*	*-42.44*
18	*69.65*	*3.529*	*190.476*	*360.5*	*1.699*	*332*	*12.36*	
19	*46.95*	*3.529*	*190.476*	*-19.2*	*0.5573*	*-19.61*	*848.90*	*-76.19*
20	*46.95*	*18.38*	*190.476*	*-17.99*	*0.5556*	*-20.16*	*849.62*	*-75.51*

State Point	Temperature	Pressure	Mass Flow Rate	Specific Enthalpy	Specific Entropy	Specific Internal Energy	Density	Specific Exergy
	T[i]	P[i]	m_dot[i]	h[i]	s[i]	u[i]	rho[i]	E
[i]	[C]	[bar]	[kg/hr]	[kJ/kg]	[kJ/kg-C]	[kJ/kg]	[kg/m^3]	[kJ/kg]
21	*46.95*	*18.38*	*154.764*	*-17.99*	*0.5556*	*-20.16*	*849.62*	*-75.51*
22	*46.95*	*18.38*	*35.694*	*-17.99*	*0.5556*	*-20.16*	*849.62*	*-75.51*
23	*99.32*	*18.38*	*35.694*	*217.8*	*1.238*	*215.4*	*791.14*	*-66.73*
24	*99.32*	*18.38*	*154.764*	*217.8*	*1.238*	*215.4*	*791.14*	*-66.73*
25	*99.32*	*18.38*	*190.476*	*217.8*	*1.238*	*215.4*	*791.14*	*-66.73*
26	*116.5*	*18.38*	*190.476*	*364.6*	*1.619*	*354*	*172.71*	*-55.95*
27	*125*	*6*	*1044.36*	*524.8*	*1.583*	*524.2*	*939.85*	
28	*141.5*	*6*	*1044.36*	*595.1*	*1.756*	*594.5*	*924.21*	
29	*5*		*1388.88*					
30	*-2.002*		*1388.88*					
31	*41.25*	*2*	*3970.8*	*172.4*	*0.5901*	*172.2*	*995.02*	
32	*41.25*	*2*	*1503.36*	*172.4*	*0.5901*	*172.2*	*995.02*	
33	*41.25*	*2*	*2466*	*172.4*	*0.5901*	*172.2*	*995.02*	
34	*41.25*	*2*	*0*	*172.4*	*0.5901*	*172.2*	*995.02*	
35	*41.25*	*2*	*1503.36*	*172.4*	*0.5901*	*172.2*	*995.02*	
36	*45.25*	*2*	*2466*	*189.2*	*0.6431*	*189*	*994.04*	
37	*41.25*	*2*	*0*	*172.4*	*0.5901*	*172.2*	*995.02*	
38	*45.38*	*2*	*1503.36*	*189.7*	*0.6447*	*189.5*	*993.05*	
39	*45.38*	*2*	*1503.36*	*189.7*	*0.6447*	*189.5*	*993.05*	
40	*45.3*	*2*	*3970.8*	*189.4*	*0.6437*	*189.1*	*994.04*	

Table 6-1 list down the state points for the proposed absorption chiller when operating under the design condition. Also, the table 6-1, provides the working medium at that state point along with the location of that state point within the proposed absorption chiller. The vapor to liquid ratio has also been provided along with ammonia mass concentration for each state point in table 6-1. All the mass, energy and exergy balance equation for the proposed absorption chiller have been solved in Engineering Equation Solver (EES). EES has the added advantage that it has an in-built library of all the thermodynamic properties for all the mixtures and solutions. While stating the thermodynamic properties, if the state of any state point is superheated, then the EES returns a vapor-liquid ratio of 1.001 whereas it returns a value of -0.001 if the state is a sub-cooled state. This explains the vapor to liquid ratio of 1.001 and -0.001 at several state points in Table 6-1 for the proposed absorption chiller.

The Table 6-2 provides the detailed thermodynamic properties for the proposed absorption chiller when operated at design conditions. The thermodynamic properties provided in table 6-2 are the temperatures, pressures, specific enthalpies, specific entropies, specific exergies, specific internal energies, densities and mass flow rates for each state point for the proposed absorption chiller when operated at the design condition. It must be noted that the specific exergies have only be determined and listed for the aqua-ammonia solution from state point 1 to state point 26. The specific exergies are required only for the aqua-ammonia solution in order to determine the exergy loss for each component of the proposed absorption chiller. Table 6-3 list down the final calculation results from the software (EES) when the proposed absorption chiller is operated at the design condition.

Table 6-3 Thermodynamic analysis results for the proposed absorption chiller at deign condition

Description	Symbol	Values
Coefficient of Performance	COP	*0.5173*
Maximum Coefficient of Performance	COP_{max}	*1.466*
Exergetic Coefficient of Performance	$ECOP$	*0.3528*
Collector Area	m^2	*42*
Circulation Ratio	CR	*5.702*
Circulation Ratio (Rectifier)	CR_{rect}	*1.182*
Circulation Ratio (Dephlegmator)	CR_{deph}	*1.096*
Total Energy into the System	$Energy_{IN}$	*30.8 [kW]*
Total Energy Rejection from the System	$Energy_{OUT}$	*30.8 [kW]*
Total Energy Recovered within the System	$Energy_{Recovery}$	*17 [kW]*
Total Initial Mass input into the System	$Mass_{initial}$	*33 [kg]*
Mass stored in the reservoir based on Ambient Temperature	$Mass_{reservoir}$	*0.35 [kg]*
Mass flow rate of refrigerant	$\dot{m}_{ref}$	*0.009279 [kg/s]*
Mass flow rate of strong solution	$\dot{m}_{ss}$	*0.05291 [kg/s]*
Mass flow rate of weak solution	$\dot{m}_{ws}$	*0.04363 [kg/s]*
Mass flow rate of the solar collector circuit	$\dot{m}_{heat}$	*0.2901 [kg/s]*
Mass flow rate of the heat rejection circuit	$\dot{m}_{rej}$	*1.103 [kg/s]*
Mass flow rate of the chilled water-glycol mixture circuit	$\dot{m}_{cool}$	*0.3858 [kg/s]*
High operating pressure	$Pressure_{high}$	*18.38 [bar]*
Low operating pressure	$Pressure_{low}$	*3.529 [bar]*
Pressure of solar collector circuit	$Pressure_{heat}$	*6 [bar]*
Pressure of the heat rejection circuit	$Pressure_{rej}$	*2 [bar]*
Pressure of the chilled water-glycol mixture circuit	$Pressure_{cool}$	*2.7 [bar]*

Description	Symbol	Values
Heat rejected by the Absorber	Q_{ABS}	*19 [kW]*
Heat rejected by the Absorber pre-cooler	Q_{APC}	*0 [kW]*
Heat rejected by the Condenser	Q_{COND}	*11.8 [kW]*
Heat recovered from the Dephlegmator	Q_{DEPH}	*2.285 [kW]*
Maximum heat recovered from the Dephlegmator	$Q_{DEPH,max}$	*2.338 [kW]*
Refrigeration effect produced at the evaporator	Q_{EVAP}	*10.5 [kW]*
Heat input into the generator	Q_{GEN}	*20.24 [kW]*
Heat recovered by the Generator Heat Exchanger	Q_{GHX}	*3.8 [kW]*
Heat rejected by the Heat Rejection Heat Exchanger	Q_{HRHX}	*30.8 [kW]*
Work Input by the Pump	Q_{PUMP}	*0.0636 [kW]*
Heat recovered by the Refrigerant Pre-Cooler	Q_{RPC}	*0.7562 [kW]*
Heat recovered by the Solution Heat Exchanger	Q_{SHE}	*10.14 [kW]*
Split ratio to the Dephlegmator	$Ratio_{deph}$	*0.1874*
Energy Recovery Ration from the Dephlegmator	$RecoveryRatio_{deph}$	*0.97*
Temperature of the Absorber Outlet	T_{abs}	*46.95 [C]*
Absorption Process Starting Temperature	$T_{abs,start}$	*72.64 [C]*
Ambient Temperature	$T_{ambient}$	*40 [C]*
Temperature of the Condensate from the Condenser	T_{cond}	*46.95 [C]*
Operating Temperature of the Evaporator	T_{evap}	*-5 [C]*
Operating Temperature of the Generator	T_{gen}	*140.5 [C]*
Generation Process Starting Temperature	$T_{gen,start}$	*110.5 [C]*
High Ammonia Mass Liquid Concentration in the System	x_{high}	*0.3935*
Low Ammonia Mass Liquid Concentration in the System	x_{low}	*0.2645*
Highest Concentration of Pure Ammonia Mixture into the System	$x_{pure,ammonia}$	*0.9826*
Total initial Ammonia Mass Concentration into the System	$x_{ss,max}$	*0.4*

It can be seen from table 6-3 that the proposed absorption chiller operates at a coefficient of performance of 0.5173 when operated at the design ambient condition of 40°C which is quite satisfactory. The refrigeration effect is produced at an evaporator temperature of -5°C and a generator temperature of 140.5°C. It can also be seen from the table 6-3 that when the ambient condition is 40°C, the absorber and condenser operates at a temperature of about 47°C. The reason for high operating temperature of absorber and condenser is that several temperature differences are added into the ambient temperature for the operation of absorber and condenser. Thus, there is approximately 2°C temperature difference between cooling water outlet temperature from the heat rejection heat exchanger and ambient temperature. Similarly there is approximately 4°C temperature difference between the inlet and outlet of cooling water within the absorber and condenser. Similarly there is approximately 1°C temperature difference between the cooling water outlet temperature and the condenser or absorber operating temperature. Also it can be seen from the table 6-3 that exergetic coefficient of performance of 0.3528 is achieved from the absorption chiller when operating at the design condition.

Also it can be seen from the table 6-3 that a total of 30.8 kW of energy input and output take place from the absorption chiller where around 17 kW of energy is recovered within the system for the proposed absorption system. Thus the design generator is for 20kW, absorber is also 20kW, condenser is 10kW and evaporator is also 10kW, the solution heat exchanger is also 10kW, refrigerant pre-cooler is 0.75kW, heat rejection heat exchanger is designed for 30kW. Under design condition, the system's high pressure is around 18 bar but the system is designed to operate below 25 bar while it can survive a pressure of 30 bar at most.

6.2 First Law of Thermodynamic Analysis

After going through the thermodynamic design for the design condition of the proposed absorption chiller in the previous section 6.1, the simulation results for the first law of thermodynamic analysis of the proposed absorption chiller has been developed in this section based on the mathematical modeling described in chapter 5.

6.2.1 Coefficient of Performance (COP)

The coefficient of performance for the proposed absorption chiller is shown in figure 6-1 when operated at varying ambient temperature and varying generator temperature. The analysis has been conducted at an evaporator temperature of -5°C, for the ambient temperatures varying from 25°C to 45°C whereas the generator temperature is varied from 90°C to 180°C. It can be seen from the figure 6-1 that, at any constant ambient temperature, the coefficient of performance of the proposed absorption chiller increases by increasing the generator temperature, becomes maximum at an optimum generator temperature and then slowly drops by further increasing the generator temperature. Similarly, it can also be seen from figure 6-1 that, at any constant generator temperature, the coefficient of performance drops with an increasing ambient temperature. Also it can be seen from figure 6-1 that the optimum generator temperature of the proposed absorption chiller increases with the increasing ambient temperature whereas the optimum coefficient of performance decreases with the increasing ambient temperature. Thus, when increasing the ambient temperature from 25°C to 45°C, the optimum generator temperature increases from 120°C to 155°C whereas the optimum coefficient of performance decreases from 0.54 to 0.48.

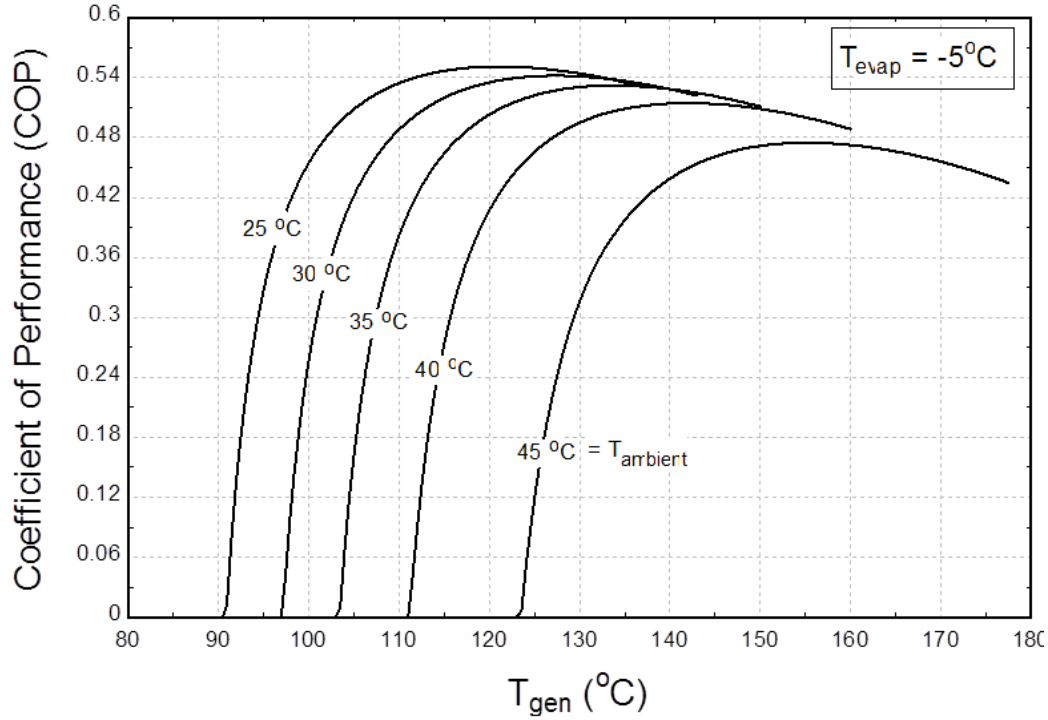

Figure 6-1 Coefficient of performance of the proposed absorption chiller against generator temperature

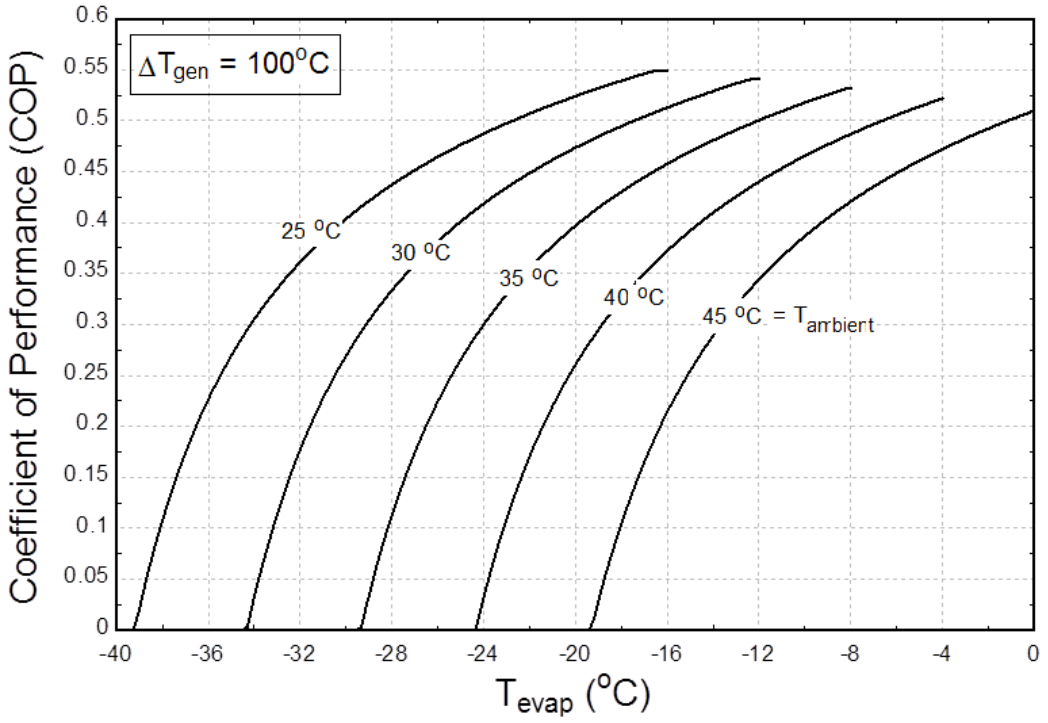

Figure 6-2 Coefficient of performance of the proposed absorption chiller against evaporator temperature

The coefficient of performance for the proposed absorption chiller is shown in figure 6-2 when operated at varying ambient temperature and varying evaporator temperature. The analysis has been conducted at a generator temperature 100°C higher than the ambient temperature, for the ambient temperatures varying from 25°C to 45°C whereas the evaporator temperature is varied from -40°C to 0°C. It can be seen from the figure 6-2 that, at any constant ambient temperature, the coefficient of performance of the proposed absorption chiller increases by increasing the evaporator temperature.

Similarly, it can also be seen from figure 6-2 that, at any constant evaporator temperature, the coefficient of performance drops with an increasing ambient temperature. Thus, when increasing the ambient temperature from 25°C to 45°C, the coefficient of performance decreases from 0.55 to 0.21 when operated at an evaporator temperature of -16°C.

6.2.2 Circulation Ratios

The circulation ratio of generator is defined as ratio of mass flow rate of the strong solution to the mass flow rate of the ammonia refrigerant vapor. The circulation ratio of generator for the proposed absorption chiller is shown in figure 6-3 when operated at varying ambient temperature and varying generator temperature. The analysis has been conducted at an evaporator temperature of -5°C, for the ambient temperatures varying from 25°C to 45°C whereas the generator temperature is varied from 90°C to 180°C. It can be seen from the figure 6-3 that, at any constant ambient temperature, the circulation ratio of generator of the proposed absorption chiller decreases by increasing the generator temperature, becomes almost constant at an optimum generator temperature and then very slowly drops by further increasing the generator temperature. Similarly, it

can also be seen from figure 6-3 that, at any constant generator temperature, the circulation ratio of generator increases with an increasing ambient temperature however it becomes almost constant for high generator temperature. Thus, at any ambient temperature from 25°C to 45°C, the circulation ratio of generator drops to as low as 4.8 when increasing the generator temperature.

The circulation ratio of generator for the proposed absorption chiller is shown in figure 6-4 when operated at varying ambient temperature and varying evaporator temperature. The analysis has been conducted at a generator temperature 100°C higher than the ambient temperature, for the ambient temperatures varying from 25°C to 45°C whereas the evaporator temperature is varied from -40°C to 0°C. It can be seen from the figure 6-4 that, at any constant ambient temperature, the circulation ratio of generator of the proposed absorption chiller decreases by increasing the evaporator temperature, becomes almost constant at an optimum evaporator temperature and then very slowly drops by further increasing the evaporator temperature. Similarly, it can also be seen from figure 6-4 that, at any constant evaporator temperature, the circulation ratio of generator increases with an increasing ambient temperature however it becomes almost constant for high evaporator temperature. Thus, at any ambient temperature from 25°C to 45°C, the circulation ratio of generator drops to as low as 4.8 when increasing the evaporator temperature.

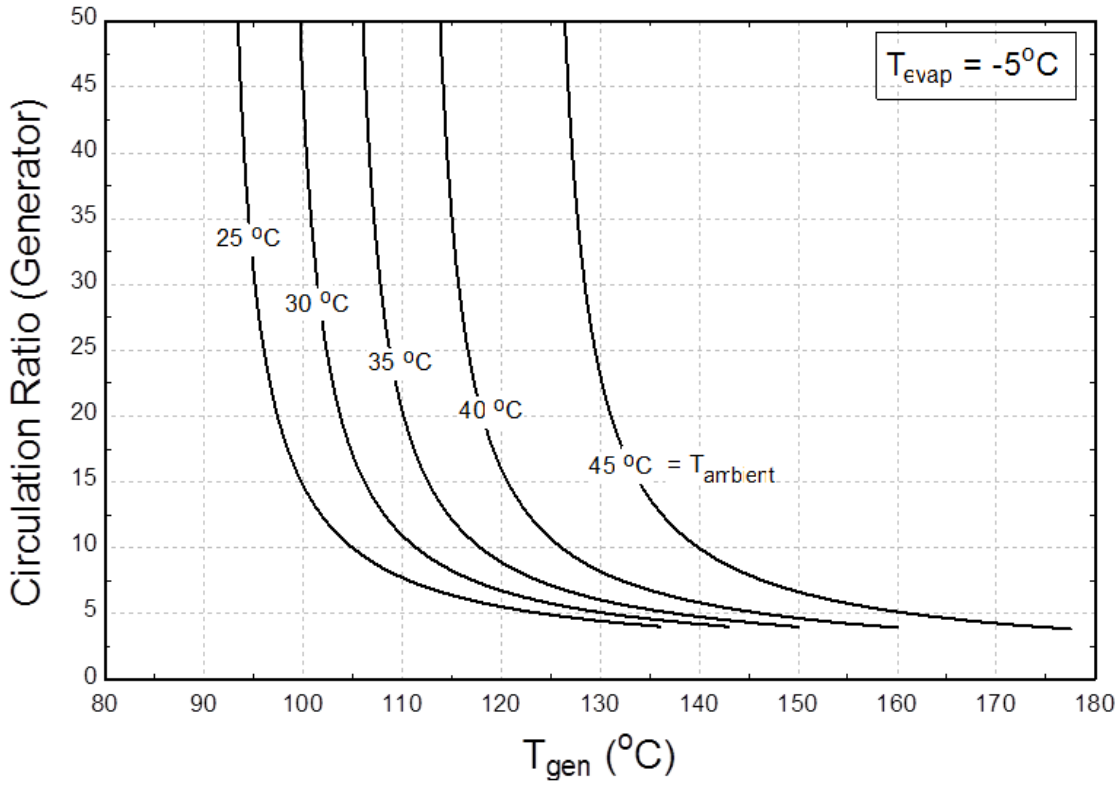

Figure 6-3 Circulation ratio for the generator against varying generator temperature

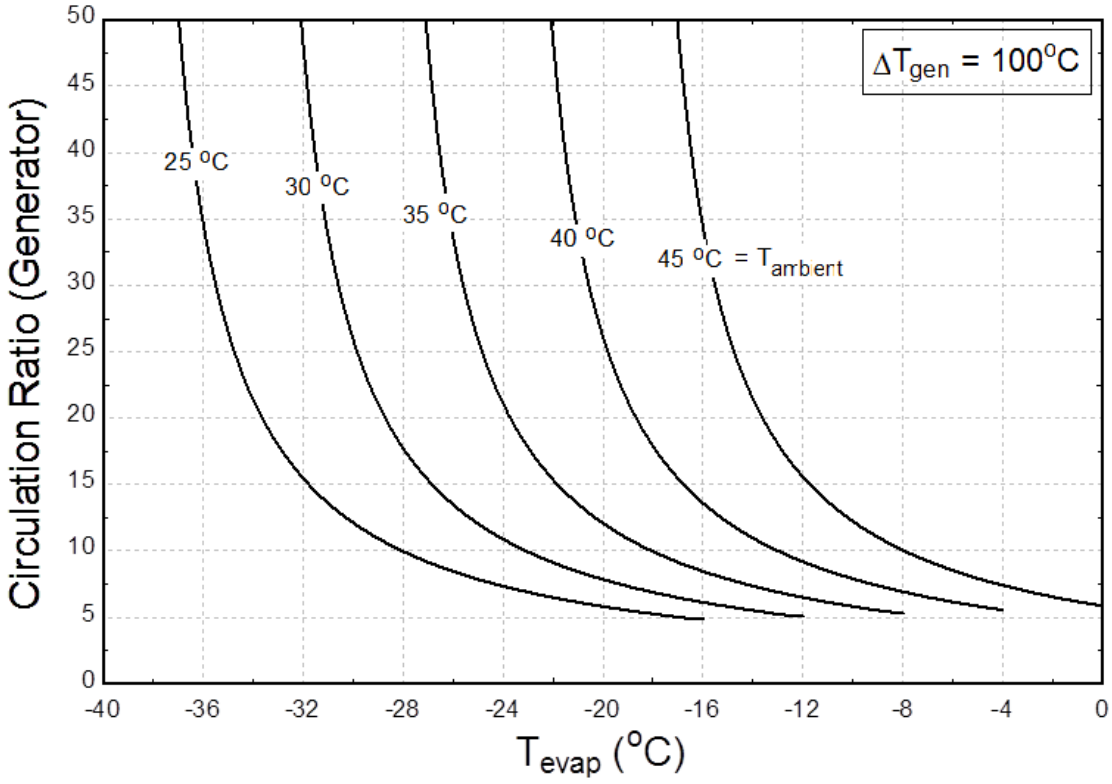

Figure 6-4 Circulation ratio for the generator against varying evaporator temperature

The circulation ratio of dephlegmator & rectifier is defined as ratio of mass flow rate of the inlet aqua-ammonia vapor to the outlet aqua-ammonia vapor from the dephlegmator and rectifier respectively. The circulation ratio of dephlegmator & rectifier for the proposed absorption chiller is shown in figure 6-5 & figure 6-6 respectively, when operated at varying ambient temperature and varying generator temperature. The analysis has been conducted at an evaporator temperature of -5°C, for the ambient temperatures varying from 25°C to 45°C whereas the generator temperature is varied from 90°C to 180°C.

It can be seen from the figure 6-5 & figure 6-6 that, at any constant ambient temperature, the circulation ratio of dephlegmator & rectifier of the proposed absorption chiller increases by increasing the generator temperature. Similarly, it can also be seen from figure 6-5 & figure 6-6 that, at any constant generator temperature, the circulation ratio of dephlegmator & rectifier decreases with an increasing ambient temperature.

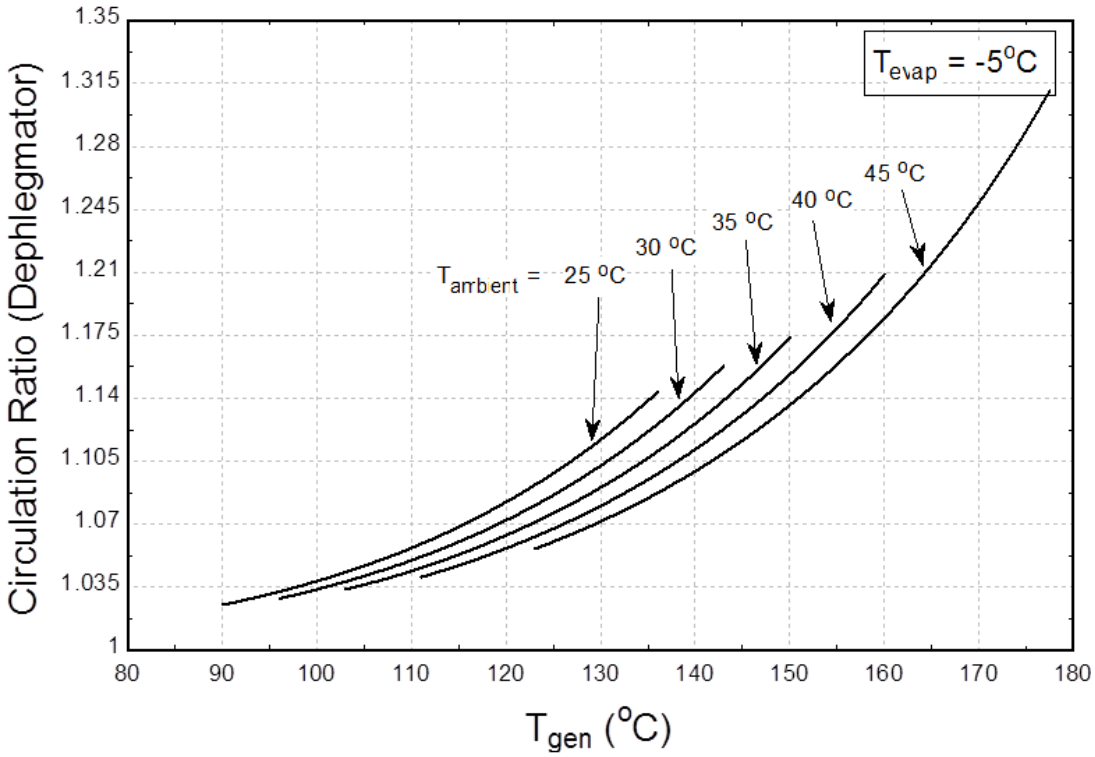

Figure 6-5 Circulation ratio for the dephlegmator against varying generator temperature

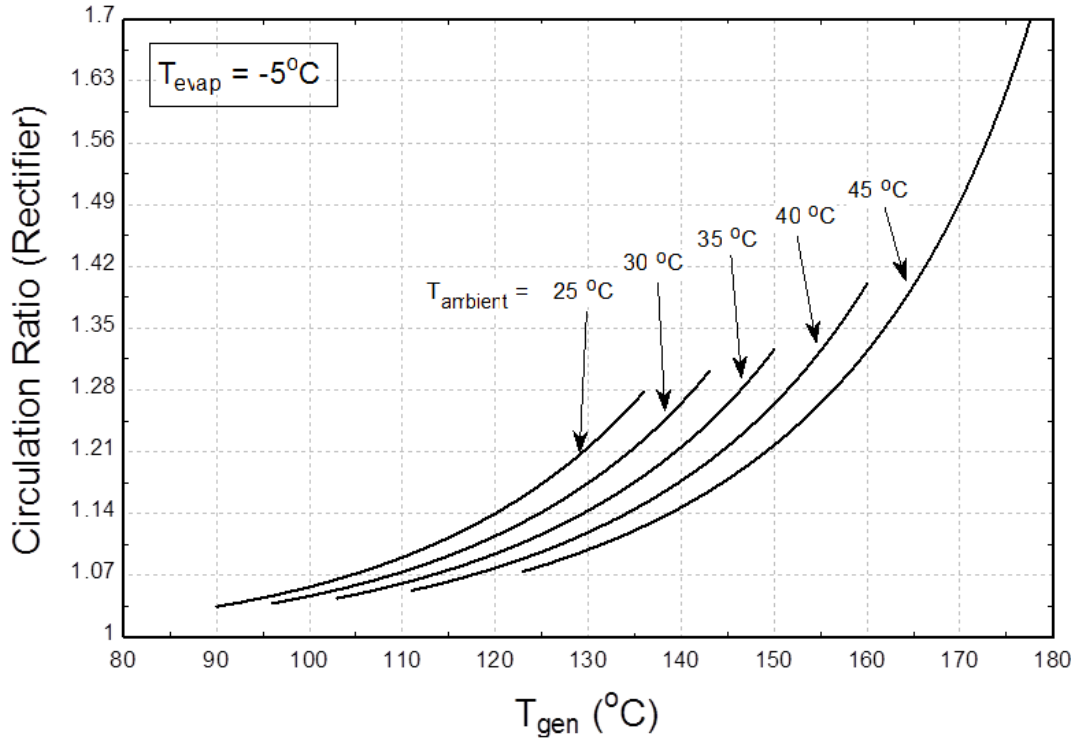

Figure 6-6 Circulation ratio for the rectifier against varying generator temperature

6.2.3 Specific Heat Capacities

The specific heat capacity is defined as the heat capacity of any component of the proposed absorption chiller per unit heat capacity of the evaporator where the heat capacity of the evaporator is the refrigeration effect produced at the evaporator. This section deals with the simulated results for the heat capacities of various components of the proposed absorption chiller.

6.2.3.1 Absorber

The specific heat capacity of absorber for varying generator and ambient temperature is shown in figure 6-7 whereas for varying evaporator and ambient temperature is shown in figure 6-8. It can be seen from the figure 6-7 & figure 6-8 that, at any constant ambient temperature, the specific heat capacity of absorber decreases by increasing the generator temperature and evaporator temperature respectively. Thus, at any ambient temperature from 25°C to 45°C, the specific heat capacity of absorber drops to as low as 1.7 when increasing the generator temperature and evaporator temperature as shown in figure 6-7 & figure 6-8 respectively.

6.2.3.2 Dephlegmator

The specific heat capacity of dephlegmator for varying generator and ambient temperature is shown in figure 6-9 whereas for varying evaporator and ambient temperature is shown in figure 6-10. It can be seen from the figure 6-9 & figure 6-10 that, at any constant ambient temperature, the specific heat capacity of dephlegmator increases by increasing the generator temperature and evaporator temperature respectively.

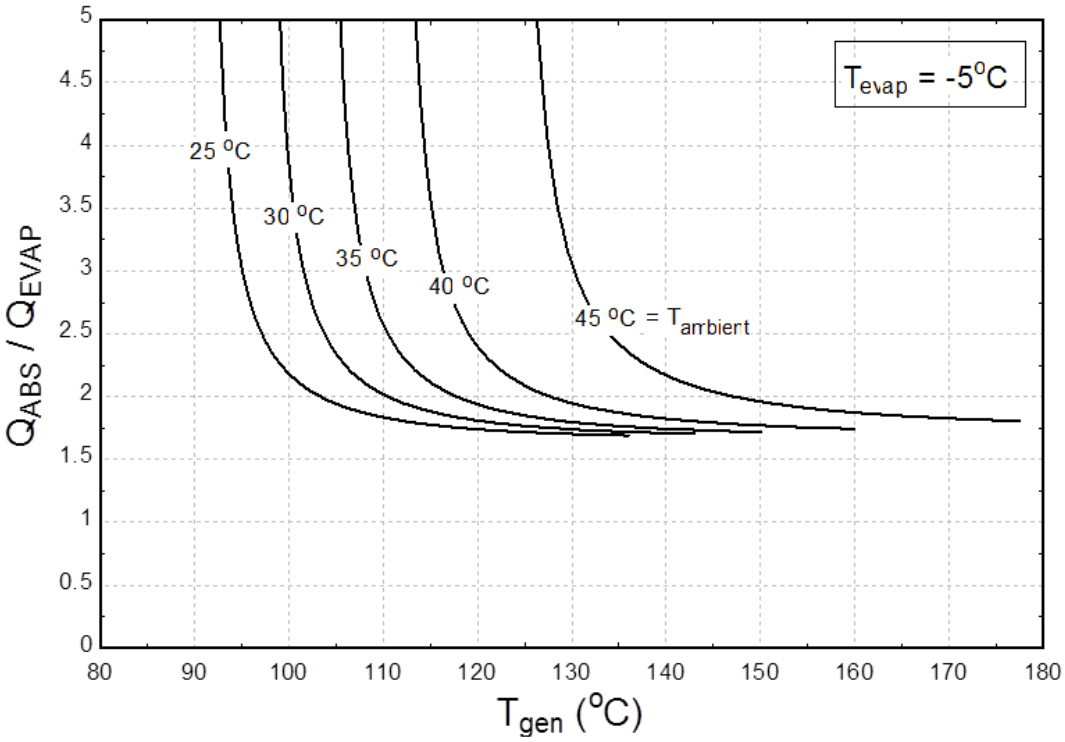

Figure 6-7 Specific heat rejected by the absorber against varying generator temperature

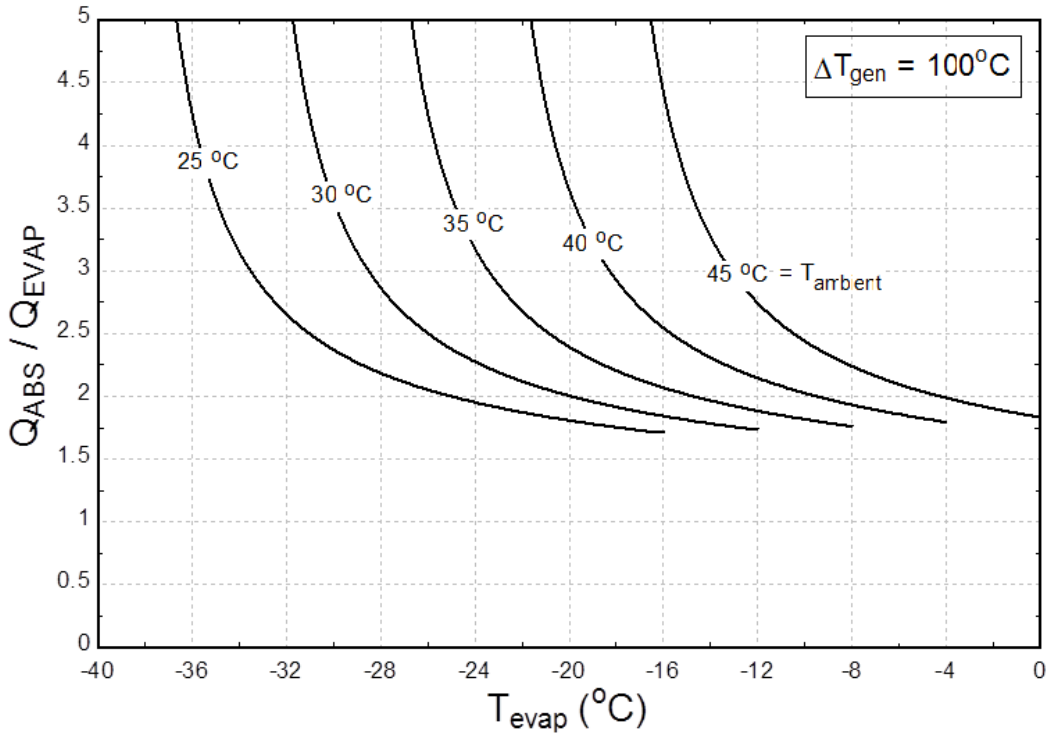

Figure 6-8 Specific heat rejected by the absorber against varying evaporator temperature

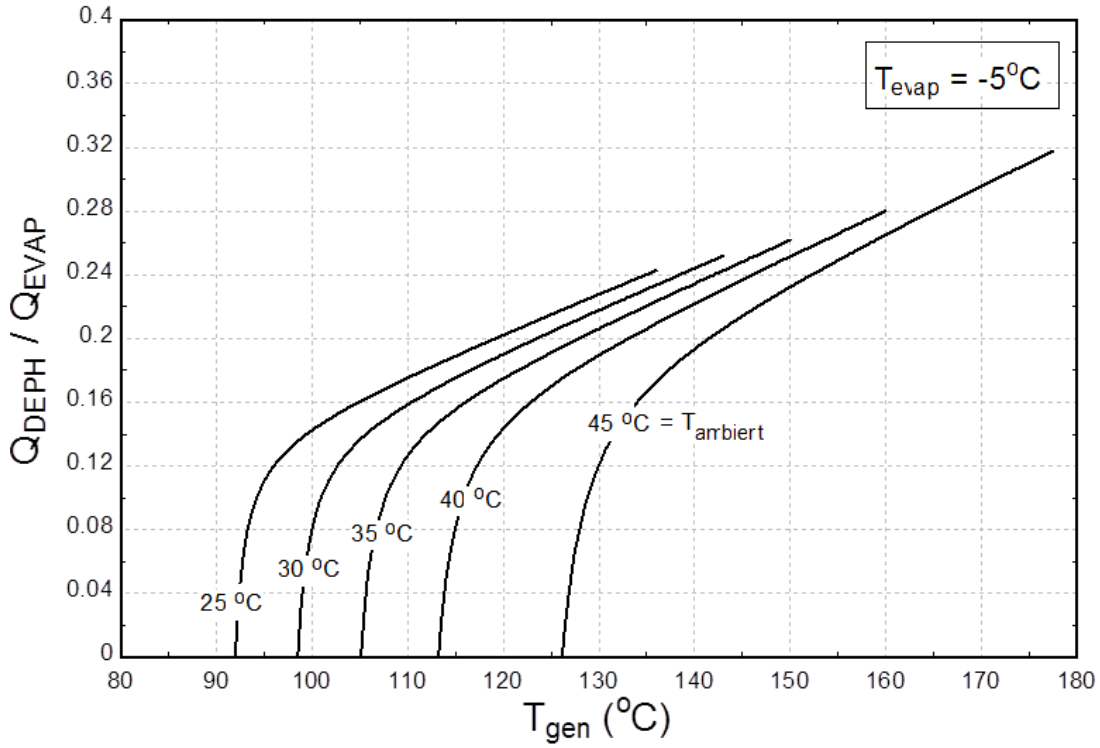

Figure 6-9 Specific heat removed at the dephlegmator against varying generator temperature

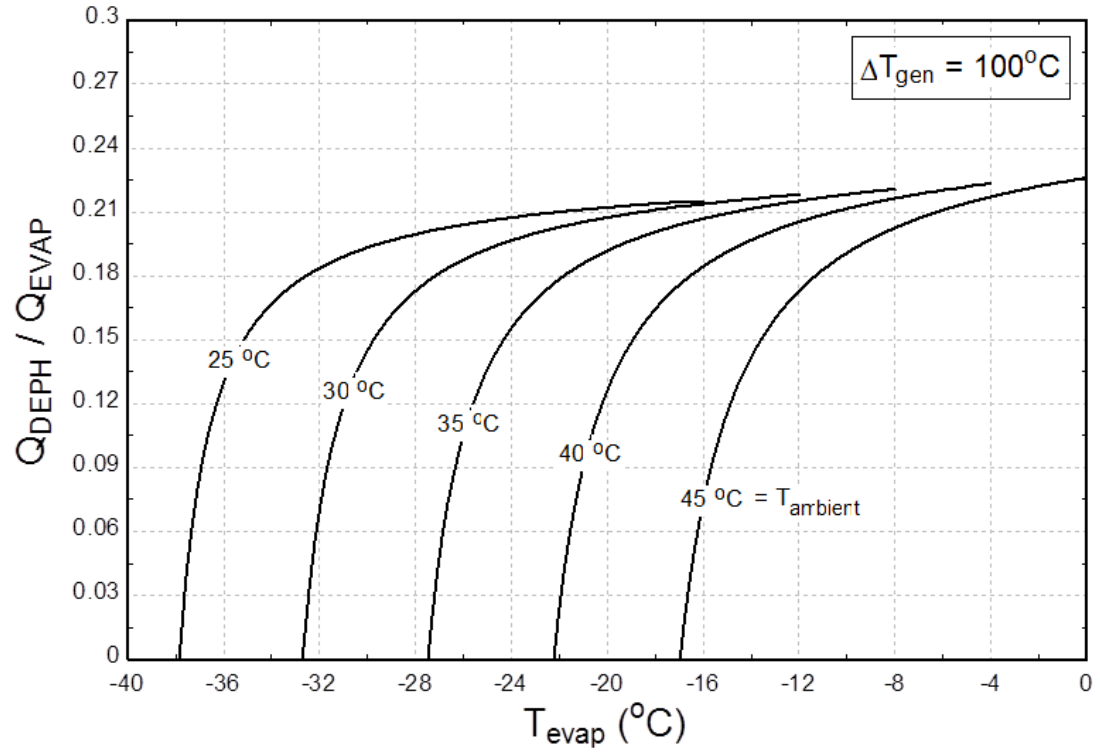

Figure 6-10 Specific heat removed at the dephlegmator against varying evaporator temperature

6.2.3.3 Generator

The specific heat capacity of generator for varying generator and ambient temperature is shown in figure 6-11 whereas for varying evaporator and ambient temperature is shown in figure 6-12. It can be seen from the figure 6-11 & figure 6-12 that, at any constant ambient temperature, the specific heat capacity of generator decreases by increasing the generator temperature and evaporator temperature respectively. Thus, at any ambient temperature from 25°C to 45°C, the specific heat capacity of generator drops to as low as 1.9 when increasing the generator temperature and evaporator temperature as shown in figure 6-11 & figure 6-12 respectively.

6.2.3.4 Heat Recovery Coils in the Generator

The specific heat capacity of heat recovery coils in the generator for varying generator and ambient temperature is shown in figure 6-13 whereas for varying evaporator and ambient temperature is shown in figure 6-14. It can be seen from the figure 6-13 & figure 6-14 that, at any constant ambient temperature, the specific heat capacity of heat recovery coils in the generator decreases by increasing the generator temperature and evaporator temperature respectively. Thus, at any ambient temperature from 25°C to 45°C, the specific heat capacity of heat recovery coils in the generator drops to as low as 0.3 when increasing the generator temperature and evaporator temperature as shown in figure 6-13 & figure 6-14 respectively.

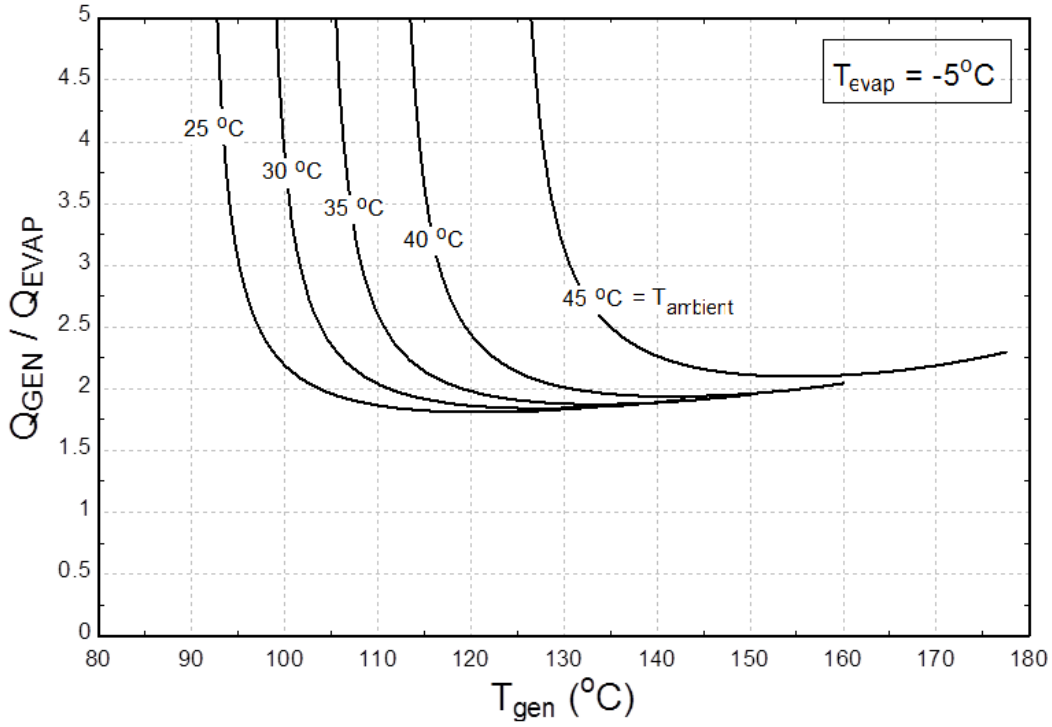

Figure 6-11 Specific heat input required at the generator for varying generator temperature

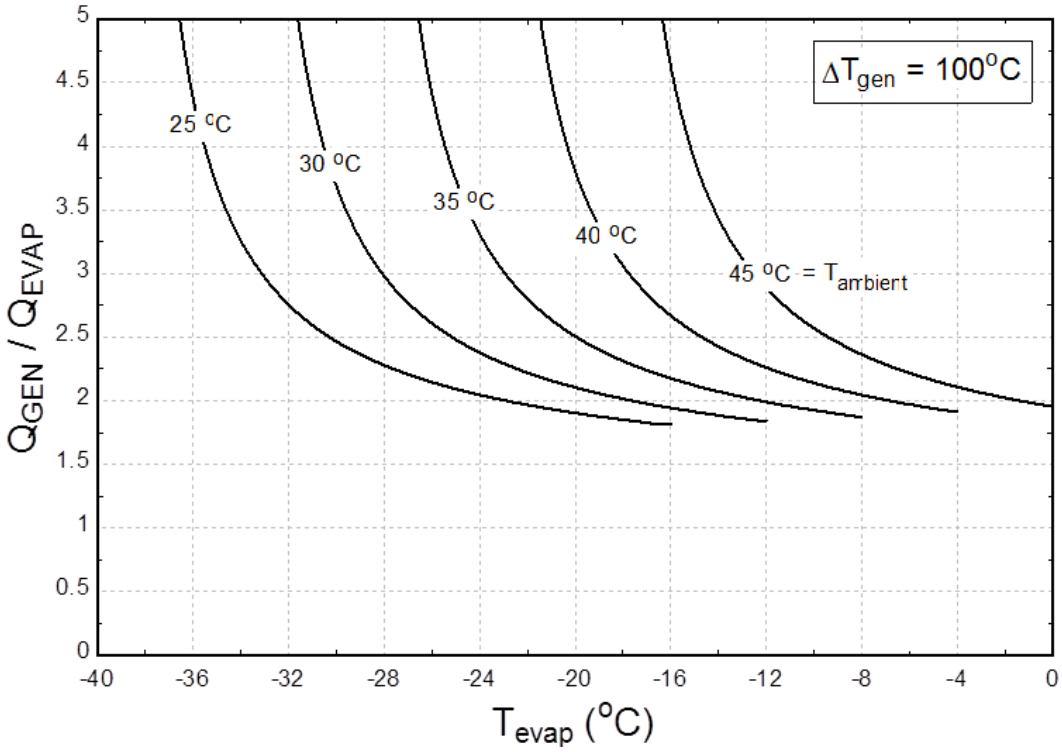

Figure 6-12 Specific heat input required at the generator for varying evaporator temperature

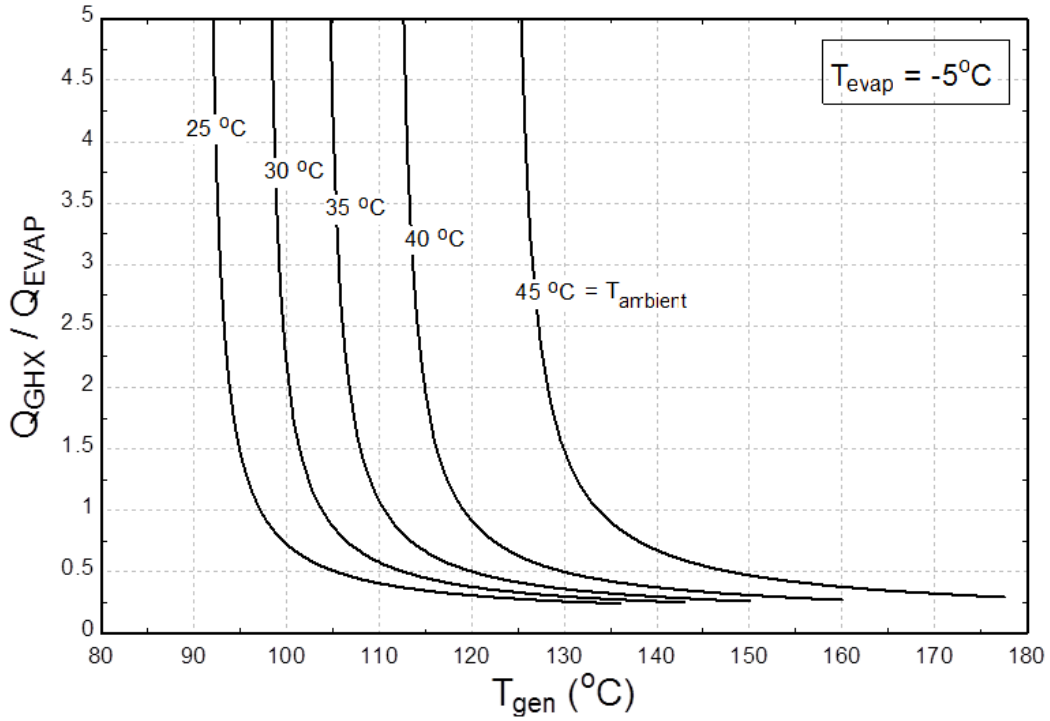

Figure 6-13 Specific heat recovery by heat exchanger coils inside generator for varying generator temperature

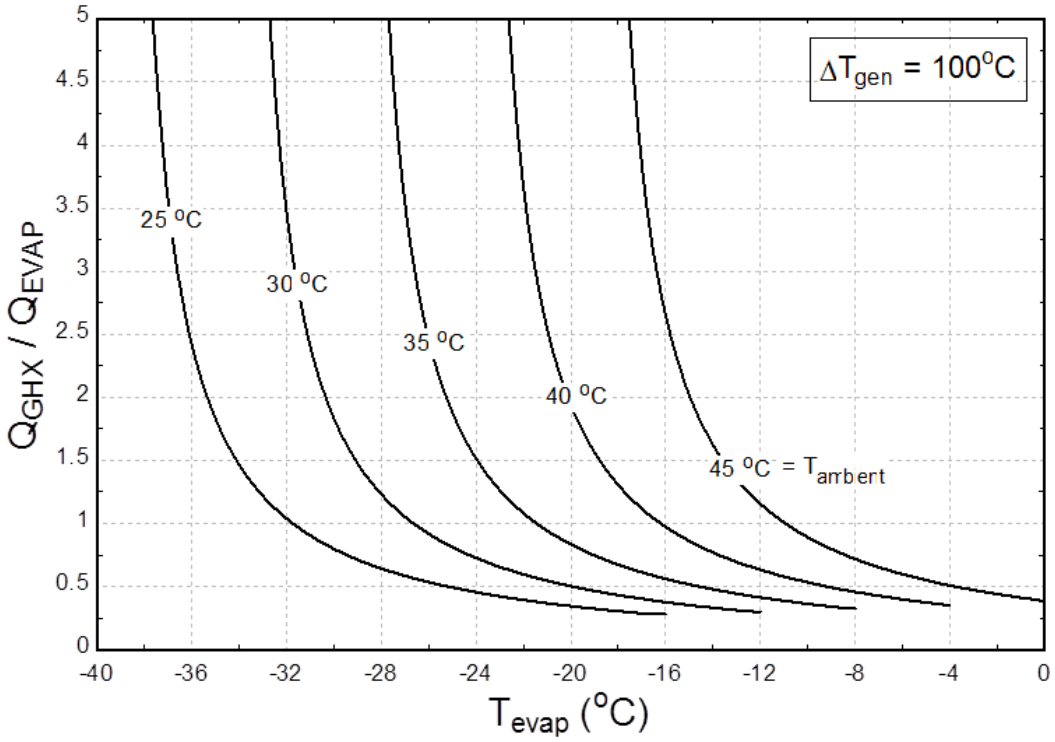

Figure 6-14 Specific heat recovery by heat exchanger coils inside generator for varying evaporator temperature

6.2.3.5 Heat Rejection Heat Exchanger

The specific heat capacity of heat rejection heat exchanger for varying generator and ambient temperature is shown in figure 6-15 whereas for varying evaporator and ambient temperature is shown in figure 6-16. It can be seen from the figure 6-15 & figure 6-16 that, at any constant ambient temperature, the specific heat capacity of heat rejection heat exchanger decreases by increasing the generator temperature and evaporator temperature respectively. Thus, at any ambient temperature from 25°C to 45°C, the specific heat capacity of heat rejection heat exchanger drops to as low as 2.75 when increasing the generator temperature and evaporator temperature as shown in figure 6-15 & figure 6-16 respectively.

6.2.3.6 Solution Pump

The specific heat capacity of solution pump for varying generator and ambient temperature is shown in figure 6-17 whereas for varying evaporator and ambient temperature is shown in figure 6-18. It can be seen from the figure 6-17 & figure 6-18 that, at any constant ambient temperature, the specific heat capacity of solution pump decreases by increasing the generator temperature and evaporator temperature respectively. Thus, at any ambient temperature from 25°C to 45°C, the specific heat capacity of solution pump drops to as low as 0.006 when increasing the generator temperature and evaporator temperature as shown in figure 6-17 & figure 6-18 respectively.

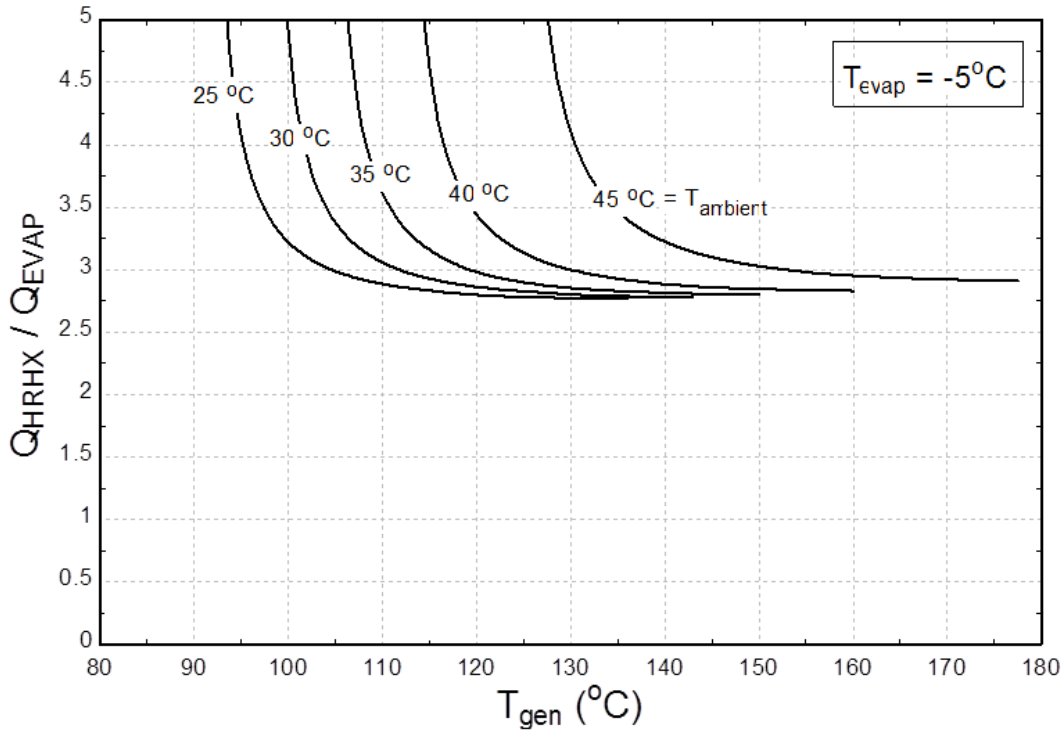

Figure 6-15 Specific heat rejection by heat recovery heat exchanger for varying generator temperature

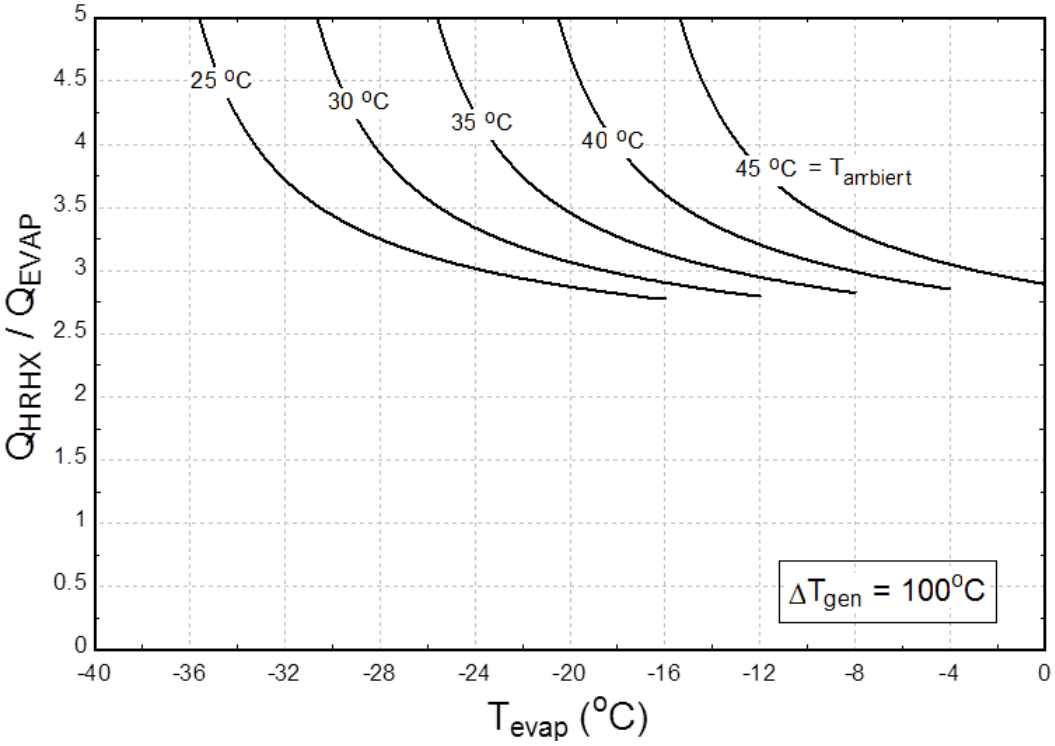

Figure 6-16 Specific heat rejection by heat recovery heat exchanger for varying evaporator temperature

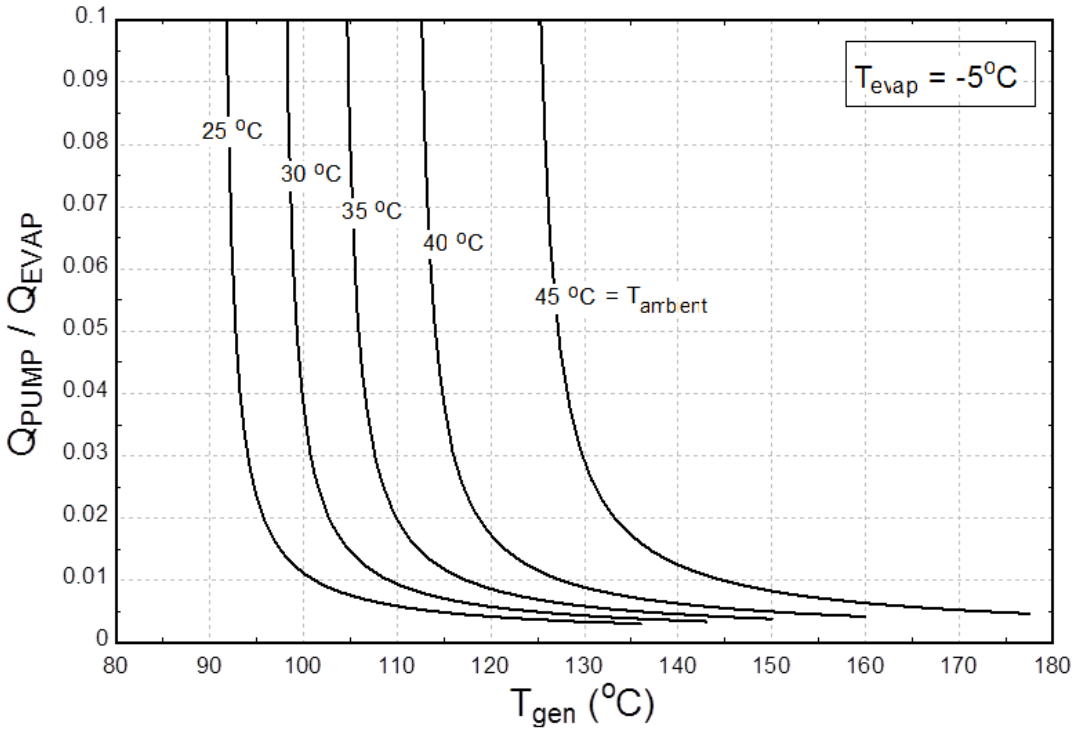

Figure 6-17 Specific Electrical energy requirement by pump for varying generator temperature

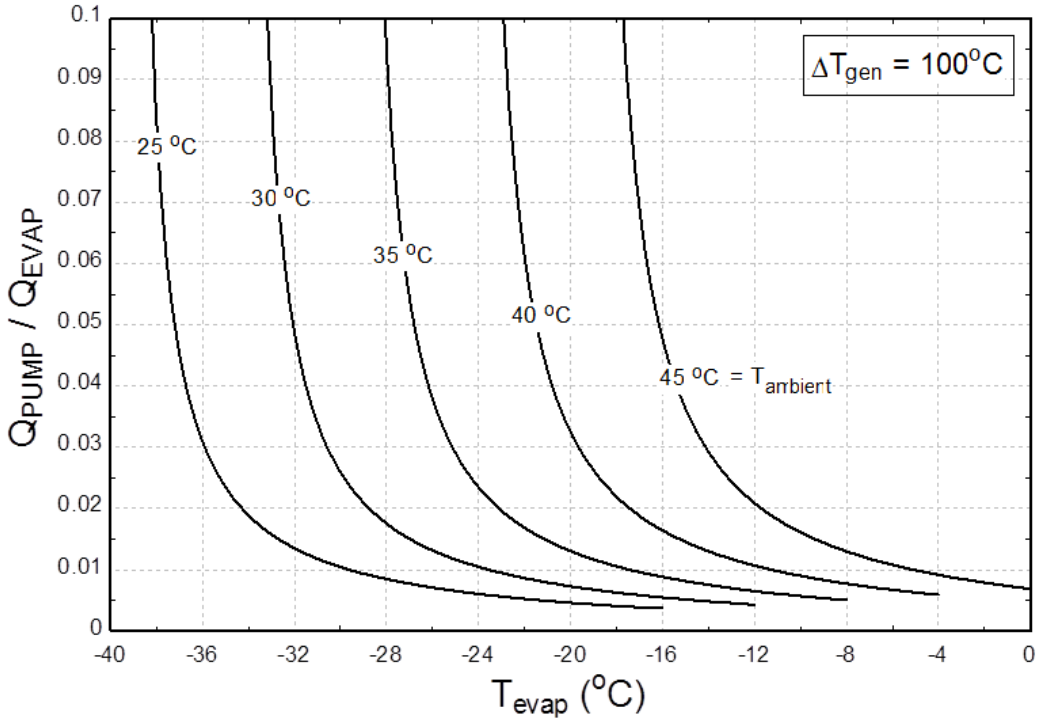

Figure 6-18 Specific Electrical energy requirement by pump for varying evaporator temperature

6.2.3.7 Refrigerant Pre-Cooler

The specific heat capacity of refrigerant pre-cooler for varying evaporator and ambient temperature is shown in figure 6-19. It can be seen from the figure 6-19 that at any constant ambient temperature, the specific heat capacity of refrigerant pre-cooler decreases by increasing the evaporator temperature. Unlike other component of the proposed absorption chiller, the refrigerant pre-cooler shows a linear drop in the specific heat for increasing evaporator temperature. It can also be seen from the figure 6-19 that specific heat of the refrigerant pre-cooler increases with an increase in the ambient temperature for a fixed evaporator temperature. However, under all the cases the specific heat of refrigerant pre-cooler remains below 0.1 thus defining a very small size of the heat exchanger

6.2.3.8 Solution Heat Exchanger

The specific heat capacity of solution heat exchanger for varying generator and ambient temperature is shown in figure 6-20 whereas for varying evaporator and ambient temperature is shown in figure 6-21. It can be seen from the figure 6-20 & figure 6-21 that, at any constant ambient temperature, the specific heat capacity of solution heat exchanger decreases by increasing the generator temperature and evaporator temperature respectively. Thus, at any ambient temperature from 25°C to 45°C, the specific heat capacity of solution heat exchanger drops to as low as 0.8 when increasing the generator temperature and evaporator temperature as shown in figure 6-20 & figure 6-21 respectively.

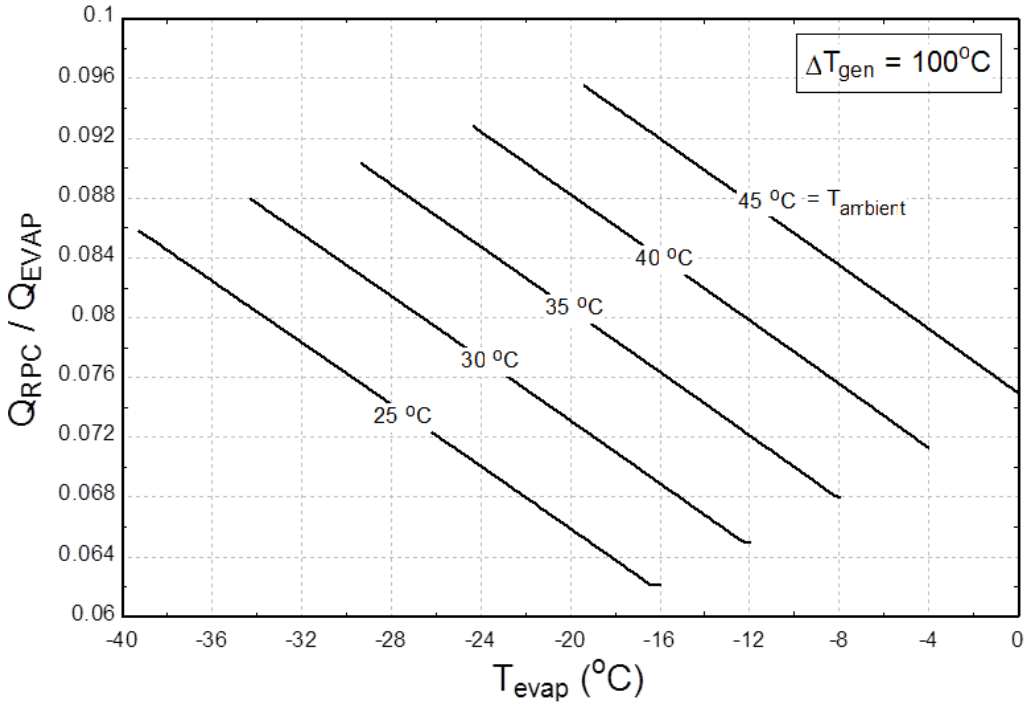

Figure 6-19 Specific heat recovered by refrigerant pre-cooler for varying evaporator temperature

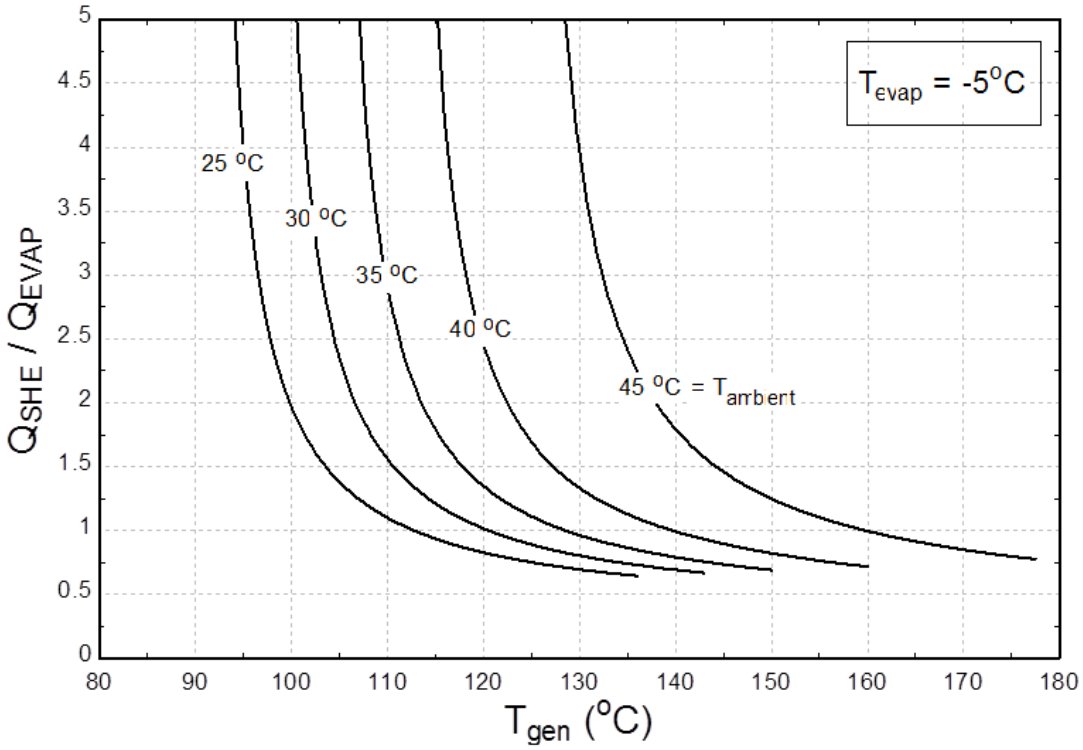

Figure 6-20 Specific heat recovered by solution heat exchanger for varying generator temperature

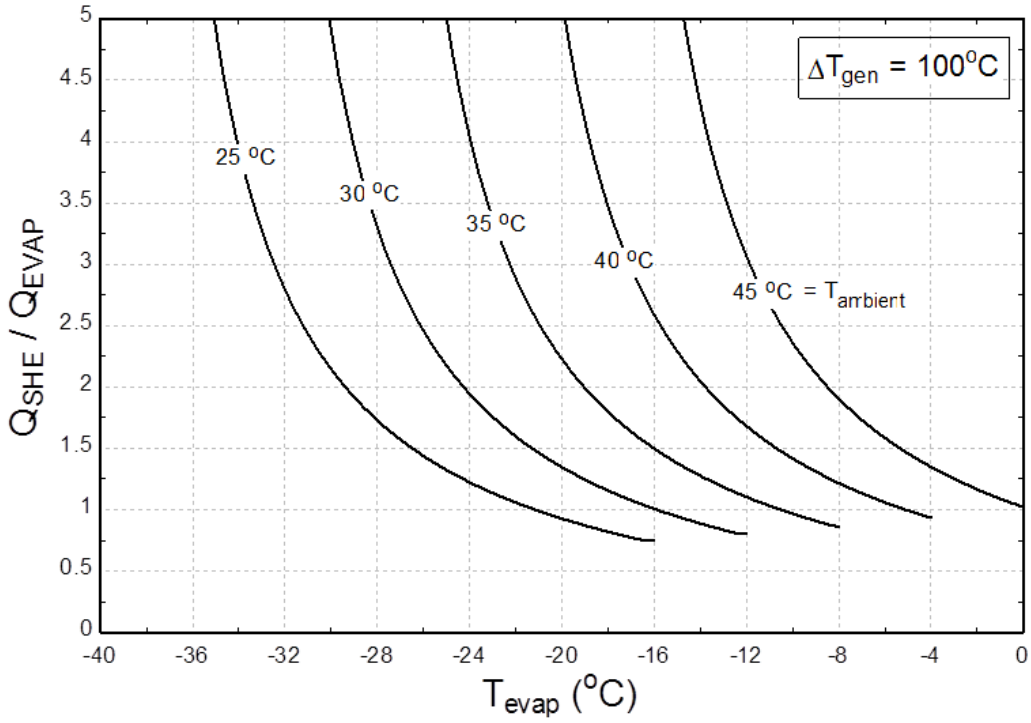

Figure 6-21 Specific heat recovered by solution heat exchanger for varying evaporator temperature

6.2.4 Aqua-Ammonia Solution Concentrations

6.2.4.1 Low Concentration

The low ammonia mass concentration for aqua-ammonia solution in the proposed absorption chiller varies with the generator temperature and the ambient temperature. The low ammonia mass concentration for varying generator and ambient temperature is shown in figure 6-22. It can be seen from the figure 6-22 that at any constant ambient temperature, the low ammonia mass concentration linearly decreases by increasing the generator temperature. It can also be seen from the figure 6-22 that low ammonia mass concentration increases with an increase in the ambient temperature for a fixed generator temperature.

6.2.4.2 High Concentration

The high ammonia mass concentration for aqua-ammonia solution in the proposed absorption chiller varies with the evaporator temperature and the ambient temperature. The high ammonia mass concentration for varying evaporator and ambient temperature is shown in figure 6-23. It can be seen from the figure 6-23 that at any constant ambient temperature, the high ammonia mass concentration linearly increases by increasing the evaporator temperature. It can also be seen from the figure 6-23 that high ammonia mass concentration decreases with an increase in the ambient temperature for a fixed evaporator temperature.

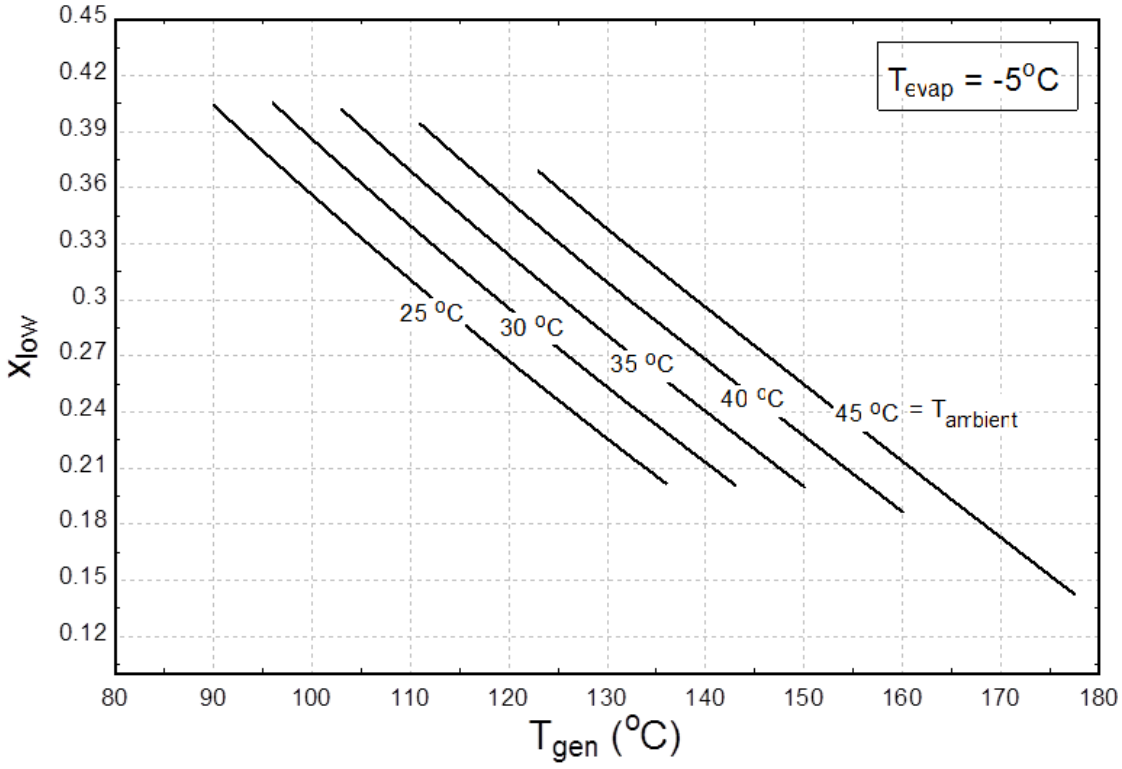

Figure 6-22 Low ammonia mass concentration for varying generator temperatures

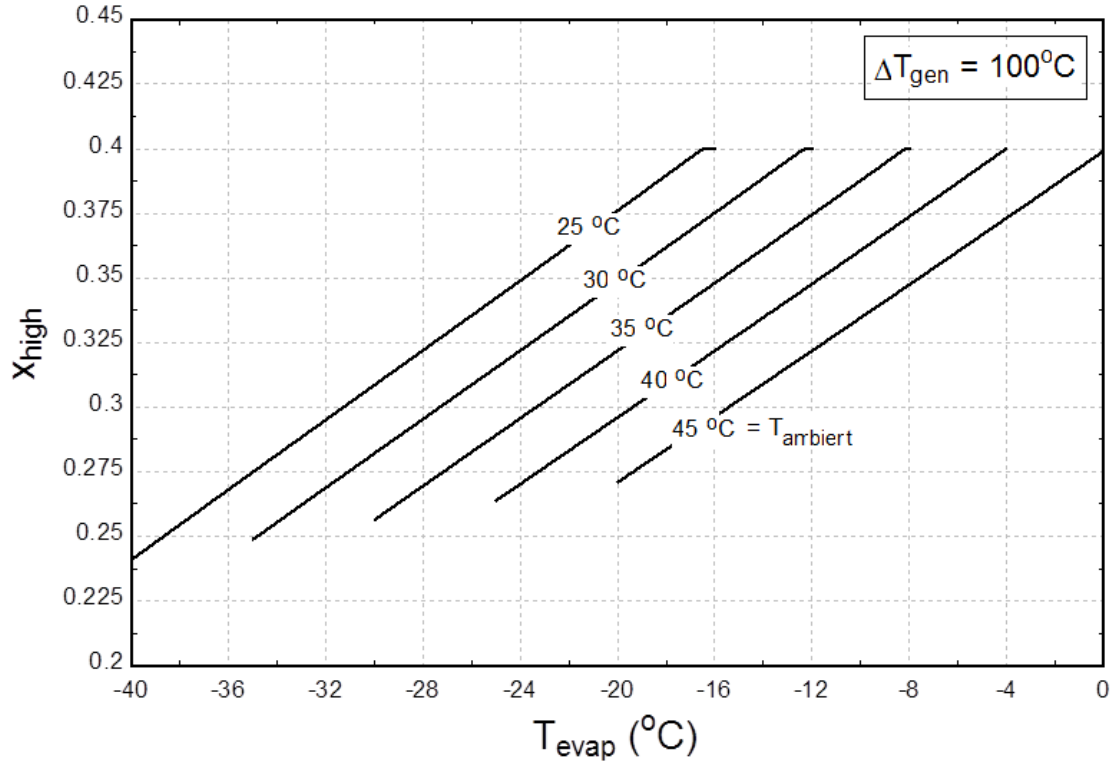

Figure 6-23 High ammonia mass concentration for varying evaporator temperatures

6.2.5 Sensitivity Analysis of Heat Recovery Components

The coefficient of performance of the proposed absorption chiller is sensitive to the effectiveness of the heat recovery components. Thus, the effectiveness of solution heat exchanger and refrigerant pre-cooler effects the coefficient of performance of the absorption chiller which is considered in this section.

6.2.5.1 Solution Heat Exchanger

The coefficient of performance for varying effectiveness of solution heat exchanger and for varying generator and evaporator temperature is shown figure 6-24 and figure 6-25 respectively. It can be seen from figure 6-24, that the optimum coefficient of performance increases from 0.32 to 0.69 for varying the effectiveness of solution heat exchanger from 0.05 to 0.95. Similarly, it can be seen from figure 6-25, that at a fixed evaporator temperature of -20°C, the coefficient of performance increases from 0.12 to 0.53 for varying the effectiveness of solution heat exchanger from 0.05 to 0.95.

6.2.5.2 Refrigerant Pre-Cooler

The coefficient of performance for varying effectiveness of refrigerant pre-cooler and for varying generator and evaporator temperature is shown figure 6-26 and figure 6-27 respectively. It can be seen from figure 6-26, that the optimum coefficient of performance increases from 0.48 to 0.52 for varying the effectiveness of refrigerant pre-cooler from 0.05 to 0.95. Similarly, it can be seen from figure 6-27, that at a fixed evaporator temperature of -20°C, the coefficient of performance increases from 0.24 to 0.28 for varying the effectiveness of refrigerant pre-cooler from 0.05 to 0.95.

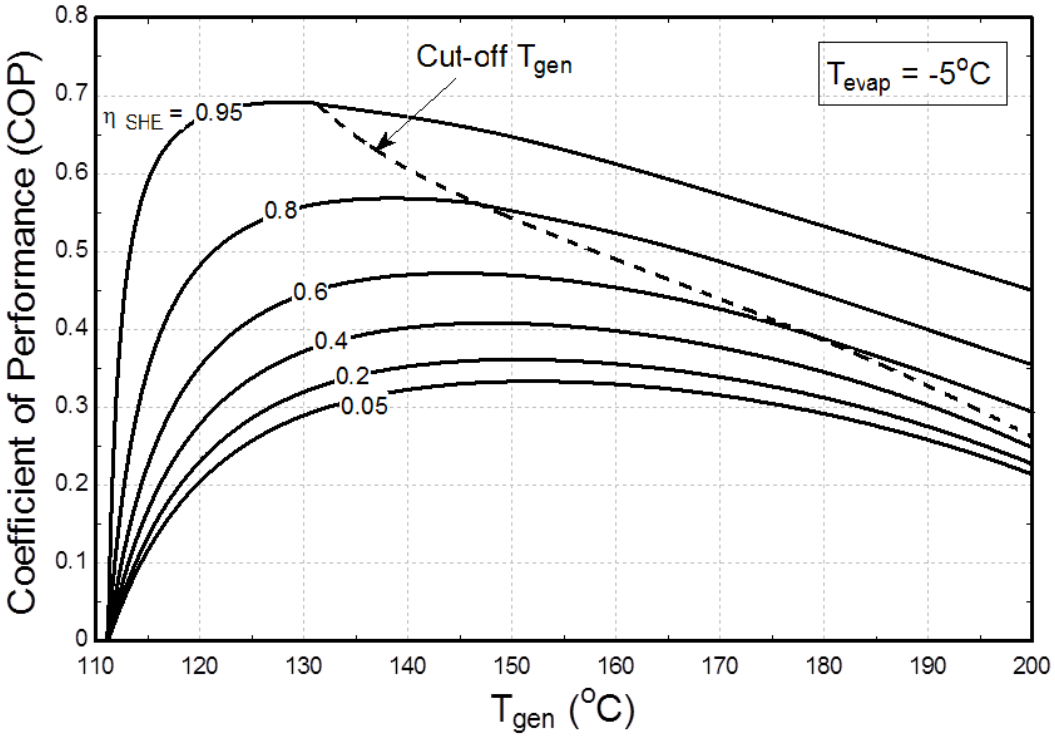

Figure 6-24 Effect of varying effectiveness of solution heat exchanger for varying generator temperature

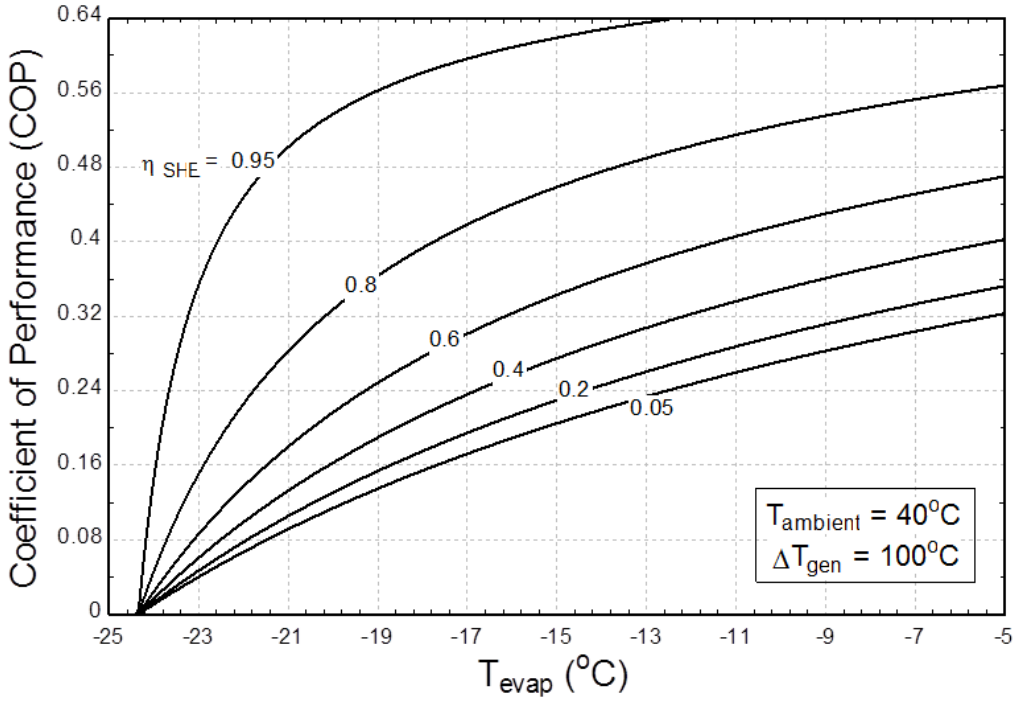

Figure 6-25 Effect of varying effectiveness of solution heat exchanger for varying evaporator temperature

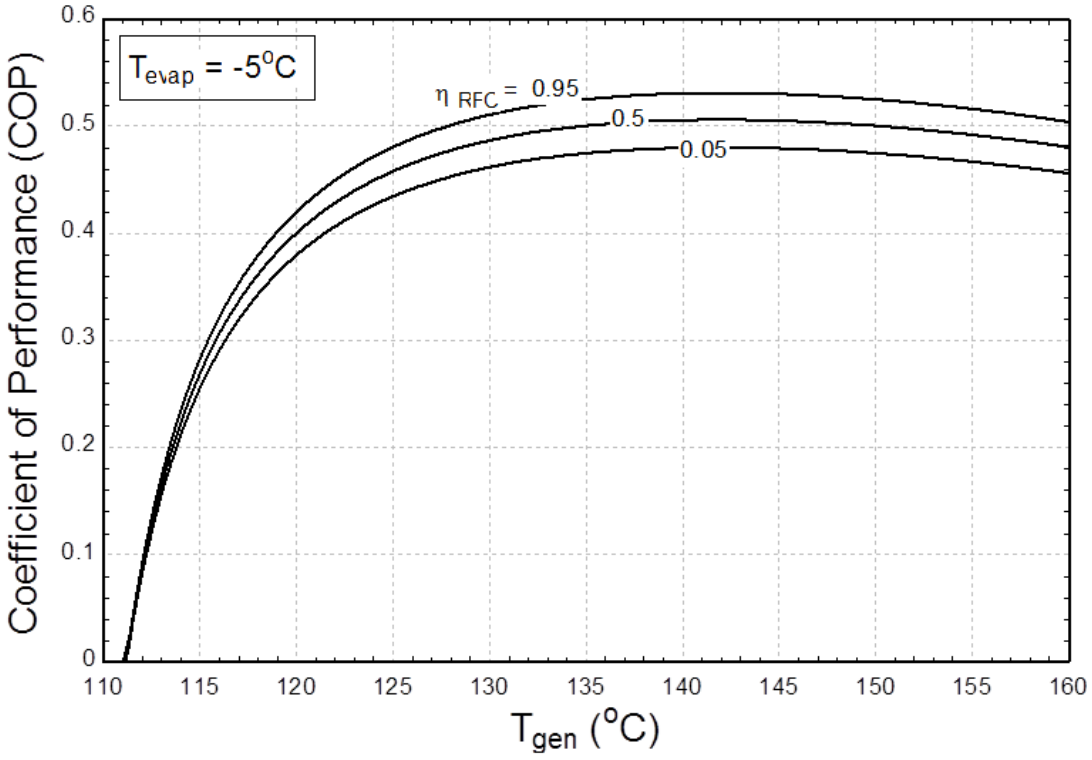

Figure 6-26 Effect of varying effectiveness of refrigerant pre-cooler for varying generator temperature

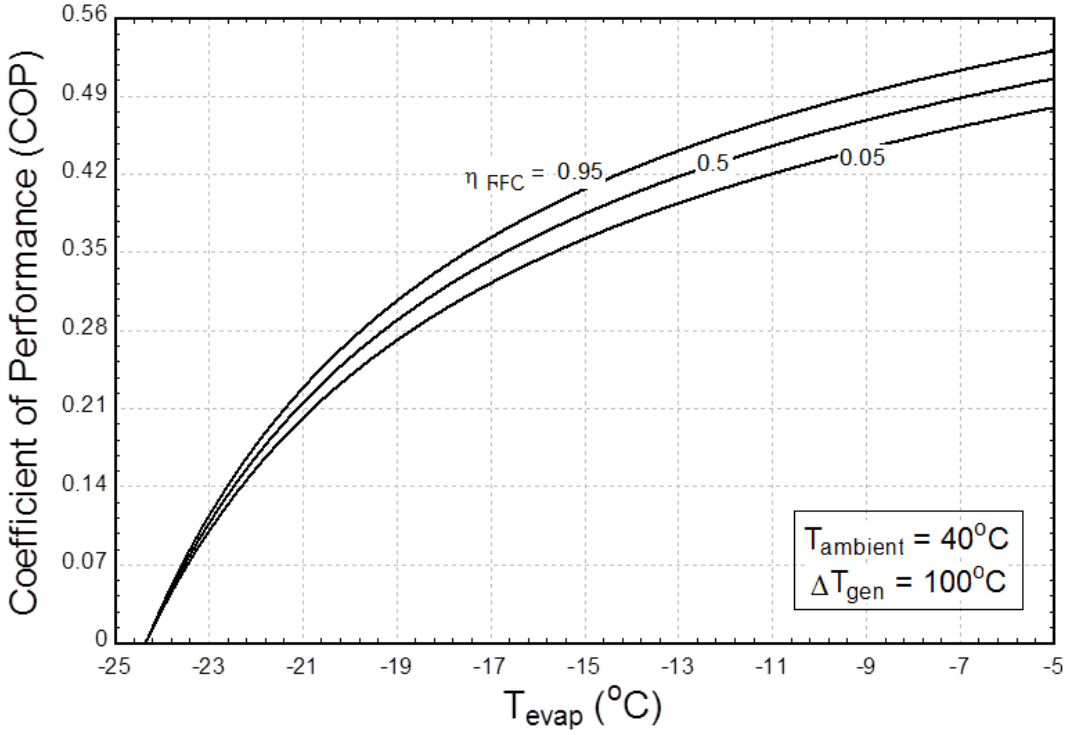

Figure 6-27 Effect of varying effectiveness of refrigerant pre-cooler for varying evaporator temperature

6.3 Second Law of Thermodynamic Analysis

After the first law thermodynamic analysis of the proposed absorption chiller in the previous section 6.2, the simulation results for the second law of thermodynamic analysis of the proposed absorption chiller has been developed in this section based on the mathematical modeling described in chapter 5.

6.3.1 Coefficient of Performance

In order to determine the second law efficiency of the proposed absorption chiller, it is initially required to determine the maximum coefficient of performance. The maximum coefficient of performance for varying generator and ambient temperature is shown in figure 6-28. The analysis has been conducted at an evaporator temperature of -5°C. It can be seen from the figure 6-28 that for any ambient temperature, the maximum coefficient of performance linearly increases with the generator temperature. Also it can be seen from the figure 6-28 that increasing the ambient temperature decreases the maximum coefficient of performance. However under any case, the maximum coefficient is performance remains above 1.

The maximum coefficient of performance for varying evaporator and ambient temperature is shown in figure 6-29. The analysis has been conducted at a generator temperature of 100°C higher than the ambient temperature. It can be seen from the figure 6-29 that for any ambient temperature, the maximum coefficient of performance increases with the evaporator temperature. Also it can be seen from the figure 6-29 that increasing the ambient temperature decreases the maximum coefficient of performance. However under any case, the maximum coefficient is performance remains above 0.9.

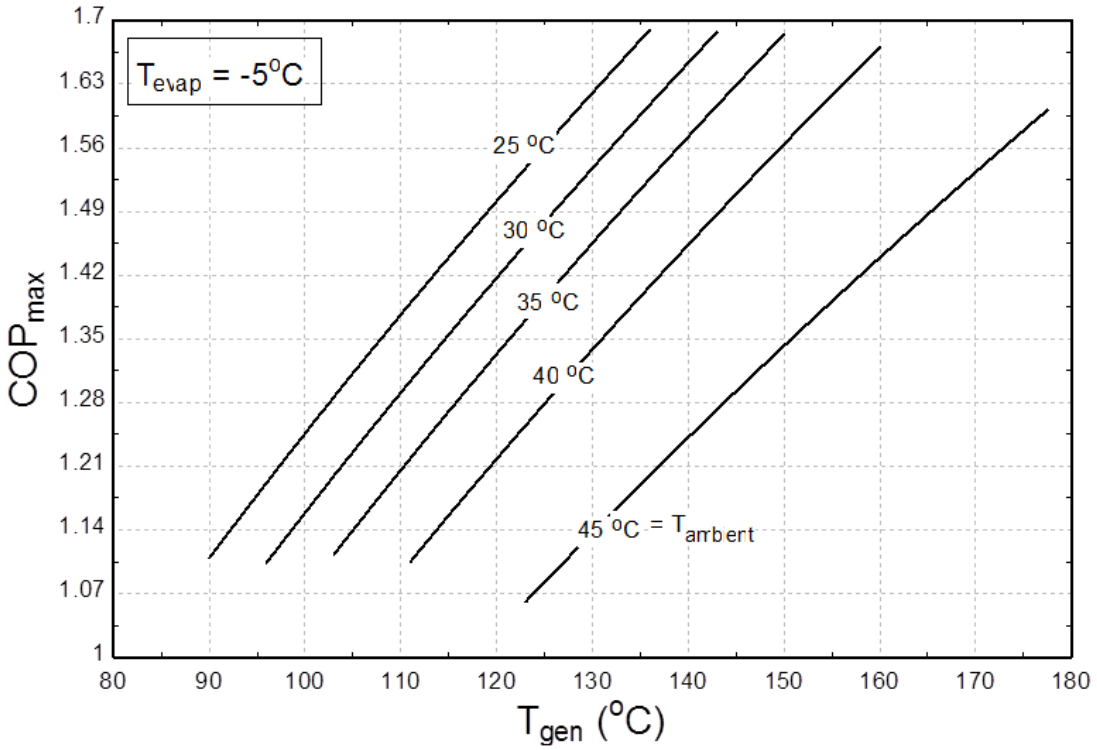

Figure 6-28 Maximum coefficient of performance for varying generator temperature

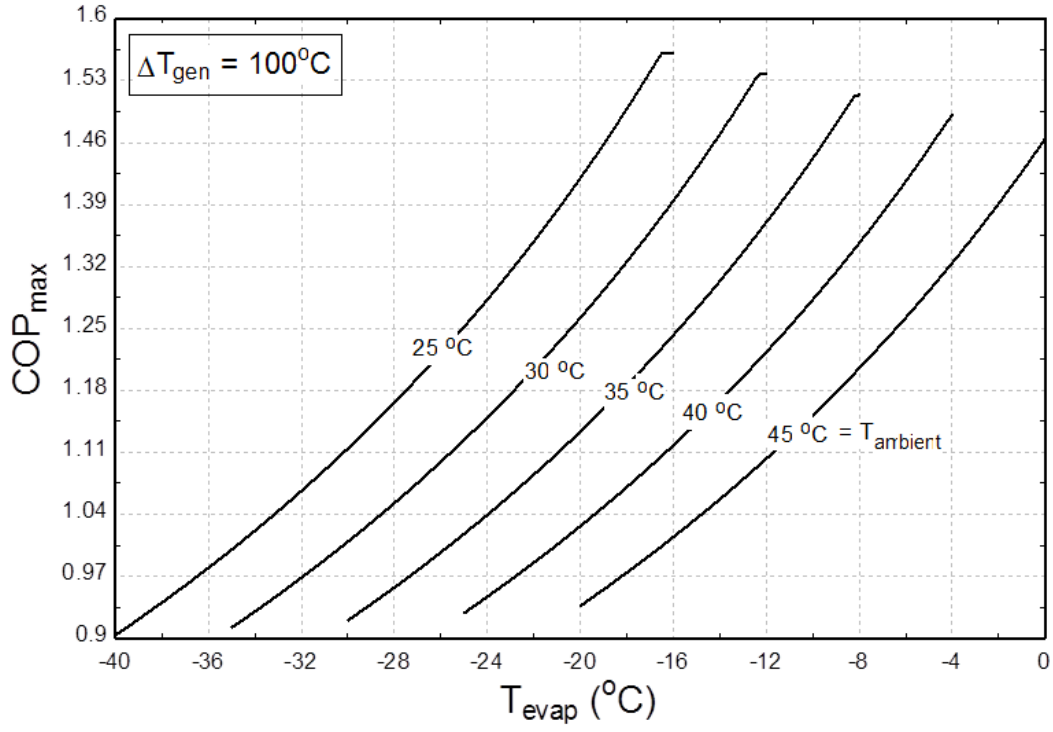

Figure 6-29 Maximum coefficient of performance for varying evaporator temperature

The exergetic coefficient of performance is shown in figure 6-30 when operated at varying ambient and generator temperature. The analysis has been conducted at an evaporator temperature of -5°C. It can be seen from the figure 6-30 that, at any constant ambient temperature, the exergetic coefficient of performance increases by increasing the generator temperature, becomes maximum at an optimum generator temperature and then slowly drops by further increasing the generator temperature. Also it can be seen from figure 6-30 that the optimum generator temperature increases with the increasing ambient temperature whereas the optimum exergetic coefficient of performance decreases with the increasing ambient temperature. Thus, when increasing the ambient temperature from 25°C to 45°C, the optimum generator temperature increases from 107°C to 145°C whereas the optimum exergetic coefficient of performance decreases from 0.39 to 0.35.

The exergetic coefficient of performance is shown in figure 6-31 when operated at varying ambient and evaporator temperature. The analysis has been conducted at a generator temperature of 100°C higher than the ambient temperature. It can be seen from the figure 6-31 that, at any constant ambient temperature, the exergetic coefficient of performance increases by increasing the evaporator temperature, becomes maximum at an optimum evaporator temperature and then slowly drops by further increasing the evaporator temperature. Also it can be seen from figure 6-31 that the optimum evaporator temperature increases with the increasing ambient temperature whereas the optimum exergetic coefficient of performance decreases with the increasing ambient temperature. Thus, when increasing the ambient temperature from 25°C to 45°C, the optimum evaporator temperature increases from -25°C to -5°C whereas the optimum exergetic coefficient of performance decreases from 0.38 to 0.36.

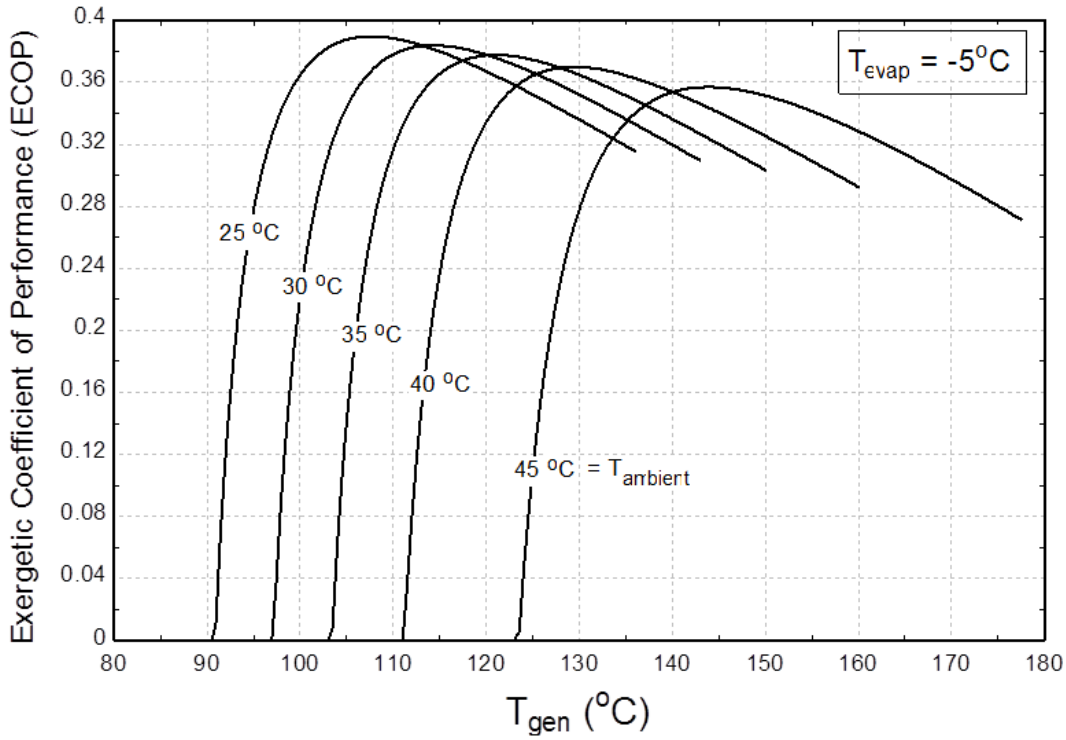

Figure 6-30 Exergetic coefficient of performance for varying generator temperature

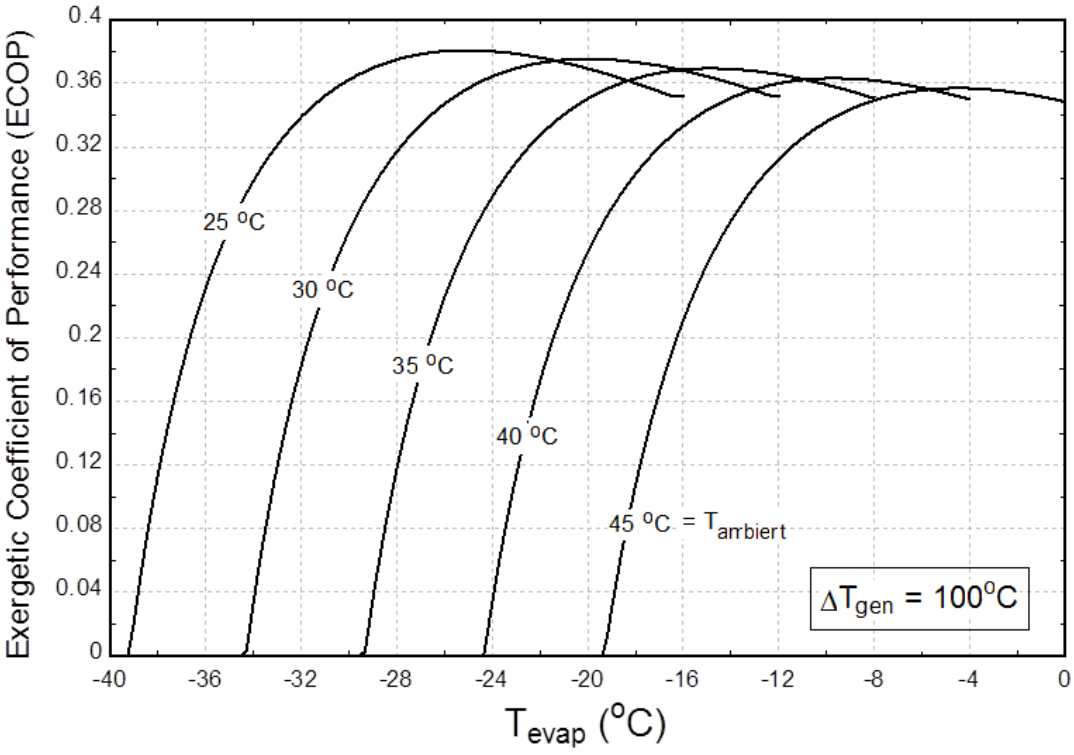

Figure 6-31 Exergetic coefficient of performance for varying evaporator temperature

The comparison between first law and second law efficiency is shown in the figure 6-32 when operated at varying ambient and generator temperature. The analysis has been conducted at an evaporator temperature of -5°C. It can be seen from the figure 6-32 that, at any constant ambient temperature, both the coefficient of performance and the exergetic coefficient of performance follows the same trend however, the values of coefficient of performance is much larger than the values of exergetic coefficient of performance. Also it can be seen from figure 6-32 that the optimum generator temperature, at a fixed ambient temperature, is higher for first law efficiency compared to second law efficiency. Thus, for an ambient temperature of 40°C, the first law efficiency is 0.52 for an optimum generator temperature of 142°C whereas the second law efficiency is 0.37 for an optimum generator temperature of 125°C.

The comparison between first law and second law efficiency is shown in the figure 6-33 when operated at varying ambient and evaporator temperature. The analysis has been conducted at a generator temperature of 100°C higher than the ambient temperature. It can be seen from the figure 6-33 that, at any constant ambient temperature, the values of coefficient of performance is much larger than the values of exergetic coefficient of performance. Also it can be seen from figure 6-33 that the optimum evaporator temperature, at a fixed ambient temperature, is higher for first law efficiency compared to second law efficiency. Thus, for an ambient temperature of 40°C, the first law efficiency is 0.52 for an optimum evaporator temperature of -5°C whereas the second law efficiency is 0.37 for an optimum evaporator temperature of -10°C.

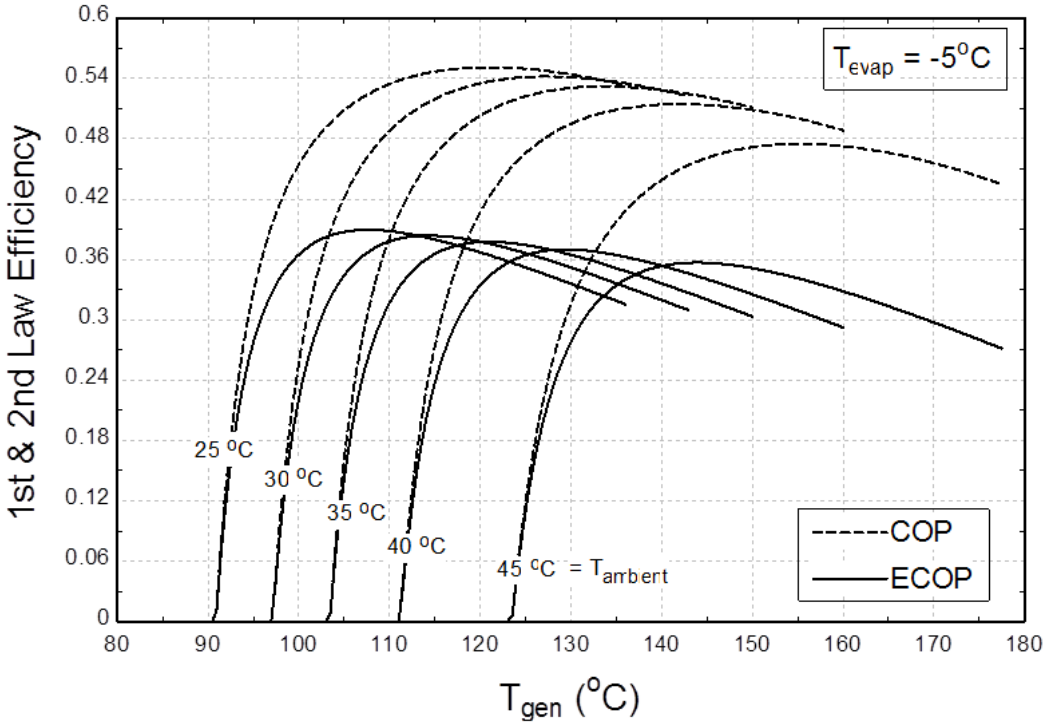

Figure 6-32 First & second law efficiency for varying generator temperature

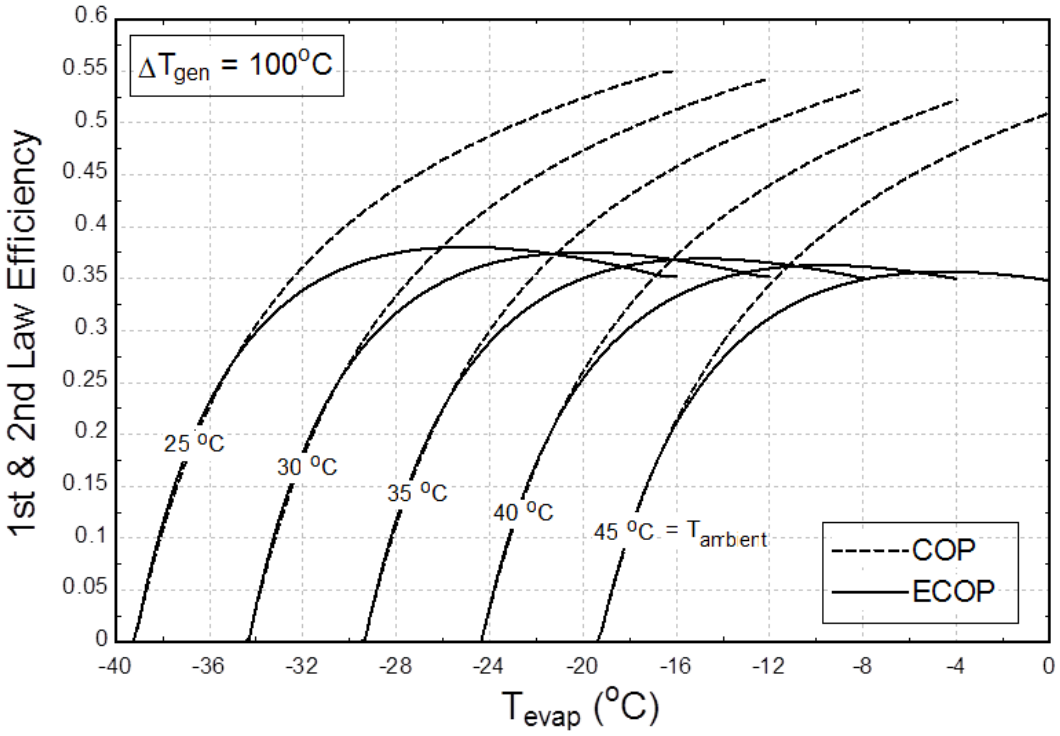

Figure 6-33 First & second law efficiency for varying evaporator temperature

6.3.2 Exergy Losses

This section deals with the simulated results for the exergy losses of various components of the proposed absorption chiller.

6.3.2.1 Total Exergy losses

The total exergy losses in the proposed absorption chiller is a sum of the exergy losses of all the components of the absorption chiller. The total exergy losses is shown in figure 6-34 when operated at varying ambient and generator temperature and at an evaporator temperature of -5°C. It can be seen from the figure 6-34 that, at any constant ambient temperature, the total exergy losses decreases by increasing the generator temperature, becomes minimum at an optimum generator temperature and then increases by further increasing the generator temperature. Also it can be seen from figure 6-34 that the optimum generator temperature increases with the increasing ambient temperature whereas the minimum total exergy losses increases with the increasing ambient temperature. Thus, when increasing the ambient temperature from 25°C to 45°C, the optimum generator temperature increases from 101°C to 136°C whereas the minimum total exergy losses increases from 2.75kW to 3.2kW.

Similarly, the total exergy losses is shown in figure 6-35 when operated at varying ambient and evaporator temperature and at a generator temperature of 100°C higher than the ambient temperature. It can be seen from the figure 6-35 that, at any constant ambient temperature, the total exergy losses decreases by increasing the evaporator temperature, becomes minimum at an optimum evaporator temperature and then increases by further increasing the evaporator temperature. Also it can be seen from figure 6-35 that the

optimum evaporator temperature increases with the increasing ambient temperature whereas the minimum total exergy losses remains constant with the increasing ambient temperature. Thus, when increasing the ambient temperature from 25°C to 45°C, the optimum evaporator temperature increases from -26°C to -4°C whereas the minimum total exergy losses remains constant at 3.3kW.

6.3.2.2 Absorber

The exergy loss ratio for the absorber is shown in figure 6-36 when operated at varying ambient and generator temperature and at an evaporator temperature of -5°C. It can be seen from the figure 6-36 that, at any constant ambient temperature, the exergy loss ratio for the absorber increases by increasing the generator temperature, becomes maximum at an optimum generator temperature and then decreases by further increasing the generator temperature. Also it can be seen from figure 6-36 that the optimum generator temperature increases with the increasing ambient temperature whereas the maximum exergy loss ratio for the absorber decreases with the increasing ambient temperature. Thus, when increasing the ambient temperature from 25°C to 40°C, the optimum generator temperature increases from 101°C to 120°C whereas the maximum exergy loss ratio for the absorber decreases from 0.08 to 0.065.

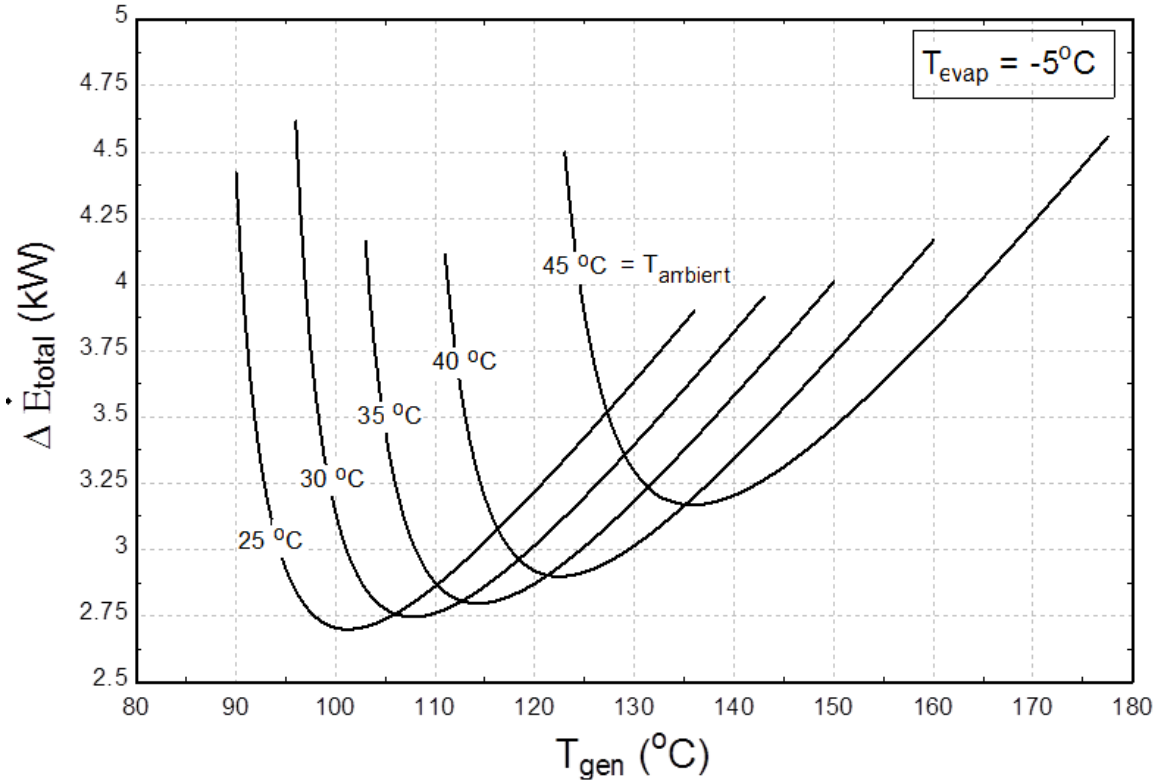

Figure 6-34 Total exergy losses for varying generator temperature

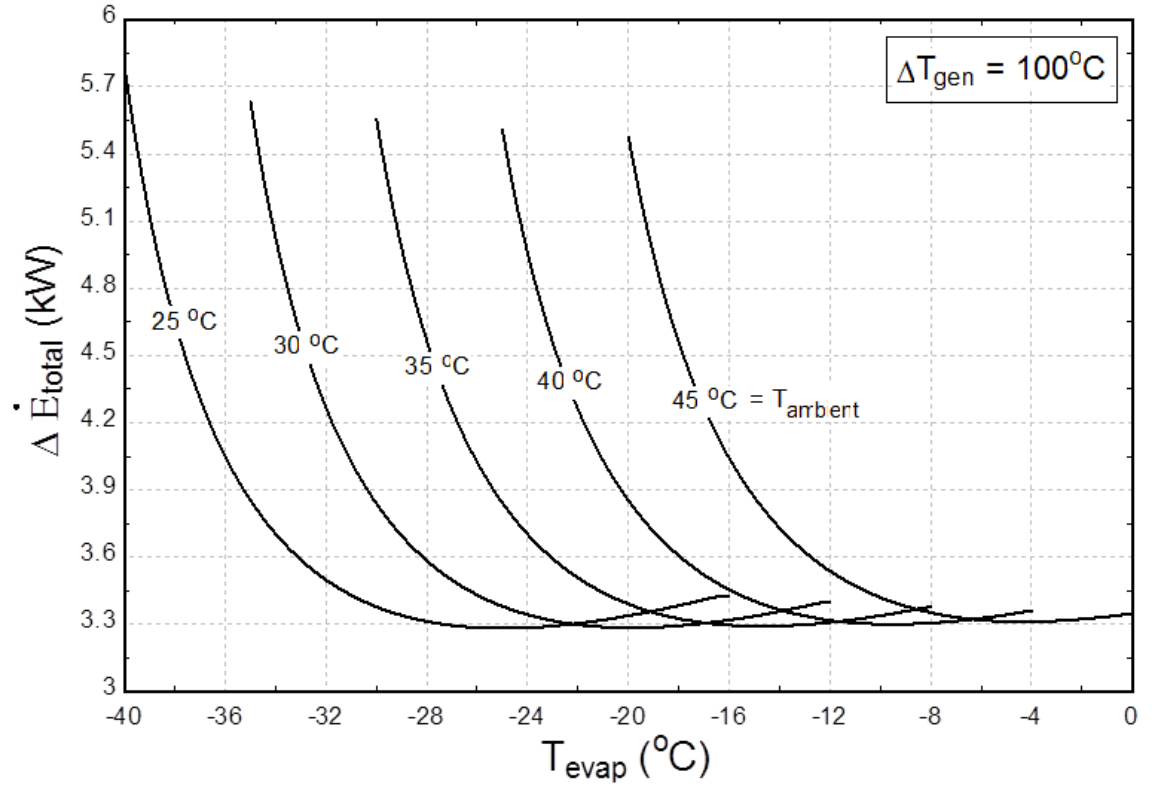

Figure 6-35 Total exergy losses for varying evaporator temperature

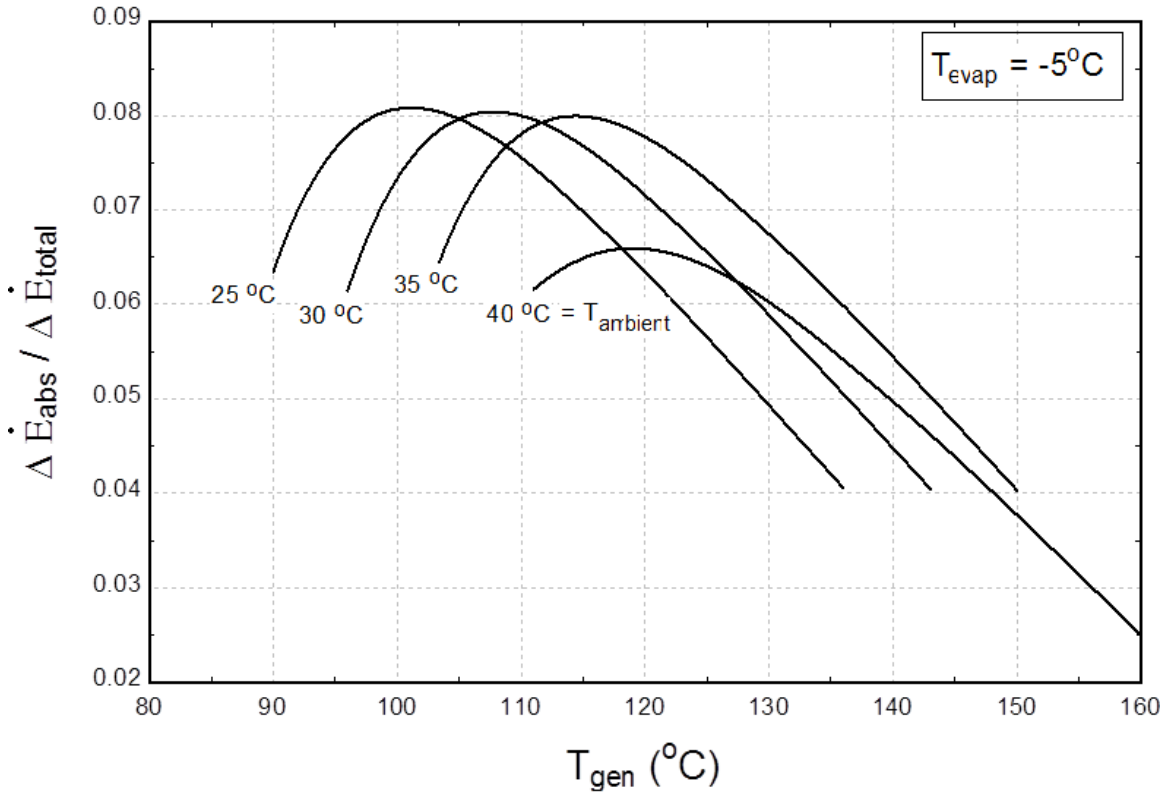

Figure 6-36 Exergy loss ratio of absorber for varying generator temperature

6.3.2.3 Condenser

The exergy loss ratio for the condenser when operated at varying ambient and generator temperature and at an evaporator temperature of -5°C is shown in figure 6-37 whereas when operated at varying ambient and evaporator temperature and at a generator temperature of 100°C higher than the ambient temperature is shown in figure 6-38. It can be seen from the figure 6-37 that, at any constant ambient temperature, the exergy loss ratio for the condenser increases by increasing the generator temperature, becomes maximum at an optimum generator temperature and then decreases by further increasing the generator temperature. However, it can be seen from figure 6-38 that the exergy loss ratio for the condenser increases by increasing the evaporator temperature.

6.3.2.4 Dephlegmator

The exergy loss ratio for the dephlegmator when operated at varying ambient and generator temperature and at an evaporator temperature of -5°C is shown in figure 6-39 whereas when operated at varying ambient and evaporator temperature and at a generator temperature of 100°C higher than the ambient temperature is shown in figure 6-40. It can be seen from the figure 6-39 that, at any constant ambient temperature, the exergy loss ratio for the dephlegmator increases by increasing the generator temperature. Similarly, it can also be seen from figure 6-40 that the exergy loss ratio for the dephlegmator increases by increasing the evaporator temperature.

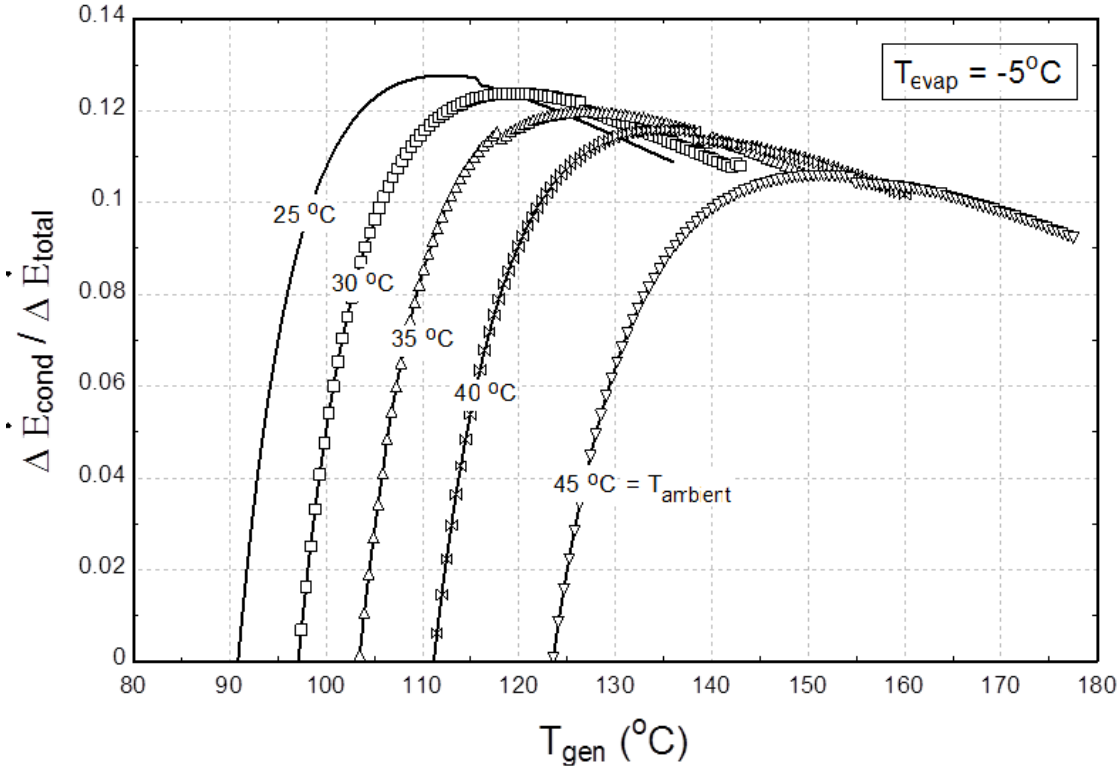

Figure 6-37 Exergy loss ratio of condenser for varying generator temperature

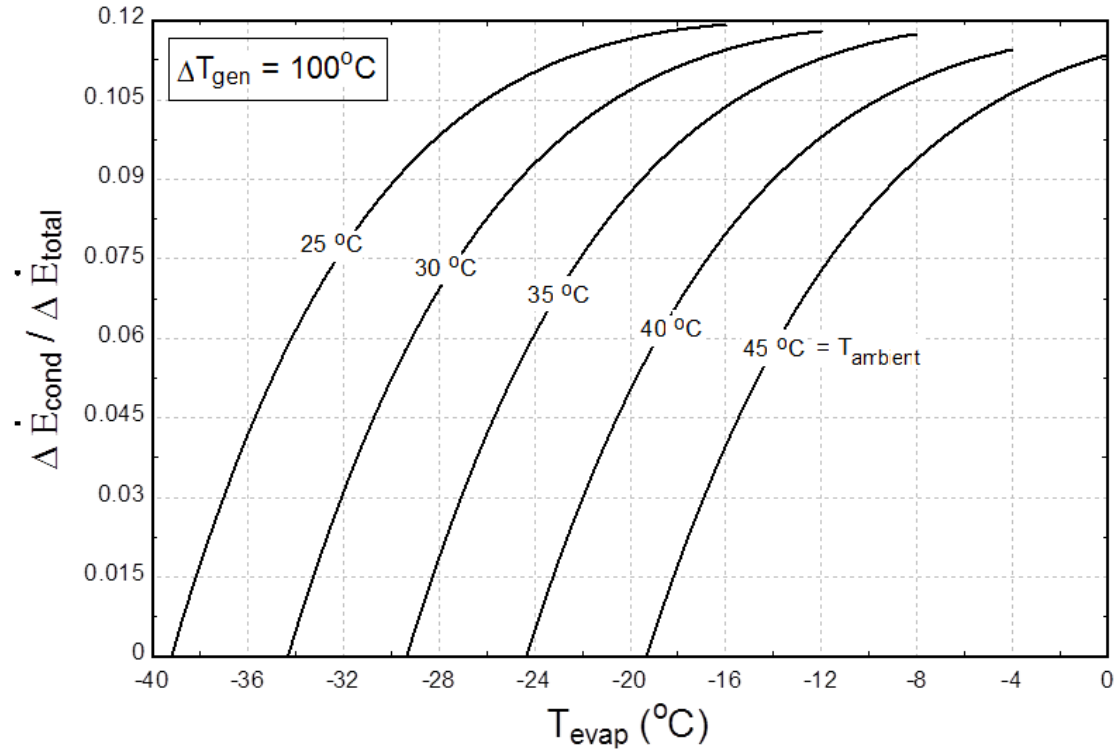

Figure 6-38 Exergy loss ratio of condenser for varying evaporator temperature

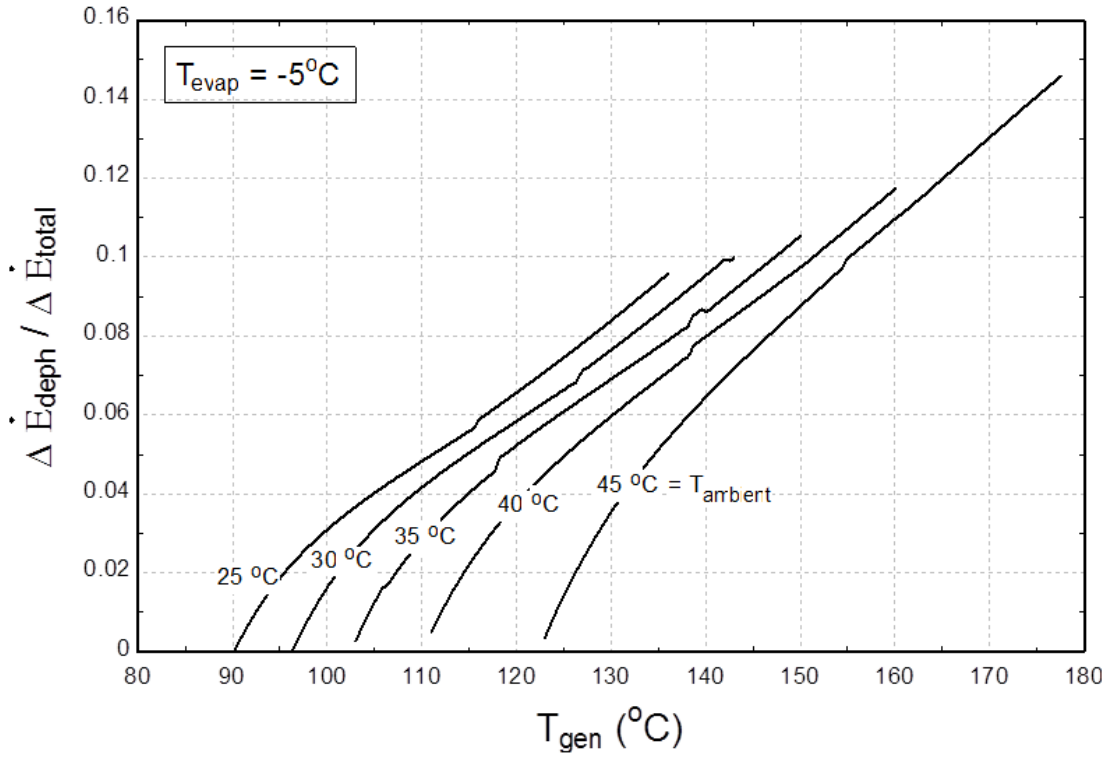

Figure 6-39 Exergy loss ratio of dephlegmator for varying generator temperature

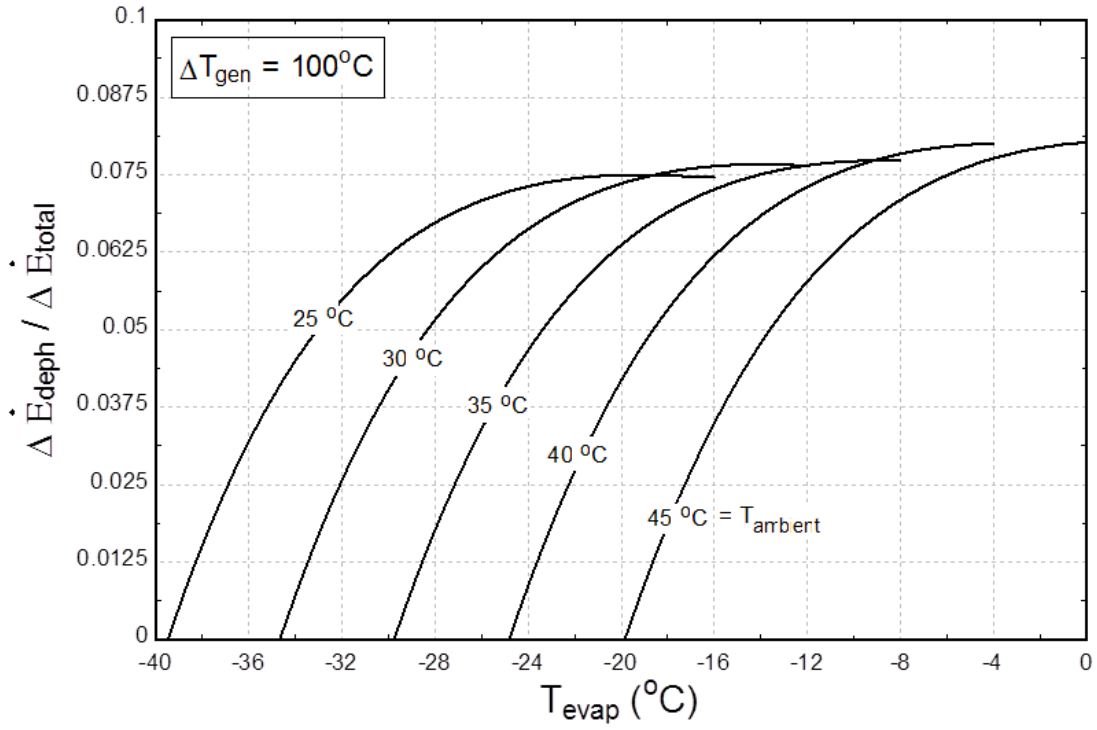

Figure 6-40 Exergy loss ratio of dephlegmator for varying evaporator temperature

6.3.2.5 Evaporator

The exergy loss ratio for the evaporator when operated at varying ambient and generator temperature and at an evaporator temperature of -5°C is shown in figure 6-41 whereas when operated at varying ambient and evaporator temperature and at a generator temperature of 100°C higher than the ambient temperature is shown in figure 6-42. It can be seen from the figure 6-41 that, at any constant ambient temperature, the exergy loss ratio for the evaporator increases by increasing the generator temperature, becomes maximum at an optimum generator temperature and then decreases by further increasing the generator temperature. However, it can be seen from figure 6-42 that the exergy loss ratio for the evaporator increases by increasing the evaporator temperature.

6.3.2.6 Refrigerant Expansion Valve

The exergy loss ratio for the refrigerant expansion valve when operated at varying ambient and generator temperature and at an evaporator temperature of -5°C is shown in figure 6-43 whereas when operated at varying ambient and evaporator temperature and at a generator temperature of 100°C higher than the ambient temperature is shown in figure 6-44. It can be seen from the figure 6-43 that, at any constant ambient temperature, the exergy loss ratio for the refrigerant expansion valve increases by increasing the generator temperature, becomes maximum at an optimum generator temperature and then decreases by further increasing the generator temperature. However, it can be seen from figure 6-44 that the exergy loss ratio for the refrigerant expansion valve increases by increasing the evaporator temperature.

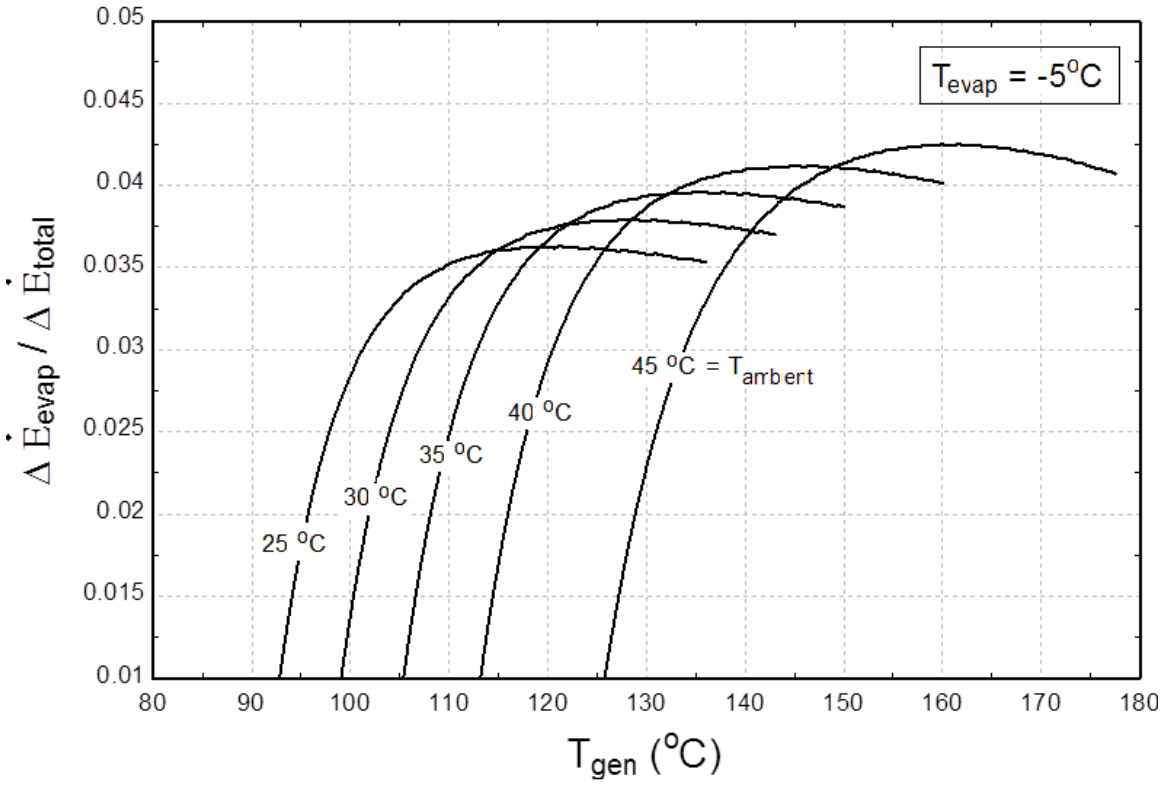

Figure 6-41 Exergy loss ratio of evaporator for varying generator temperature

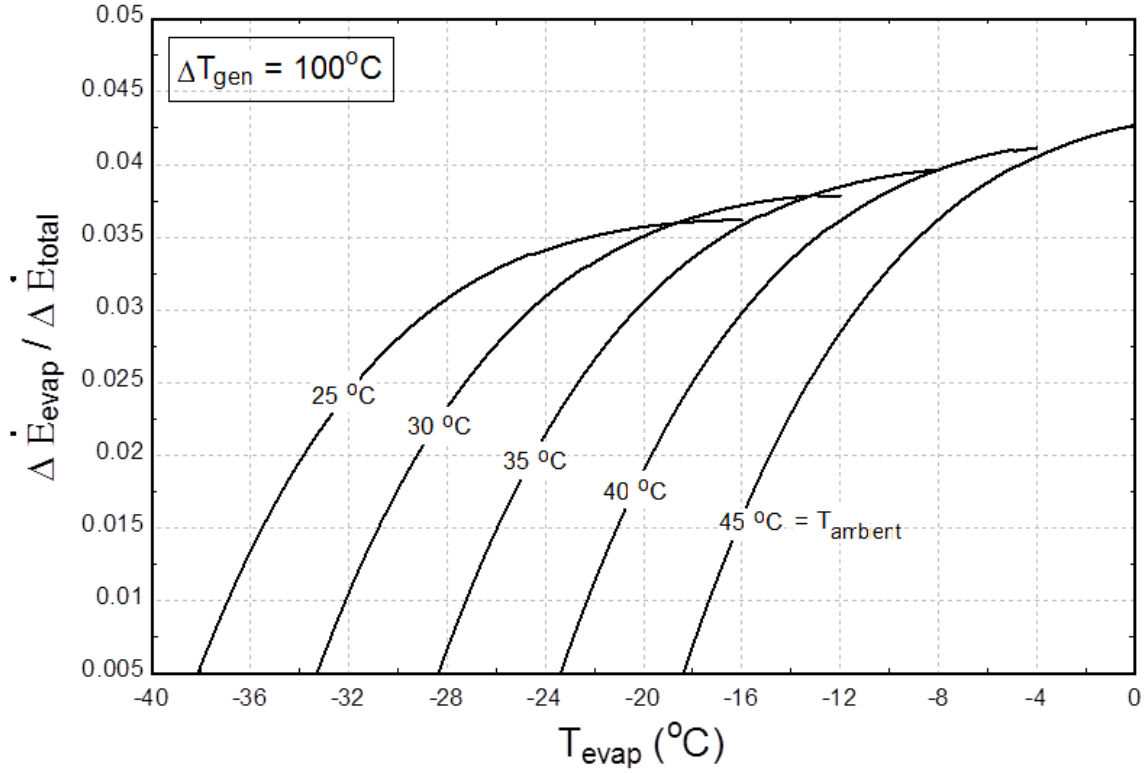

Figure 6-42 Exergy loss ratio of evaporator for varying evaporator temperature

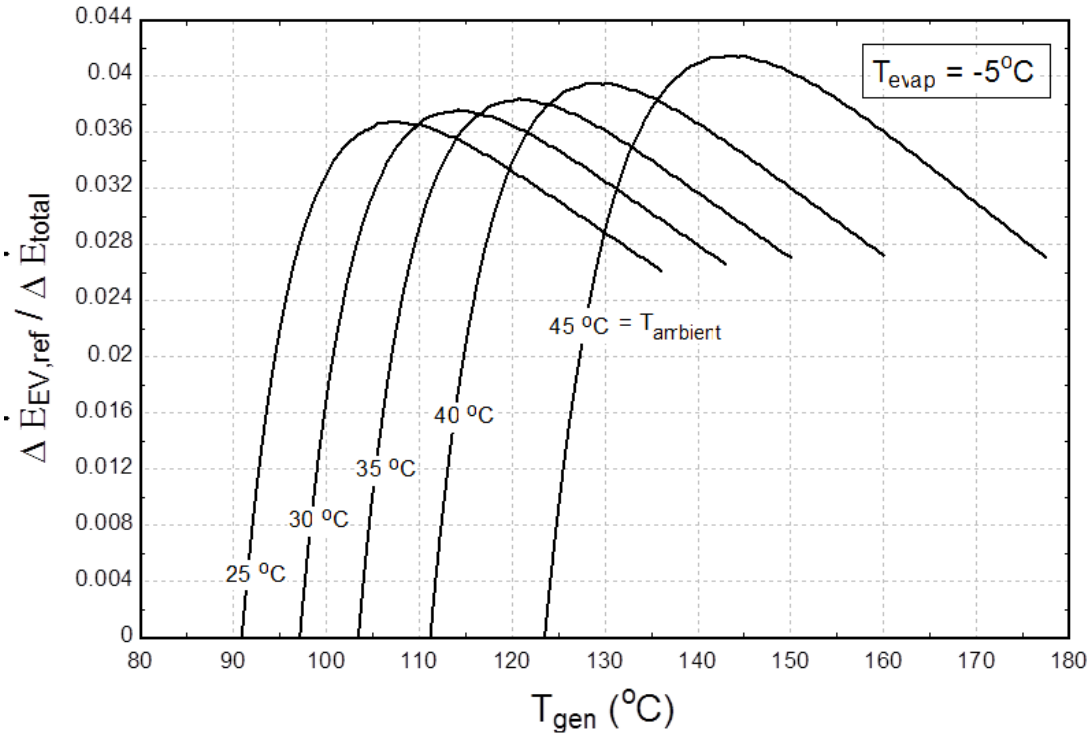

Figure 6-43 Exergy loss ratio of refrigerant expansion valve for varying generator temperature

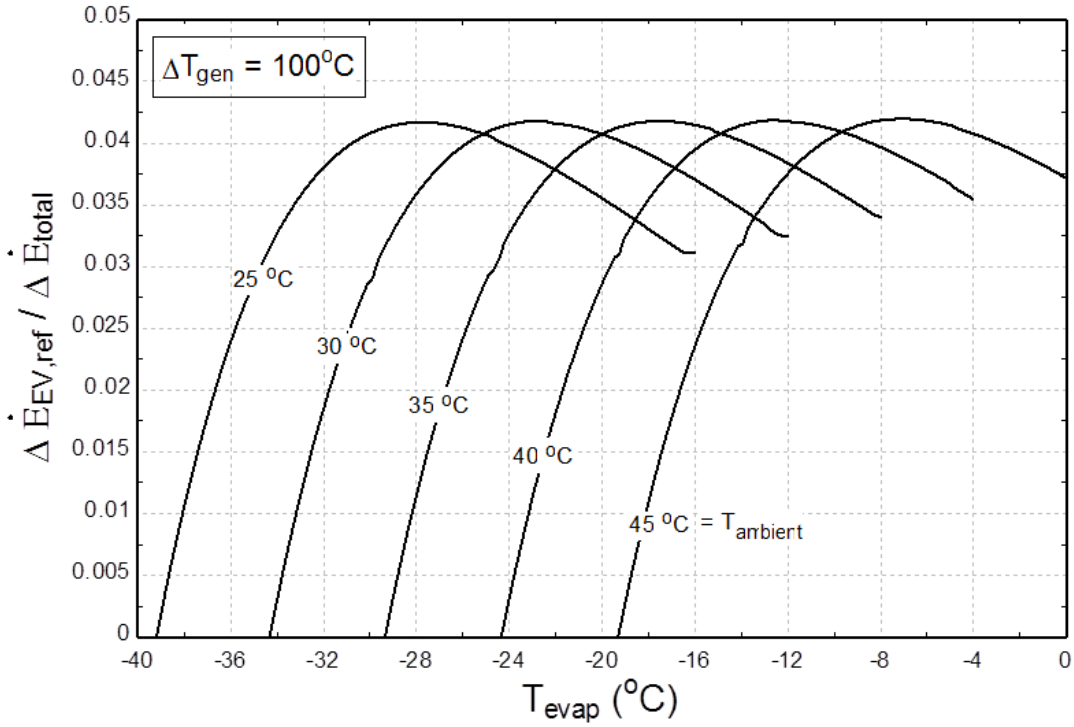

Figure 6-44 Exergy loss ratio of refrigerant expansion valve for varying evaporator temperature

6.3.2.7 Solution Expansion Valve

The exergy loss ratio for the solution expansion valve when operated at varying ambient and generator temperature and at an evaporator temperature of -5°C is shown in figure 6-45 whereas when operated at varying ambient and evaporator temperature and at a generator temperature of 100°C higher than the ambient temperature is shown in figure 6-46. It can be seen from the figure 6-45 that, at any constant ambient temperature, the exergy loss ratio for the solution expansion valve decreases by increasing the generator temperature, becomes approximately constant at very high generator temperature. Similarly, it can be seen from figure 6-46 that the exergy loss ratio for the solution expansion valve decreases by increasing the evaporator temperature.

6.3.2.8 Generator

The exergy loss ratio for the generator when operated at varying ambient and generator temperature and at an evaporator temperature of -5°C is shown in figure 6-47 whereas when operated at varying ambient and evaporator temperature and at a generator temperature of 100°C higher than the ambient temperature is shown in figure 6-48. It can be seen from the figure 6-47 that, at any constant ambient temperature, the exergy loss ratio for the generator decreases by increasing the generator temperature, becomes minimum at an optimum generator temperature and then increases by further increasing the generator temperature. However, it can be seen from figure 6-48 that at any constant ambient temperature, the exergy loss ratio for the generator increases by increasing the evaporator temperature, becomes maximum at an optimum evaporator temperature and then decreases by further increasing the evaporator temperature.

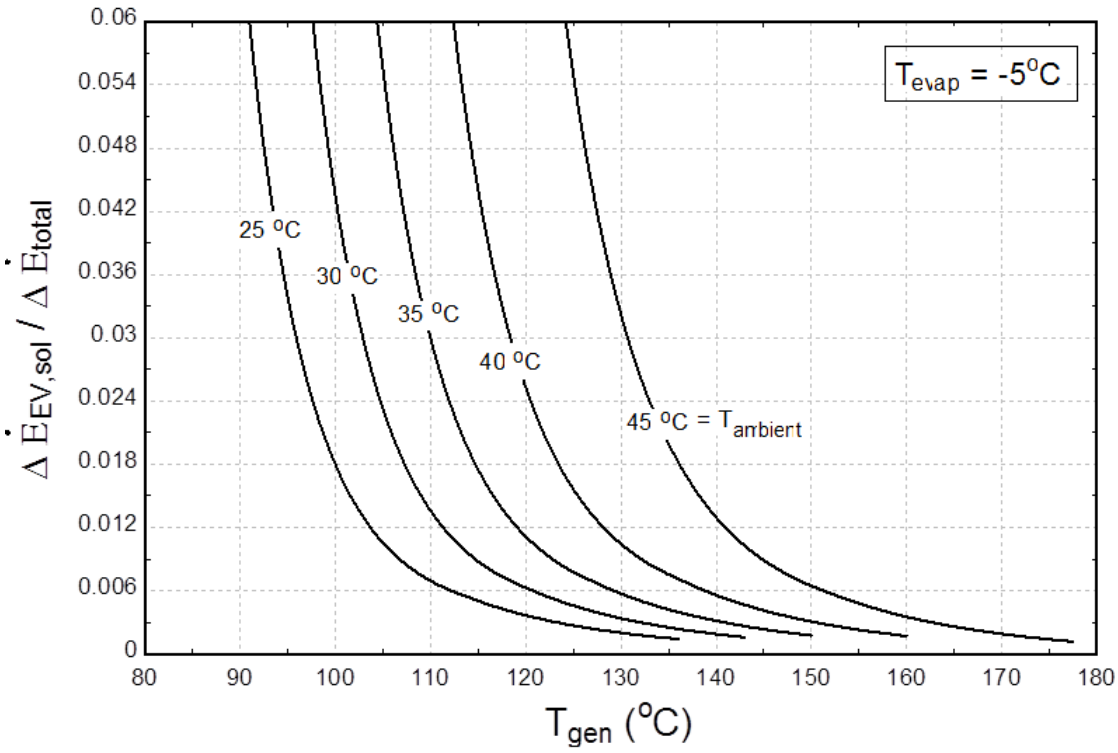

Figure 6-45 Exergy loss ratio of solution expansion valve for varying generator temperature

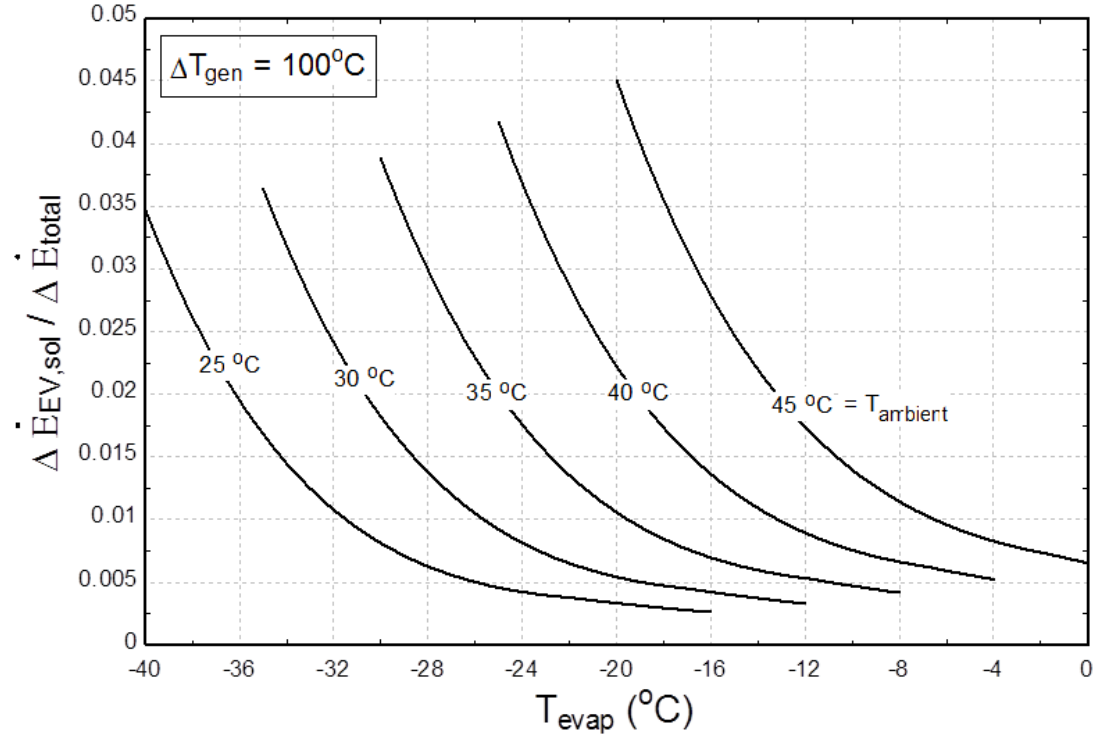

Figure 6-46 Exergy loss ratio of solution expansion valve for varying evaporator temperature

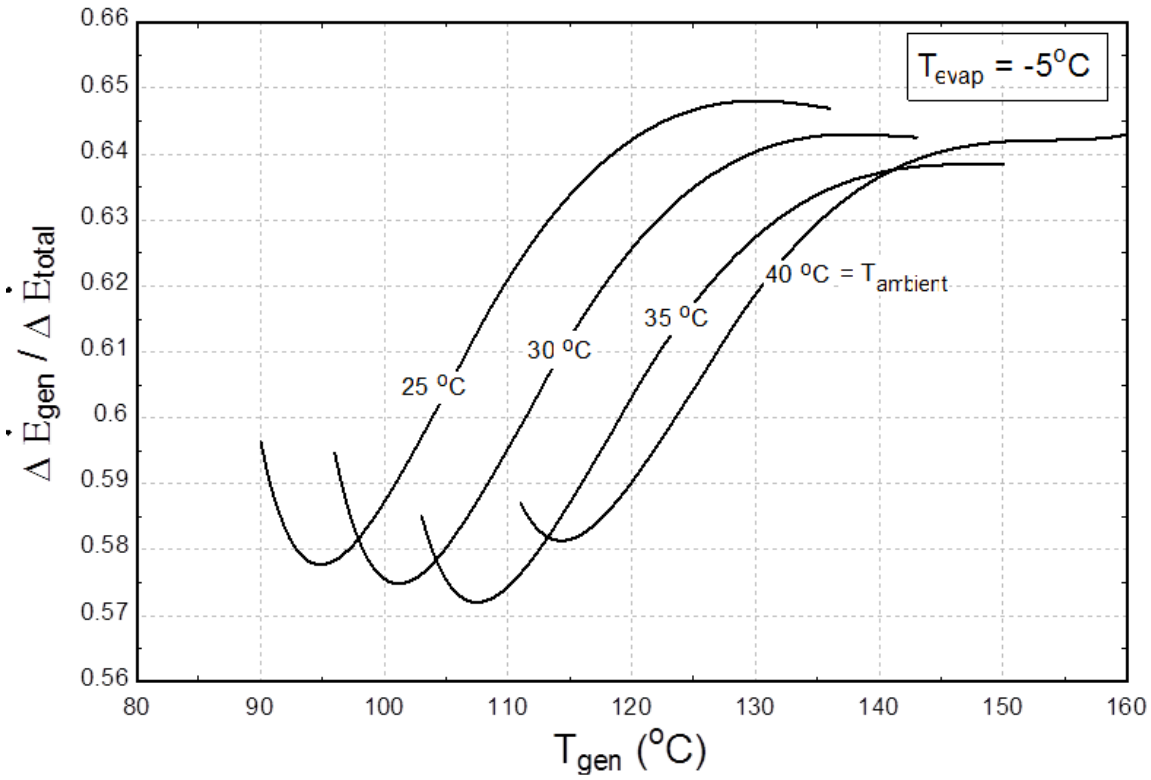

Figure 6-47 Exergy loss ratio of generator for varying generator temperature

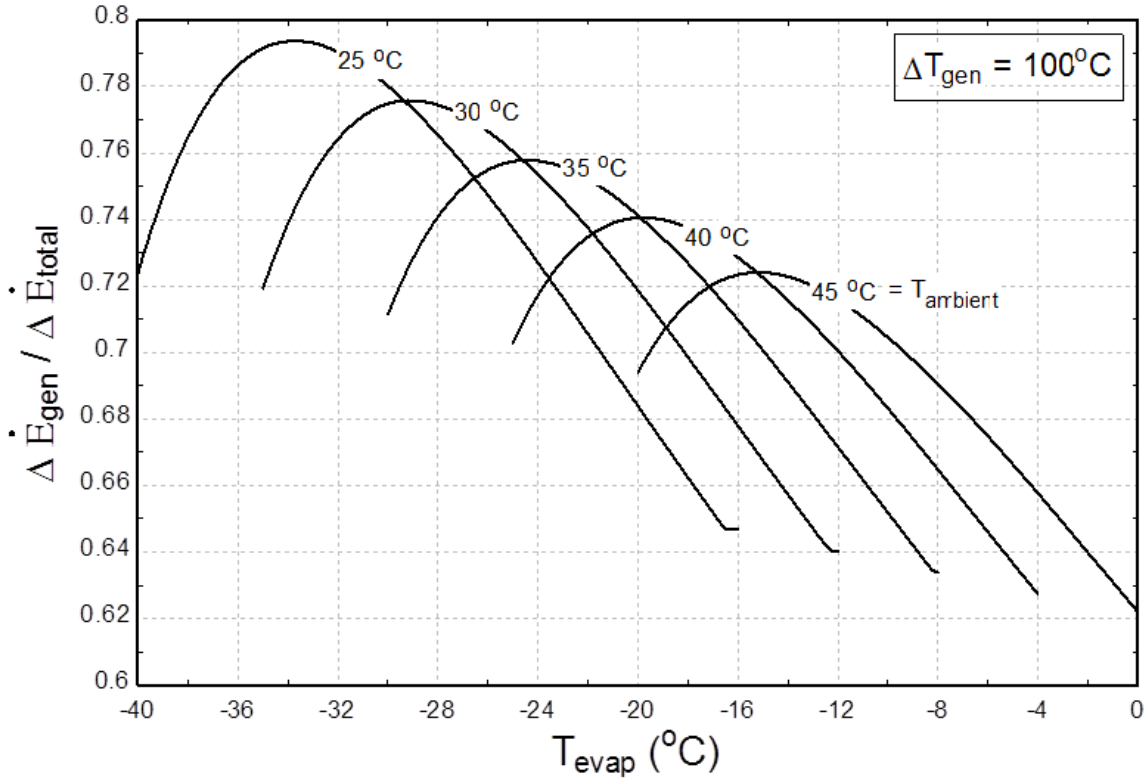

Figure 6-48 Exergy loss ratio of generator for varying evaporator temperature

6.3.2.9 Heat Recovery Coils inside Generator

The exergy loss ratio for the heat recovery coils inside generator when operated at varying ambient and generator temperature and at an evaporator temperature of -5°C is shown in figure 6-49 whereas when operated at varying ambient and evaporator temperature and at a generator temperature of 100°C higher than the ambient temperature is shown in figure 6-50. It can be seen from the figure 6-49 that, at any constant ambient temperature, the exergy loss ratio for the heat recovery coils inside generator decreases by increasing the generator temperature, becomes minimum at an optimum generator temperature and then increases by further increasing the generator temperature. However, it can be seen from figure 6-50 that at any constant ambient temperature, the exergy loss ratio for the heat recovery coils inside generator increases by increasing the evaporator temperature, becomes maximum at an optimum evaporator temperature and then decreases by further increasing the evaporator temperature.

6.3.2.10 Solution pump

The exergy loss ratio for the solution pump when operated at varying ambient and generator temperature and at an evaporator temperature of -5°C is shown in figure 6-51 whereas when operated at varying ambient and evaporator temperature and at a generator temperature of 100°C higher than the ambient temperature is shown in figure 6-52. It can be seen from the figure 6-51 that, at any constant ambient temperature, the exergy loss ratio for the solution pump decreases by increasing the generator temperature, becomes approximately constant at very high generator temperature. Similarly, it can be seen from figure 6-52 that the exergy loss ratio for the solution pump decreases by increasing the evaporator temperature.

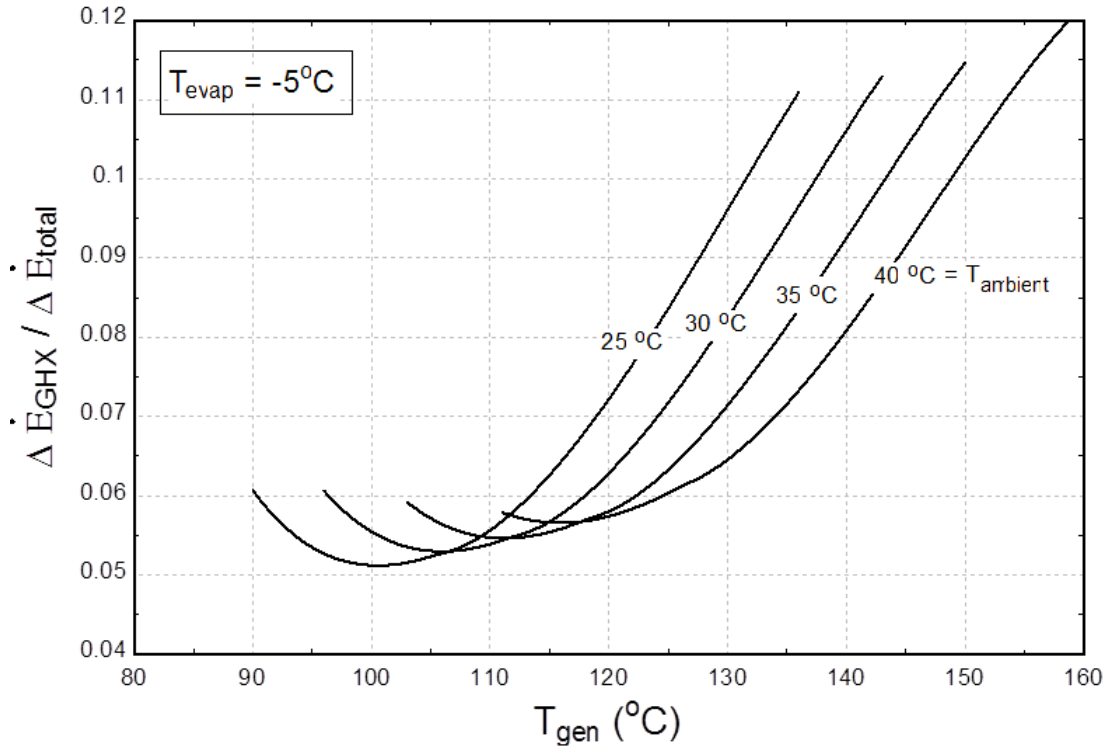

Figure 6-49 Exergy loss ratio of heat exchanger coils in the generator for varying generator temperature

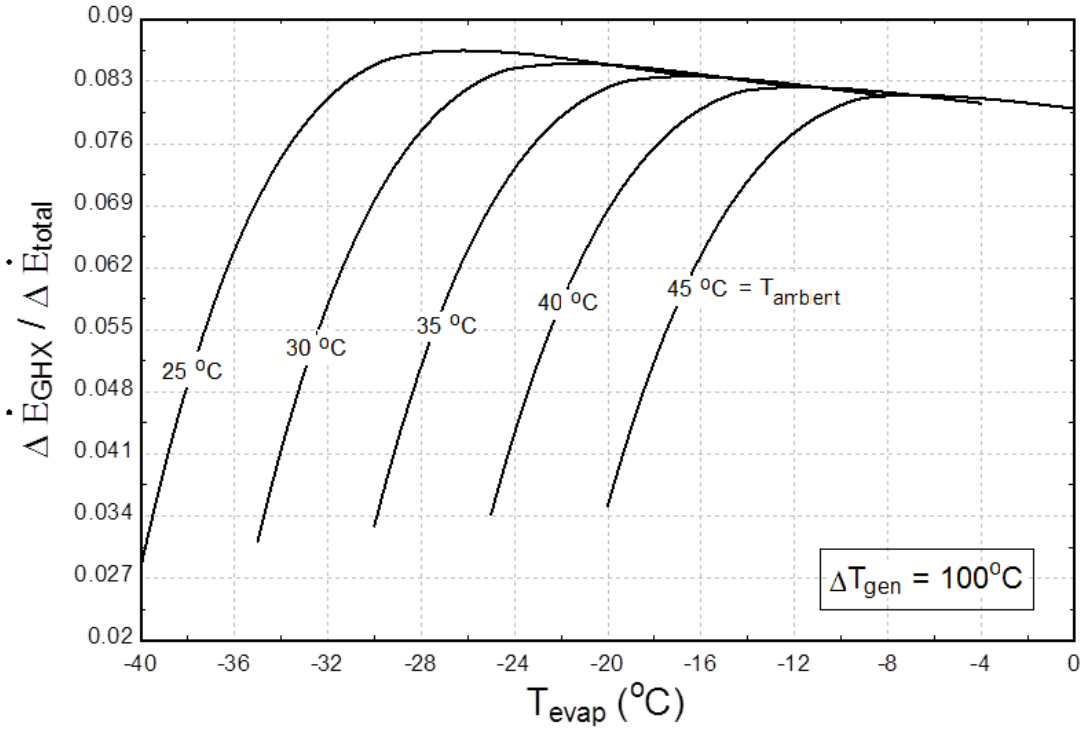

Figure 6-50 Exergy loss ratio of heat exchanger coils in the generator for varying evaporator temperature

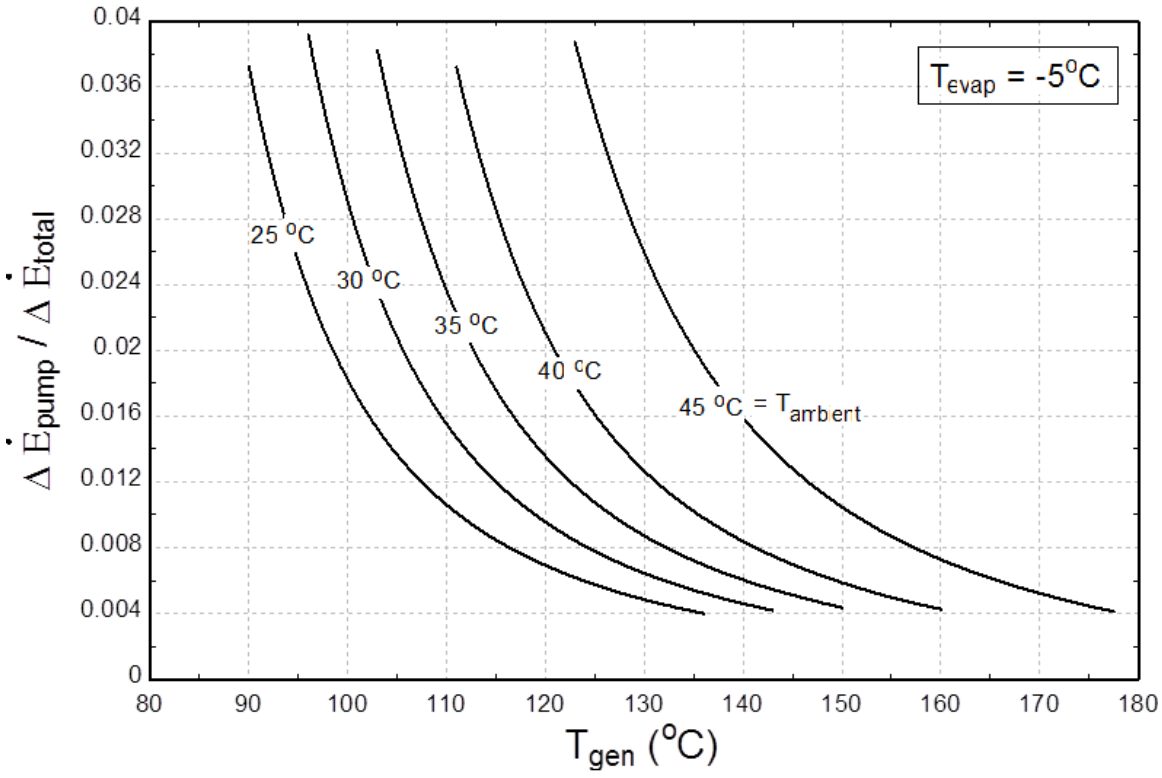

Figure 6-51 Exergy loss ratio of solution pump for varying generator temperature

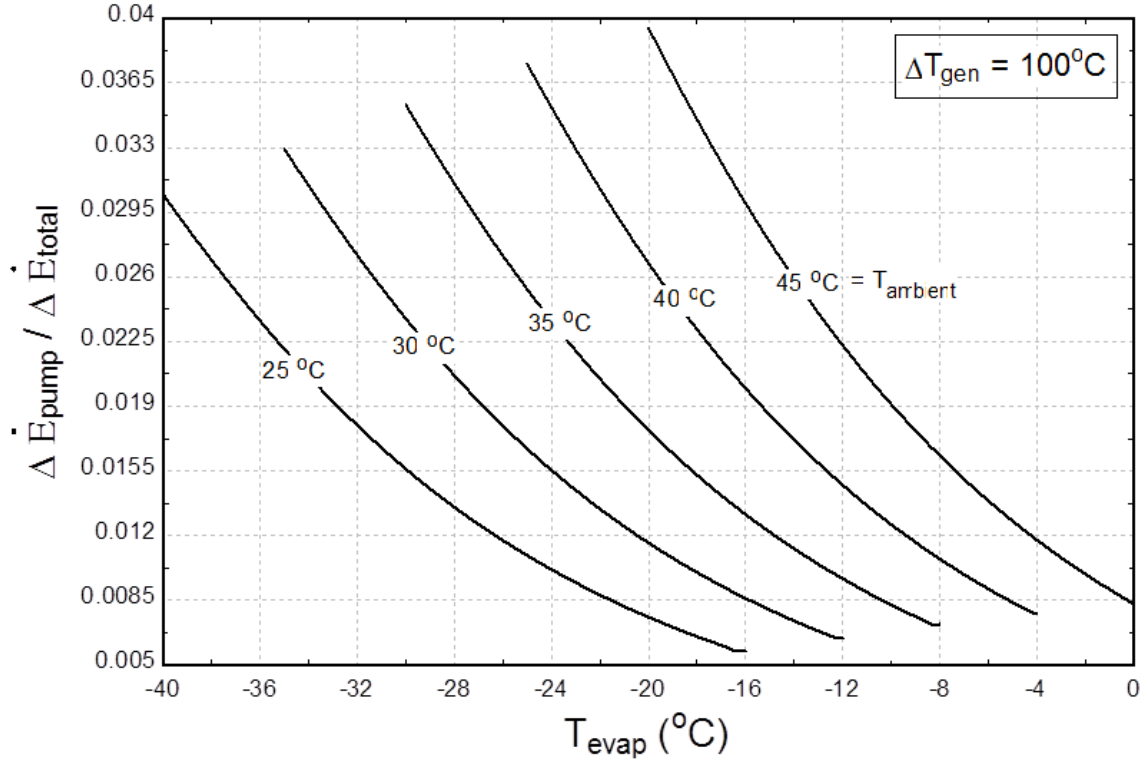

Figure 6-52 Exergy loss ratio of solution pump for varying evaporator temperature

6.3.2.11 Refrigerant Pre-Cooler

The exergy loss ratio for the refrigerant pre-cooler when operated at varying ambient and generator temperature and at an evaporator temperature of -5°C is shown in figure 6-53 whereas when operated at varying ambient and evaporator temperature and at a generator temperature of 100°C higher than the ambient temperature is shown in figure 6-54. It can be seen from the figure 6-53 that, at any constant ambient temperature, the exergy loss ratio for the refrigerant pre-cooler increases by increasing the generator temperature, becomes maximum at an optimum generator temperature and then decreases by further increasing the generator temperature. However, it can be seen from figure 6-54 that the exergy loss ratio for the refrigerant pre-cooler increases by increasing the evaporator temperature.

6.3.2.12 Solution Heat Exchanger

The exergy loss ratio for the solution heat exchanger when operated at varying ambient and generator temperature and at an evaporator temperature of -5°C is shown in figure 6-55 whereas when operated at varying ambient and evaporator temperature and at a generator temperature of 100°C higher than the ambient temperature is shown in figure 6-56. It can be seen from the figure 6-55 that, at any constant ambient temperature, the exergy loss ratio for the solution heat exchanger decreases by increasing the generator temperature, becomes approximately constant at very high generator temperature. Similarly, it can be seen from figure 6-56 that the exergy loss ratio for the solution heat exchanger decreases by increasing the evaporator temperature.

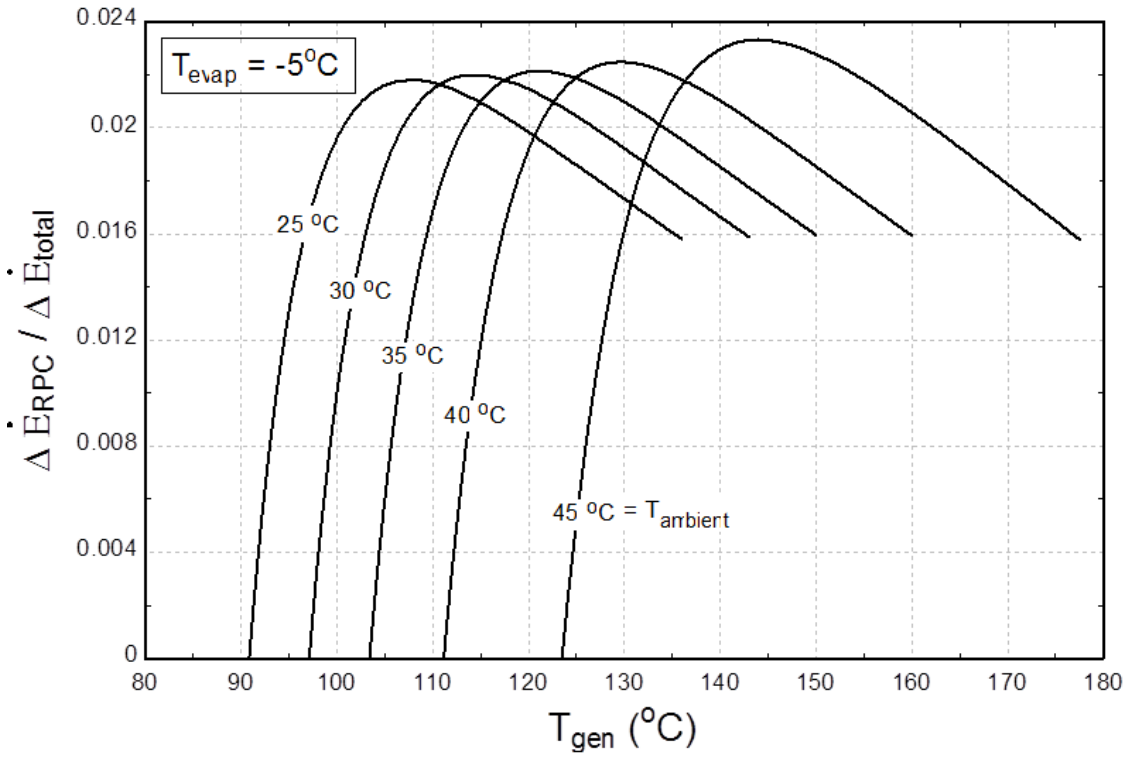

Figure 6-53 Exergy loss ratio of refrigerant pre-cooler for varying generator temperature

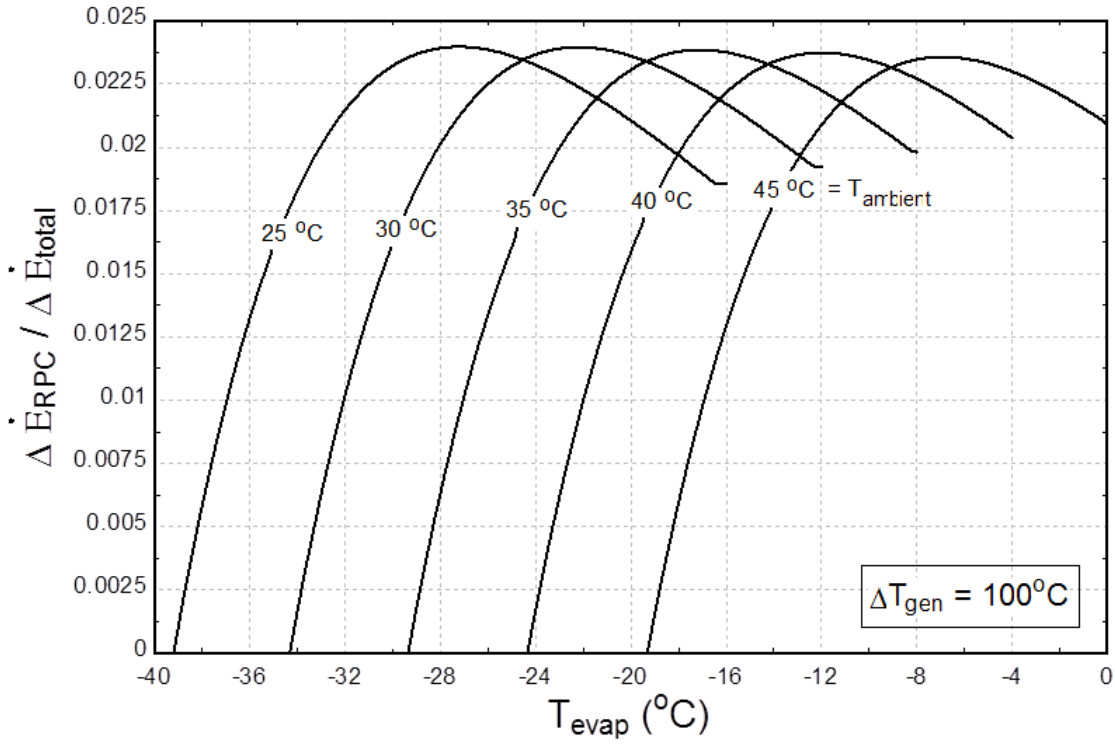

Figure 6-54 Exergy loss ratio of refrigerant pre-cooler for varying evaporator temperature

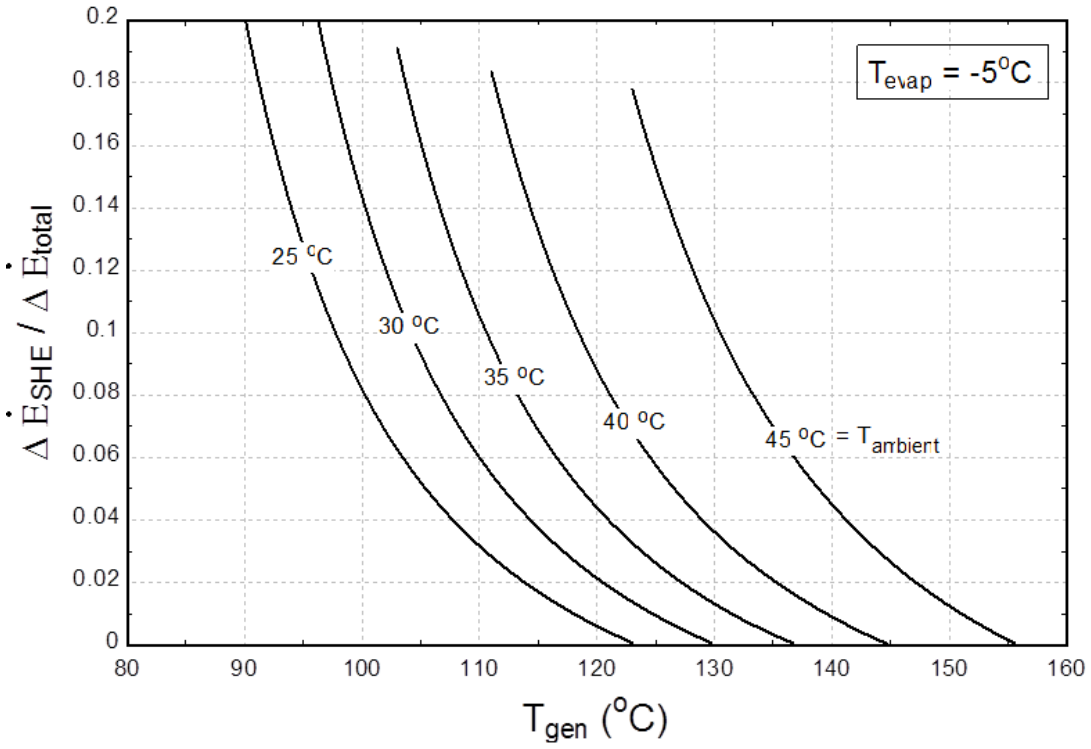

Figure 6-55 Exergy loss ratio of solution heat exchanger for varying generator temperature

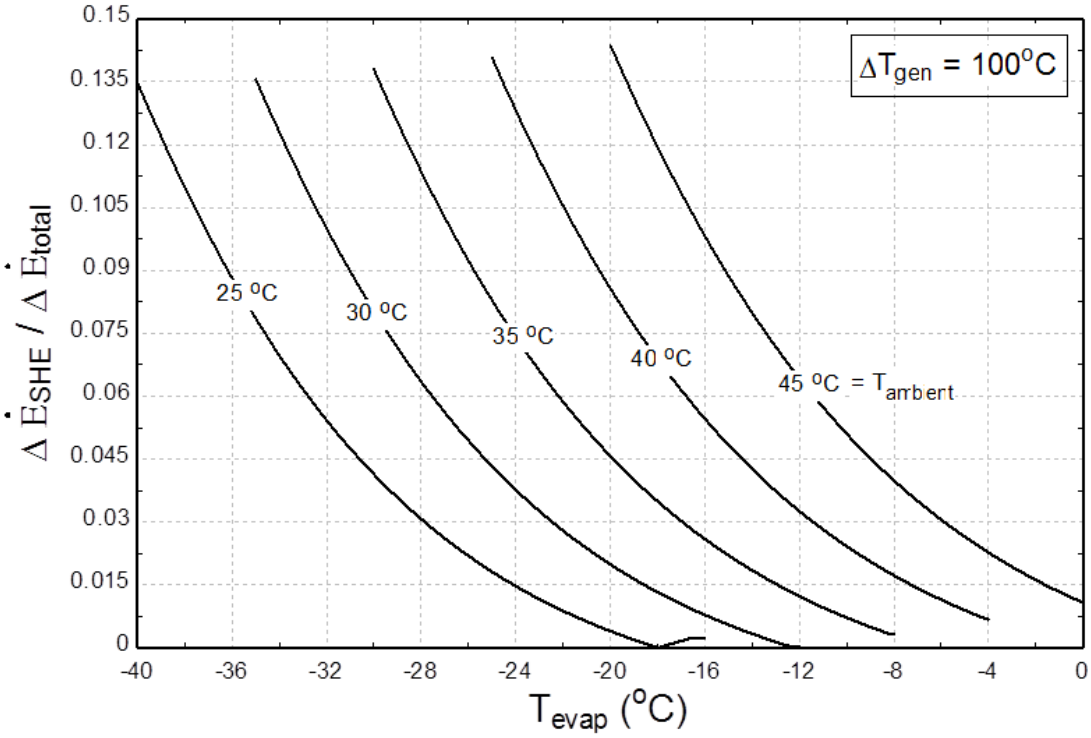

Figure 6-56 Exergy loss ratio of solution heat exchanger for varying evaporator temperature

6.4 Effect of Dephlegmator Heat Recovery

After the first and second law thermodynamic analysis of the proposed absorption chiller in the previous sections 6.2 & 6.3 respectively, this section elaborates, in detail, the effect of dephlegmator heat recovery over the performance of proposed absorption chiller. The simulation results for the proposed energy efficient solar powered aqua-ammonia vapor absorption refrigeration and air-conditioning system is compared to the conventional system based on the mathematical modeling described in chapter 5.

6.4.1 Coefficient of Performance

Using the dephlegmator heat recovery within the proposed absorption causes an increase in the coefficient of performance of the proposed absorption chiller compared to conventional system. Figure 6-57 shows the coefficient of performance of the proposed absorption chiller compared to the conventional systems for varying generator and ambient temperatures when operated at an evaporator temperature of 5°C. Similarly, figure 6-58 shows the coefficient of performance of the proposed absorption chiller compared to the conventional systems for varying evaporator and ambient temperatures when operated a generator temperature of 100°C higher than the ambient temperature.

It can be seen from figure 6-57 that the increase in the coefficient of performance due to heat recovery from the dephlegmator is much more visible at high generator temperature. Similarly, it can also be seen from figure 6-58 that the increase in the coefficient of performance due to heat recovery from the dephlegmator is much more visible at high evaporator temperature.

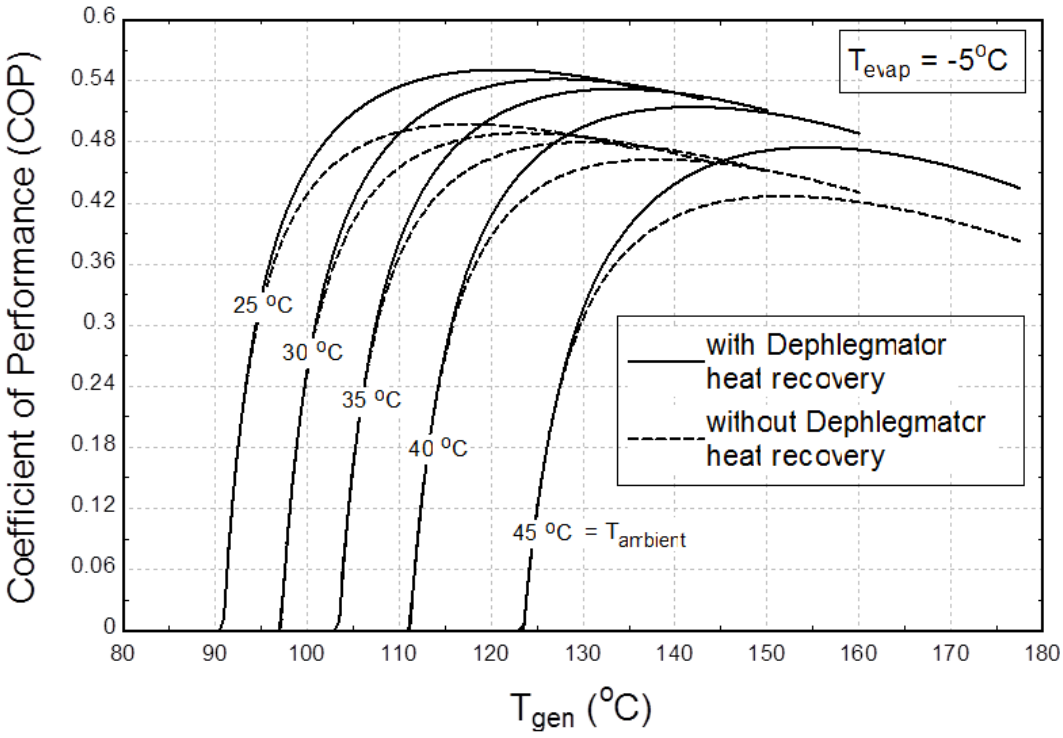

Figure 6-57 Effect of dephlegmator heat recovery over the COP for varying generator temperature

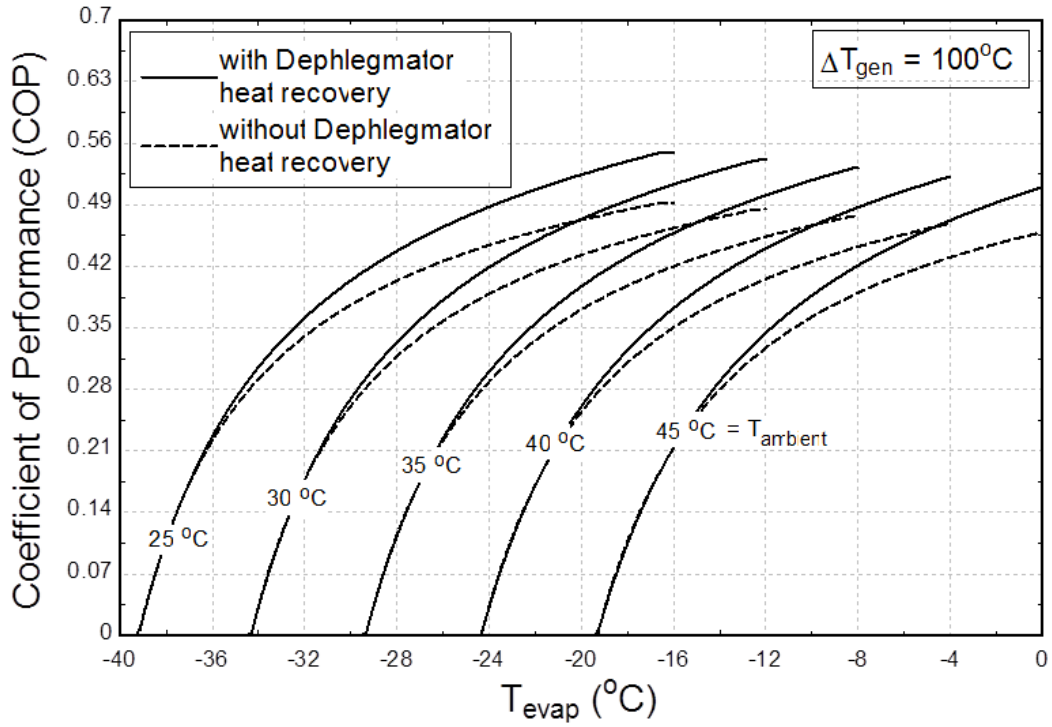

Figure 6-58 Effect of dephlegmator heat recovery over the COP for varying evaporator temperature

The percentage increase in the coefficient of performance for the proposed absorption chiller using dephlegmator heat recovery compared to conventional systems is shown in figure 6-59 when operated at varying ambient temperature and varying generator temperature. The analysis has been conducted at an evaporator temperature of -5°C, for the ambient temperatures varying from 25°C to 45°C whereas the generator temperature is varied from 90°C to 180°C. It can be seen from the figure 6-59 that the percentage increase in the coefficient of performance increases with an increase in the generator temperature at a constant ambient temperature whereas it decreases with an increase in the ambient temperature at constant generator temperature. It can also be seen from the figure 6-59 that at any ambient temperature, the percentage increase in the coefficient of performance for the proposed absorption chiller could be as high as 12%.

The percentage increase in the coefficient of performance for the proposed absorption chiller using dephlegmator heat recovery compared to conventional systems is shown in figure 6-60 when operated at varying ambient temperature and varying evaporator temperature. The analysis has been conducted at a generator temperature of 100°C higher than the ambient temperature, for the ambient temperatures varying from 25°C to 45°C whereas the evaporator temperature is varied from -40°C to 0°C. It can be seen from the figure 6-60 that the percentage increase in the coefficient of performance increases with an increase in the evaporator temperature at a constant ambient temperature whereas it decreases with an increase in the ambient temperature at constant evaporator temperature. It can also be seen from the figure 6-60 that at any ambient temperature, the percentage increase in the coefficient of performance for the proposed absorption chiller could be as high as 10%.

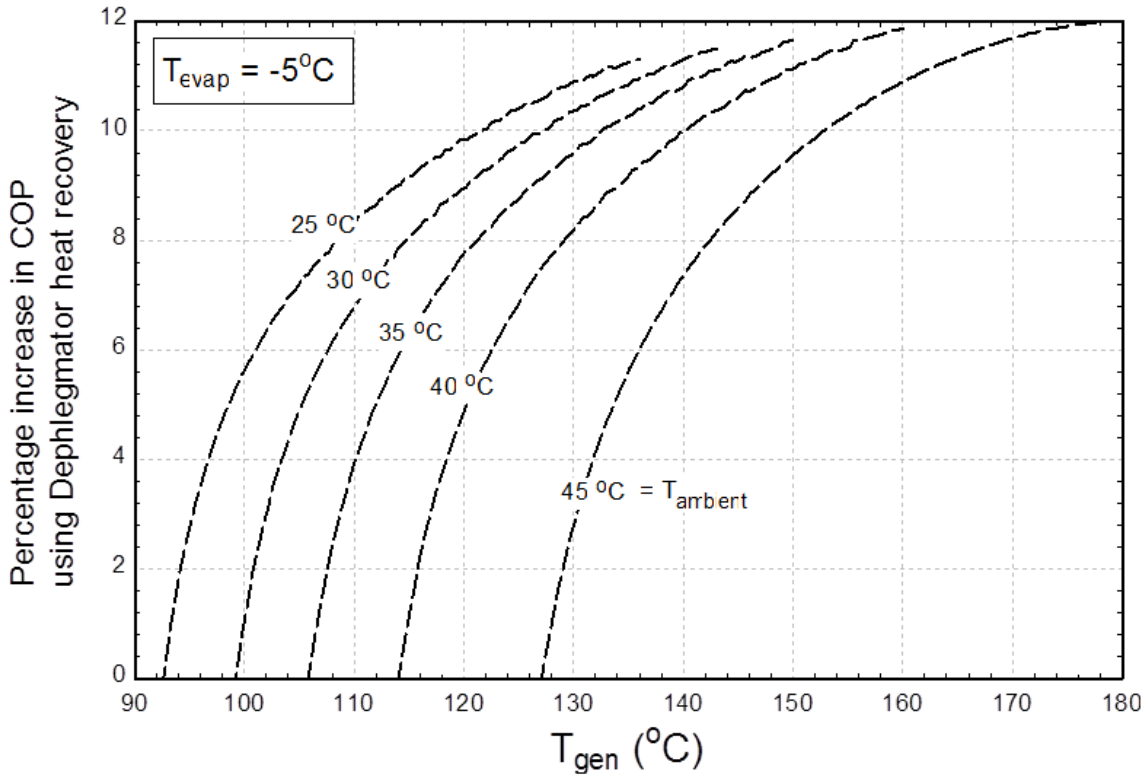

Figure 6-59 Percentage increase in COP for varying generator temperature

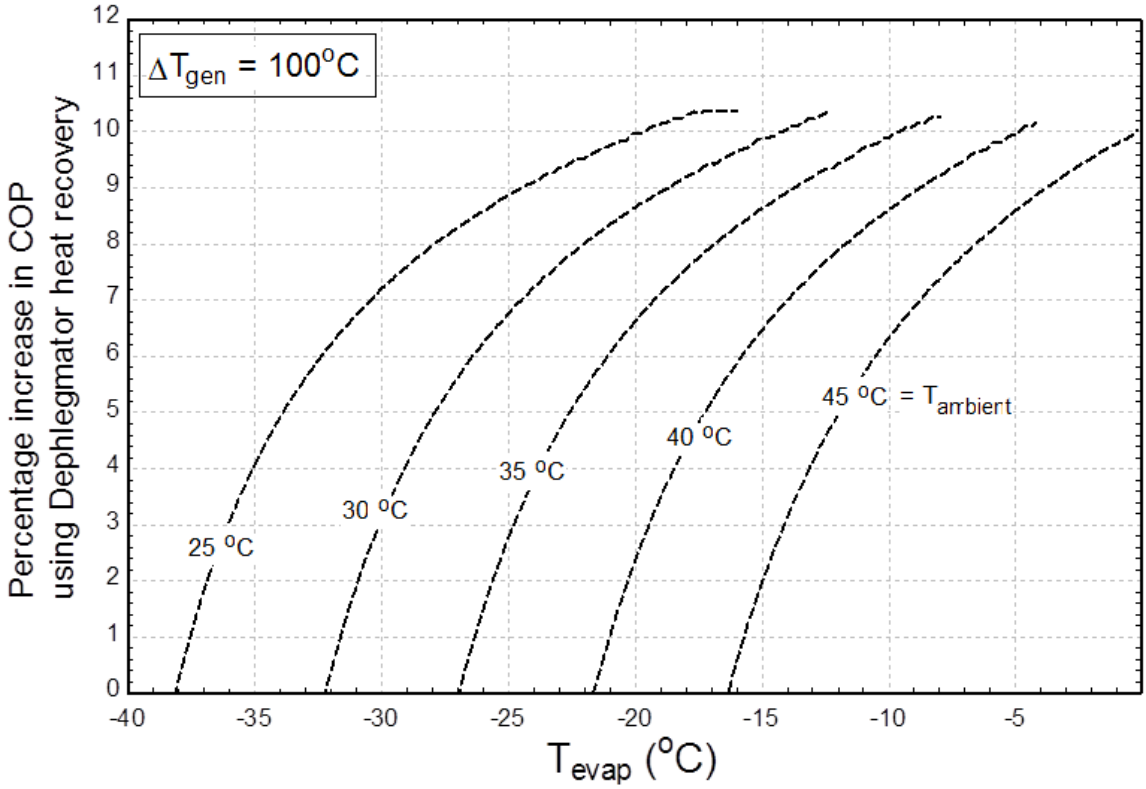

Figure 6-60 Percentage increase in COP for varying evaporator temperature

6.4.2 Optimum Split Ratio

Within the proposed absorption system, both dephlegmator and solution heat exchanger are used to recover heat. The dephlegmator heat recovery is a result of splitting the mass flow rate of the strong aqua-ammonia solution from the outlet of solution pump between the dephlegmator and solution heat exchanger. Thus, the dephlegmator split ratio is defined as the ratio of the mass flow rate of the strong solution in the dephlegmator to the total mass flow rate of strong solution within the absorption chiller. Figure 6-61 shows the effect of varying the dephlegmator split ratio over the coefficient of performance of the proposed absorption chiller at varying generator temperatures. It can be seen from the figure 6-61 that, at any fixed generator temperature, increasing the dephlegmator split ratio will initially increase the coefficient of performance until an optimum split ratio is reached.

The optimum dephlegmator split ratio is the split ratio at which coefficient of performance of the proposed absorption chiller becomes maximum. After optimum split ratio is reached, further increasing the split ratio will result in a decrease in the coefficient of performance of the absorption. The reason for initial increase in the coefficient of performance is that, the dephlegmator heat recovery adds into the overall heat recovery within the absorption chiller without causing a drop in the heat recovery from the solution heat exchanger. When the optimum split ratio is reached, further increase in the split ratio will cause a large decrease in the heat recovery from the solution exchanger, thus causing an overall reduced heat recovery within the absorption chiller. The overall reduced heat recovery within the absorption chiller results in an overall decrease in the coefficient of performance of the proposed absorption chiller.

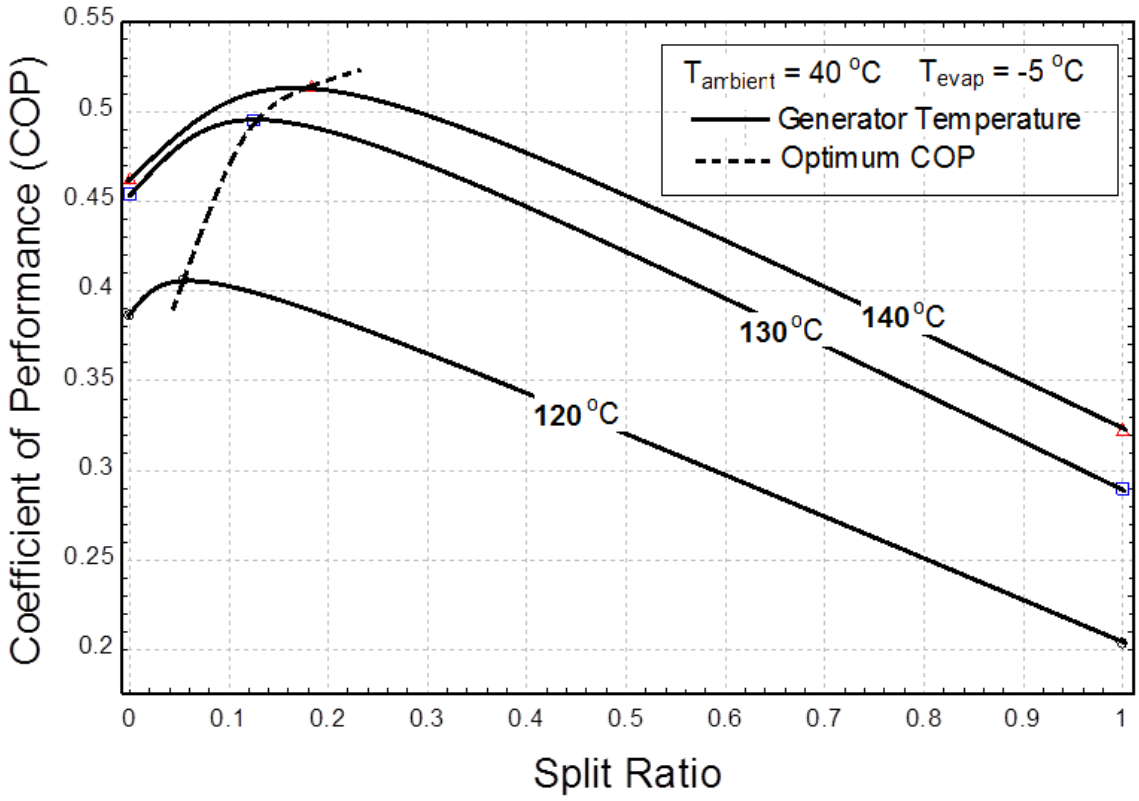

Figure 6-61 Effect of varying dephlegmator split ratio over the COP of the proposed absorption chiller

The dephlegmator split ratio for the proposed absorption chiller is shown in the figure 6-62 when operated at varying ambient temperature and varying generator temperature. The analysis has been conducted at an evaporator temperature of -5°C, for the ambient temperatures varying from 25°C to 45°C whereas the generator temperature is varied from 90°C to 180°C. It can be seen from the figure 6-62 that dephlegmator split ratio increases with an increase in the generator temperature at a constant ambient temperature whereas it decreases with an increase in the ambient temperature at constant generator temperature. It can also be seen from the figure 6-62 that at any ambient temperature, the dephlegmator split ratio for the proposed absorption chiller could be as high as 0.3.

The dephlegmator split ratio for the proposed absorption chiller is shown in the figure 6-63 when operated at varying ambient temperature and varying evaporator temperature. The analysis has been conducted at a generator temperature of 100°C higher than the ambient temperature, for the ambient temperatures varying from 25°C to 45°C whereas the evaporator temperature is varied from -40°C to 0°C. It can be seen from the figure 6-63 that the dephlegmator split ratio increases with an increase in the evaporator temperature at a constant ambient temperature whereas it decreases with an increase in the ambient temperature at constant evaporator temperature. It can also be seen from the figure 6-63 that at any ambient temperature, the dephlegmator split ratio for the proposed absorption chiller could be as high as 0.23.

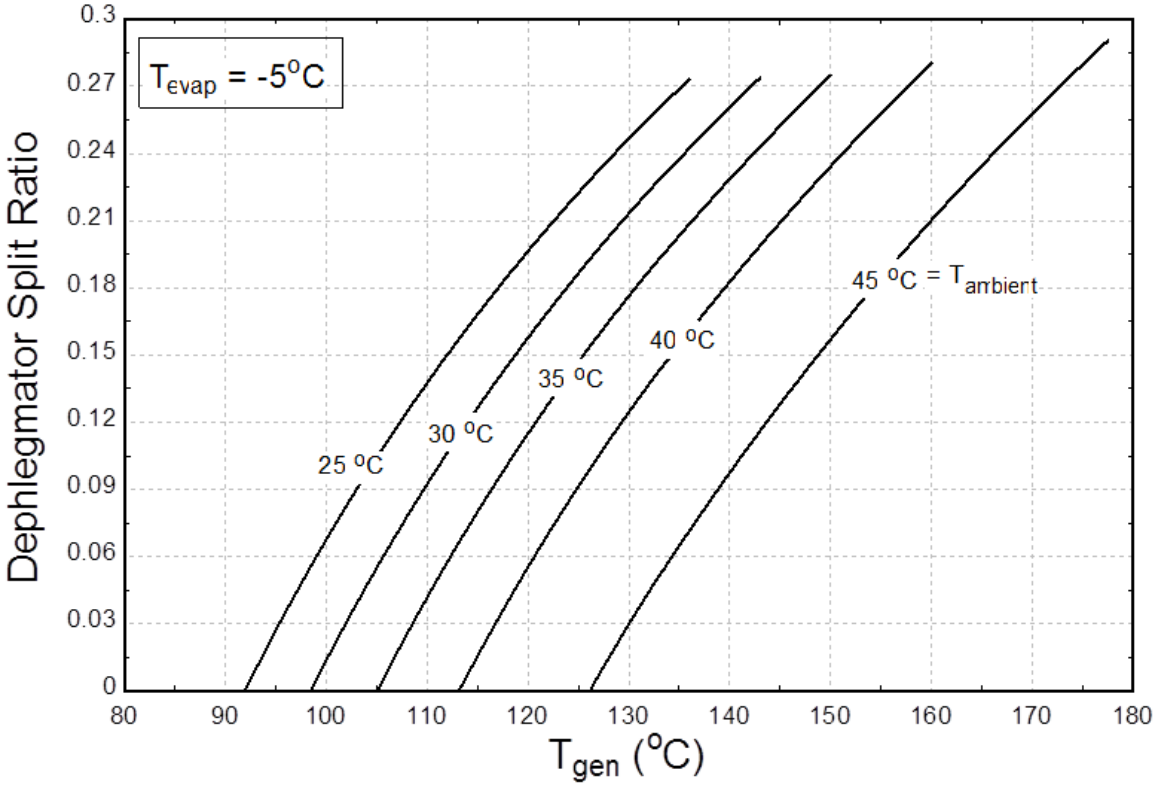

Figure 6-62 Dephlegmator split ratio for varying generator temperature

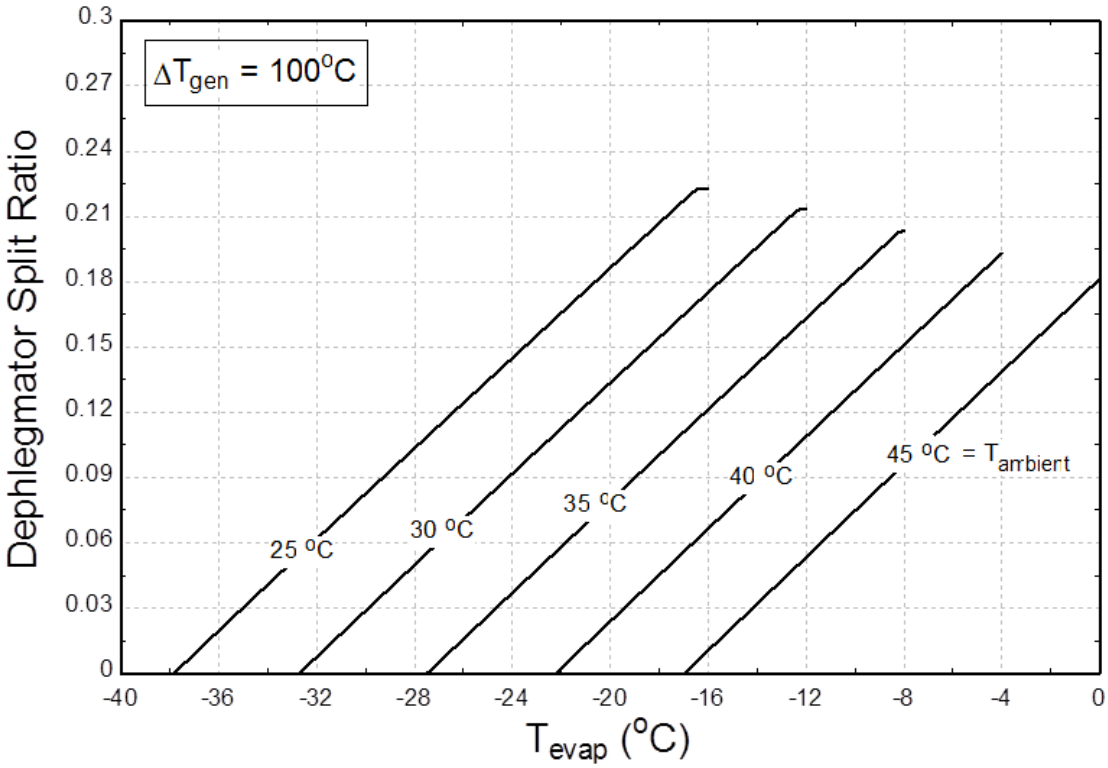

Figure 6-63 Dephlegmator split ratio for varying evaporator temperature

6.4.3 Generator Energy Input

Using the dephlegmator heat recovery within the proposed absorption causes a decrease in the generator energy input requirement for the proposed absorption chiller compared to conventional system. Figure 6-64 shows the generator energy input requirement for the proposed absorption chiller compared to the conventional systems for varying generator and ambient temperatures when operated at an evaporator temperature of 5°C. Similarly, figure 6-65 shows the generator energy input requirement for the proposed absorption chiller compared to the conventional systems for varying evaporator and ambient temperatures when operated a generator temperature of 100°C higher than the ambient temperature.

It can be seen from figure 6-64 that the decrease in the generator energy input requirement due to heat recovery from the dephlegmator is much more visible at high generator temperature. Similarly, it can also be seen from figure 6-65 that the decrease in the generator energy input requirement due to heat recovery from the dephlegmator is much more visible at high evaporator temperature.

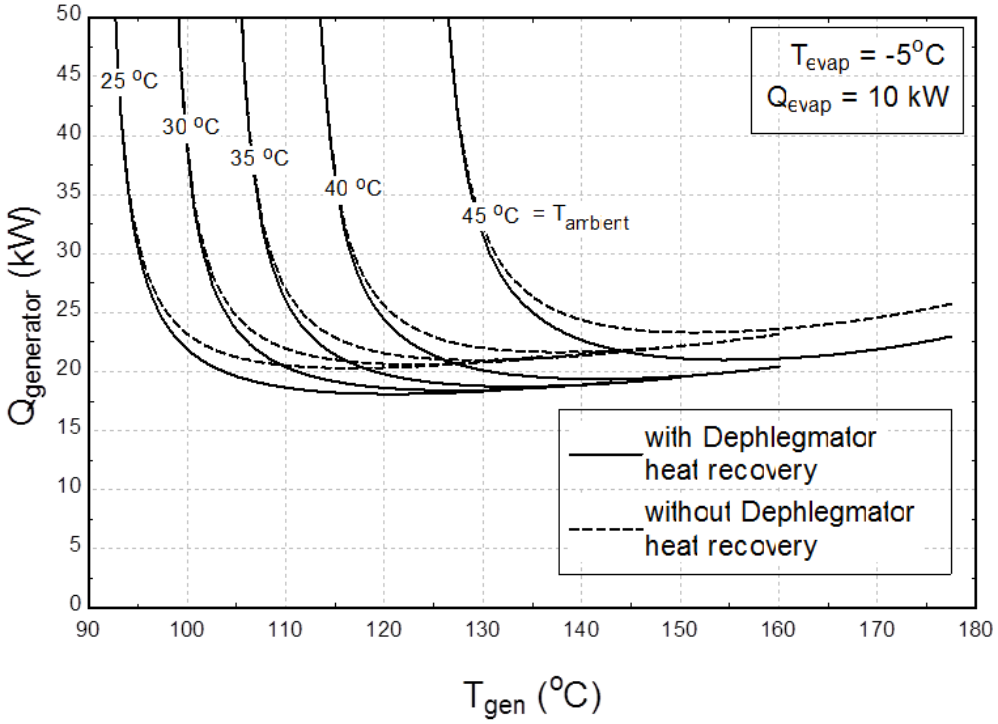

Figure 6-64 Effect of dephlegmator heat recovery over the generator energy input for varying generator temperature

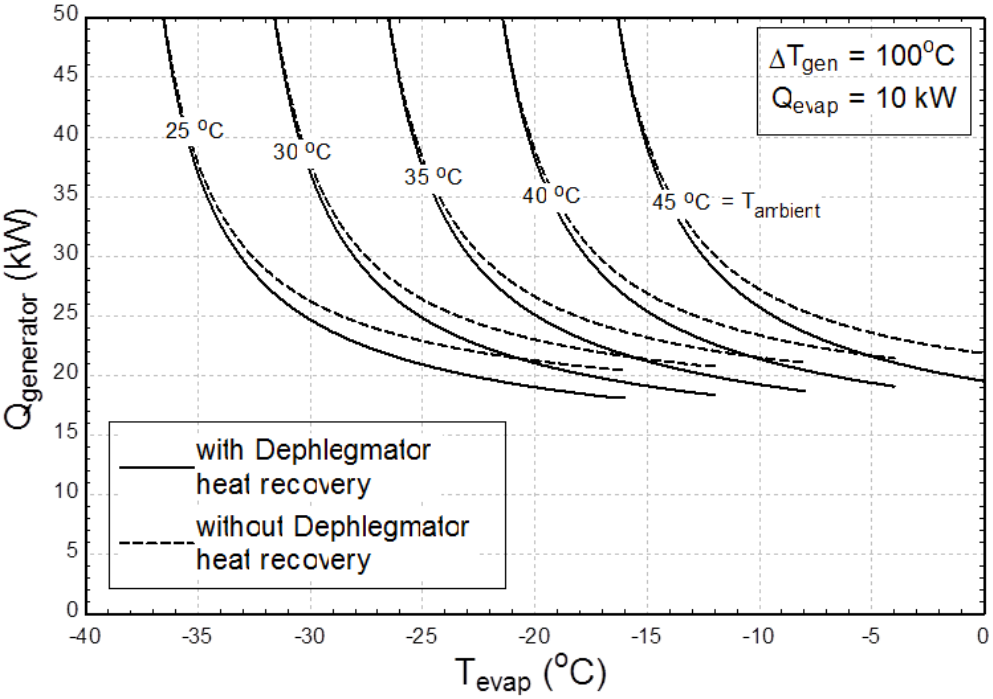

Figure 6-65 Effect of dephlegmator heat recovery over the generator energy input for varying evaporator temperature

6.4.4 Energy Recovery Ratio

Based on the optimum split ratio for the dephlegmator, the actual amount of heat recovery from the dephlegmator is limited compared to the maximum possible heat recovery from the dephlegmator. Thus, the energy recovery ratio of the dephlegmator can be defined as the ratio of energy recovered from the dephlegmator at optimum dephlegmator split ratio to the maximum possible energy recovery from the dephlegmator.

The dephlegmator energy recovery ratio for the proposed absorption chiller is shown in the figure 6-66 when operated at varying ambient temperature and varying evaporator temperature. The analysis has been conducted at a generator temperature of 100°C higher than the ambient temperature, for the ambient temperatures varying from 25°C to 45°C whereas the evaporator temperature is varied from -40°C to 0°C. It can be seen from the figure 6-66 that the dephlegmator energy recovery ratio increases with an increase in the evaporator temperature at a constant ambient temperature until it becomes approximately constant at high evaporator temperature. Whereas, the dephlegmator energy recovery ratio decreases with an increase in the ambient temperature at constant evaporator temperature. It can also be seen from the figure 6-66 that at any ambient temperature, the dephlegmator energy recovery ratio for the proposed absorption chiller could be as high as 0.95.

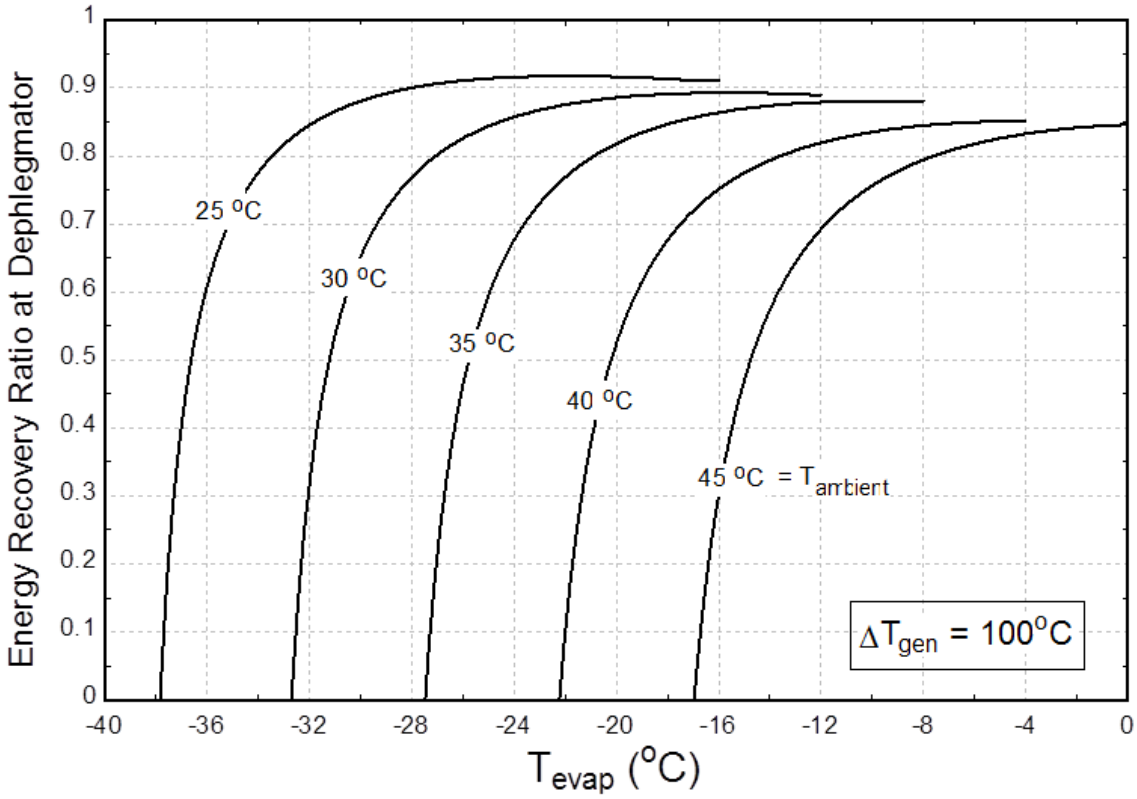

Figure 6-66 Energy recovery ratio of the dephlegmator for varying evaporator temperature

6.5 Effect of Refrigerant Storage Unit

After describing the effect of dephlegmator heat recovery over the performance of the proposed absorption chiller in the previous section 6.4, this section elaborates, in detail, the effect of refrigerant storage unit over the performance of proposed absorption chiller. The simulation results for the proposed energy efficient solar powered aqua-ammonia vapor absorption refrigeration and air-conditioning system is compared to the conventional system based on the mathematical modeling described in chapter 5.

6.5.1 Coefficient of Performance

When an absorption system operates at an ambient temperature lower than the design temperature, its coefficient of performance increases above the design coefficient of performance as shown in figure 6-67. There are two reasons for increase in the coefficient of performance at lower ambient temperatures compared to the design temperature. One reason is that, at lower ambient temperature, the condenser operating pressure reduces which allows more ammonia vapor generation causing an increase in the coefficient of performance. The other reason is that, at lower ambient temperature, the absorber has more capacity to absorber ammonia vapor producing much strong solution in the absorber thus causing an increase in the coefficient of performance of the absorption system.

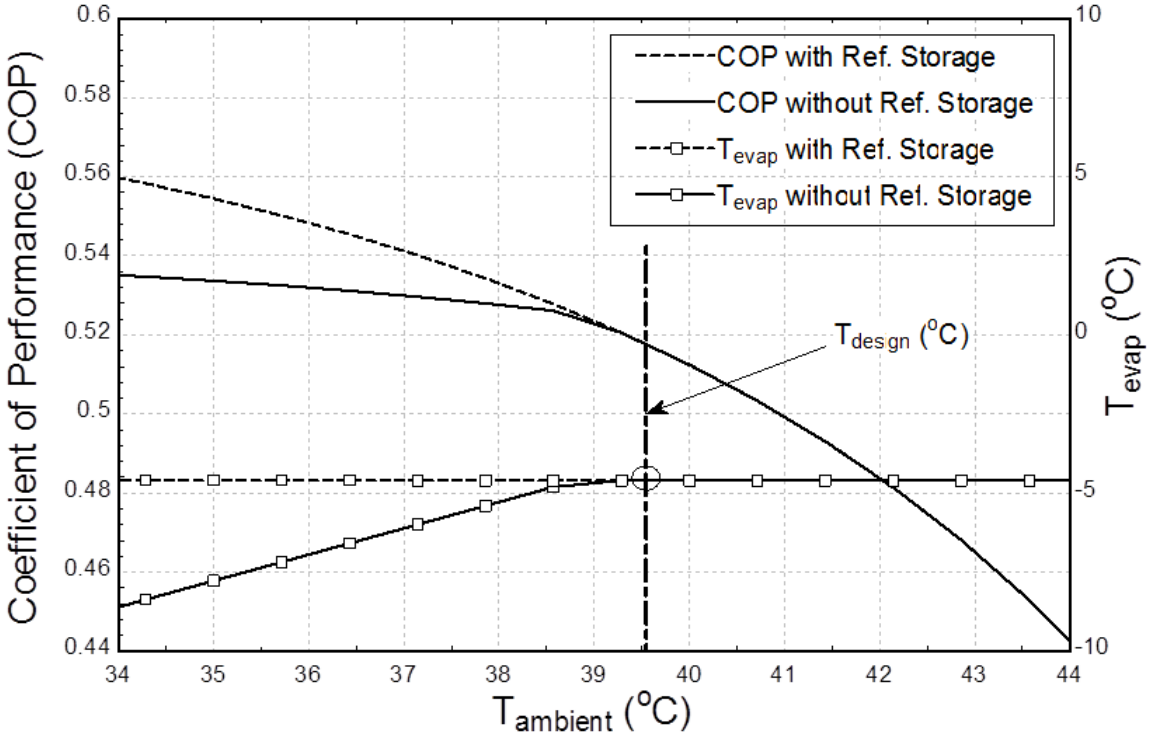

Figure 6-67 Effect of refrigerant storage over the performance of the proposed absorption chiller

In the absence of a refrigerant storage unit, the rise in the coefficient of performance at lower ambient temperatures is only due to decrease in condenser pressure because the concentration of strong solution is limited by the initial concentration of the strong solution with which the absorption chiller was filled during the manufacturing stage. Thus at lower ambient temperatures, the absorption chiller although operates at slightly high coefficient of performance yet it do not operate at full potential. Since the ambient temperature is low but due to the unavailability of additional ammonia in the system, the absorber absorbs more ammonia vapors causing a drop in the pressure of the absorber. The drop in the pressure of the absorber causes a drop in the pressure of the evaporator as well. This unnecessary drop in the pressure of the evaporator causes a drop in the evaporator temperature.

Hence, at lower ambient temperatures, the potential of the absorption chiller is utilized in producing evaporation temperature lower than the required evaporator temperature. Therefore, additional ammonia is required to allow the absorption chiller to operate at full potential hence signifying the importance of a refrigerant storage unit in the proposed absorption chiller. This effect can be visualized in figure 6-67. When the ambient temperature drops below the design temperature from 39.5°C to 34°C, it can be seen that, without the refrigerant storage unit, the coefficient of performance rises from 0.52 to just 0.535 however the evaporator temperature unnecessarily drops from -5°C to -8°C. Whereas, with the refrigerant storage unit, the coefficient of performance rises from 0.52 to 0.56 while keeping the evaporator temperature fixed at -5°C.

6.5.2 Refrigerant Storage Unit

The size of the refrigerant storage unit can be determined using the figure 6-68. Figure 6-68 determines the mass of ammonia refrigerant required per unit mass of the water in the absorber of the absorption chiller. The actual amount of water in the absorption chiller is filled based on the concentration of strong aqua-ammonia solution at the time of manufacturing of the absorption chiller which is based on the design ambient temperature. Thus for varying evaporator temperatures and varying ambient temperature, the amount of ammonia required in the refrigerant storage unit can be determined using figure 6-68. Thus for our case, when the absorption chiller is designed to operate at an ambient temperature of 40°C, by allowing the tolerance of ambient temperature till 30°C, the ratio of ammonia required in the refrigerant storage unit per unit mass of water in the absorber is 0.2.

The mass of refrigerant stored in the reservoir for the proposed absorption chiller is shown in the figure 6-69 when operated at varying ambient temperature and varying evaporator temperature. The analysis has been conducted at a generator temperature of 100°C higher than the ambient temperature, for the ambient temperatures varying from 25°C to 45°C whereas the evaporator temperature is varied from -40°C to 0°C. It can be seen from the figure 6-69 that the mass of refrigerant stored in the reservoir decreases with an increase in the evaporator temperature at a constant ambient temperature whereas it increases with an increase in the ambient temperature at constant evaporator temperature. It can also be seen from the figure 6-69 that at any ambient temperature, the mass of refrigerant stored in the reservoir for the proposed absorption chiller could be as high as 7 kg.

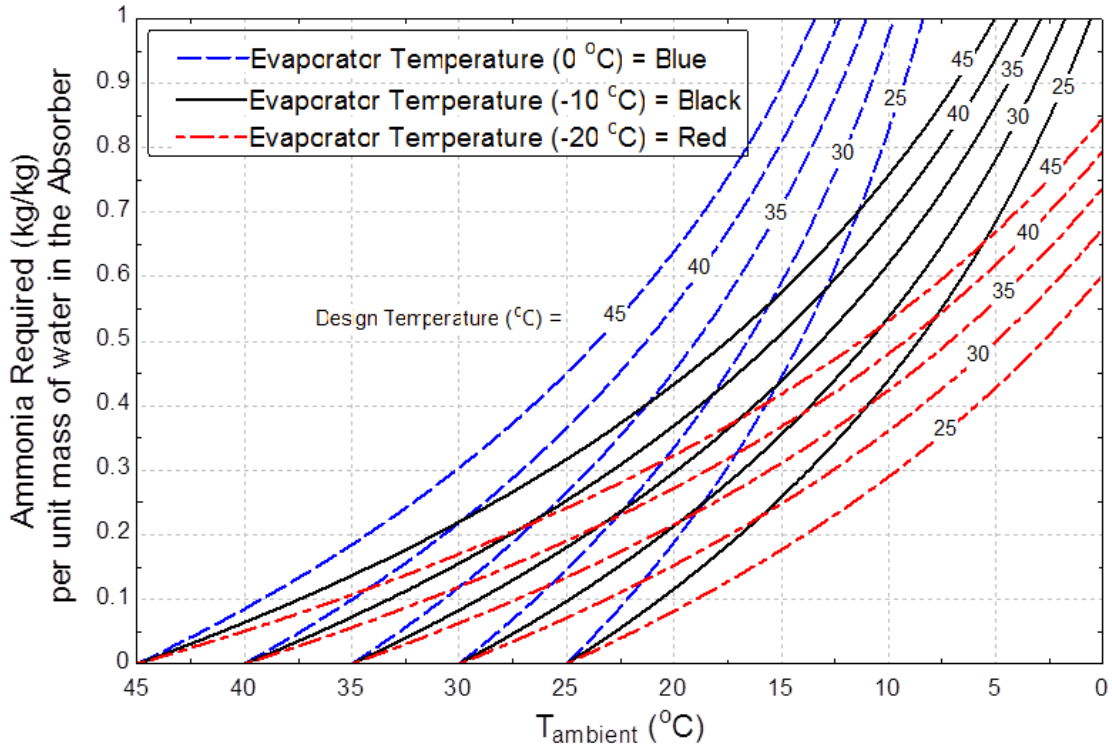

Figure 6-68 Additional ammonia requirement for the proposed absorption chiller

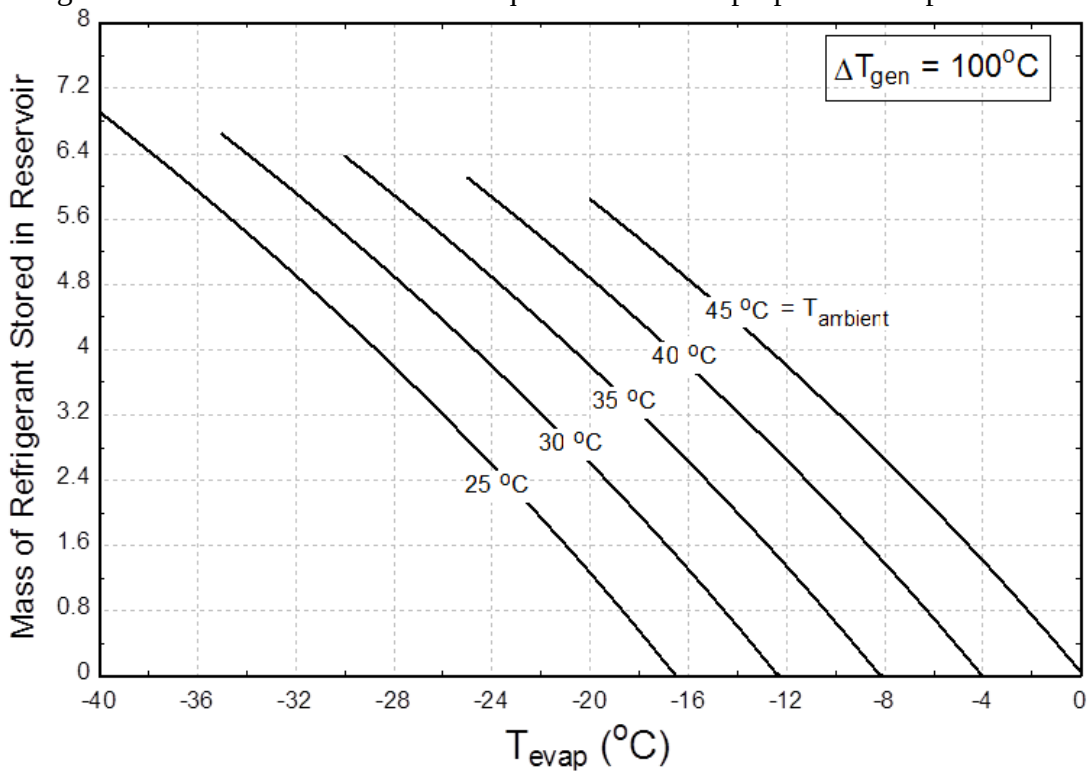

Figure 6-69 Effect of evaporator temperature over the mass of ammonia stored in the refrigerant storage unit

6.5.3 Dhahran Weather Data

In order the analyze the advantage of using refrigerant storage unit in the proposed absorption chiller, it is required to simulated the performance of the proposed absorption chiller for Dhahran ambient conditions. The Dhahran ambient conditions include the hourly solar radiation data and the hourly temperature data. Figure 6-70 represents the solar radiation data for Dhahran, KSA for the year 2012. Similarly, the figure 6-71 represents the temperature data for Dhahran, KSA for the year 2012.

It can be seen from figure 6-70 that in Dhahran during summer, the solar radiation reaches upto more than 8000 W-hr/m^2/day. Similarly, it can also be seen from figure 6-70 that the variation in solar radiation during summer season for Dhahran for year 2012 is around 1200 W-hr/m^2/day. Similarly, it can be seen from figure 6-71 that in Dhahran during summer, the average temperature reaches up to 40°C whereas the maximum temperature during summer may reach up to 47°C. Also, it can be seen from the figure that there is an approximately 10°C temperature difference between day and night time temperatures for Dhahran in the summer season.

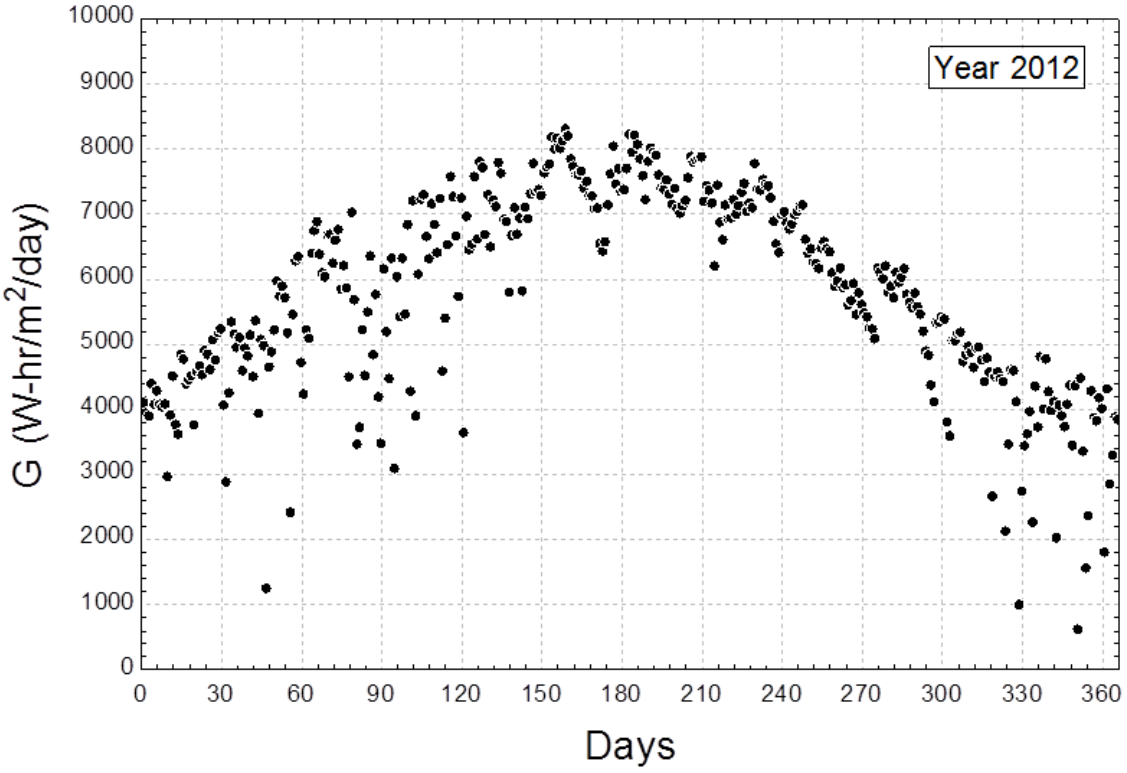

Figure 6-70 Solar Irradiation data for Dhahran KSA for 2012

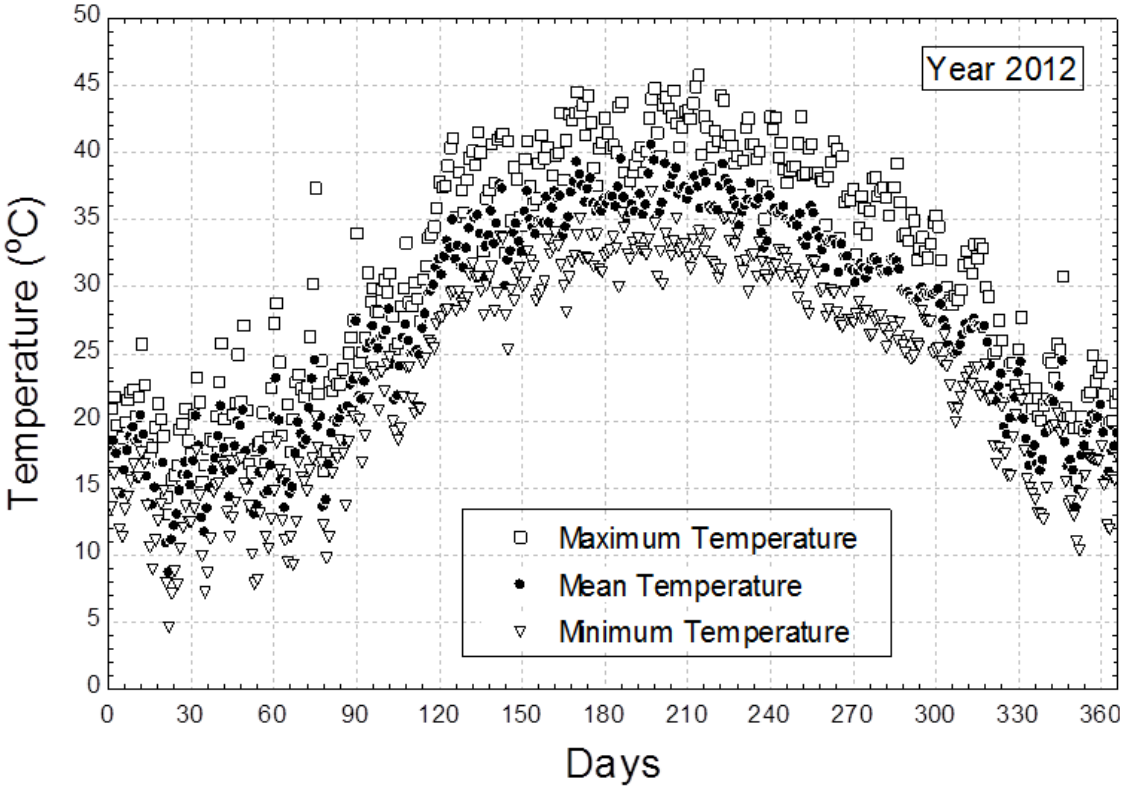

Figure 6-71 Weather temperature data for the Dhahran KSA for 2012

6.5.4 Selection of Summer Season

Since the absorption chiller produces the cooling effect, it is desired to be operated during the summer season. Thus, for simulation purposes, it is very important to select the summer season from the complete year weather data of Dhahran, KSA for the year 2012. Therefore, the analysis of hourly temperature data for the Dhahran for the year 2012 is shown in figure 6-72. Also the selection of summer season for the year 2012 for Dhahran is shown in figure 6-73. It can be seen from figure 6-73 that a period starting from April 15, 2012 to November 15, 2012 could be taken as the summer season period for Dhahran since the average temperature for the selected period is more than 30°C. This concludes that the performance of the proposed absorption chiller is desired to be simulated for the selected seven month period for the year 2012 for Dhahran, Saudi Arabia. The temperature analysis for the selected summer season for the year 2012 is shown in detail in figure 6-72. It can be seen from the figure 6-72 that, in the year 2012, there are a total of 8784 hours, out of which 3264 hours lies in the winter season while the rest of 5160 hours lies in the summer season. Out of this 5160 hours, 2181 hours are without any available solar radiation i.e. represents the night time during which absorption system cannot be operated. While the rest of the 2979 hours does have the available solar radiation. Now the temperature analysis for this 2979 selected hours for the year 2012 reveals that only 12% of hours lies approximately at the design condition (39°C to 41°C), whereas the 7% of hours lies above the design condition (greater than 41°C) and 81% of hours lies below the design condition (less than 39°C). Thus, the use of refrigerant storage unit in the proposed absorption chiller will significantly increase the performance of the proposed absorption chiller.

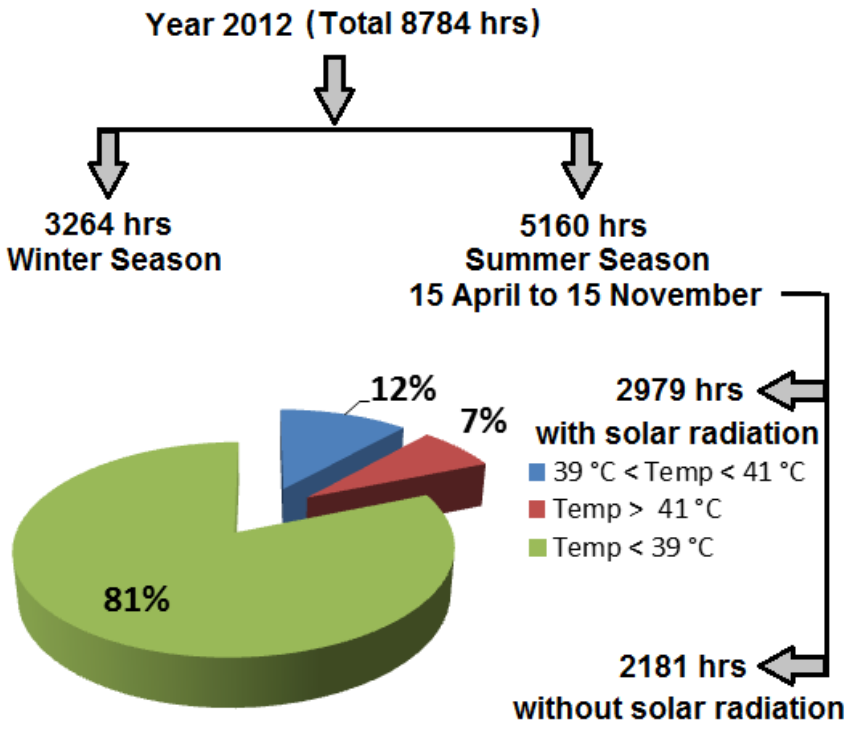

Figure 6-72 Weather temperature distribution for Dhahran KSA for 2012

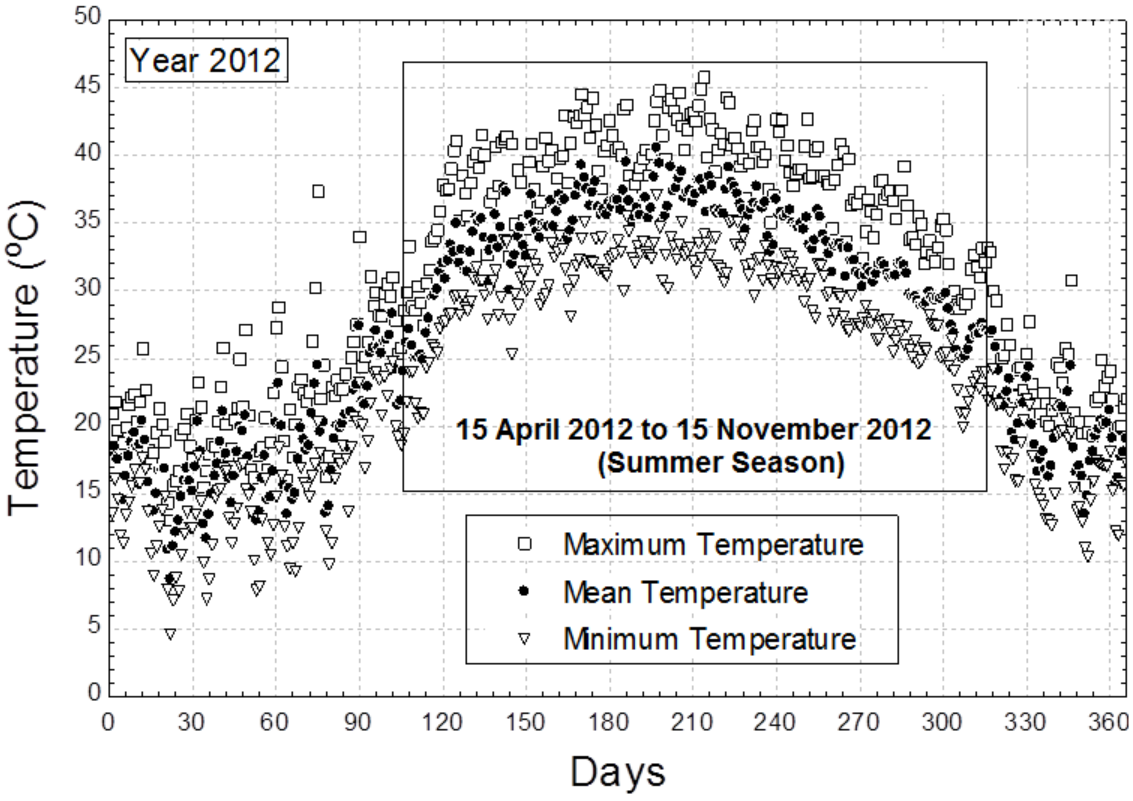

Figure 6-73 Selection of summer season for Dhahran KSA for 2012

6.5.5 Performance of the Proposed Absorption Chiller

The performance of the proposed absorption chiller for the selected summer season is evaluated based on the coefficient of performance of the proposed absorption system along with the equivalent ice production. The equivalent ice production is the conversion of refrigeration effect produced at the evaporator of the proposed absorption chiller into the equivalent amount of ice that could be produced using that refrigeration effect of the proposed absorption chiller. Figure 6-74 shows the equivalent ice production for the proposed absorption chiller when operated on a representative day (May 15, 2012) of the selected summer season. It can be seen from the figure 6-74, using the proposed absorption chiller with refrigerant storage, large amount of equivalent ice can be produced when compared to the absorption chiller without the refrigerant storage since the average ambient temperature throughout the representative day varied between 30°C to 33°C.

Similarly, Figure 6-75 shows the coefficient of performance for the proposed absorption chiller when operated on a representative day. It can be seen from the figure 6-75, using the proposed absorption chiller with refrigerant storage, the chiller could be operated at higher coefficient of performance when compared to the absorption chiller without the refrigerant storage since the average ambient temperature throughout the representative day varied between 30°C to 33°C. Figure 6-86 shows the additional cumulative equivalent ice production by the proposed absorption chiller with refrigerant storage unit when operated in the selected summer season for the year 2012. It can be seen from figure 6-76 that an additional 3500 kg of ice can be produced when operating the proposed absorption chiller using refrigerant storage unit in the summer season.

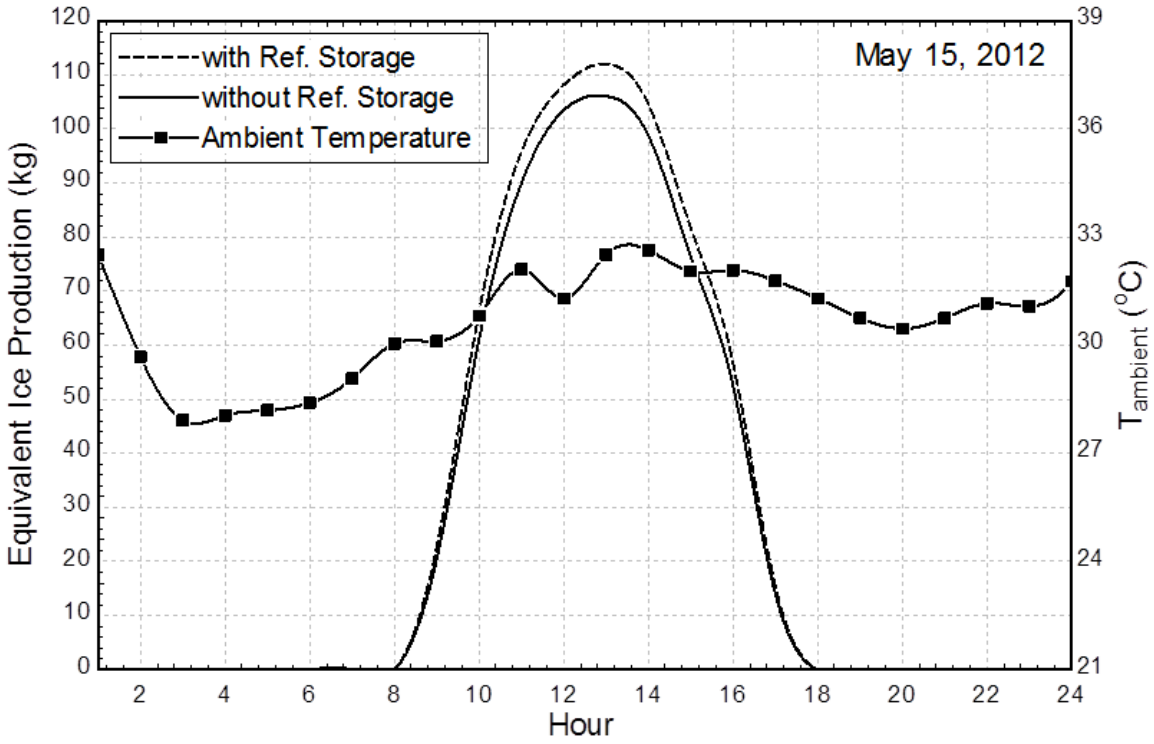

Figure 6-74 Effect of refrigerant storage unit over equivalent ice production for the proposed chiller

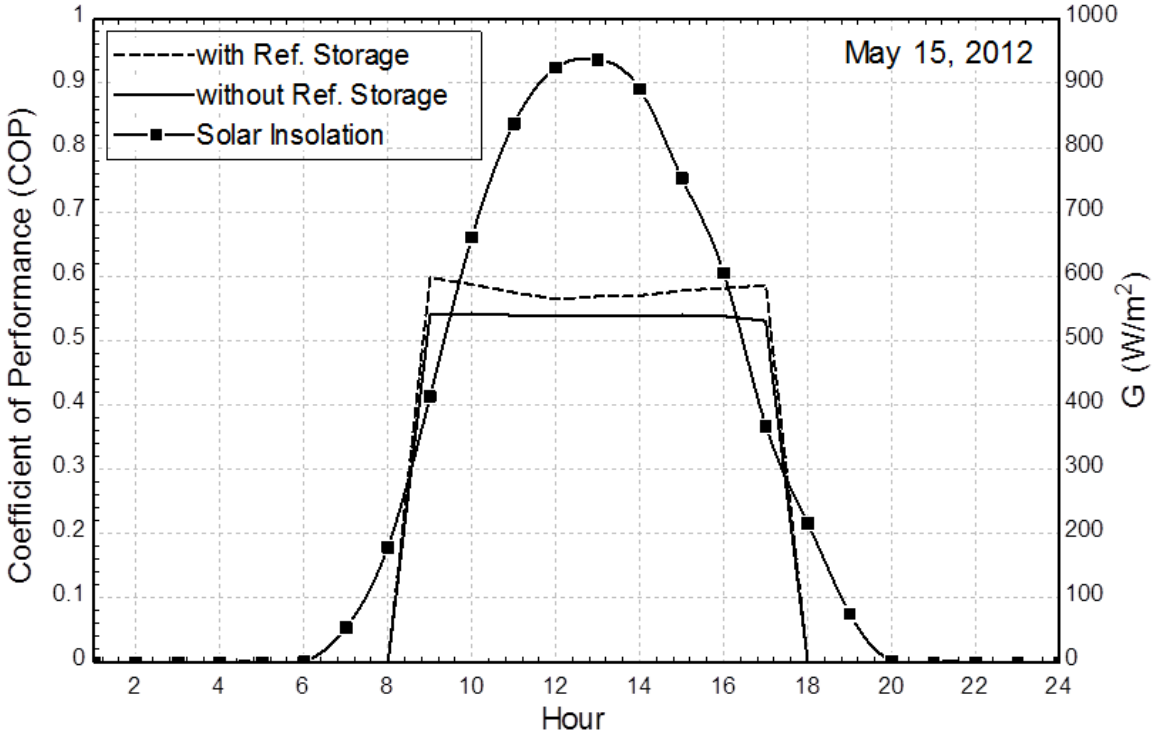

Figure 6-75 Effect of refrigerant storage unit over the COP for the proposed absorption chiller

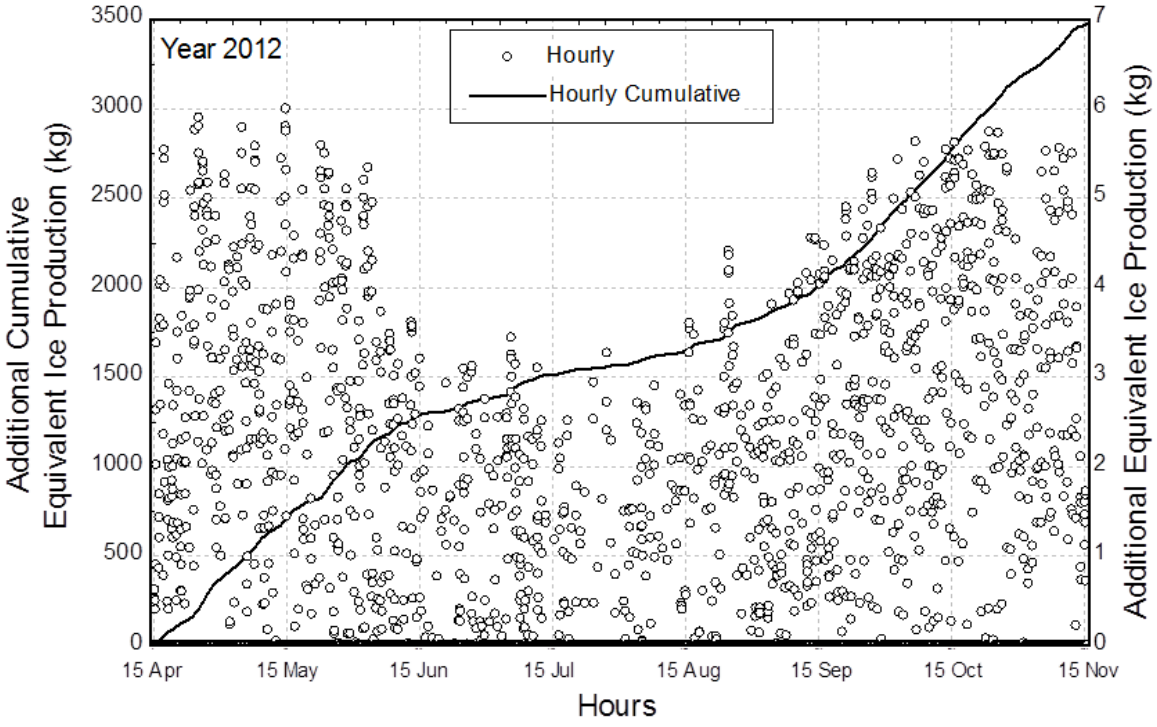

Figure 6-76 Additional equivalent cumulative ice production for the selected summer season of 2012 for the proposed absorption chiller

CHAPTER 7

EXPERIMENTAL VALIDATION

After simulating the performance of the proposed absorption system in Chapter 6, this chapter provides the experimental validation of the simulation carried out over the proposed absorption chiller. In this chapter, the specific focus has been given to the experimental setup of the absorption chiller and comparison of simulation results with the experimental results.

7.1 Experimental Setup

The proposed absorption chiller, described in Chapter 4, is basically one component of the complete absorption system. The complete absorption system consist of several other auxiliary systems that work together in an experimental setup to ensure the proper working of the absorption chiller. Therefore, the main components of the complete absorption cooling system, shown in figure 7-1, are listed as follows:-

1. Solar Collector field
2. Absorption Chiller
3. Heat Rejection System
4. Cold Storage System (Ice Storage Units)
5. Air-Conditioning System (Air Handling Units) &
6. Data Acquisition System.

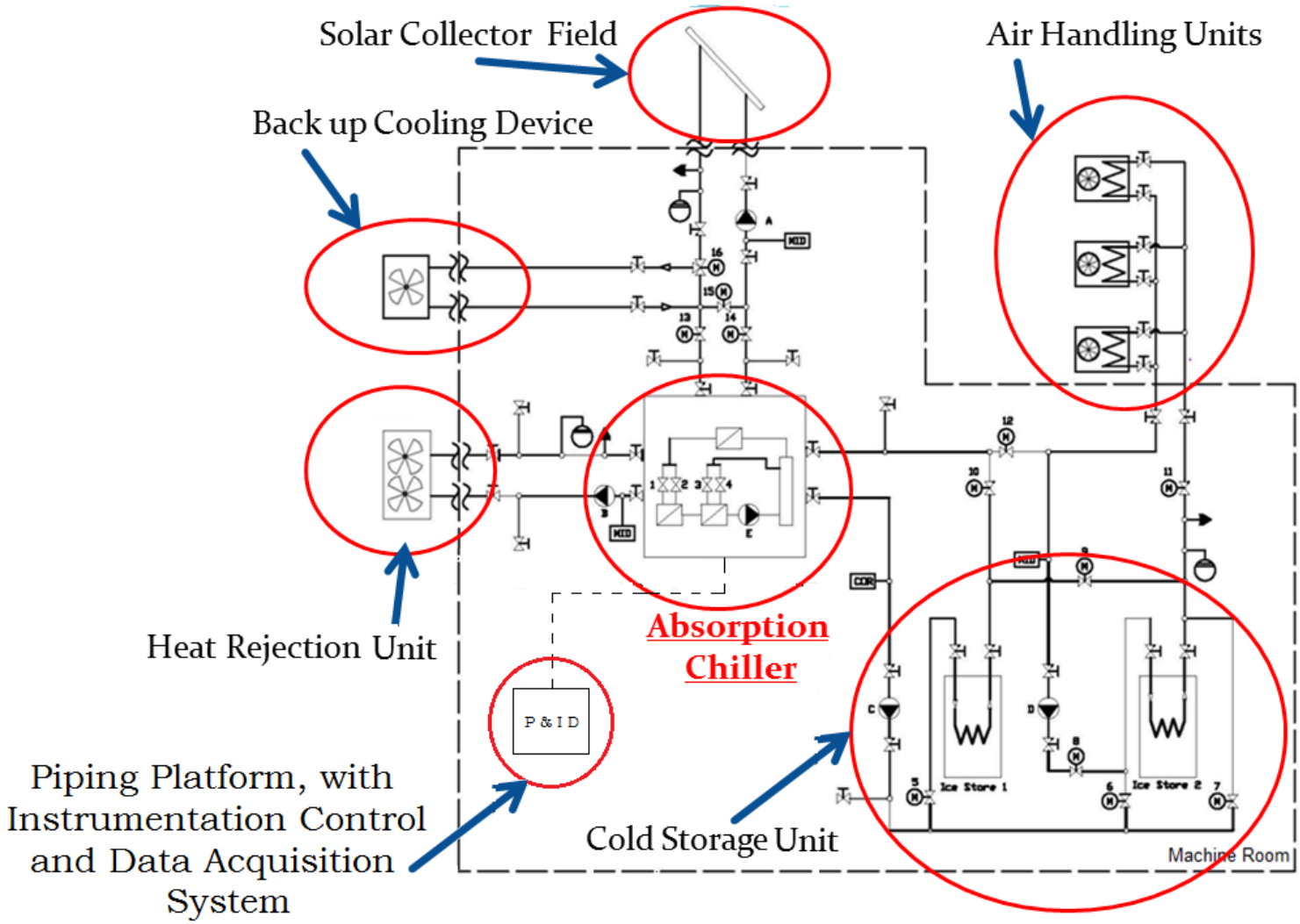

Figure 7-1 Schematic Diagram of Complete Absorption System

The site selected, for the installation of the proposed absorption cooling system, is a building located at Ali Street, near the faculty housing at KFUPM, Dhahran, KSA. The maximum cooling load requirement for the main hall of the installation site is around 10.0 kW, hence the absorption system is required to be designed to provide the cooling requirement of the main hall. The solar collector field consist of solar collector panels that collect the solar energy and supply it to the cooling plant. In the present experimental setup, the solar collectors are purchased from Millennium Energy Industries (MEI). The solar collector field is also connected with an emergency cooler which is a backup-cooling device through a 3-way valve. In case, the cooling plant is not running, the solar energy collected by the collector field will heat up the water within the solar circuit. This will cause a significant rise in the temperature and pressure inside the collector field. In order to avoid any kind of damage to the solar collector field, the 3-way valve will open the flow to the emergency cooler which will reject heat to the environment. Thus the emergency cooler ensures the safety of the collector field in case of high temperature and high pressure development within the solar collector field.

For the experimental setup, evacuated tubular solar collectors CPC-18 are purchased from MEI. The purchased solar collector field consist of a set of 14 evacuated tubular solar collectors CPC-18 installed at the roof of the solar cooling laboratory at KFUPM. The evacuated tubular solar collectors are arranged in 4 rows with 2 rows of three collectors in series and 2 rows of four collectors in series. The evacuated tubular collectors are required to provide the maximum heating power of 20 kW with an average temperature of 140 ºC of the fluid in the collectors. The heating flow rate is 1 m^3/hr. The aperture area of each solar collector panel is 3 m^2. The solar collector field area is 65 m^2

at the roof of the solar laboratory for the installation of solar panels. The collectors are installed facing south at an angle of inclination of 25º from the roof surface. The solar collectors can reach a stagnation temperature of 276 ºC and a pressure of 8 bar. Each collector panel can hold a total of 2.4 liters of water

The heat rejection system is required to reject heat from the absorption chiller. The heat rejection is required from the absorber, condenser and the absorber pre-cooler of the proposed absorption system. In the experimental setup developed, the heat rejection unit is purchased from the THERMFIN company in Germany. This heat rejection unit is an air-cooled heat rejection heat exchanger. It is composed of copper finned tubes containing the heat rejection fluid. The copper finned tubes are placed in a casing with two induced draft fans installed horizontally at the top of the casing. Ambient air is from the bottom of the heat rejection heat exchanger. The air handling unit is required to provide the air-conditioning requirement of the building. This air handling unit is also composed of copper finned tubes which takes in the room air, cools it down and supply it back to the room. In the experimental setup developed, this air handling unit is purchased from JOHNSON's & Controls.

The ice storage system is required to store the cold produced by the absorption chiller. This ice storage unit is also composed of copper tubes placed in an insulated water container. The copper tubes contains water glycol mixture of 40%. Ice is formed at the surface of copper tubes and keeps on increasing in thickness until the whole of the ice storage unit is filled with ice. In the experimental setup developed, two ice storages are used with each having a capacity of 500 kg of ice in it.

7.2 Validation

The proposed absorption chiller described in chapter 4 has been manufactured and tested based on the experimental setup developed as described in the previous section 7.1. The simulation results for the proposed absorption chiller has been developed based on the mathematical modeling described in chapter 5. Hence by comparing the simulated results with the experimental results, this section provides the experimental validation of the simulation results for the proposed absorption chiller.

7.2.1 Operating Conditions

The experimental setup developed for the proposed absorption chiller is tested on February 10, 2014 (Monday) & February 11, 2014 (Tuesday). The operating conditions for the manufactured absorption chiller within the absorption cooling system is determined based on the two main input parameters, i.e. incident solar energy (G) and the temperature of cooling water inlet within the absorption chiller. All other parameters within the absorption chiller are a function of these two input parameters.

Figure 7-2 represents the operating conditions for the absorption chiller tested on February 10, 2014 whereas the figure 7-3 represents the operating conditions for the absorption chiller tested on February 11, 2014. It must be noted that the temperature of the cooling water inlet to the absorption system can be adjusted based on the heat rejection from the heat rejection heat exchanger.

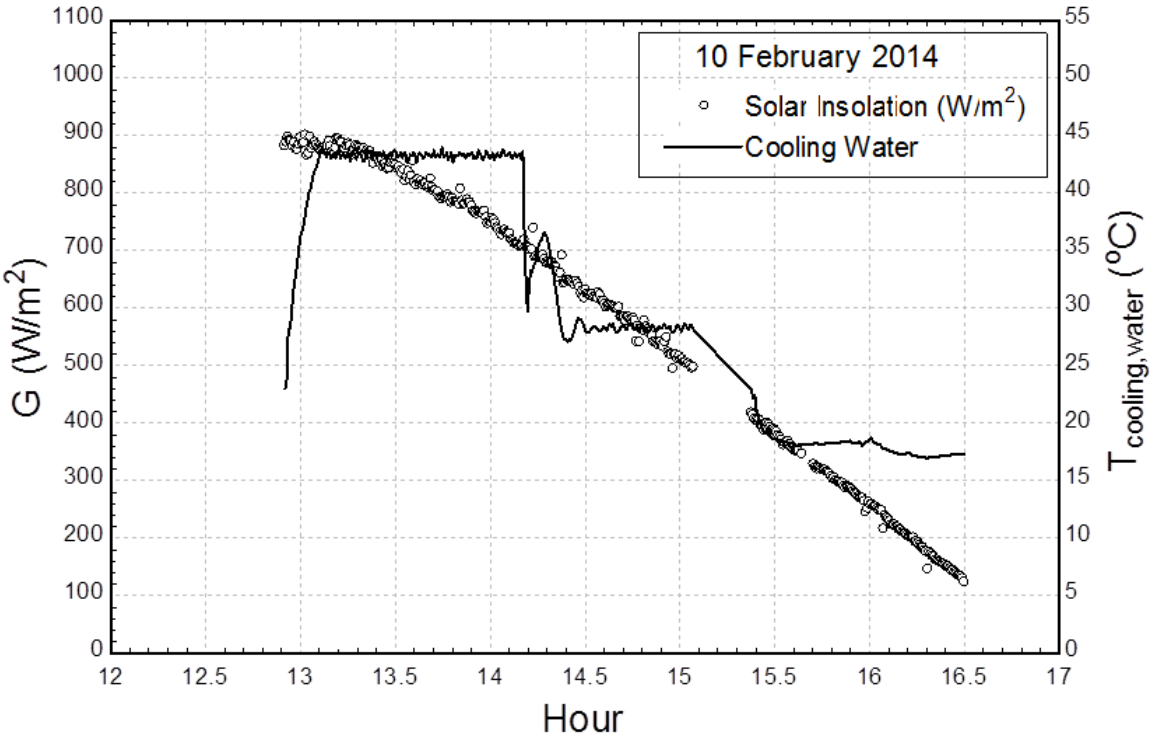

Figure 7-2 Operating conditions for 10 February 2014

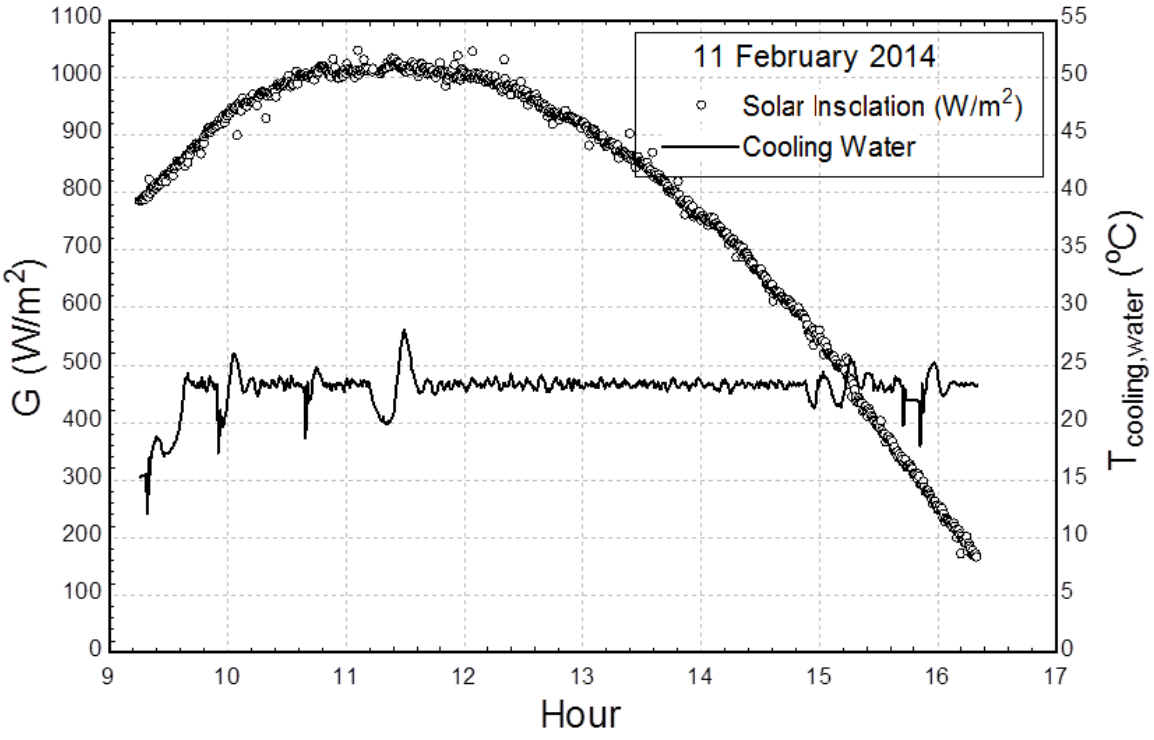

Figure 7-3 Operating conditions for 11 February 2014

Hence, using the variable frequency modulator, the speed of the rotating fan of the heat rejection heat exchanger could be adjusted to vary the temperature of the cooling water inlet to the absorption chiller. Thus decreasing the fan speed will result in comparatively small heat rejection causing an increase in the cooling water inlet temperature. Similarly, increasing the fan speed will result in comparatively high heat rejection causing a decrease in the cooling water inlet temperature. However, it must be noted that in any of the case, the cooling water inlet temperature cannot go below the ambient temperature since the heat rejection heat exchanger is intended to reject heat to the ambient. In fact, the experimental results showed that, when operating at the maximum fan speed, the cooling water inlet temperature is still approximately 0.7 to 1.9°C higher than the ambient temperature.

It can be seen from the figure 7-2 that the experimental testing started from 1:00 p.m. in the afternoon till the sunset. During this period, the incident solar radiation could be seen to gradually decrease from 900 W/m^2 to 100 W/m^2. However, during this period, the cooling water inlet to the absorption chiller, is initially set to 44°C, then approximately after one hour it was set to 28°C and then after further one and a half hour it was set to be below 20°C as per the ambient temperature conditions. The variation in the cooling water inlet temperature was made by adjusting the fan speed of the heat rejection heat exchanger as described above.

Similarly, it can be seen from the figure 7-3 that the experimental testing started early morning from 9:00 a.m. till the sunset. During this period, the incident solar radiation could be seen to initially gradually increase from 800 W/m^2 to 1000 W/m^2 and then gradually decrease from 1000 W/m2 to 100 W/m2. During this period, the cooling water inlet to the absorption chiller was varying as per the ambient conditions.

7.2.2 Performance of the Absorption Chiller

The performance of the proposed absorption chiller was experimentally tested based on the mathematical modeling developed in chapter 5. The simulated and experimental refrigeration effect produced for the proposed absorption chiller operated on February 10, 2014 is shown in figure 7-4. Similarly, the simulated and experimental refrigeration effect produced for the proposed absorption chiller operated on February 11, 2014 is shown in figure 7-5.

It can be seen from figure 7-4 that when operated at an incident solar radiation of 900W/m^2, the refrigeration effect produced for the proposed absorption chiller was around 8.5kW. However, as the incident solar radiation over the solar collectors reduced to 100W/m^2, the refrigeration effect produced for the proposed absorption chiller also dropped and when the solar radiation was approximately 380W/m^2, the produced refrigeration effect dropped to zero as there was not enough solar radiation available to generate ammonia vapors in the generator of the proposed absorption chiller. It can be seen from figure 7-5 that when operated at an incident solar radiation of 800W/m^2, the refrigeration effect produced for the proposed absorption chiller was around 8kW. However, as the incident solar radiation over the solar collectors increased, the refrigeration effect produced for the proposed absorption chiller also increased and when

the solar radiation was approximately 1050W/m^2, the produced refrigeration effect increase to 11kW. Similarly, as the incident solar radiation over the solar collectors gradually reduced to 100W/m^2, the refrigeration effect produced for the proposed absorption chiller also gradually dropped and when the solar radiation was approximately 300W/m^2, the produced refrigeration effect dropped to 0.8kW. It can also be seen from the figure 7-4 & figure 7-5, that the experimental results for the refrigeration effect produced for the proposed energy efficient solar powered aqua-ammonia vapor absorption refrigeration and air-conditioning system are in very good agreement with the simulated results with a maximum deviation of 6%.

The small increment in the measured values of incident solar radiation is ±1 W/m^2 and the one in the measured values of ambient temperature is ± 0.01 °C. Performing uncertainty analysis gives an uncertainty of ±0.00008917 for the coefficient of performance and the uncertainty of ±0.0145 kW for the produced refrigeration effect. Therefore, the uncertainty as a percentage of the values of coefficient of performance and refrigeration effect are 0.017% and 0.138% respectively. The calculated uncertainty for the COP and refrigeration effect provide a high level of confidence in the measured data.

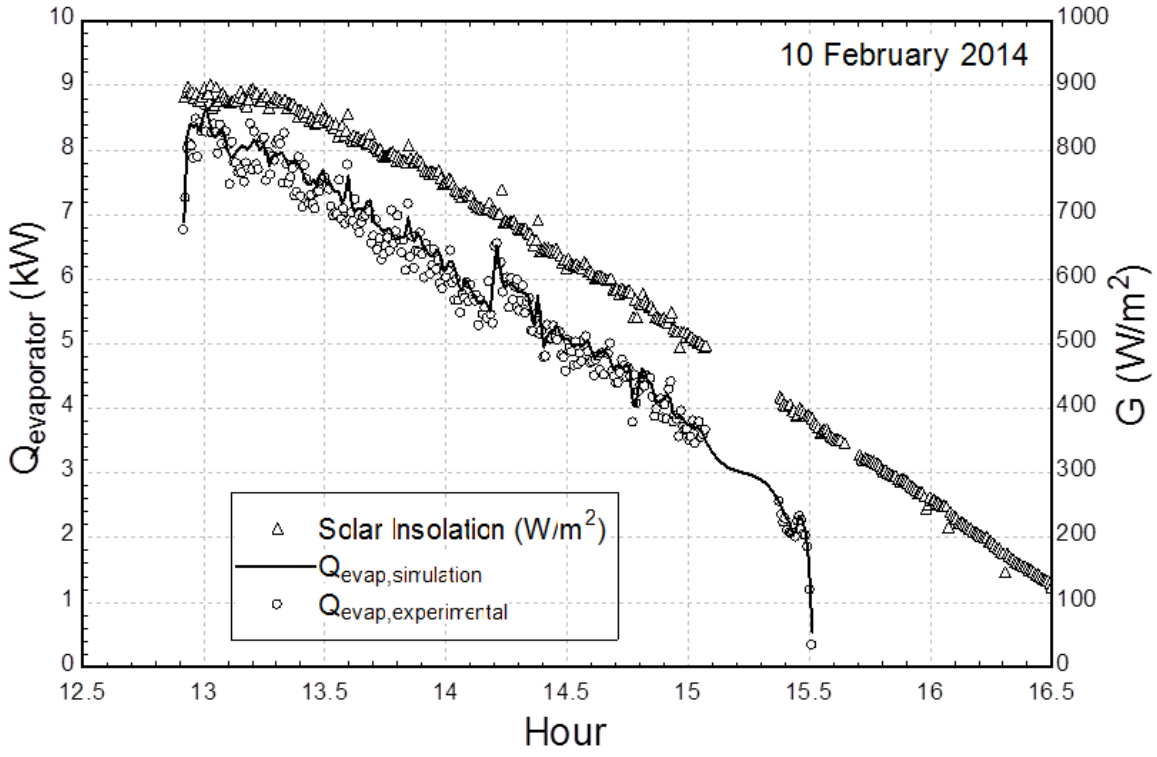

Figure 7-4 Refrigeration Effect produced by the proposed absorption chiller on 10 February 2014

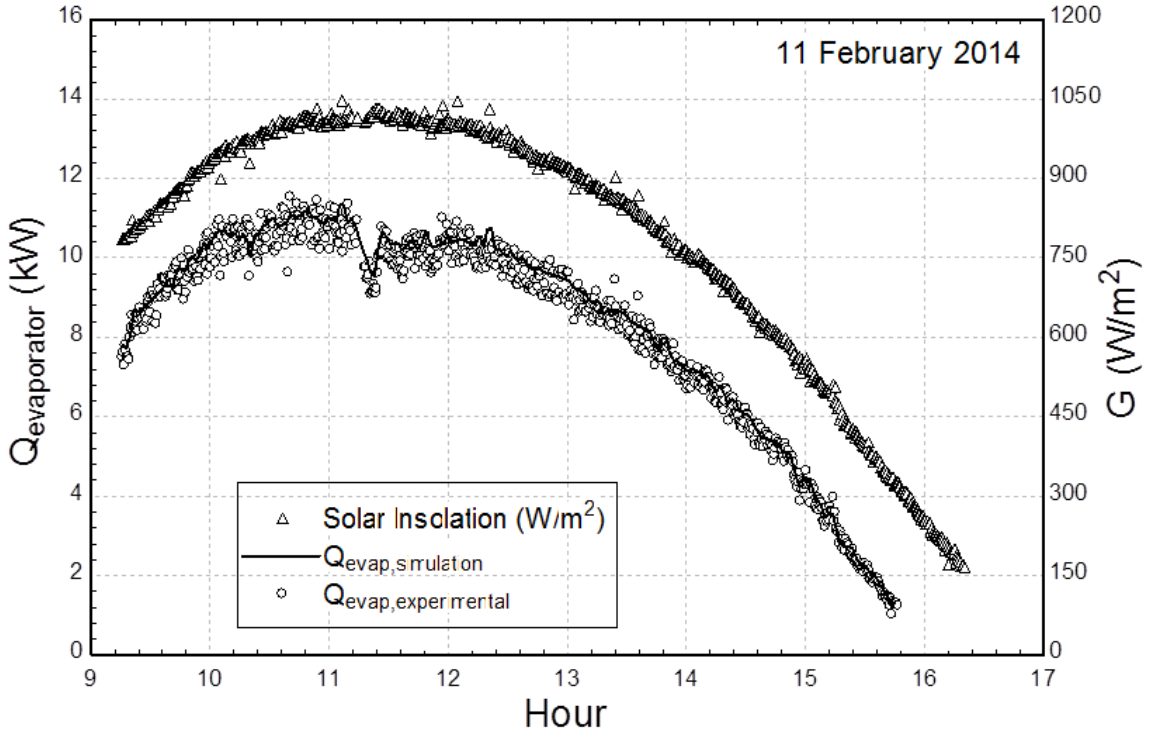

Figure 7-5 Refrigeration Effect produced by the proposed absorption chiller on 11 February 2014

CHAPTER 8

CONCLUSIONS AND RECOMMENDATIONS

In this dissertation, a design of an energy efficient solar powered aqua-ammonia vapor absorption refrigeration and air-conditioning system is proposed. The proposed design is a modified form of conventional aqua-ammonia absorption system aimed at improving its performance by heat recovering from the dephlegmator. The proposed system is also designed to operate at full cooling capacity with varying ambient conditions by introducing a refrigerant storage in the design of the system.

This dissertation also describes the details of the experimental setup established to practically analyze the performance of the proposed energy efficient solar powered aqua-ammonia vapor absorption refrigeration and air-conditioning system. The specific focus has been given to the different auxiliary systems attached to the absorption chiller, the construction of the absorption chiller, data acquisition system and operation procedure of the developed experimental setup.

This dissertation also develops the mathematical modeling for simulating the performance of the proposed energy efficient solar powered aqua-ammonia vapor absorption refrigeration and air-conditioning system. The specific focus has been given to the first and second laws of thermodynamic analysis conducted over the proposed absorption chiller.

Initially, the experimental validation of the simulated results has been conducted by simulating the performance of the proposed absorption chiller for February 10, 2014 & February 11, 2014 and comparing the simulated results with the experimental results. This experimental validation is followed by the first and second law thermodynamic analysis of the proposed absorption chiller.

The results for recovering heat from the dephlegamtor showed that the coefficient of performance of the proposed absorption chiller is 12% higher than the conventional absorption systems. The proposed absorption chiller is then analyzed for the selected summer season for the year 2012 under Dhahran ambient conditions. The results of the analysis over proposed absorption chiller for the summer season indicated that an additional 3500 kg of ice could be produced by introducing a refrigerant storage unit in the absorption system thus allowing the system to operate at full potential throughout the summer season.

Based on the results of the present dissertation analysis, it is recommended to analyze the proposed absorption system throughout the summer season in Saudi-Arabia. The proposed absorption system uses a refrigerant storage unit and cold storage units, however it is also recommended to analyze the performance of the system using heat storage units. The heat storage unit could be composed of hot water storage or phase change materials (PCM). Thus, in future, it is recommended to produce the day and night cooling using absorption chiller allowing the absorption chiller to utilize the advantage of diurnal temperature change in the hot and humid climatic regions.

References

[1] Choudhury B, Saha BB, Chatterjee PK, Sarkar JP. An overview of developments in adsorption refrigeration systems towards a sustainable way of cooling. Applied Energy 2013; 104: 554–567.

[2] Balaras CA, Grossman G, Henning HM, Infante-Ferreira CA, Podesser E, Wang L, Wiemken E. Solar air conditioning in Europe — an overview. Renewable and Sustainable Energy Reviews 2007; 11: 299–314.

[3] Solanki CS. Solar Photovoltaic Technology and Systems. 2013; 1: 23-24.

[4] Ministry of water & electricity, KSA Annual Report 2010.

[5] Faisal MZ. Impacts of Climate Change on Water Resources in Saudi Arabia. 3rd International Conference on Water Resources and Arid Environments 2008.

[6] Said SAM, Habib MA, Iqbal MO. Database for building energy prediction in Saudi Arabia. Energy Conversion and Management 2003; 44: 191–201.

[7] Fan Y, Luo L, Souyri B. Review of solar sorption refrigeration technologies: Development and applications. Renewable and Sustainable Energy Reviews 2007; 11: 1758–1775.

[8] Kim DS, Ferreira CAI. Solar refrigeration options – a state-of-the-art review. International Journal of Refrigeration 2008; 31: 3–15.

[9] Otanicar T, Taylor RA, Phelan PE. Prospects for solar cooling — an economic and environmental assessment. Solar Energy 2012 ; 86 : 1287–1299.

[10] Sarbu I, Sebarchievici C. Review of solar refrigeration and cooling systems. Energy and Buildings (2013); Accepted Manuscript: 1-24.

[11] Afshar O, Saidur R, Hasanuzzaman M, Jameel M. A review of thermodynamics and heat transfer in solar refrigeration system. Renewable and Sustainable Energy Reviews 2012; 16: 5639–5648.

[12] Chidambaram LA, Ramana AS, Kamaraj G, Velraj R. Review of solar cooling methods and thermal storage options. Renewable and Sustainable Energy Reviews 2011; 15: 3220-3228.

[13] Wang SG, Wang RZ. Recent developments of refrigeration technology in fishing vessels. Renewable Energy 2005; 30: 589-600.

[14] Trombe F, Foex M. The production of cold by means of solar radiation. Solar Energy 1957; 1(1): 51-52.

[15] Chinnappa JCV. Experimental study of the intermittent vapor absorption refrigeration cycle employing the refrigerant-absorbent systems of ammonia-water and ammonia-lithium nitrate. Solar Energy 1961; 5:1-18

[16] Chinnappa JCV. Performance of an intermittent refrigerator operated by a flat-plate collector. Solar Energy 1962; 6: 143-150.

[17] Kundu B, Mondal PK, Datta SP, Wongwises S. Operating design conditions of a solar-powered vapor absorption cooling system with an absorber plate having different profiles: An analytical study. International Communications in Heat and Mass Transfer 2010; 37: 1238–1245.

[18] Fernandez-Seara J, Uhia FJ, Sieres J. Research on the condensation of the ammonia–water mixture on a horizontal smooth tube. International Journal of Refrigeration 2008; 31: 304-314.

[19] Venegas M, Rodrıguez P, Lecuona A, Izquierdo M. Spray absorbers in absorption systems using lithium nitrate–ammonia solution. International Journal of Refrigeration 2005; 28: 554–564.

[20] Sozen A. Effect of heat exchangers on performance of absorption refrigeration systems. Energy Conversion and Management 2001; 42: 1699-1716.

[21] Fernandez-Seara J, Sieres J. The importance of the ammonia purification process in ammonia–water absorption systems. Energy Conversion and Management 2006; 47: 1975–1987.

[22] Sieres J, Fernandez-Seara J. Evaluation of the column components size on the vapour enrichment and system performance in small power NH3–H2O absorption refrigeration machines. International Journal of Refrigeration 2006; 29: 579-588.

[23] Sieres J, Fernandez-Seara J. Mass transfer characteristics of a structured packing for ammonia rectification in ammonia-water absorption refrigeration systems. International Journal of Refrigeration 2007; 30: 58-67.

[24] Sieres J, Fernandez-Seara J, Uhia FJ. Experimental characterization of the rectification process in ammonia–water absorption systems with a large-specific area corrugated sheet structured packing. International Journal of Refrigeration 2009; 32: 1230-1240.

[25] Sieres J, Fernandez-Seara J, Uhia FJ. Experimental analysis of ammonia–water rectification in absorption systems with the 10mm metal Pall ring packing. International Journal of Refrigeration 2008; 31: 270-278.

[26] Fernandez-Seara J, Sieres J, Vázquez M. Heat and mass transfer analysis of a helical coil rectifier in an ammonia–water absorption system. International Journal of Thermal Sciences 2003; 42: 783–794.

[27] Raghuvanshi S, Maheshwari G. Analysis of Ammonia –Water (NH3-H2O) Vapor Absorption Refrigeration System based on First Law of Thermodynamics. International Journal of Scientific & Engineering Research 2011; 2(8): 1-7.

[28] Said SAM, El-Shaarawi MAI, Siddiqui MU. Alternative designs for a 24-h operating solar-powered absorption refrigeration technology. International Journal of Refrigeration 2012; 35(7): 1967-1977.

[29] Darwish NA, Al-Hashimi SH, Al-Mansoori AS. Performance analysis and evaluation of a commercial absorption–refrigeration water–ammonia (ARWA) system. International Journal of Refrigeration 2008; 31: 1214–1223.

[30] Beccali M, Cellura M, Longo S, Nocke B, Finocchiaro P. LCA of a solar heating and cooling system equipped with a small water–ammonia absorption chiller. Solar Energy 2012; 86: 1491–1503.

[31] Mohanraj M, Jayaraj S, Muraleedharan C. Applications of artificial neural networks for refrigeration, air-conditioning and heat pump systems — A review. Renewable and Sustainable Energy Reviews 2012; 16: 1340–1358.

[32] Sencan A. Artificial intelligent methods for thermodynamic evaluation of ammonia–water refrigeration systems. Energy Conversion and Management 2006; 47: 3319 –3332.

[33] Sencan A. Performance of ammonia–water refrigeration systems using artificial neural networks. Renewable Energy 2007; 32: 314–328.

[34] Sun DW. Thermodynamic design data and optimum design maps for absorption refrigeration systems. Applied Thermal Engineering 1997; 17(3):211–21.

[35] Bangotra A, Mahajan A. Design Analysis of 3 TR Aqua Ammonia vapor Absorption Refrigeration System. International Journal of Engineering Research & Technology 2012; 1(8)

[36] Lavanya RS, Murthy BSR. Design of solar water cooler using aqua-ammonia absorption refrigeration system. International Journal of Advanced Engineering Research and Studies 2013; 2(2): 20-24.

[37] Abdulateef JM, Sopian K, Yahya M, Zaharim A, Alghoul MA. Optimization of the thermodynamic model of a solar driven Aqua-ammonia absorption refrigeration system. 2nd WSEAS/IASME International Conference on Renewable Energy Sources Corfu, Greece, 2008: 112-117.

[38] Chua HT, Toh HK, Ng KC. Thermodynamic modeling of an ammonia–water absorption chiller. International Journal of Refrigeration 2002; 25: 896–906.

[39] Lostec BL, Millette J, Galanis N. Finite time thermodynamics study and exergetic analysis of ammonia-water absorption systems. International Journal of Thermal Sciences 2010; 49: 1264-1276

[40] Caciula B, Popa V, Costiuc L. Theoretical study on solar powered absorption cooling system. Termotehnica 2013; 1; 130-134.

[41] Cai W, Sen M, Paolucci S. Dynamic simulation of an ammonia-water absorption refrigeration system. Department of Aerospace and Mechanical Engineering University of Notre Dame 2010; IN 46556.

[42] Kim B, Park J. Dynamic simulation of a single-effect ammonia-water absorption chiller. International Journal of Refrigeration 2007; 30: 535-545.

[43] Kim DS, Wang L, Machielsen CHM. Dynamic modelling of a small-scale NH3/H2O absorption chiller. International Congress of Refrigeration 2003; ICR0210: 1-8.

[44] Ozgoren M, Bilgili M, Babayigit O. Hourly performance prediction of ammonia-water solar absorption refrigeration. Applied Thermal Engineering 2012; 40: 80-90.

[45] Lin P, Wang RZ, Xia ZZ. Numerical investigation of a two-stage air-cooled absorption refrigeration system for solar cooling: Cycle analysis and absorption cooling performances. Renewable Energy 2011; 36: 1401-1412.

[46] Rogdakis ED, Antonopoulos KA. Performance of a low-temperature NH_3-H_2O absorption refrigeration system. Energy 1992; 17(5): 477-484.

[47] Bayramoglu M, Bulgan AT. Sensitivity analysis of an aqua-ammonia absorption refrigeration system (AARS). Energy 1995; 20(6): 567-571.

[48] Misra RD, Sahoo PK, Gupta A. Thermoeconomic evaluation and optimization of an aqua-ammonia vapour-absorption refrigeration system. International Journal of Refrigeration 2006; 29: 47–59.

[49] Ziegler B, Trepp C. Equation of state for ammonia-water mixtures. International Journal of Refrigeration 1984; 7(2): 101-106.

[50] BoopathiRaja V, Shanmugam V. A review and new approach to minimize the cost of solar assisted absorption cooling system. Renewable and Sustainable Energy Reviews 2012; 16: 6725–6731.

[51] Gomri R. Second law comparison of single effect and double effect vapour absorption refrigeration systems. Energy Conversion and Management 2009; 50: 1279–1287.

[52] Onan C, Ozkan DB, Erdem S. Exergy analysis of a solar assisted absorption cooling system on an hourly basis in villa applications. Energy 2010; 35: 5277-5285.

[53] Somers C, Mortazavi A, Hwang Y, Radermacher R, Rodgers P, Al-Hashimi S. Modeling water/lithium bromide absorption chillers in ASPEN Plus. Applied Energy 2011; 88: 4197–4205.

[54] Cascales JRG, García FV, Izquierdo JMC, Marín JPD, Sánchez RM. Modelling an absorption system assisted by solar energy. Applied Thermal Engineering 2011; 31: 112-118.

[55] Balghouthi M, Chahbani MH, Guizani A. Solar Powered air conditioning as a solution to reduce environmental pollution in Tunisia. Desalination 2005; 185: 105–110.

[56] Balghouthi M, Chahbani MH, Guizani A. Feasibility of solar absorption air conditioning in Tunisia. Building and Environment 2008; 43: 1459–1470.

[57] Ortiz M, Barsun H, He H, Vorobieff P, Mammoli A. Modeling of a solar-assisted HVAC system with thermal storage. Energy and Buildings 2010; 42: 500–509.

[58] Eicker U, Pietruschka D, Pesch R. Heat rejection and primary energy efficiency of solar driven absorption cooling systems. International Journal of Refrigeration 2012; 35: 729-738.

[59] Hong DL, Chen GM, Tang LM, He YJ. Simulation research on an EAX (Evaporator-Absorber-Exchange) absorption refrigeration cycle. Energy 2011; 36: 94-98.

[60] Kaynakli O, Kilic M. Theoretical study on the effect of operating conditions on performance of absorption refrigeration system. Energy Conversion and Management 2007; 48: 599–607.

[61] Gomri R. Investigation of the potential of application of single effect and multiple effect absorption cooling systems. Energy Conversion and Management 2010; 51: 1629–1636.

[62] Kaushik SC, Arora A. Energy and exergy analysis of single effect and series flow double effect water–lithium bromide absorption refrigeration systems. International Journal of Refrigeration 2009; 32: 1247-1258.

[63] Kilic M, Kaynakli O. Second law-based thermodynamic analysis of water-lithium bromide absorption refrigeration system. Energy 2007; 32: 1505–1512.

[64] Kouremenos DA, Rogdakis E, Antonopoulos KA. A high-efficiency, compound NH3/H20-H20/LIBR absorption-refrigeration system. Energy 1989; 14(12): 893-905.

[65] Micallef D, Micallef C. Mathematical model of a vapor absorption refrigeration unit. International Journal of Simulation Model 2010; 9(2): 86-97.

[66] Eicker U, Pietruschka D. Design and performance of solar powered absorption cooling systems in office buildings. Energy and Buildings 2009; 41: 81–91.

[67] Florides GA, Kalogirou SA, Tassou SA, Wrobel LC. Modelling and simulation of an absorption cooling system for Cyprus. Solar Energy 2002; 72(1): 43-5I.

[68] Farshi LG, Mahmoudi SMS, Rosen MA, Yari M, Amidpour M. Exergoeconomic analysis of double effect absorption refrigeration systems. Energy Conversion and Management 2013; 65: 13–25.

[69] Koroneos C, Nanaki E, Xydis G. Solar air conditioning systems and their applicability—an exergy approach. Resources, Conservation and Recycling 2010; 55: 74–82.

[70] Abdulateef JM, Sopian K, Alghoul MA. Optimum design for solar absorption refrigeration systems and comparison of the performances using ammonia-water, ammonia-lithium nitrate and ammonia-sodium thiocyanate solutions. International Journal of Mechanical and Materials Engineering 2008; 3(1): 17-24.

[71] Saghiruddin M, Siddiqui A. Economic analysis of two stage dual fluid absorption cycle for optimizing generator temperatures. Energy Conversion and Management 2001; 42: 407-437.

[72] Medrano M, Bourouis M, Coronas A. Double-lift Absorption Refrigeration cycles driven by low temperature heat sources using organic fluid mixtures as working pair. Applied Energy 2001; 68: 173-185.

[73] Pilatowsky I, Rivera W, Romero RJ. Thermodynamic analysis of monomethylaminewater solutions in a single-stage solar absorption refrigeration cycle at low generator temperatures. Solar Energy Materials & Solar Cells 2001; 70: 287-300.

[74] Fong KF, Lee CK, Chow CK, Yuen SY. Simulation-optimization of solar-thermal refrigeration systems for office use in subtropical Hong Kong. Energy 2011; 36: 6298-6307.

[75] Crepinsek Z, Goricanec D, Krope J. Comparison of the performances of absorption refrigeration cycles. WSEAS Transactions on heat and mass transfer 2009; 3(4): 65-76.

[76] Brendel T, Zetzsche M, Müller-Steinhagen H. Development of Small Scale Ammonia/Water Absorption Chiller. 9th IIR Gustav Lorentzen Conference, Sydney, 2010; 1: 469-474.

[77] Lostec BL, Galanis N, Millette J. Experimental study of an ammonia-water absorption chiller. International Journal of Refrigeration 2012; 35: 2275-2286.

[78] Albers J, Ziegler F. Analysis of the part load behaviour of sorption chillers with thermally driven solution pumps. Proceedings of the XXI IIR International Congress Refrigeration 2003; ICR0570 (Washington, DC, USA).

[79] Asdrubali F, Grignaffini S. Experimental evaluation of the performances of a H2O-LiBr absorption refrigerator under different service conditions. International Journal of Refrigeration 2005; 28: 489-497.

[80] Cerezo J, Bourouis M, Vallès M, Coronas A, Best R. Experimental study of an ammonia water bubble absorber using a plate heat exchanger for absorption refrigeration machines. Applied Thermal Engineering 2009; 29: 1005–1011.

[81] Cerezo J, Best R, Bourouis M, Coronas A. Comparison of numerical and experimental performance criteria of an ammonia–water bubble absorber using plate heat exchangers. International Journal of Heat and Mass Transfer 2010; 53: 3379–3386.

[82] De-Francisco A, Illanes R, Torres JL, Castillo M, De-Blas M, Prieto E, Garcia A. Development and testing of a prototype of low power water-ammonia absorption equipment for solar energy applications. Renewable Energy 2002; 25: 537-544.

[83] Boudéhenn F, Demasles H, Wyttenbach J, Jobard X, Chèze D, Papillon P. Development of a 5 kW cooling capacity ammonia-water absorption chiller for solar cooling applications. Energy Procedia 2012; 30: 35 – 43.

[84] Sohel MI, Dawoud B. Dynamic modeling and simulation of a gravity-assisted solution pump of a novel ammonia–water absorption refrigeration unit. Applied Thermal Engineering 2006; 26: 688–699.

[85] Abdulateef JM, Alghoul MA, Zaharim A, Sopian K. Experimental Investigation on Solar Absorption Refrigeration System in Malaysia. Proceedings of the 3rd WSEAS International Conference on Renewable Energy Sources, 2010.

[86] Arias-Varela HD, Soto-Gomez W, Castillo-Lopez O, Best-Brown R. Thermodynamic design of a solar refrigerator to preserve sea products. 2000; California 22370: http://www.cientificosaficionados.com/energia%20solar/termodinamica.pdf

[87] Chua HT, Toh HK, Malek A, Ng KC, Srinivasan K. Improved thermodynamic property fields of LiBr±H2O solution. International Journal of Refrigeration 2000; 23: 412-429.

[88] Agyenim F, Knight I, Rhodes M. Design and experimental testing of the performance of an outdoor LiBr/H2O solar thermal absorption cooling system with a cold store. Solar Energy 2010; 84: 735–744.

[89] Balghouthi M, Chahbani MH, Guizani A. Investigation of a solar cooling installation in Tunisia. Applied Energy 2012; 98: 138–148.

[90] Darkwa J, Fraser S, Chow DHC. Theoretical and practical analysis of an integrated solar hot water-powered absorption cooling system. Energy 2012; 39: 395-402.

[91] Hu JS, Chao CYH. Study of a micro absorption heat pump system. International Journal of Refrigeration 2008; 31: 1198-1206.

[92] Bermejo P, Pino FJ, Rosa F. Solar absorption cooling plant in Seville. Solar Energy 2010; 84: 1503–1512.

[93] Praene JP, Marc O, Lucas F, Miranville F. Simulation and experimental investigation of solar absorption cooling system in Reunion Island. Applied Energy 2011; 88: 831–839.

[94] Sumathy K, Huang ZC, Li ZF. Solar absorption cooling with low grade heat source - A strategy of development in south china. Solar Energy 2002; 72(2): 155-165.

[95] Zhu L, Wang S, Gu J. Performance investigation of a thermal-driven refrigeration system. International Journal of Energy Research 2008; DOI: 10.1002.

[96] E1-Shaarawi MAI, Ramadan RA. Effect of condenser temperature on the performance of intermittent solar refrigerators. Energy Conversion and Management 1987; 27(1): 73-81.

[97] E1-Shaarawi MAI, Ramadan RA. An additional parameter in evaluating the performance of intermittent solar refrigerators. Energy Conversion and Management 1988; 28(2): 143-150.

[98] E1-Shaarawi MAI, Ramadan RA. Technical Note:-Variation of the performance of intermittent solar Refrigerators with initial Temperature. Solar and Wind Technology 1988; 5(3): 278-299.

[99] El-Shaarawi MAI, Said SAM, Siddiqui MU. Comparative analysis between constant pressure and constant temperature absorption processes for an intermittent solar refrigerator. International Journal of Refrigeration 2014; Accepted for publication

[100] El-Shaarawi MAI, Said SAM, Siddiqui MU. New Simplified Correlations for Aqua-Ammonia Intermittent Solar-Powered Absorption Refrigeration Systems. International Journal of Air-Conditioning and Refrigeration 2012; 20(2): 1250008.

[101] Said SAM, El-Shaarawi MAI, Siddiqui MU. Intermittent absorption refrigeration system equipped with an economizer. Energy 2013; 61: 332-344.

[102] Rivera CO, Rivera W. Modeling of an intermittent solar absorption refrigeration system operating with ammonia-lithium nitrate mixtures. Solar Energy Materials and Solar Cells 2003; 76: 417-427.

[103] E1-Shaarawi MAI, Ramadan RA. Solar refrigeration in the Egyptian climate. Solar Energy 1986; 37(5): 347-361.

[104] El-Ghalban AR. Operational results of an intermittent absorption cooling unit. International Journal of Energy Research 2002; 26: 825–835.

[105] Hernandez JA, Rivera W, Colorado D, Moreno-Quintanar G. Optimal COP prediction of a solar intermittent refrigeration system for ice production by means of direct and inverse artificial neural networks. Solar Energy 2012; 86: 1108–1117.

[106] Rasul MG, Murphy A. Solar Powered intermittent Absorption Refrigeration unit. Australasian Power Engineering Conference AUPEC 2006.

[107] Park YM, Sonntag RE. Thermodynamic properties of ammonia-water mixtures: A generalized equation-of-state approach. ASHRAE Transactions 1990; 97(1): 150.

[108] Macrisis RA, Eakin BE, Ellington RT, Huebler J. Physical and thermodynamic properties of ammonia-water mixtures. Research Bulletin 34, Institute of Gas Technology–Chicago 1964.

[109] Ibrahim OM, Klein SA. Thermodynamic properties of ammonia-water mixtures. ASHRAE Transactions 1993; 99(1): 1495.

[110] Patek J, Klomfar J. Simple functions for fast calculations of selected thermodynamic properties of the ammonia-water system. International Journal of Refrigeration 1995; 18(4): 228.

[111] Tillner-Roth R, Friend DG. Survey and assessment of available measurements on thermodynamic properties of the mixture (water-ammonia). Journal of Physical Chemistry 1998; 27(1): 45.

[112] Klein SA. Engineering Equation Solver. Academic Professional version 8.427-3D. Department of Mechanical Engineering, University of Wisconsin-Madison, Madison, WI 2009.

[113] El-Shaarawi MAI, Said SAM, Siddiqui MU. New Correlation Equations for Ammonia-Water Vapor-Liquid Equilibrium (VLE) Thermodynamic Properties. ASHRAE Transactions 2013; 119(1): DA-13-025.

Vitae

Name	Muhammad Umar Siddiqui
Nationality	Pakistani
Date of Birth	May 03, 1985
Email	umar_tuwairqi@yahoo.com
Address	KFUPM P.O.BOX 925, Dhahran, 31261, KSA
Academic Background	MS. Mechanical Eng. (2011) KFUPM - KSA
	BE. Mechanical Eng. (2007) NEDUET - PAKISTAN

Publications

1. El-Shaarawi MAI, Said SAM, ***Siddiqui MU***. New Simplified Correlations for Aqua-Ammonia Intermittent Solar-Powered Absorption Refrigeration Systems. International Journal of Air-Conditioning and Refrigeration 2012; 20(2): 1250008.

2. Said SAM, El-Shaarawi MAI, ***Siddiqui MU***. Alternative designs for a 24-h operating solar-powered absorption refrigeration technology. International Journal of Refrigeration 2012; 35(7): 1967-1977.

3. El-Shaarawi MAI, Said SAM, ***Siddiqui MU***. New Correlation Equations for Ammonia-Water Vapor-Liquid Equilibrium (VLE) Thermodynamic Properties. ASHRAE Transactions 2013; 119(1): DA-13-025.

4. Said SAM, El-Shaarawi MAI, ***Siddiqui MU***. Intermittent absorption refrigeration system equipped with an economizer. Energy 2013; 61: 332-344.

5. El-Shaarawi MAI, Said SAM, ***Siddiqui MU***. Comparative analysis between constant pressure and constant temperature absorption processes for an intermittent solar refrigerator. International Journal of Refrigeration 2014; Accepted for publication

Patent

1. Said SAM, El-Shaarawi MAI, ***Siddiqui MU***. Hybrid Aqua-Ammonia & LiBr-water Absorption Chiller. USPTO Serial # 14/043,745. Filed on October 01, 2013. ***Accepted*** on January 09, 2014.